T.C.

YEDİTEPE UNIVERSITY

INSTITUTE OF HEALTH SCIENCES

DEPARTMENT OF PROSTHETIC DENTISTRY

EVALUATION OF MECHANICAL AND OPTICAL PROPERTIES OF DIFFERENT CAD-CAM MATERIALS AFTER GASTRIC ACID EXPOSURE

DOCTOR OF PHILOSOPHY THESIS

ELİFNAZ ÖZEN, DDS

SUPERVISOR
PROF. PINAR KURSOĞLU

İSTANBUL-2021

THESIS APPROVAL FORM

Institute	:	Yeditepe University Institute of Health Sciences
Programme	:	Prosthetic Dentistry
Title of the Thesis	:	Evaluation of Optical and Mechanical Properties of Different Cad-Cam Materials After Gastric Acid Exposure
Owner of the Thesis	:	Elifnaz Özen, DDS, PhD.
Examination Date	:	30.06.2021

This study have approved as a Doctorate Thesis in regard to content and quality by the Jury.

Chair of the Jury:	PROF. ENDER KAZAZOĞLU (Yeditepe University)
Supervisor:	PROF. PINAR KURSOĞLU (Yeditepe University)
Member/Examiner:	PROF. NURAY ÇAPA YILDIRIM (Yeditepe University)
Member/Examiner:	PROF. VOLKAN GÜNAY (Yeditepe University)
Member/Examiner:	PROF. OLCAY ŞAKAR (İstanbul University)

APPROVAL

This thesis has been deemed by the jury in accordance with the relevant articles of Yeditepe University Graduate Education and Examinations Regulation and has been approved by Administrative Board of Institute with decision dated .... and numbered ....

PROF. BAYRAM YILMAZ
Director of Institute of Health Science

DECLARATION

I hereby declare that this thesis is my own work and that, to the best of my knowledge and belief, it contains no material previously published or written by another person nor material which has been accepted for the award of any other degree except where due acknowledgment has been made in the text.

30.06.2021

ELİFNAZ ÖZEN, DDS

DEDICATION

I dedicate my thesis to my beloved family…

ACKNOWLEDGEMENTS

I would like to express my endless gratitude to my dear family; my mother **Fatma ÖZEN**, my father **İlhan ÖZEN** and my sister **Ezginur ÖZEN**, who stand behind me in all circumstances and surround me with their love and support. I am here where I stand now thanks to them and their endless belief in me.

I kindly would like to present my deepest gratitude to my very dear advisor, mentor, teacher **Prof. Pınar KURSOĞLU**, who encouraged me to continue on this path and to move forward under all circumstances, who did not spare her support, belief, guidance, kindness and love. I am so grateful that she did not give me the fish, but she taught me to fish. I was and I will always be deeply honored and feel as the luckiest to be her student.

My greatest gratitude is for my very much respected mentor, **Prof. Ender KAZAZOĞLU**, who always makes us feel his support, is not only a teacher, but a person I am honored to know and whose ideas I always value very much. I would like to express my heartfelt thanks to him for his support, guidance and help.

I am so thankful and grateful to know one of my most trustful mentors, dearest teacher **Prof. Nuray ÇAPA YILDIRIM,** who means so much to me and who is always very valuable to me with her guidance, support and belief.

I would like to express my deepest gratitude to my dear teacher **Prof. Volkan GÜNAY** for always being there and being very supportive. His presence is so valuable and precious.

My endless thanks are for all my teachers in our department, who never hesitate to share their knowledge and experiences during my undergraduate and doctorate education, for being very generous and warm-hearted.

I want to express my gratitude coming from the deep of my heart to my best friend **DDS. PhD. İzim TÜRKER,** who has always been with me through all this hard, long, sometimes full of tears and mostly very joyful journey for nine years. Her kind perspective, support, valuable friendship was and always will be very precious for me. I hope our paths will always go side by side.

I sincerely thank my dearest **Samet SÜTÜVEN**, who witnessed this process closely in every detail, never spared his support from me, and was always by my side, ready to help with every opportunity. This process would be very hard without him.

My dearest friends from high school, they are my second family and I could not make it here without them. Thank you for always being by my side, guiding, loving, supporting, leading to the best paths.

I want to thank all my friends in our department for being so supportive and loving people. It is always very lovely to work with them.

I also would like to express my gratitude to **İsmehan DERE** for being very helpful and open to share her knowledge about my experiments held at Hard Tissue Laboratory.

I am very grateful to **Optimal Dental Laboratory**, especially to **Cdt. Hasan ALKAÇ and Cdt. Burak ÜNAL** for their very kind help and support.

I would like to thank **Assist. Prof. Elif Çiğdem ALTUNOK** and **Ebru OSMANOĞLU AKYOL** for the statistical analysis of my thesis.

For my 3D optical profilometer evaluations, I would like to thank **Prof. Bahri ŞAHİN** and **Prof. Aysel KANTÜRK FİGEN**, who showed kind interest and support.

For my scanning electron microscope evaluations, I would like to thank **Doctor Ali ABDİ** and **PhD. Pınar AKKUŞ SÜT** for their meticulous cooperation.

I want to thank "TÜBİTAK 2211-A National PhD Scholarship Program" that has supported my PhD education and my PhD thesis.

TABLE OF CONTENTS

APPROVAL…………………………………………………………………………… ii
DECLARATION………………………………………………………..…….. iii
DEDICATION…………………………………………………………………..iv
ACKNOWLEDGEMENTS…………………………………………………….....v
TABLE OF CONTENTS…………………………………………..……..... vii
LIST OF TABLES……………………………………………………………….. xii
LIST OF FIGURES……………………………………………………….. xv
LIST OF SYMBOLS AND ABBREVIATIONS…………………..………………... xix
ABSTRACT………………………………………………………………… xxii
ABSTRACT (Turkish)……………………………………………………….. xxiii
1. INTRODUCTION AND PURPOSE 1
2. GENERAL INFORMATIONS... 3
2.1. Dental Ceramics... 3
2.1.1. Properties of Dental Ceramics 4
2.1.2. Classification of Dental Ceramics 5
2.1.2.1. Glass-Matrix Ceramic Family 6
2.1.2.2. Polycrystalline Ceramic Family... 11
2.1.2.3. Resin-Matrix Ceramics 16
2.2. Brief History of Subtractive CAD-CAM Systems 18
2.3. Surface Treatments of Ceramic Restorations 20
2.3.1. Glazing.. 20
2.3.1.1. Glazing Methods.. 21
2.3.2. Polishing 21
2.3.2.1. Steps of Finishing and Polishing Procedures... 22
2.3.2.2. Factors Affecting the Polishing Efficiency.. 23
2.3.2.3. Wear Tribology... 23
2.3.3. Glaze versus Polishing on CAD-CAM Ceramics... 24
2.4. Erosion... 27

2.4.1. Extrinsic Erosion 28
2.4.2. Intrinsic Erosion 28
2.4.2.1. Blumia Nervosa 29
2.4.3. Clinical Presentation of Erosion 33
2.4.4. Corrosion on Dental Ceramics 34
2.5. Assessment Methods of Corrosion and Erosion 35
2.5.1. Surface Roughness Assessment 35
2.5.1.1. Methods of Measuring Surface Roughness 36
2.5.2. Surface Topography Assessment 39
2.5.3. Surface Microhardness Assessment 40
2.5.3.1. Methods of Measuring Surface Microhardness 41
2.5.4. Fracture Toughness Assessment 41
2.5.4.1. Indentation Fracture Toughness Test 42
2.6. Optical Parameters of Esthetic Restorations 43
2.6.1. Color Determinant 43
2.6.1.1. Definition and Perception of Color 43
2.6.1.2. Color Systems 44
2.6.1.3. Main Definitions Related to Color and Appearance 49
2.6.1.4. Color Measurement Methods 50
2.6.2. Translucency Determinant 53
2.6.2.1. Translucency Parameter (TP) 53
2.6.2.2. Contrast Ratio (CR) 54
2.6.2.3. Translucency Thresholds 55
2.6.2.4. Factors Affecting Translucency Measurement 55
3. MATERIALS AND METHODS 56
3.1. Power Analysis 56
3.2. Sample Preparations 56

3.2.1. Lithium Disilicate and Zirconia Reinforced Lithium Silicate Samples................ 59
3.2.2. Monolithic Zirconia Samples... 61
3.2.3. Sinterization of the Monolithic Zirconia Samples... 63
3.2.4. Grinding Step 64
3.2.5. Crystallization of the Lithium Disilicate and Zirconia Reinforced Lithium Silicate Samples.. 66
3.2.6. Intra Oral Polishing Step and Cleaning of Samples 67
3.2.7. Subgroup Formations.. 70
3.3. Solution Preparations 71
3.4. Measurements 73
3.4.1. Color Measurements 75
3.4.2. Translucency Measurements.. 76
3.4.3. Surface Roughness Measurements 77
3.4.4. Surface Microhardness Measurements 79
3.4.5. Fracture Toughness Measurements 81
3.4.6. Surface Topography.. 82
3.5. Statistical Analysis.. 84
4. RESULTS 85
4.1. Mechanical Properties... 85
4.1.1. Surface Roughness... 85
4.1.1.1. Baseline (T_0) Surface Roughness (Ra) Evaluations among CAD-CAM Materials 87
4.1.1.2. Surface Roughness (Ra) Evaluations After Solution Exposures (T_1) Among CAD-CAM Materials 88
4.1.1.3. Surface Roughness (Ra) Evaluations of Each Subgroup Before and After the Solution Exposure (T_0-T_1) 88
4.1.1.4. Comparison of Surface Roughness Changes (ΔRa) on Different CAD-CAM Materials Exposed to Different Solutions.. 89

4.1.2. Surface Microhardness ... 91

4.1.2.1. Baseline (T_0) Surface Microhardness (VHN) Evaluations Among CAD-CAM Materials ... 93

4.1.2.2. Surface Microhardness (VHN) Evaluations After Solution Exposures (T_1) Among CAD-CAM Materials ... 94

4.1.2.3. Surface Microhardness (VHN) Evaluations of Each Subgroup Before and After the Solution Exposure (T_0-T_1)... 95

4.1.2.4. Comparison of Surface Microhardness Changes (ΔVHN) on Different CAD-CAM Materials Exposed to Different Solutions... 96

4.1.3. Fracture Toughness... 99

4.1.3.1. Baseline (T_0) Fracture Toughness (K_{Ic}) Evaluations among CAD-CAM Materials ... 101

4.1.3.2. Fracture Toughness (K_{Ic}) Evaluations After Solution Exposures (T_1) Among CAD-CAM Materials ... 102

4.1.3.3. Fracture Toughness (K_{Ic}) Evaluations of Each Subgroup Before and After the Solution Exposure (T_0-T_1)... 103

4.1.3.4. Comparison of Fracture Toughness Changes (ΔK_{Ic}) on Different CAD-CAM Materials Exposed to Different Solutions ... 104

4.1.4. Surface Topography... 107

4.1.4.1. 3D Optical Profilometer Evaluations... 107

4.1.4.2. Scanning Electron Microscope (SEM) Evaluations ... 110

4.2. Optical Properties ... 113

4.2.1. Color ... 113

4.2.1.1. Baseline (T_0) Color Parameter (L*, a*, b*) Evaluations among CAD-CAM Materials ... 116

4.2.1.2. Evaluations of Color Parameters (L*, a*, b*) After Solution Exposures (T_1) Among CAD-CAM Materials...119

4.2.1.3. Evaluations of Color Parameters (L*, a*, b*) of Each Subgroup Before and After the Solution Exposure (T_0-T_1)... 122

4.2.1.4. Comparison of Color Changes (ΔE) on Different CAD-CAM Materials Exposed to Different Solutions…………………………………………………..……....124

4.2.2. Translucency Results 127

4.2.2.1. Baseline (T_0) Evaluations of Translucency Parameter (TP) Among CAD-CAM Materials...129

4.2.2.2. Translucency Parameter (TP) Evaluations After Solution Exposures (T_1) Among CAD-CAM Materials……………………………………………….……130

4.2.2.3. Translucency Parameter (TP) Evaluations of Each Subgroup Before and After the Solution Exposure (T_0-T_1)………………………………………………….. 131

4.2.2.4. Comparison of Translucency Parameter Changes (ΔTP) on Different CAD-CAM Materials Exposed to Different Solutions.. 132

5. DISCUSSION 135

6. CONCLUSIONS 156

7. REFERENCES 158

LIST OF TABLES

Table 2.1. Corrosion Determinants Affecting the Durability of Dental Ceramics 34

Table 3.1. Material contents 58

Table 3.2. Characteristics of samples 59

Table 3.3. Optra Fine Intra Oral Polishing Kit 68

Table 3.4. Solution formulas and pH's table 71

Table 4.1. Descriptive statistics on surface roughness (µm) of six subgroups before and after the solution exposures 86

Table 4.2. Baseline surface roughness (µm) evaluations among different materials and solutions. 87

Table 4.3. Surface roughness (µm) evaluations among different materials and solutions at T_1. 88

Table 4.4. Ra (µm) evaluations of six subgroups before and after (T_0-T_1) the solution exposure. 89

Table 4.5. ΔRa (µm) Evaluation on Different Materials and Solutions 90

Table 4.6. Evaluation of the common effect of material and solution on ΔRa 91

Table 4.7. Descriptive statistics on surface hardness (VHN) of six subgroups before and after the solution exposures 92

Table 4.8. Baseline surface microhardness (VHN) evaluations among different materials and solutions. 93

Table 4.9. Surface microhardness (VHN) evaluations among different materials and solutions at T_1. 94

Table 4.10. VHN evaluations of six subgroups before and after (T_0-T_1) the solution exposure. 95

Table 4.11. ΔVHN Evaluation on Different Materials and Solutions 96

Table 4.11.a. Multiple comparisons of blumic subgroups' surface hardness values 97

Table 4.11.b. Multiple comparisons of control subgroups' surface hardness values 97

Table 4.12. Evaluation of the common effect of material and solution on ΔVHN 98

Table 4.13. Descriptive statistics on fracture toughness (K_{Ic}) of six subgroups before and after the solution exposures 100

Table 4.14. Baseline fracture toughness ($MPa.m^{1/2}$) evaluations among different materials and solutions. 101

Table 4.15. Fracture toughness (MPa.m$^{1/2}$) evaluations among different materials and solutions at T_1. 102
Table 4.16. K_{Ic} (MPa.m$^{1/2}$) evaluations of six subgroups before and after (T_0-T_1) the solution exposure. 103
Table 4.17. ΔK_{Ic} (MPa.m$^{1/2}$) Evaluation on Different Materials and Solutions 104
Table 4.17.a. Multiple comparisons of blumic subgroups' fracture toughness values 105
Table 4.17.b. Multiple comparisons of control subgroups' fracture toughness values 105
Table 4.18. Evaluation of the common effect of material and solution on ΔK_{Ic} 106
Table 4.19.a. Descriptive statistics on color parameter (L*) of six subgroups before and after the solution exposures 113
Table 4.19.b. Descriptive statistics on color parameter (a*) of six subgroups before and after the solution exposures 114
Table 4.19.c. Descriptive statistics on color parameter (b*) of six subgroups before and after the solution exposures 115
Table 4.20. Descriptive statistics on color parameter (ΔE) of six subgroups before and after the solution exposures 116
Table 4.21. Baseline L* parameter evaluations among different materials and solutions. 116
Table 4.22. Baseline a* parameter evaluations among different materials and solutions. 117
Table 4.23. Baseline b* parameter evaluations among different materials and solutions. 118
Table 4.24. L* value evaluations among different materials and solutions at T_1. 119
Table 4.25. a* value evaluations among different materials and solutions at T_1. 120
Table 4.26. b* value evaluations among different materials and solutions at T_1. 121
Table 4.27. L* value evaluations of six subgroups before and after (T_0-T_1) the solution exposure. 122
Table 4.28. a* value evaluations of six subgroups before and after (T_0-T_1) the solution exposure. 123
Table 4.29. b* value evaluations of six subgroups before and after (T_0-T_1) the solution exposure. 123
Table 4.30. ΔE Evaluation on Different Materials and Solutions 124
Table 4.30.a. Multiple comparisons of blumic subgroups' color change values 125

Table 4.30.b. Multiple comparisons of control subgroups' color change values 125
Table 4.31. Evaluation of the common effect of material and solution on ΔE 126
Table 4.32. Descriptive statistics on translucency parameter (TP) of six subgroups before and after the solution exposures 128
Table 4.33. Baseline TP parameter evaluations among different materials and solutions. 129
Table 4.34. Translucency parameter evaluations among different materials and solutions at T_1. 130
Table 4.35. TP evaluations of six subgroups before and after (T_0-T_1) the solution exposure. 131
Table 4.36. ΔTP Evaluation on Different Materials and Solutions 132
Table 4.36.a. Multiple comparisons of blumic subgroups' translucency change Values 133
Table 4.36.b. Multiple comparisons of control subgroups' translucency change Values 133
Table 4.37. Evaluation of the common effect of material and solution on ΔTP 134

LIST OF FIGURES

Figure 2.1. First generation of zirconia (3Y-HA TZP) having larger alumina content, while second generation of zirconia having smaller alumina content (3Y-TZP). 14
Figure 2.2. Steps of finishing and polishing starting from the bottom to the top. 22
Figure 2.3. Classification of the finishing and polishing methods according to abrasive-wear modes. 24
Figure 2.4. Diagram of white light interferometer 37
Figure 2.5. Shape and mark of Vickers indenter 41
Figure 2.6. Cylindrical illustration of Munsell Color Scale 45
Figure 2.7. Color diagram according to CIELab* system 47
Figure 3.1. IPS e.max CAD C14 block, Ivoclar Vivadent, Schaan, Liechtenstein 56
Figure 3.2. Celtra Duo CAD C14 block, Dentsply Sirona, York, Pennsylvania 57
Figure 3.3. Ceramill Zolid HT+ 16 mm thick disc, Amann Girrbach AG, Koblach, Austria 57
Figure 3.4. and Figure 3.5. E and C blocks stabilized onto metal-acrylic holder 60
Figure 3.6. and Figure 3.7. Polywax sticky wax, Bilkimya, İzmir, Turkey 60
Figure 3.8. Isomet 1000 sectioning saw, Buehler, Lake Bluff, Illinois 60
Figure 3.9. Block hold by metal-acrylic piece installed onto the sectioning saw 61
Figure 3.10. Samples designed onto disc by Ceramill Mind 1.0 software, Amann Girrbach GmbH, Pforzheim, Germany 61
Figure 3.11. and Figure 3.12. Disc milled by Ceramill Motion 2, Amann Girrbach GmbH, Pforzheim, Germany 62
Figure 3.13. Z sample milled %25 bigger than desired dimensions 62
Figure 3.14. and Figure 3.15. Before and after the sintering process 63
Figure 3.16. HT Speed Sintering Furnace, MIHM-VOGT GmbH & Co., Stutensee, Germany 63
Figure 3.17. Ecomet 250 automatic polishing machine, Buehler, Lake Bluff, Illinois 64
Figure 3.18., Figure 3.19. and Figure 3.20. 600- 800- 1200- 2500 grit silicon carbide papers (English Abrasives & Chemicals Ltd., Stafford, UK; Buehler, Lake Bluff, Illinois) 65
Figure 3.21. Digital caliper (Mitutoyo Corp., Kanagawa, Japan) measuring final thickness as 1.50 mm 65

Figure 3.22. E samples before crystallization with Programat P500, Ivoclar Vivadent, Schaan, Lichtenstein 66
Figure 3.23. E samples after crystallization with Programat P500, Ivoclar Vivadent, Schaan, Lichtenstein 66
Figure 3.24. and Figure 3.25. C samples before and after crystallization with Focus 2010 Furnace, Shenpaz, Tel Aviv, Israel 67
Figure 3.26. Optra Fine 3 step intra oral polishing kit, Ivoclar Vivadent, Schaan, Liechtenstein 68
Figure 3.27. Contra-angled hand piece and micro motor (W&H, Salzburg, Austria; A-dec, Newberg, Oregon) 69
Figure 3.28. Samples cleaned in distilled water for 20 minutes with ultrasonic cleaner (AS 8772 Ultrasonic Cleaner, General Home Orsay Ltd. Şti., İstanbul, Turkey) 69
Figure 3.29. Plastic box and upright standing samples via plexi glass holder 70
Figure 3.30 and Figure 3.31. Different color coded boxes 70
Figure 3.32. Blumia Nervosa Solution (Blumic Subgroup Solution) 71
Figure 3.33. Artificial Saliva Solution (Control Subgroup Solution) 71
Figure 3.34. MP 220 Digital pH meter, Mettler Toledo, Greifensee, Switzerland 72
Figure 3.35. Samples stored in the incubator at 37°C (Memmert BE 500 Incubator, Memmert GmbH + Co. KG, Schwabach, Germany) 73
Figure 3.36. Summary of study design 74
Figure 3.37. and Figure 3.38. Spectrophotometer (CM-2600d, Konica Minolta, Tokyo, Japan) and sample positioned on the center of white background 75
Figure 3.39. Spectrophotometer set up and Spectra Magic 3.1 Software, Konica Minolta, Tokyo, Japan 76
Figure 3.40. and Figure 3.41. Sample over white and black backgrounds 77
Figure 3.42. Contact profilometer (Perthometer M1, Mahr GmbH, Ingolstadt, Germany) 78
Figure 3.43. Settings of contact profilometer 78
Figure 3.44. Measuring the surface roughness on the center of a sample 78
Figure 3.45. and Figure 3.46. Microhardness tester equipment (Micromet 5114D, Buehler, Lake Bluff, Illinois) and indentation made on the center of sample 79
Figure 3.47. and Figure 3.48. Vickers indentation mark and border lines to measure d_1 and d_2 distance 80

Figure 3.49. Screen showing the calculation of the Vickers Hardness Number (VHN) 80
Figure 3.50. and Figure 3.51. Cracks formed on a sample by indentation 81
Figure 3.52. Vacuum sputter coater (SCD 005 Sputter Coater, Bal-Tec, Balzers, Liechtenstein) 82
Figure 3.53. and Figure 3.54. Scanning electron microscope (EVO 40, Carl Zeiss Microscopy, Oberkochen, Germany) and positioning of samples for examination 83
Figure 3.55. 3D Optical Profilometer (Nanomap-500LS, AEP Technology, Santa Clara, California, USA) 83
Figure 4.1. Surface roughness change evaluations on different materials and solutions 90
Figure 4.2. Surface microhardness change evaluations on different materials and solutions 98
Figure 4.3. Fracture toughness change evaluations on different materials and solutions 106
Figure 4.4. 3D topographic images of IPS e.max taken by 3D optical profilometer. A, before solution exposure. B, after exposure of blumic solution. C, after exposure of control solution. 107
Figure 4.5. 3D topographic images of Celtra Duo taken by 3D optical profilometer. A, before solution exposure. B, after exposure of blumic solution. C, after exposure of control solution. 108
Figure 4.6. 3D topographic images of Ceramill Zolid taken by 3D optical profilometer. A, before solution exposure. B, after exposure of blumic solution. C, after exposure of control solution. 109
Figure 4.7. SEM images of IPS e.max with x10.000 original magnification. A, before solution exposure. B, after blumic solution exposure. C, after control solution exposure. 110
Figure 4.8. SEM images of Celtra Duo with x10.000 original magnification. A, before solution exposure. B, after blumic solution exposure. C, after control solution exposure. 111

Figure 4.9. SEM images of Ceramill Zolid with x10.000 original magnification. A, before solution exposure. B, after blumic solution exposure. C, after control solution exposure. 112

Figure 4.10. Color change evaluations on different materials and solutions 126

Figure 4.11. Translucency change evaluations on different materials and solutions 134

LIST OF SYMBOLS AND ABBREVIATIONS

ΔE_{00}	Color change based on CIE2000 color system
ΔE_{ab}	Color change based on CIELab* color system
^{o}	Degrees
^{o}C	Degrees celcius
µm	Micrometer, micron
%	Percent
3D	Three dimensional
3Y-TZP	Tetragonal zirconia polycrystals stabilized with %3 mol yttria
4Y-PSZ	Partially stabilized zirconia stabilized with %4 mol yttria
5Y-PSZ	Partially stabilized zirconia stabilized with %5 mol yttria
6Y-PSZ	Partially stabilized zirconia stabilized with %6 mol yttria
AFM	Atomic force microscope
Al_2O_3	Aluminum oxide
AN	Anorexia nervosa
ANOVA	Analysis of variance
Ar/Kr	Argon/Krypton
ATZ	Alumina toughened zirconia
B_2O_3	Boron trioxide
BN	Blumia Nervosa
$Ca_5(PO_4)_3F$	Fluoroapatite crystal
CAD-CAM	Computer aided design and Computer aided manufacturing
CaO	Calcium oxide
CeO_2	Cerium oxide
CIE	Confocal laser scanning microscope
CLSM	Chevron Notch Beam
CNB	Commission International de l'Eclairage
CR	Contrast ratio
EDTA	Ethylene diamine tetra acetic acid
FSZ	Fully stabilized zirconia
GERD	Gastro esophageal reflux disease
GPa	Gigapascal
He/Ar	Helium/Argon

HF	Hydrofluoric acid
HT	High translucent
HP	High polishing
K_2O	Potassium oxide
K_2O-Al_2O_3-6 SiO_2	Potassium aluminum silicate, potash feldspar
kg.f	Kilogram force
K_{Ic}	Fracture toughness
LTD	Low temperature degradation
mm	Millimeter
mm^2	Millimeter square, definition of area
MgO	Magnesium oxide
MgO-PSZ	Partially stabilized zirconia stabilized with magnesium oxide
MPa	Megapascal
MPa.m1/2	Fracture toughness unit
n	Population of samples
N	Newton
Na_2O	Sodium oxide
Na_2O-Al_2O_3-6 SiO_2	Soda aluminum silicate, soda feldspar
nm	Nanometer
OH^-	Hydroxide ion
p	Statistical significance sign
PC	Polychromatic
PICN	Polymer infiltrated ceramic network
PSZ	Partially stabilized zirconia
Ra	2D surface roughness parameter, arithmetic mean of the surface
rpm	Rotation per minute
RTP	Relative translucency parameter
Sa	3D surface roughness parameter, arithmetic mean of the surface
SCF	Surface Crack in Flexure
SD	Standard deviation
SE	Standard error
SEM	Scanning electron microscope
SEPB	Single Edge Pre-Cracked
SEVBN	Single Edge 'V' Notched Beam

SiO_2	Silicon dioxide, silica
TEGDMA	Triethylene glycol dimethacrylate
TP	Translucency parameter
TZP	Tetragonal zirconia polycrystals
UDMA	Urethane dimethacrylate
UV	Ultraviolet
VIF	Vickers indentation fracture
VHN	Vickers hardness number
$\bar{x}$	Arithmetical mean
Y_2O_3	Yttrium oxide, yttria
ZrO_2	Zirconium dioxide
ZTA	Zirconia toughened alumina

ABSTRACT

Özen, E. (2021). Evaluation of Mechanical and Optical Properties of Different CAD-CAM Materials After Gastric Acid Exposure. Yeditepe University, Institute of Health Sciences, Department of Prosthetic Dentistry, PhD Thesis, İstanbul.

The aim was observation of changes in optical and mechanical characteristics of CAD-CAM restorative materials under the well-established blumia nervosa (BN) and control conditions. Three different CAD-CAM materials chosen as A1 shade and high translucent (HT) [IPS e.max CAD (E), Celtra Duo CAD (C), Ceramill Zolid HT+ PS (Z)]. All samples (N=120) with 1.5 mm were polished with 3 step Optra Fine Intra Oral Polishing Kit. Samples were distributed into 6 subgroups (n=18), 2 samples from each group were chosen for topography evaluations. The exposure time was 486.5 hours to simulate patients who have BN for five years. Blumic subgroups were stored in BN solution with 1.6 pH and control subgroups were stored in artificial saliva with 7 pH. Measurements were done for parameters as color and translucency change (ΔE, ΔTP) by spectrophotometer, surface roughness change (ΔRa) by contact profilometer, surface microhardness and fracture toughness change (ΔVHN, ΔK_{Ic}) by Vickers hardness device, and surface topography by scanning electron microscope and 3D optical profilometer. As a result, the ΔRa value of Z samples exposed to blumic solution was significantly higher than those exposed to control solution (p=0.004). Control solution significantly increased the VHN of E samples more than blumic solution (p=0.000). Blumic solution significantly decreased the VHN of C samples (p=0.000) and K_{Ic} of E and Z samples more than control solution (p=0.000, p=0.000). The ΔE after the blumic solution exposures were significantly higher than the control solution exposures among three materials (p=0.000, p=0.000, p=0.000). Blumic solution significantly decreased the TP of E and Z samples more than control solution (p=0.000, p=0.000), while control solution changed the TP value on C samples more than blumic solution (p=0.000). In non-blumic patients, Ceramill Zolid HT+ PS was found as the most stable material choice, and then IPS e.max CAD follows as the second stable material. In blumic patients, all materials' mechanical properties were found sufficient, but color stabilities of IPS e.max CAD and Celtra Duo CAD were superior to Ceramill Zolid HT+ PS. In blumic patients, high color change of polished Ceramill Zolid HT+ PS restricted its use at anterior region.

Key Words: Blumia nervosa, Gastric acid, Artificial saliva, CAD-CAM materials

"The PhD education and the PhD thesis study were supported by TUBITAK 2211-A National PhD Scholarship Program."

ÖZET

Özen, E. (2021). Farklı CAD-CAM Materyallerinin Gastrik Aside Maruz Bırakılmasının Ardından Mekanik ve Optik Özelliklerinin Değerlendirilmesi. Yeditepe Üniversitesi, Sağlık Bilimleri Enstitüsü, Protetik Diş Tedavisi Anabilim Dalı, Doktora Tezi, İstanbul.

Çalışmanın amacı, farklı bakış açısıyla kurgulanmış blumia nervoza (BN) ve kontrol koşulları altında üç farklı CAD-CAM materyalinin optik ve mekanik özelliklerindeki değişikliklerin gözlemlenmesidir. A1 renk ve yüksek ışık geçirgenliğine (HT) sahip olarak seçilen örnekler (N=120) [IPS e.max CAD (E), Celtra Duo CAD (C), Ceramill Zolid HT+ PS (Z)] 1,5 mm kalınlığa kadar zımparalanmıştır ve 3 basamaklı Optra Fine ağız içi cilalama kiti ile cilalanmıştır. Örnekler 6 alt gruba ayrılmıştır (n=18), topografi değerlendirmeleri için her alt gruptan 2 örnek seçilmiştir. BN hastalarının beş yıllık gastrik aside maruz kalma süresi 486.5 saat olarak hesaplanmıştır. Blumik alt gruplar BN solüsyonunda (pH=1.6), kontrol alt grupları ise yapay tükürükte (pH=7) bekletilmiştir. Renk ve translusensi değişimi (ΔE, ΔTP) spektrofotometre ile, yüzey pürüzlülüğü değişimi (ΔRa) kontakt profilometre ile, yüzey mikro sertliği ve kırılma tokluğu değişimleri (ΔVHN, ΔK_{Ic}) Vickers sertlik ölçme cihazı ile, ve yüzey topografisindeki değişiklikler taramalı elektron mikroskobu (SEM) ve 3 Boyutlu Optik Profilometre ile incelenmiştir. Z örneklerinin blumik alt grubunun ΔRa değeri kontrol alt grubundan anlamlı derecede daha yüksek bulunmuştur (p=0.004). Kontrol solüsyonu E örneklerinin VHN değerini blumik solüsyona göre anlamlı derecede daha fazla artırmıştır (p=0.000). Blumik solüsyon C örneklerinin VHN değerini ve E ve Z örneklerinin K_{Ic} değerlerini kontrol solüsyonuna göre anlamlı derecede daha fazla azaltmıştır (p=0.000, p=0.000, p=0.000). Üç materyalin blumik alt gruplarının ΔE değerleri kontrol alt gruplarına göre anlamlı derecede daha yüksek bulunmuştur (p=0.000, p=0.000, p=0.000). Blumik solüsyon, E ve Z örneklerinin TP değerini kontrol solüsyonuna göre anlamlı derecede daha çok düşürürken (p=0.000, p=0.000), kontrol solüsyonu C örneklerinin TP değerini blumik solüsyona göre anlamlı derecede daha fazla değiştirmiştir (p=0.000). Blumik olmayan hastalarda en stabil materyal seçiminin Ceramill Zolid HT+ PS olduğu ve bunu IPS e.max CAD'in takip ettiği görülmüştür. BN simülasyonunda üç materyalin de mekanik özellikleri yeterli bulunmuştur fakat IPS e.max CAD ve Celtra Duo CAD'in renk stabiliteleri Ceramill Zolid HT+ PS'ye göre daha üstün bulunmuştur. Blumik hastalarda Ceramill Zolid HT+ PS'nin yüksek renk değişikliği göstermesi ön bölgede kullanımını kısıtlamıştır.

Anahtar Kelimeler: Blumia nervoza, Gastrik asit, Yapay tükürük, CAD-CAM materyalleri.

"Doktora eğitimim ve doktora tezim TÜBİTAK 2211-A Genel Yurtiçi Doktora Burs Programı tarafından desteklenmiştir."

1. INTRODUCTION AND PURPOSE

In recent years, materials fabricated by computer-aided design and computer-aided manufacturing (CAD-CAM) were introduced. This technique enables the fabrication of esthetic monolithic restorations in a single patient visit.[1] Lithium disilicate glass ceramics, zirconia-reinforced lithium silicate ceramics and monolithic zirconia are among these materials. After entering the market, many researches have been conducted on comparison of the durabilities under the challenges such as thermocycling and mechanical aging.[2–6] However, studies evaluating the effect of acidic chemicals which may affect the durability of materials were less in number.[7–9]

Chemical environment of oral cavity may affect the longevity of restorations by impairing their mechanical and optical characteristics.[10] Little is known about how their surface behaves in the presence of intrinsic acidic (gastric acid) substances.[7] Gastric acid can reach the oral cavity and cause chemical attacks leading degradation of restorative dental ceramics as much as dental hard tissues as a result of bulimia nervosa (BN), gastroesophageal reflux disease (GERD) or prolonged severe nausea during pregnancy.[11]

BN is a multifactorial disorder characterized by recurrent binge eating cycles followed by compensatory behaviors such as self-induced vomiting, misuse of purgative medicines, fasting or over-exercising.[9,12,13] Gastric juice directly contacts with dental hard and soft tissues by self-induced vomiting. The gastric juice produced a more severe degradation of dental structures than dietary acids.[8] Low pH of gastric acid ($pH<2$) induces destruction of dental hard tissues which may lead to the decrease of vertical dimension of occlusion, teeth sensitivity and consequently a need for restorations.[14]

Adequate salivary flow and buffering efficiency provide protection against acid attacks in healthy patients. However, there may be restricted period for protective action of saliva before erosion occurs in blumia nervosa patients because gastric juice directly contacts with dental hard tissues and pH remains low for a while. Thereby, the buffering effect of saliva on neutralizing the acidic pH may not completely prevent erosion resulting from BN.[15]

Restoring destructed tooth structure after erosion can be challenging, because the predisposing factor may still be present in the environment. Only few studies[7–9,16–20] have evaluated the change in characteristics of different materials exposed to acidic environment simulating erosive challenges. As a result of these studies[7–9,16–20], it was found that leached ion concentrations may significantly change among different material types, on different solution pH's and different exposure time. Dental ceramics were found susceptible to remarkable degradation against low pH solutions.[21]

Chemical deterioration of dental ceramics may resulted in surface roughness increase, which may lead to abrasion of the opposing dentition or restoration, increase in plaque retention and possible release of detrimental elements from ceramics.[22] Roughness increase may lead to stress accumulation on restoration and initiate crack formation followed by crack propagation. In addition to alterations in mechanical properties, color and translucency of the restoration may also be influenced after acidic challenge due to change in surface texture.

Dentists treat blumic patients more often while blumia nervosa prevalence increases[12,13,23]. However, in vitro simulation of blumia nervosa is not well established in the literature.[16,18] Observing the changes in the optical and mechanical characteristics of CAD-CAM restorative materials under the well-established acidic conditions was considered necessary. The appropriate material that will be chosen in rehabilitation of erosion patients and the effect of intrinsic erosive situations on ceramic restorations will be determined to find out with this research.

The aim of the current study is evaluating the mechanical properties such as surface roughness, surface microhardness, fracture toughness and surface topography and optical properties such as color and translucency of three different polished CAD-CAM restorative materials (lithium disilicate glass ceramic, zirconia reinforced lithium silicate ceramic and monolithic zirconia) under blumic condition compared to control condition which was chosen as immersion in artificial saliva.

First null hypothesis is that 'there are no statistically significant changes in terms of mechanical (Ra, VHN, K_{Ic}) and optical (L*, a*, b*, TP) properties of different CAD-CAM materials after exposure to acidic blumia nervosa solution and artificial saliva solution'. Second null hypothesis is that 'solutions with different pH similarly affect the mechanical (ΔRa, ΔVHN, ΔK_{Ic}) and optical (ΔE_{ab}, ΔTP) properties' changes of a CAD-CAM material'. Third null hypothesis is that 'blumic solution affects the selected three CAD-CAM materials similarly on mechanical (ΔRa, ΔVHN, ΔK_{Ic}) and optical (ΔE_{ab}, ΔTP) properties' changes'. Fourth null hypothesis is that 'control solution affects the selected three CAD-CAM materials similarly on mechanical (ΔRa, ΔVHN, ΔK_{Ic}) and optical (ΔE_{ab}, ΔTP) properties' changes'.

2. GENERAL INFORMATIONS

2.1. Dental Ceramics

In dentistry, generally four classes of materials are used for rehabilitation of tooth loss and dental tissue loss which are ceramics, metals, polymers and composites. Properties of high translucency, good light transmission and ideal biocompatibility contribute choosing the dental ceramic for highly-demanded esthetic restorations. Besides optimal optical and biological characteristics, sufficient mechanical properties as high Vickers hardness, high fracture toughness, wear resistance, high flexural strength and low abrasiveness have been important reasons for being common choice.[24]

General structure of dental ceramic is consisted of metallic and non-metallic elements such as silicates, oxides, nitrides or carbides stabilized with atomic bonds including both covalent and ionic character. Most of dental ceramics are based on silica which has high affinity to bind to oxygen. However, there is different class of dental ceramics known as polycrystalline ceramics which have no silica ingredient.[25]

Composition of typical dental ceramic is mainly %70-90 feldspar minerals, %11-18 quartz (silica) particles and %5-10 kaolin fillers. Additionally, glass modifiers, coloring pigments and oxide particles providing opacity are added to the main composition.[26]

Feldspar is a mineral naturally found in nature as potassium aluminum silicate (K_2O-Al_2O_3-6 SiO_2) (also called as potash feldspar) and soda aluminum silicate (Na_2O-Al_2O_3-6 SiO_2) (also called as soda feldspar). Current dental ceramics contain potash feldspar mostly due to providing translucency to the fired restoration when it fuses with kaolin and quartz. As a result of this fusion, feldspar turns into a translucent glassy matrix which helps maintaining the form with quartz as a skeleton for other materials to fuse.[25,27] Quartz contributes as a framework when fused with feldspar and remains the same form during high temperature firing and prevents shrinkage. It brings translucency, however it is not strong enough to prevent mechanical failure, so some particles like alumina is added for reinforcement.[25,27] Kaolin is clay like filler that holds other particles together at the unfired stage. Due to the opacity of kaolin, its composition is very limited in the dental ceramics.[25] Glass modifiers decrease the viscosity, while the color pigments give the specific shade to dental ceramic.[25] For instance, indium contributes to yellowness and chromium gives pink shade. Iron oxide makes the ceramic blacker in shade and darker while salts of cobalt add blueness to the ceramic.[28]

2.1.1. Properties of Dental Ceramics

In dentistry, ceramics are commonly used due to high esthetics and biocompatibility. Even though metal-ceramic restorations may be chosen as a treatment option on rehabilitation of missing or defective teeth, using opaque metal core may limit the use of them in esthetic areas due to the unwanted color formations below the ceramic. Another disadvantage of metal-ceramic restorations is that they may lead to metal allergy in some patients. These deficits of metal substructure have led to the fabrication of all-ceramic systems. All-ceramics do not contain any metal and dark-colored core. Thereby they can be used at the esthetic regions with their high translucent feature.[29]

Besides being chemically inert in the mouth, dental ceramics are very biocompatible with the dental soft tissues. Especially all-ceramic monolithic systems possess excellent esthetics owing to favorable light transmission and desired color achievements.[30] Dental ceramics successfully resist against the compressive stresses; whereas they are very fragile against tensile and shear stresses. That situation brings the brittle characteristic of ceramic, making it in danger under tensile forces.[31] Dental ceramics isolate thermal stimulants very well, and their thermal expansion coefficient is very similar with tooth. Additionally due to the high surface hardness, dental ceramics may abrade the opposing dentition or restoration.[32]

Defects may be caused due to fabrication technique faults and due to high or inappropriately designed occlusal forces.[32] Cracks on ceramics may start as sub-millimetric micro-cracks from the occlusal contact point, from the cementation surface underneath the occlusal contact point, from the cementation margins of crowns and from connectors of bridge restorations.[33] Structural defects and cracks may be resulted in the failure in dental ceramic restorations.

Durability and long-lasting use of dental ceramic restorations were determined by strength against fatigue. Fatigue may be explained by crack growth in the presence of moist and oral fluids, and cyclic application of occlusal forces.[34] When water molecules infiltrate through the sub-millimetric cracks, it goes forward by breaking the chemical bonds that holds the crack walls as a whole unit. This results in the slow propagation of crack which is accelerated at higher occlusal loads and finally results in failure.[33]

Durability of dental ceramic restorations was also determined by the proper adhesion with resin cements to the tooth. Proper adhesion depends on the use of the luting agent and cementation technique.[35] Increasing the adhesion and retention can be provided by etching the intaglio surface of ceramic in order to elevate the width of adhesion surface mechanically or by altering the ceramic intaglio surface affinity to the adhesive resins chemical by silanation process.[36] In order to enhance the bond strength of adhesives to dental ceramics, mechanical and chemical conditioning methods are used in combination without damaging the ceramic by over-etching or over-roughening.[37]

2.1.2. Classification of Dental Ceramics

There have been many classifications for dental ceramics according to composition, processing technique, fusion temperature, microstructure, translucency, fracture resistance and abrasiveness.[27,38–41]

Ho et al.[27] classified ceramics by restoration type as follows: all-ceramics and metal-ceramic systems. Helvey[38] made a classification based on processing method as powder-liquid building, slip casting, hot ceramic pressing and additive or subtractive CAD-CAM. Kelly and Benetti[39] classified dental ceramics according to their glass content as predominantly glass ceramics, particle filled glass ceramics and polycrystalline ceramics. Datla et al.[40] made a classification according to the processing techniques as sintered ceramic, castable glass ceramics, slip cast ceramics, hot-pressed-injection-molded ceramics and machinable ceramics.

In current study, latest classification according to the phases in ceramic’s chemical composition made by Gracis et al.[41] will be detailed as follows:

- Glass-matrix ceramics,
- Polycrystalline ceramics,
- Resin-matrix ceramics.

2.1.2.1. Glass-Matrix Ceramic Family

Gracis et al.[41] sub-classified this family into three as; naturally occurred feldspathic ceramics, synthetic ceramics and glass-infiltrated ceramics.

2.1.2.1.A. Feldspathic Ceramics

They are primarily composed of clay/kaolin, quartz (silica) and naturally occurred feldspar (mixture of potash feldspar and soda feldspar). Potash feldspar turns into the leucite crystals after firing process, hence both elevates the internal strength of the ceramic and makes it translucent. This type of glassy matrix ceramic may be used as veneering ceramic on metal or ceramic substructures, or as monolithic restoration directly bonded to dental hard tissues.[41]

Feldspathic ceramic is resistant to compressive forces but not to shear forces because of the low tensile strength, eventually fractures may occur. They are known with advanced esthetics presenting high translucency, optimal transmission of light, natural tooth like appearance and great biocompatibility.[24]

Some examples are Vita VM9, Vita VMK Master, Vitablocs Mark II, TriLuxe, TriLuxe forte and Vitablocs RealLife (VITA Zahnfabrik, Bad Säckingen, Germany).[25] Those types of ceramics may be fabricated with refractory die method, platinum foil processing technique, by pressing method and with CAD-CAM methods. They may be used as veneering ceramics or monolithic restorations.[41] After the etching process with hydrofluoric acid (HF), many pores, channels and degenerated ceramic particles was observed on Vita Mark II material.[42]

2.1.2.1.B. Synthetic Ceramics

In case of lacking the raw minerals found in nature, synthetic particles for ceramics were produced in the laboratory. Producers added more crystals in order to strengthen the material, to decrease the crack formation risk and even the crack has formed, propagation would be diminished. Mechanical properties of the subgroup were superior to naturally occurred feldspathic ceramic. Crystals like leucite or lithium disilicate was dispersed in a translucent glassy matrix. These crystals were artificially produced from a core with process called controlled nucleation and crystallization. Therefore producers may fabricate the crystals as desired size, number and geometry, and the desired homogenity as well.[25]

Mainly four subgroups are organized in synthetic ceramic glass-matrix ceramics;

- leucite-reinforced ceramic,
- lithium disilicate ceramic,
- zirconia-reinforced lithium silicate and
- fluoroapatite-glass ceramics.[25]

- **Leucite-reinforced Ceramics**

In a glassy matrix, leucite crystals, measured as only few microns, were embedded and dispersed regularly and grown from the feldspar particles by controlled firing and slow crystallization which is called surface crystallization. [24] Leucite particles grow from the boundaries to the center of grain. This crystalline content improves the mechanical properties compared with feldspathic ceramic, and high silica content contributes to the optimum translucency, opalescence and optical properties.[25]

Some examples may be given as GC Initial LRF Block (GC Corp., Tokyo, Japan), IPS Empress and IPS Empress CAD (Ivoclar Vivadent, Schaan, Liechtenstein), Paradigm C (3M ESPE, Seefeld, Germany).[25] When etched with HF, honeycomb like pattern occurs on IPS Empress CAD.[42]

While monolithic products may be the first option, increased crystal content enables to make frameworks for single restorations. These types of restorations are fabricated by pressing from ingots or CAD-CAM methods.[41] When the pressing method was selected, wax analog of desired restoration was invested and burned out. Then the IPS Empress ingots were pressed at high temperature into the investment. The process is called ‘hot-pressing’.[24]

Leucite-reinforced ceramics have low flexural strength values approximately 100-120 MPa.[43] Hence, their use on anterior region where esthetics is predominated as single crown or laminate veneer is suitable. As a perceptible evidence for indication, survival rate was found %98.9 for single anterior crowns and diminished survival rate for posterior single crowns was presented as %84.4 in an 11 years clinical study.[44] In a meta-analysis, survival rate was found %92.4 for laminate veneers after 5 years of clinical use.[45]

- **Lithium disilicate Ceramics**

In 1990's, lithium disilicate ceramic was introduced with the name of 'IPS Empress 2' (Ivoclar Vivadent, Schaan, Liechtenstein). It consists of %65 lithium disilicate particles dispersed into glass matrix. These particles are small needle-shaped crystals (3–6 μm in length and 0.8 μm in width). Flexural strength of the material was 350 MPa.[46] At first, only the core of a restoration was fabricated with IPS Empress 2 by hot-pressed ingots, then the cores were veneered with fluoroapatite feldspathic ceramic.[47] In 2005, Ivoclar Vivadent was introduced a new lithium disilicate glass ceramic formula into the market known as IPS e.max Press. This material exerted better optical and mechanical properties as 370 to 460 MPa increased flexural strength, with smaller and more regularly dispersed crystals.[47] While the older version, IPS Empress II was used only for core productions, IPS e.max Press was used for both core and monolithic restoration production owing to increased strength.[47]

Due to enlarging CAD-CAM industry, lithium disilicate ceramics were fabricated as CAD-CAM blocks, mostly known is IPS e.max CAD. High volume of lithium orthosilicate crystals are dispersed into the translucent glass matrix before slow firing. With partial crystallization, %40 of crystals turns into lithium metasilicate and the state called 'intermediate crystalline phase' or 'blue state'.[25] Thus, the pre-crystallized IPS e.max CAD block has blue-purplish color. In addition to lithium metasilicate crystals, it contains lithium disilicate nuclei crystals. In that blue state, material has approximately 130 MPa flexural strength and gives opportunity for easier milling via CAD-CAM milling devices.[47] After final crystallization, randomly-oriented long-thin lithium disilicate crystals are formed in the glass matrix and strength of the material is the highest at this form.[25] Different colors are available through different coloring ions, while different translucency is gathered by different sizes and distributions of particles.[47]

Some current examples for this type of ceramic are IPS e.max press, IPS e.max CAD (Ivoclar Vivadent, Schaan, Liechtenstein), VITA Ambria (VITA Zahnfabrik, Bad Säckingen, Germany), GC Initial LiSi Press (GC Corp. Tokyo, Japan). These restorative materials are milled with CAD-CAM systems or pressed and used as framework or monolithic restoration on natural tooth or implant as single unit anterior or posterior crown or up to three unit bridges (extended utmost to second premolar), besides being used as laminate veneer or posterior inlay, onlay, overlay.[25,41,47] When etched with HF, glassy matrix dissolves and shallow irregularities of lithium disilicate crystals become visible under scanning electron microscopy imaging.[42]

- **Zirconia-reinforced Lithium Silicate Ceramics**

Alternative searches in CAD-CAM market led to new materials with enhanced translucency. Zirconia reinforced lithium silicate is one of them and obtained by strengthening a homogenous lithium disilicate particles containing glass matrix with tetragonal zirconia filler %10 by weight. Thus, elevated flexural strength (approximately 445 MPa, higher than other glass ceramics) and increased translucency were gained compared to feldspathic ceramics and lithium disilicate glass ceramics.[48] Additionally, enhanced polishability is an advantage especially after the intraoral occlusal adjustments. Such properties allow the material to be used as inlay, onlay, overlay, table top restoration with no preparation, partial crown and laminate veneer, anterior or posterior single crown on natural tooth or an implant.[47,48]

Zirconia reinforced lithium silicate material is produced in three stages. Firstly, lithium orthosilicate particles were present and thermal pretreatment called as nucleation/precrystallization applied to form lithium metasilicate crystals. In the second stage, only lithium metasilicate crystals were found dispersed in glassy matrix. That state comes with easier machinability on milling devices. At last stage, short heat treatment applied and final crystallization occurs as same with lithium disilicate glass ceramics. Final crystallized state has final desired color and improved mechanical and optical properties; containing more lithium metasilicate than lithium disilicate. Zirconia particles act as nucleating agent during the second and third stages. They are dispersed in the glassy matrix and bring enhanced flexural strength in fully crystallized state.[25]

Despite being thought that zirconia particles bring more opacity to material, zirconia reinforced lithium silicate materials have enhanced esthetic, translucency, opalescence and chameleon effect similar to natural tooth. When etched with HF, glassy matrix dissolves revealing densely aligned lithium silicate crystals like lithium disilicate ceramics.[25,42] These crystals are composed by the fusion of zirconia particles with lithium metasilicates, forming fine grained microstructure (Li_2O-ZrO_2-SiO_2).[49]

Two brands produced zirconia reinforced lithium silicate materials; Celtra Press and Celtra Duo CAD (Dentsply Sirona, York, Pennsylvania) and Vita Suprinity PC (Vita Zahnfabrik, Bad Säckingen, Germany). Vita Suprinity is served as partially crystallized, whereas Celtra Duo is ready to be used after milling. Although additional heat treatment is not necessary for crystallization of Celtra Duo, firing process has been reported to enhance the flexural strength greater than the as-milled material.[50] Lithium metasilicate crystals were smaller on Vita Suprinity than Celtra Duo, this might be due to different crystallization processes; additional firing time of Vita Suprinity is shorter than Celtra Duo CAD.[51]

When compared with lithium disilicate ceramics having needle shaped crystals, zirconia reinforced lithium silicate has finer crystalline structure with rod like rounded tip. Lithium disilicate has higher crystalline content.[48,51] According to a recent literature review, Zarone et al.[51] stated that; although zirconia reinforced lithium silicate has tetragonal zirconia, there is no exact evidence that it has more mechanical strength than lithium silicate ceramics. When fracture toughness and Vickers hardness were evaluated, fully crystallized zirconia reinforced lithium silicate material exhibited higher values compared to pressed and milled lithium disilicate materials.[52–54] In addition, it has way too higher values compared to dental enamel.[55]

- **Fluoroapatite Glass Ceramics**

In the glass matrix, there are fluoroapatite crystals [$Ca_5(PO_4)_3F$] in different sizes. These crystals are responsible for coherence on thermal expansion with metals, for improved strength and for opalescence of restoration.[25,41] IPS e.max Ceram and IPS e.max ZirPress (Ivoclar Vivadent, Schaan, Liechtenstein) are examples of that type of glass ceramic.

IPS e.max Ceram is powder formed material and used as a veneering ceramic on glass or oxide ceramics substructures or as veneer. IPS e.max ZirPress is in the form of pressable ingots and used as veneering ceramic on zirconia substructures using press-on-zirconia technique or as veneer. Both materials cannot be used as a core or in substructure form due to low flexural strength than any other glass ceramic material, approximately 90-110 MPa.[25]

In 2015, further research has concluded with the production of a new experimental glass ceramic called fluorophlogopite glass ceramic.[56] Differently from other glass ceramics, it releases fluoride ions to the oral environment as a contribution to biocompatibility. Flexural strength is 120 MPa, similar to leucite reinforced glass ceramic, lower than lithium disilicate and zirconia reinforced lithium silicate glass ceramics, whereas Vickers hardness was found lower than feldspathic ceramics, lithium disilicate and resin matrix ceramics.

2.1.2.1.C. Glass-infiltrated Ceramics

There are two interpenetrated glass ceramic phases in one material. It can be fabricated by two techniques; slip-cast method or CAD-CAM production method. In slip-casting method, slurry densely packaged ceramic particles applied onto a refractory die and then sintered. In CAD-CAM production method, ceramic powder which has been densely packaged dry-pressed into the CAD-CAM block formed mold. Then, blocks were milled. In the end of two methods, porous skeleton core material was prepared. This opaque core material then has been infiltrated with lanthanum glass by second firing process. After all, the strength of restoration has been increased. Different core composition indicates the mechanical and optical properties of final restoration.[25,57]

There are three types of glass-infiltrated ceramics; Vita In-Ceram Spinell, Vita In-Ceram Alumina, Vita In-Ceram Zirconia (VITA Zahnfabrik, Bad Säckingen, Germany). In 1994, In-Ceram Spinell core has magnesia and alumina particles, contributing high translucency and low strength (flexural strength approximately 400 MPa). Thus this material is indicated for anterior single crowns. In 1989, In-Ceram Alumina has %80 alumina particle content, coming with optimal translucency and approximately 500 MPa flexural strength. It is indicated for both anterior or posterior single unit restorations, and anterior 3-unit bridges. In-Ceram Zirconia has alumina particles strengthened with zirconia, having highest flexural strength (approximately 600 MPa) among glass-infiltrated ceramics. It may be used in single posterior restorations and 3–unit bridges on any location.[25]

HF does not roughen the intaglio surface of restoration.[58] Currently this class of material is not used due to complex fabrication methods and developed superior properties of lithium disilicate and zirconia materials.[25]

2.1.2.2. Polycrystalline Ceramic Family

Subgroups of this family possess fine grained crystal particles containing no glassy phase. Thus, these materials are not capable of being etched by HF and translucency is low.[59] Crystal particles contribute to high strength and high fracture toughness due to preventive mechanism on crack propagation.[57] These crystals particles are mainly alumina and zirconia.

2.1.2.2.A. Alumina

Alumina material has %99.5 aluminum oxide (Al_2O_3) which has emerged naturally and used as a core material in 1950's fabricated by milling. In order to process easily, blocks milled in bigger dimensions as partially sintered, then sintered and shrinkage occurs. Grinding after sintering does not initiate phase transformation. Some examples for this material are Procera® AllCeram (Nobel Biocare, Kloten, Switzerland), the first completely compact polycrystalline ceramic, and In-Ceram® AL (VITA Zahnfabrik, Bad Säckingen, Germany).[25,41]

Alumina has high hardness and highest elastic modulus (300 GPa), thus originates bulk fractures.[60] Core fractures were the disadvantage of this material. Thereby the use of alumina was diminished due to both weak fracture resistance and newly developed improved materials having mechanism such as transformation toughening.[41]

2.1.2.2.B. Stabilized Zirconia

Zirconia name comes from ancient times, two Persian words; 'Zar' meant 'Gold' and 'Gun' meant 'Color'. Origin of the zirconia is a gemstone named zircon from ancient history. In 1789, Martin Heinrich Klaproth who was a chemist, had heated up some zircon gems and named the obtained product as a metal oxide, zirconium dioxide (ZrO_2) and then mixed with other earth oxides and used as pigment for ceramics.[61] In 1969, Helmer and Driskell[62] mentioned the biomedical use of zirconia as surgical implants. In 1988, Christel et al.[63] published an article about use of zirconia in the hip replacement as a prosthetic head. Zirconia was presented to the dental field as a CAD-CAM material in 1998.[64] It is biocompatible, not cytotoxic, has ideal radio-opacity,[65] low corrosion[66] and provides less bacterial adhesion than titanium.[67]

Pure zirconia is in polymorph structure and has three allotropes at three temperature intervals:

- At room temperature to 1170^{o}C, material is in monoclinic (m) phase,
- From 1170^{o}C to 2370^{o}C, zirconia is in tetragonal (t) phase,
- From 2370^{o}C which is the melting point, to 2370^{o}C, it is in cubic (c) phase.[61]

After sintering process during cooling down, particles transform from metastable tetragonal (t) phase into more stable monoclinic (m) phase spontaneously. A recognizable volume rise takes place during this transformation and crystals grows %4-5 by size, thus creating great compressive stresses inside the material. In order to prevent this stress-creating situation so called 'phase transformation', researchers added some cubic-phased oxides such as MgO, CaO, Y_2O_3 and CeO_2 to stabilize the tetragonal phase in room temperature.[24,61]

Classification for stabilized zirconia material used in dentistry according to the microstructure has been made as;

- Tetragonal zirconia polycrystals (TZP),
- Partially stabilized zirconia (PSZ),
- Fully stabilized zirconia (FSZ).[68]

- **Tetragonal zirconia polycrystals (TZP)**

Tetragonal zirconia polycrystals (TZP) are monolithic materials composed of only tetragonal (t) phase, mostly stabilized by %3 yttria (Y_2O_3) or ceria content[68], so called monophasic.[24,66]

At first, conventional tetragonal zirconia polycrystals (TZP) has been stabilized with %3 mol of yttria and with %0.25 weight of alumina (3Y-HA) and 3Y-HA TZP was gathered as first generation dental zirconia. It was aimed to be used as a ceramic substructure instead of metal. 3Y-HA did not have enough translucency, so zirconia core was veneered with feldspathic ceramic. However, the strength of the veneering ceramic was too low to stand against the occlusal forces in the posterior area.[64] As a result many ceramic chipping failures were reported.[69,70]

When researches were continuing on making zirconia more translucent, high translucent zirconia was introduced in 2011, in which the tetragonal zirconia polycrystals (TZP) were stabilized with %3 mol of yttria in addition with less than %0.05 weight of alumina (Figure 2.1.). This material was called yttria-stabilized tetragonal zirconia polycrystals referred as 3Y-TZP (second generation dental zirconia). Due to its increased translucency, this material has not needed to be veneered with feldspathic ceramic, and it is indicated as a monolithic zirconia crown. The risk of ceramic chipping failure was decreased very well. Additionally, tooth preparation was reduced owing to the removal of ceramic veneer layer.[64]

3Y-HA TZP has increased density and decreased porosity, while having the highest strength - in preventing crack formation and highest fracture toughness - in providing damage control after crack formation, after milling and sintering.[41,66,71,72] It has been the mostly used type of zirconia for dental restorations and applications; such as fixed prosthesis for indirect prosthodontics[73], orthodontic brackets[74] and endodontic posts[75].

Second generation 3Y-TZP ceramics were more translucent owing to the decrease of alumina crystals content which has light scattering effect[72,76,77] and had higher strength and stability after aging processes.[76]

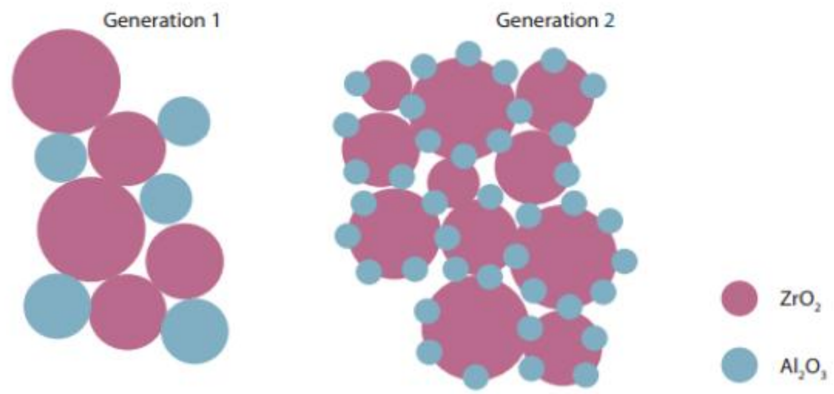

Figure 2.1. First generation of zirconia (3Y-HA TZP) having larger alumina content, while second generation of zirconia having smaller alumina content (3Y-TZP).[76]

Tetragonal zirconia polycrystals having great birefringence effect[77] in general 3Y-TZP ceramics still allow limited light transmission when compared to glass ceramics.[78] Birefringent materials are optically anisotropic, light was scattered in different crystallographic directions when reflected through grain boundaries.[76,77]

- **Partially stabilized zirconia (PSZ)**

Partially stabilized zirconia (PSZ) is composed of tetragonal or monoclinic zirconia particles in nano sizes dispersed in a matrix of cubic zirconia particles,[25,41] thus creating a two-phased material.

Before the classification of generations on zirconia has been made, first partially stabilized zirconia was introduced as magnesium partially stabilized zirconia (Mg-PSZ).[79] Zirconia was stabilized with %8-10 mol MgO. Denzir-M® (Dentronic AB, Skellefteå, Sweden) is the only available Mg-PSZ product for CAD-CAM system.[25]

This material had low stability, great porosity and framework wear when occlusal forces had applied on a substructure.[61] Mg-PSZ could not reach great popularity and use due to weak mechanical characteristics especially when compared to 3Y-TZP.[66]

Recently, the need of more translucent zirconia materials among yttria stabilized zirconia after second generation 3Y-TZP has been emerged. PSZ containing %4-5 yttria content higher than 3Y-TZP, have been introduced in 2014, in order to increase light transmission by reducing the birefringence. As a result, third-generation dental zirconia has been emerged.[76,77,80]

At first, PSZ has been stabilized with %5 mol yttria and 5Y-PSZ material introduced in 2014. 5Y-PSZ is highly translucent due to higher light transmission through cubic crystals and thus it may be used as anterior monolithic crown. Whereas the optical properties were superior, mechanical properties were diminished that as half strength of 3Y-TZP.[64]

Secondly, PSZ was stabilized with %4 mol of yttria, resulting as 4Y-PSZ. It has mechanical properties better than 5Y-PSZ but weaker than 3Y-TZP, while having more translucency than 3Y-TZP but lower than 5Y-PSZ. Thus, an intermediate type of zirconia between 3Y-TZP and 5Y-PSZ was emerged.[64]

Recently, high translucent PSZ stabilized with %6 mol of yttria (6Y-PSZ) and pre-shaded half sintered discs were introduced in 2017.[64]

- **Fully stabilized zirconia (FSZ)**

In fully stabilized zirconia (FSZ), %8 mol yttrium oxide (Y_2O_3) is used to stabilize zirconia in its cubic form.[41] The importance of cubic form is that it is stable under stress and water conditions and does not transform into tetragonal or monoclinic phases.[81] PSZ composed of tetragonal and cubic forms, has %40 to %70 cubic phased zirconia particles.[81] Sometimes PSZ is called as fully stabilized zirconia or cubic zirconia when the proportion of cubic zirconia was closer to %70 and stabilized with >%6-8 mol yttria.[82,83] Also the FSZ is classified as third generation zirconia.[76]

When the tetragonal phase presents in material, the crack propagation is disturbed. Yet crack formation could not be prevented but fracture toughness and strength was increased.[24,61] When there is a mechanical or thermal stimulant ending up a crack tip, stress concentration may break the polycrystalline bonds and results in a phase transformation from tetragonal to monoclinic crystals. %4-5 volume increase caused by monoclinic crystals restricted to the crack surrounding particles follows that transformation and results in the compressive stresses. These compressive stresses are used in the favor of limiting the crack propagation.[79] This crack propagation limiting mechanism is called as ‘transformation toughening’ or ‘phase transformation toughening’.[24,84]

The main reason that third generation partially stabilized zirconia and fully stabilized zirconia materials have reduced mechanical properties is due to lower volume of tetragonal phase content when compared to second generation TZP materials.[76,85,86]

2.1.2.2.C. Zirconia Toughened Alumina & Alumina Toughened Zirconia

Zirconia toughened alumina (ZTA) was mentioned previously as ‘glass-infiltrated zirconia-toughened alumina’. It is also two-phased material.[24] Transformable tetragonal zirconia particles were scattered in an alumina matrix.[25] In Ceram Zirconia is an example for that type and zirconia was used in a dental ceramic for the first time in this material. It is used as a core material containing %67 weight of aluminum oxide and %33 weight of %12 mol cerium-partially stabilized zirconium oxide.[87] When there is a mechanical stimuli, crack tip generally propagates through the borders of aluminum oxide matrix surrounding the transformed crystals.[66] This material can be manufactured by two ways; soft milling or slip-casting. It has poor mechanical properties and higher porosity especially produced with slip-casting, when compared with 3Y-TZP.[66] However, due to cerium content, it has increased thermal stability and it is resistant to ‘low temperature degradation’ (LTD). Esthetic properties were not enough to be used as anterior crown.[24]

Alumina toughened zirconia (ATZ) was also two-phased and contains more than %50 by weight of zirconia particles.[41] It has also resistance to LTD compared to 3Y-TZP, high strength and fracture toughness than Y-TZP.[24,41]

2.1.2.3. Resin-Matrix Ceramics

Resin matrix ceramics are composed of an organic matrix and great amount of ceramic filler particles. The aim of producing that material is absorbing the high occlusal stresses owing to the same elastic modulus of hybrids with dentin tissue when compared with glass ceramics and polycrystalline ceramics. Hybrids are recommended for implant supported crowns in order to compensate the shock absorber properties which normally provided by periodontal ligament. They are wear resistant and do not cause antagonist wear as well.[88] Hybrids are easier to mill compared to glass ceramics and polycrystalline ceramics; furthermore the milling time is shorter. Milled hybrid restoration is not further required to be sintered or crystallized, finishing and polishing is made by surface polishing with specific polishing systems. Although the chipping risk was very minimal on hybrids, repair may be made intra-orally and easily with composite resins.[25,41]

Hybrid ceramics are classified according to their inorganic composition as;

- Resin nano ceramic
- Polymer infiltrated ceramic network (PICN)
- Flexible nano ceramic

2.1.2.3.A. Resin Nano Ceramic

Lava Ultimate (3M ESPE, Seefeld, Germany) is the main material known as resin nano ceramic. In a highly cross-linked polymer matrix, %80 by weight of nano ceramic particles were dispersed.[41] Nano ceramic particles are composed of silica nanomeric particles in 20 nm diameter and zirconia nanomeric particles in 4-11 nm diameter, and two nanomer types were coming together to synthesize nanomer clusters. Due to these ceramic particles, material has high polishability and good optical properties. When compared to composite resins, Lava Ultimate has increased flexural strength (200 MPa), fracture and wear resistance. Material is not brittle compared to ceramics and has shock absorber characteristics. It is not indicated for full-coverage restorations despite increased ceramic content, yet indicated for inlays, onlays and veneers.[25]

2.1.2.3.B. Polymer Infiltrated Ceramic Network (PICN)

VITA Enamic (Vita Zahnfabrik, Bad Säckingen, Germany) is the main material produced as PICN. It has dual network as; %86 by weight of feldspathic ceramic network and %14 by weight of polymer network. Ceramic network consists of SiO_2, Al_2O_3, Na_2O, K_2O, B_2O_3, ZrO_2, CaO; whereas polymer network consists urethane dimethacrylate (UDMA) and triethylene glycol dimethacrylate (TEGDMA).[41] Fabrication steps of blocks are as follows; ceramic powders are pressed and sintered into the block form in order to form porous ceramic network, then coupling agent is applied to prepare the ceramic matrix to emerge with polymer network via chemical bonds. Finally polymer monomers are infiltrated into the ceramic network. Additional final heat induced polymerization is made to finalize the polymer network construction.[25] Flexural strength is approximately 150-160 MPa, while the elastic modulus was 30.14 GPa, between the enamel and dentin.[89,90] Same wear characteristics with enamel were observed for Vita Enamic.[25,91]

2.1.2.3.C. Flexible Nano Ceramic

GC Cerasmart (GC Corp., Tokyo, Japan) is the major material that has been produced as flexible nano ceramic. It has small and neatly dispersed alumina-barium-silicate particles into the polymer matrix. Flexural strength was found higher than Lava Ultimate and Vita Enamic (approximately 240 MPa), while Vickers hardness number (VHN) value was found lower than the other two hybrids (approximately 64 VHN).[92]

Lava Ultimate hybrid ceramic is indicated only for veneers, inlays and onlays but not for crowns; whereas VITA Enamic and GC Cerasmart are indicated for same restorations as Lava Ultimate, additionally anterior or posterior tooth-supported and implant-supported crowns.[25]

2.2. Brief History of Subtractive CAD-CAM Systems

The traditional methods of dental ceramic restoration production were considered as time-consuming, technique sensitive and unpredictable due to the many variables.[93] Therefore, there has been a search to make productions easier and more predictable.

From the beginning of mid 1980's different digital systems were invented as; computer-aided machining 'in the size of final shape' from solid, fully crystallized or sintered blocks with CEREC system (CEREC, Sirona, Bensheim, Germany)[94]; computer-aided production of a larger-sized prepared tooth, pressing the alumina powder on that die and formation of a larger-sized core and sinterization of the core to the intended size with Procera system (Procera, Nobel Biocare, Kloten, Switzerland)[95]; and computer-aided fabrication of larger-sized restorations through machining the half sintered discs of zirconia and alumina, then sintering them to the intended size with various brands of materials (Cercon, Lava, Vita YZ, Ivoclar e.max zirCAD).[96]

As a cornerstone, a French dentist Dr. Duret has taken comprehensive steps on the improvement of CAD-CAM System.[97] He has introduced 'Sopha system' as a first prototype of a CAD-CAM device, which had shed light to the further implications for CAD-CAM systems in dentistry.[98] He produced first chair-side crown in 1983 by taking the impression of a prepared tooth by intra-oral scanning.[97]

In 1987, Mörmann and Brandestini[94] have developed a prototype device which could receive the three dimensional projection of a prepared tooth. They used a software to design three-dimensional restoration and then led to mill inlays and onlays by computer-aiding from dense blocks of glass ceramics. They called this device and system as 'Chair side Economic Restoration of Esthetic Ceramics' which is 'CEREC' shortly (CEREC I, Siemens Dental, Long Island City, New York then and now CEREC, Dentsply Sirona, York, Pennsylvania).[39,40]

Other very popular CAD-CAM system, the Celay system (Mikrona Technologie, Spreitenbach, Switzerland) has used copy-milling technology. Ceramic inlays, onlays were first fabricated as resin analogs, and then they were machined by copy-milling from ceramic materials. Celay system is worked with pantographic tracing of a model.[40]

Other popular CAD-CAM system is Procera All Ceram (Nobel Biocare, Kloten, Switzerland). This system which was the pioneer on providing data for production by internet connection, was presented by Dr. Andersson[95]. Master model of prepared tooth was scanned, scanning images were sent to the processing center or laboratory through the internet. A bigger-sized abutment tooth was manufactured by computer-aided milling machine to overcome the firing shrinkage. Then aluminum oxide powder was compacted and pressed on that abutment, and coping was milled via computer-aided milling machine as well.[40,95]

Other systems can be listed as; DCS Precident system having a laser scanner, Cercon system without CAD software and CICERO (computer integrated crown reconstruction) system.[40] Recently, Lava system (3M ESPE, Seefeld, Germany) is developed and indicated in zirconia core production from Y-TZP for all-ceramic restorations. Laser optical scanner of Lava system obtains the data. The Lava CAD software draws the margin by itself automatically and offers a pontic design, while Lava CAM fabricates an oversized substructure to overcome the sintering shrinkage.[40]

CAD-CAM technology broadened the scope of machinable ceramic production by utilizing intra-oral or model scanning, designing, and milling of both a monolithic full contour restoration and a framework for single or multiple unit restoration with the help of computer.[1] The advantages of CAD-CAM systems may be explained as follows; reducing the time required to produce restoration of high strength ceramics by up to 90%,[57] reducing chair-side period of time due to lack of taking conventional impressions, preventing cross-contamination among patient-dental technician and dentist, providing deliveries of restorations in single appointment, more homogenously fabricated blocks[99], leading the way to produce polycrystalline ceramics like stabilized zirconia which would not be easily fabricated via conventional laboratory techniques.[39,57] However, there are some disadvantages of CAD-CAM systems including; high prices of equipments, requirement of adequate knowledge of dentist/technician.[40]

2.3. Surface Treatments of Ceramic Restorations

Since 1728, the year of first use of ceramics in dentistry, many in-vitro and in-vivo researches have been done in the aim to develop a dental ceramic to meet esthetic, mechanical and optical requirements of a dental restoration.[100] Main goal is always gathering the smoothest restoration surface. Smooth ceramic surface is linked with good periodontal and dental health, because the bacteria can not adhere well to the smooth surface.[101] When the average roughness (Ra) of a surface is higher than 0.2 μm, bacteria retention begins and biologic complications start to occur.[102] A flat and smooth surface reflects the light more regularly like natural teeth in contrast to rough surfaces diffusing it.[103] Rough surfaces may absorb the staining pigments. Hence, smooth surface texture determines the optical properties. Additionally rough surfaces may cause harmful stress concentrations, strength reductions of material and may lead to antagonist tooth and restoration wear.[104] Patient comfort is also related with the smooth surface of a restoration.[105] Patients tend to feel discomfort and the tongue starts to feel discrepancies when the average roughness of a surface is higher than 0.5 μm.[106]

In the light of these informations, two methods have been applied during the delivery of ceramic restoration as glazing or polishing, in order to obtain highest smoothness to lower the failure risks.

2.3.1. Glazing

Glazing is the application of a thin layer of glassy-ceramic by brushes or by spraying on a restoration surface. Glaze material is composed of glass powder without any color pigments and ceramic liquid. It may applied onto the fired ceramic surface, however newer techniques were evolved as application of glazing spray or paste before firing process.[100,107]

The purpose is reducing the surface roughness, increasing the proper light reflection thus surface looks shiny, enhancing esthetics, protecting the strength of material, protecting the antagonist wear and decreasing the biofilm formation.[108,109]

2.3.1.1. Glazing Methods

Glazing contains a firing cycle that the temperature is elevated up to the ceramic's sinterization temperature.[110] During that process, surface particles of glass ceramic fuses and fills the porosities. If this firing is carried out with no application of an additional glass powder, this process is referred as ‘auto-glazing’.[111]

Traditional glaze application is mixing the glaze powder and glaze liquid according to the manufacturer’s instructions and applying thin glaze layer glaze onto fired restoration.[107] It may be called as ‘over-glazing’ due to addition of glazing material.[111]

Recently there have been new techniques on glaze application which are glazing paste application and glazing spray application. These methods were aiming the decrease in the laboratory steps, because they can be applied before the crystallization firing so that an extra glaze firing step may be diminished. Crystallization and glazing were accomplished in the same firing. Spray formed glaze is implicated by uniformly spreading onto the restoration. Paste formed glaze is applied homogenously with a brush.[107]

2.3.2. Polishing

Polishing is basically a process of removal of chipping.[112] Generally it is mentioned together with the finishing process. These procedures are consisted of three major steps as seen in the Figure 2.2.[113]

Figure 2.2. Steps of finishing and polishing starting from the bottom to the top[113]

Aims of these procedures are listed below;

- Removal of excess irregularities and refinement the borders of restoration,
- Reduction in fracture risk, because rough surfaces may be prone to fracture,
- Production of a smooth surface where plaque could not accumulate, thus increasing oral hygiene,
- Improvement of oral functions and chewing. Food slips over smooth surfaces easily,
- Production of smooth occlusal and interproximal contacts, resulting in less wear on opposite dentition and neighboring tooth,
- Delivering a more esthetic, light-reflecting restoration like enamel surface.[114]

Improper applications of finishing and polishing may lead to higher plaque accumulation, periodontal reactions, increased restoration staining and bad esthetic of the restored teeth.[113]

2.3.2.1. Steps of Finishing and Polishing Procedures

As seen in the Figure 2.2., these procedures are consisted of gross contouring, initial polishing and final polishing.

2.3.2.1.A. Gross Contouring

It can be detailed as gross reduction, coarse finishing and margination. The purpose is reaching the desired contour and anatomy of the restoration by eliminating the irregularities and smoothing the possible roughnesses during gross reduction and coarse finishing.[113] Effective abrasion and elimination of irregularities are assured by using coarse diamond burs and discs having grains bigger than 100 μm.[115] If any excess restorative material was present in the margin of restoration, elimination was provided during the margination by appropriate tools. Final marginal junction should be smooth, well-adapted and in the correct anatomical shape.[113]

2.3.2.1.B. Initial Polishing

Scratches and surface imperfections occurred in finishing, gross reduction and contouring steps are removed.[113] Surface gets smoother initially at this step. Homogenous surface with minimal microscopic defects is obtained. At this step, abrasive grain sizes should be bigger than 15-20 μm and smaller than 100 μm.[115]

2.3.2.1.C. Final Polishing

The aim is to obtain a restoration surface as smooth and light-reflective as natural enamel.[113] High-gloss polishing pastes are generally used as last step for final polishing. Scratches cannot be seen by bare looks after final polishing. Polishing tools have abrasive grains in 0.3-20 μm sizes.[115,116]

2.3.2.2. Factors Affecting the Polishing Efficiency

The efficiency of finishing and polishing process and the final surface roughness of restoration are affected by several elements listed below:

- Structural and physical properties of polished material,
- Difference in hardness between tool and polished material,
- Type, hardness, size, shape, number of abrasives,
- Hardness, elasticity, flexibility, thickness, porosity of the backing and bonding material carrying the abrasive particles,
- Speed and pressure applied onto the tool
- Whether any lubricants such as water, glycerin, vaseline are used.[113]

2.3.2.3. Wear Tribology

Finishing and polishing procedures are meant to generate intended, selective and controlled wear on restoration surfaces. Wear can be expressed as a cumulative material loss, in which particles are disappeared from material surface as small debris, mostly via mechanical processes.

The four significant wear mechanisms can be expressed as; adhesion, abrasion, surface fatigue and tribochemical reactions. The situation is generally abrasive wear when polishing was done with abrasives; however, other wears may have minor roles. The classification of the finishing and polishing methods according to abrasive-wear modes is seen on Figure 2.3.

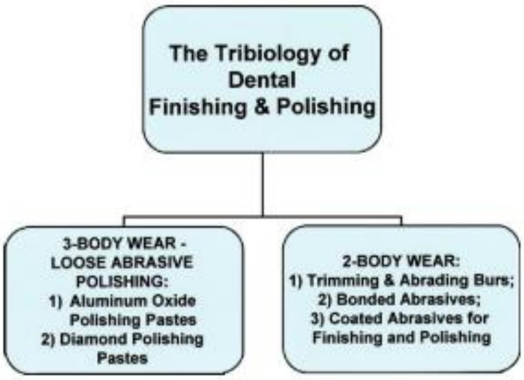

Figure 2.3. Classification of the finishing and polishing methods according to abrasive-wear modes

When a two-body wear is occurred, the 'bonded' abrasive particles come in direct contact with restoration surface. When a three-body wear is occurred, an additional paste may be placed between the material surface and polishing tool. Therefore, these particles of slurry like pastes are referred as free or loose third body particles found in environment. The loose particles in that mode may be either deliberately placed abrasive slurries like polishing pastes, or eliminated debris resulted by abraded material.

Finishing and polishing tools generally work in two-body mode. Even so, dentists and dental technicians still prefer the three-body abrasives by using polishing pastes. Three-body wear is observed if free particles are placed purposefully on the junction of material surface and the polishing tool as in the final polishing step with tiny grain sized wet abrasive pastes. This mode may also happen if minor particles are removed from the polished material and become trapped or circulate within the interface between the two bodies (abrasive tool and material surface).[113]

2.3.3. Glaze versus Polishing on CAD-CAM Ceramics

In order to obtain long-term clinical success and durability for ceramic restorations, all materials should be sufficiently smoothened.[117] Glazing and polishing create smoother surfaces by different mechanisms. By polishing, surface defects and flaws are eliminated, uniformity of surface particles is provided and roughness is decreased. By glazing, depth and sharpness of scratches and cracks on the surface are decreased, micro-cracks are filled and micro-porosities are covered by the application of a thin low fusing glass ceramic overcoat.[118]

Once the CAD-CAM materials are milled, the restorations are coarse in texture and require finishing by hand-piece burrs, polishing with or without glossy paste or glazing to smoothen the texture before delivery.[119–122] Manual polishing and glazing have different effects on surface smoothness.[119,122]

It has always been a controversial issue whether the glazing or polishing of a material acquires the best optical and mechanical properties. There is no consensus about which protocol has a great influence on preserving the properties of ceramic, when capacity of mechanical polishing kits is evolving every day to provide as smooth surfaces as glazing do.[3,10,39,47,105,109,119,123–130]

There are many researches suggesting that glazing exhibits better mechanical and optical properties.[3,124,125,131] Final glazing was suggested providing highly desired smooth ceramic surface.[131] Color difference was found higher on polished CAD-CAM materials compared to glazed ones after staining with coffee solution, however the color change was under the clinically perceptible threshold.[3]

On the contrary of superior esthetic properties, there are some findings related to poorer mechanical attributions. An important observation is the worse mechanical performance of materials with glazing especially on monolithic zirconia. A fine glaze coat would fill any existing scratch and pore, thus improve mechanical properties on glass-based dental ceramics.[132] However, Y-TZP ceramics are polycrystalline containing no glassy matrix, thus an unsatisfactory bonding between Y-TZP ceramic and glaze is obtained.[133] If a bi-layer interface could be created, under tensional forces the material-glaze union would behave mechanically similar to that as if the system is composed of only glaze layer.[134] When there is poor bonding between the layers, this situation is more dominant.[135]

Additionally, there may be air pores inside the glaze coat which were formed during the preparation of glaze by mixing liquid and powder or during sintering process.[136] These pores may decrease the success rate on this interface. Furthermore, the thickness of glaze coat may influence the success. The more thickness of glaze, the more risk of cohesive split inside the layer and the more risk of pore containment. These may be related to the strength decrease of this surface treatment.

Although glazing promotes surface smoothing, it has harmfully impacted the material's fatigue strength.[109] Despite decreasing the roughness of material, additional firings during glaze application might be problematic for delivering time of the restoration.[39] Multiple firings may cause defect formation on ceramic surfaces, which lead to permanent corruption.

It was stated that if there are not any esthetic necessities for glazing, polishing should be done to lithium disilicate ceramics especially on the occlusal surfaces of posterior restorations, glazing might be avoided.[47]

Polishing is easier and simpler compared to glaze firings. Chair-side CAD-CAM restorations may be polished by dentists.[105] If glaze firing is non-applicable, just polishing is the greatest option.[132]

Although it is suggested that the glaze perfectly smoothness the surface, the resistance of the glaze is questionable when the restoration is in function.[123] It was seen that glazed zirconia resulted in more antagonist enamel wear than polished zirconia.[127,137] This has been explained by that: the glaze layer rapidly worns out after functioning along a period or abraded via chair-side adaptation, exposing underlying unpolished rough material. Therefore, some researchers suggested polishing ceramics prior to glazing to avoid the antagonist enamel abrasion.[127]

On the contrary, polishing was found more durable and promising according to recent researches.[10,39,47,83,105,123,126,128–130] Smooth and polished surfaces contribute to the good esthetics of dental restorations by stabilizing color and translucency[138], increasing luster[104], minimize bacterial adhesion[139] and improving biocompatibility[102] through increasing the adherence and reproduction of epithelial cells and fibroblasts of gingiva to the lithium disilicate glass ceramic besides diminishing the plaque retention.[47,140,141], diminish the material exhaustion and risk of chipping or fracture[142], and enhance flexural strength[143]. Furthermore, smooth surfaces experience lesser wear.[144,145] Consequently, they extend the lifetime of both the restoration and antagonist, because smooth surfaces lead to less antagonist wear as well.[144] Besides, intraoral polishing aids in reducing the susceptibility to cross-contamination by removing requirements for recurring laboratory steps.[143]

Fracture toughness is influenced by the depth of a crack. Especially superficial cracks may result in the crack initiation or further crack propagation. Here the polishing and smoothing of the surface is resulted in an increase in fracture toughness and strength. High-gloss polishing is essential, since it may significantly decrease the roughness and hereby the risk of crack formation of the restoration.[129]

Re-polishing regularly reduces the stresses concentration and the asperity amount, and consequently decreases the abrasion of opposing teeth.[132] Re-polishing of occlusal surfaces may also be required after repeated exposure to carbonated beverages and/or acidulated phosphate fluoride[132] or after removal of orthodontic brackets bonded to ceramic restorations.[146]

When compared to glazing, polishing results in better smoothness on ceramics similar to natural enamel regardless of the ceramic type.[39,128] Glazed surfaces were found rougher than polished surfaces.[10,47,147]

It was suggested that, adequate polishing may re-establish the smoothness after occlusal adjustments.[109] For monolithic zirconia, sufficient polishing decreases surface roughness, improves fatigue strength and decreases m-phase content as reversing the monoclinic phase back to tetragonal phase. Polishing enhances fatigue behavior rather than glazing. In the obligation of glazing the restorations for esthetic purposes, especially Y-TZP restorations, it is highly recommended to apply sufficient polishing prior to glazing to diminish surface defects and obtain a smooth surface to decrease material exhaustion.[109]

It was proposed that polished zirconia surfaces showed the smoothest surface compared to the polished then re-glazed and glazed surfaces. The polished zirconia led to least wear of antagonist enamel; whereas glazed zirconia resulted in the highest antagonist wear and polished, then re-glazed zirconia had moderate wear. Interestingly, polished one resulted in less wear compared to enamel to enamel abrasion.[127,137]

Incorporation of a high-gloss polishing step with diamond polishing paste, as recommended in Optra Fine polishing kit, showed a significant improvement in surface smoothness ($Ra<0.2$ μm) for all specimens regardless of the ceramic system.[10,105,123,129] With this extra polishing step, obtaining a surface smoothness comparable to the glazed surface was possible.[123]

2.4. Erosion

Dental erosion is progressive demolishment of dental hard tissue substances via chemical process caused by exogenous or endogenous acids, without bacterial action.[148]

Causes have been linked to ingestion of acidic foods[149], BN[150], rumination and GERD.[151]

Erosion is initiated as surface demineralization of tooth enamel, which eventually leads to dissociation of underlying structures and loss of great amount of hard tissue. Acids having 5.5 pH or lower, which is critical limit, dissolves the hydroxyapatite crystals in enamel.[152] Erosion patients often display severe and generalized defects that gradually expose the dentin.[153]

Enamel erosion is a phenomenon that results in centripetal mineral loss.[154–156] However, erosion process took place in dentin is totally different. After the minerals of enamel is dissolved, the organic matrix of dentin mainly consisted by collagens[157] is brought open into the environment.[158] A thicker organic matrix retards the erosion, since the collagens behave as a protective shield against diffusion of acid.[159,160] Thus, dentin erosion process depends on the diffusion rate.

As a result, erosion is a general reason for dental tissue destruction, ranging between superficial enamel loss and direct exposure of the dentin. The source of acid may be internal or external.[161]

2.4.1. Extrinsic Erosion

Extrinsic causes may be carbonated or acidic drinks, acidic foods[149], citric pastilles, various medicines, oral hygiene swab sticks, saliva substitutes, exposure to water of gas-chlorinated swimming pools[11] and exposure to occupational corrosive agents as battery acid fumes and industry aerosols.[11,162]

2.4.2. Intrinsic Erosion

Predisposing situations leading to intrinsic erosion are bulimia nervosa, rumination or voluntary reflux phenomenon, subclinical regurgitation caused by chronic gastritis associated with alcoholism, xerostomia, malabsorption syndrome, chronic vomiting during pregnancy and GERD.[11,163,164]

Gastric juice containing hydrochloric acid is very acidic with a pH of 1-3[165], thus has an elevated potential for erosion leads to quick advancement of endogenous erosion in enamel.[166] Gastric juice is also consisted of proteolytic enzyme ‘pepsin’. When the pepsin reaches to the oral cavity via intrinsic erosive situations, it threatens the exposed organic matrix due to the capacity of degrading fully demineralized collagen of dentin.[167,168] Therefore, pepsin leads to enzymatic removal of collagens in dentin and accelerates the erosion progression.[159] Consequently, it was suggested that if the mineralized parts of dentin is removed by acidic conditions, collagen network is not able to prevent erosion anymore due to the fragility against pepsin enzyme.

Intrinsic erosion destroys dental hard tissues more than extrinsic erosion due to lower pH of exposure.[8,161] This intrinsic erosion is usually seen on BN or GERD sufferers.[16]

2.4.2.1. Blumia Nervosa

BN is a disorder, which may have multiple causes, defined as binge eating cycles and subsequent compensative acts like self-induced vomiting or over-exercising.[12]

2.4.2.1.A. Brief History of Blumia Nervosa

In 1979, British psychiatrist Gerald Russell[169] has defined anorexia nervosa (AN) patients as ‘the victims of powerful and irresistible urge to overeat’ and ‘morbidly fearful of becoming fat’. These patients developed compensative behaviors as self-induced vomiting, over-use of purgatives (laxatives), diuretics, or amphetamines, or over-extended hunger durations.[12]

The word ‘bulimia’, meaning ‘ox hunger’ in Greek, was used to underline the basic property of ‘gross over-eating’ shown in all blumic patients. When compared to anorexics, Russell[169] defined bulimics as; on normal weight or sometimes overweight, with less menstrual disturbances, higher sexual activity and higher depression levels. At first, Russell has accepted blumia as a ‘chronic stage of AN’, but not a distinct disorder. Those patients with blumia stage had poorer prognosis, more resistance to treatment, increased susceptibility to dangerous physical complications and elevated risk for suicide.[169]

In 2004, Russell has retracted his previous review and accepted that ‘Blumia Nervosa’ is a distinct disorder different form ‘AN’.[170] He stated that bulimic patients have a more favoured long-term prognosis than anorexia nervosa, despite high risks of relapse and complications. Being recognized as a disorder of blumia nervosa is crucial, as bulimics have more susceptibility to comorbid psychiatric conditions, morbidity and mortality resulted by compensative behaviors they perform to prevent weight gain.

Bulimics may be unwilling to share their symptoms; because they may feel privacy and shame over the binging or purging behaviors.[171] Their families and physicians could not detect the disorder easily due to normal or sometimes over the normal weight. Moreover, patients have no medical complaint such as absence of menses differently from anorexia nervosa. Electrolyte instability and behavioral alterations may be alarming signs of blumia nervosa.

2.4.2.1.B. Diagnosis of Blumia Nervosa

According to the third edition of the Diagnostic and Statistical Manual of Mental Disorders (DSM-III) published in 1980, blumia is firstly explained with the words of 'only the presence of binge eating acts'.[172]

The DSM-III-R, revised edition published in 1987, has initially mentioned the term 'bulimia nervosa' and described similar to Russell's genuine definition of binge eating accompanied by compensatory acts.[173] The word "nervosa" attached to keep the disease in the psychiatric nature and to emphasize the trouble of the disorder similar to anorexia nervosa.[174]

The DSM-IV, in 1994, has published a list of criteria for BN as; having binge eating intervals with compensatory acts occurring minimum two times in seven days for at least 3 months, on average.[175] Moreover, two subtypes of BN were described: a purging type, on patients performing self-induced vomiting or misuse of laxatives, diuretics or enemas; and a non-purging type, on patients choosing different compensatory acts like over-exercising or fasting.

As an exception, in many cases a great amount of purging was performed yet no binge eating was witnessed. These were described as having 'Eating Disorder Not Otherwise Specified' (EDNOS) in the DSM-IV. EDNOS patients did not possess all criteria for AN or BN.[175]

In DSM-V, several changes were determined for BN.[13] Firstly, the frequency of symptoms were changed into one time in seven days for 3 months. Thereby, patients having lower frequency are accounted as blumic.[176] Furthermore, purging and non-purging subtypes were removed, since no proof was there for distinct paths or responses along the management.[177] Lastly, the severity of compensatory behaviors is categorized based on frequency as; mild type were experienced one to three times in seven days; moderate compensatory behaviors were experienced four to seven episodes per week, severe compensatory behaviors were experienced as eight to thirteen episodes per week, and extreme compensatory behaviors were experienced fourteen or more times per week.[13]

The incidence of mild cases were found %39, while moderate cases were found %34. Majority of cases were encountered on these two types. Rest of the cases was encountered as follows; %16 with severe type and %11 with extreme type. Patients in the extreme type were found more prone to be concerned about what they eat and to be depressed compared to other types.[178]

2.4.2.1.C. Current Criteria in Diagnosis of Blumia Nervosa

The essential criteria of BN are listed as;[13]

- ‘recurrent binge eating episodes’
- ‘compensatory behaviors to overcome weight gain’
- ‘obligation of experiencing each binging and compensatory acts minimum one time in seven days along at least 3 months on average’
- ‘being unnecessarily concerned about the body figure and weight after insistent self-evaluations, despite being in normal weight or sometimes a little above’.

People usually introduce themselves unnecessarily as ‘bulimic’, when self-induce vomiting is performed but binging is not involved. However, patients with BN disorder should not be confused with the binge eating/purging subtype of AN, purging disorder, or binge eating disorder.[12]

Binge eating is described as episodes of consuming huge portions of food with a lack of control feeling more than most would not normally consume in similar time. Patients usually experience ‘numbness’ or ‘feeling of nothing’ during the binge. This is an important finding to distinguish subjective binging in which bigger portions are consumed than intended from objective binging in which control is lost and great amount of food is consumed in a short period.[12] Foods are usually chosen as easy digestible during the binge; other types have been avoided due to being anxious about putting on weight.

Binging patients generally perform it in privacy. Triggers may be stressful situations, eating a specific food intentionally abstained before and feeling bored. They may feel a relief at first which is temporary, and then guilt follows. That emotional guilt and stress lead to a struggle to be freed from the calories. Following compensatory behaviors may be ‘self-induced vomiting’, ‘misuse of laxatives, diuretics, enemas or other medications’, ‘fasting’ or ‘over-exercising’.[12]

2.4.2.1.D. Epidemiology of Blumia Nervosa

The prevalence is approximately %2-3 with the new criteria of decreased frequency of symptoms to one time in seven days, and average time of onset is 16–17 years old.[12,13,179]

According to the DSM-5 criteria, the currency on young females is %1. Gender differences occur in a female-to-male ratio of 3:1; %0.9–1.5 among women and %0.1–0.5 among men.[13]

Highest currency were observed in the Hispanic/Latino population (%2), moderate in African-Americans and rarest in non-Latino whites with %0.51, which is quite dissimilar from the frequency among ethnicities declared for AN.[180]

2.4.2.1.E. Etiology of Eating Disorders

Eating disorders are multifactorial, with contribution of genetic predispositions, environmental factors and psychology of an individual. Proofs have been shown on that eating disorders were inheritable; children of patients having eating disorders present a 10 times increased susceptibility to have an eating disorder.[181] If parents had rigid adverse thoughts on weight, AN, BN, mental disorder especially bipolar disorder, personality disorder, anxiety disorder and other types of eating disorders, patient tends to have susceptibility to have eating disorders.[182] Having decreased self-esteem, depression and social anxiety, and having a childhood trauma due to sexual or physical abuse, were found more prone to develop BN.[183]

2.4.2.1.F. Medical Comorbidities in Blumia Nervosa

- Electrolyte imbalance, cardiac arrhythmia, seizure, and death,
- Hypokalemia,
- Sub-conjunctival hemorrhages and/or epistaxis,
- Inflammatory changes of larynx and vocal cords, a raucous voice, chronic cough, sore throat and difficulty swallowing,

- Parotid gland enlargement, sialadenosis,
- Minor or bigger ruptures on esophagus, blood in the vomitus or cough
- Acid reflux, dyspepsia and dysphagia, susceptibility to Barrett's esophagus and malignancy,
- Dental lesions, tooth discolorations, elevated dental sensitivity, oral mucositis and chelitis,
- Perimyolysis which is the damage seen on the buccal and lingual sides of teeth. Lack of perimyolysis does not show that the patient does not have self-induced vomiting.[14]

2.4.2.1.G. Management of Blumia Nervosa

Initial intervention for the patient is to provide medical stabilization and balancing the electrolyte instability, if needed. Admission to hospital might be necessary on dehydration, hypokalemia, arrhythmia, severe conditions such as bradycardia, orthostatic hypotension, seizures, inevitable binging and purging, susceptibility to commit suicide, or unsuccessful outpatient treatment.[184]

Behavioral treatment of patients should satisfy the physical, psychological, social absences for appropriate healing. Team of recovery should contain a doctor, dentist, psychotherapist, dietetics expert if the condition includes medical, dental, nutritional and psychiatric impairments.[185]

2.4.3. Clinical Presentation of Erosion

The mandibular molars are subjected to erosion mostly.[186] Patients suffering from extrinsic erosion have more destruction on the labial or occlusal surfaces of upper anteriors; severity decreases through the posteriors. On the other hand, intrinsic erosion leads to more destruction on the lingual surfaces. Results of intrinsic erosion might be alleviated via preventive effect of tongue, transmitting the acid through palate and buccal vestibule.[162]

As a results enamel gets thinner leading a undesired yellowish color to the tooth. Eroded tooth may exhibit and appearance as if it has been lightly prepared ceramic restoration with a chamfer marginal line. Since the protective enamel was disappeared, tooth becomes susceptible to further abrasion. Restorations on tooth may appear highly polished and seems like elevated from the surface. Tooth sensitivities to hot, cold, sweet and tactile might appear due to exposed dentin tubules. Pulp may be affected resulted in the need for endodontic treatment.[11,162,187]

Further tooth substance loss may result in spontaneous un-occluded teeth eruption, tipping and drifting, diastema formation, vertical dimension loss, which all lead to rotation of lower jaw and overjet decrease into edge-to-edge incisal relationship or class III skeletal relation. These series of changes may be fastened if attrition from bruxism is added onto erosion. Acidic environment or erosion increases the risk of caries.

2.4.4. Corrosion on Dental Ceramics

Corrosion is the subsequent destruction of dental materials due to environmental chemical reactions. Despite high chemical inertness of ceramics, their integrity might be influenced by microstructure, surface finish, pH and temperature of corrosive environment exposed for a certain period.[188,189] Decreased durability may be resulted in alterations of hardness, frictional resistance, surface roughness and fracture toughness (Table 2.1.)[189].

Table 2.1. Corrosion Determinants Affecting the Durability of Dental Ceramics

Physical Factors	Microstructural Change	Chemical Degradation	Surface Finish
Hardness	Porosity	Acidic Liquids	Unglazed
Surface Roughness Frictional Resistance	Crystals	Neutral Liquids	Glazed
Fracture Toughness	Shading	Alkali Liquids	Polished

Although silicon dioxide is not soluble on fluids with pH 7 at temperatures lower than 250°C, glass network of ceramic is tend to be solved by two mechanism in a wet environment which has pH fluctuations. These mechanisms which occurred simultaneously are explained as ionic exchange in an acidic solution and breakdown of silicon-oxygen-silica bonds in a basic solution.[190,191]

In chemical corrosion appeared in the acidic environment with ion exchange mechanism, water molecules diffuse into silica molecules found in glass and consequent formation of hydroxyl ions (-OH) by reaction with non-bridging oxygen atoms.[192] Hydroxyl ions leaches out to maintain electrical balance.[22,192–194] In an alkali medium, the hydroxyl ions presented in environment destruct the glass matrix by tearing silicon-oxygen bonds off, hence leading generalized dissolution. In 7 pH, a mixture of two reactions happens. As a result, exposure to alkali pH leads to a total destruction in glass network compared to the acidic pH leading selective ionic removals in the silica.[21]

Corrosion is also determined by the microstructure of the glass matrix and crystal composition. Soda (Na_2O) glasses are more resistant due to the addition of calcium, magnesium, stroncium, zinc, barium, zirconium ions which stabilizes alkali ions than those made of potash (K_2O).[22]

Gastric contents due to very low pH may have corrosive effect on glassy restorative materials. Some organic acids as 'ethylene diamine tetra acetic acid (EDTA)' and citric acid dissolves glass ceramics.[191] Fluoride agents applied topically for caries prevention may degrade the glass matrix in an acidic environment.[195] Therefore, dental ceramics are very susceptible to be corroded by acidulated fluoride solutions with especially lower pH. Dental ceramic corrosion exposes a rough surface and increases the abrasion of opposing teeth. Additionally wear resistance of ceramic also decreases. Obtained vertical dimension by these restorations may also be decreased due to wear.

2.5. Assessment Methods of Corrosion and Erosion

2.5.1. Surface Roughness Assessment

As a determinant of surface texture, surface roughness influences the quantity and direction of reflected beams from surface,[196,197] mechanical characteristics such as fracture and flexural strength by altering stress concentration, wear of the opposing tooth associated with the friction coefficient alteration[145,198] and biological answer of the gingiva.[112,199] The fact that majority of ceramic restorations are selectively adjusted chair-side to arrange the shape or occlusal contacts, surface roughness increase is a big deal to detect and overcome. Various parameters were introduced to calculate roughness by measuring the distance between highest and lowest points of surface profile.[200] Average height of these peaks and valleys are called as average roughness and referred as Ra when the measurement is two dimensional, and as Sa when it is measured with three dimensional devices. Ra value is mostly used in dental studies[201], however it does not define the surface characteristic in detail. It is an estimation of roughness and calculated easily, but it may not distinguish the peaks from valleys. Therefore, detailed profile may be measured by another parameter such as average roughness depth Rz.[202,203]

2.5.1.1. Methods of Measuring Surface Roughness

Contact stylus profilometer, laser profilometer, and 3D optical profilometer are among the types of profilometers a quantitative measurement of surface roughness[200,204]. It was observed that contact profilometer was the most preferred type.[205] Besides these devices, microscopes such as atomic force microscopes (AFM) and confocal laser scanning microscopy (CLSM) may be chosen to evaluate qualitative properties of a surface texture and to measure quantitative values. Both contact and non-contact types of profilometer are good options in measuring corroded surfaces.[206]

2.5.1.1.A. Contact (Stylus) Profilometer

The stylus follows the path on a tracing line and provides a quantitative result.[201,207,208] Contact stylus applies a force 1/1000 of 1 N. However the contact of stylus may lead to scratch marks on the sample.

It provides correct measurements on roughness for flat samples contained under corrosive design and correct evaluation on marginal discrepancies of restorations in vitro.[205]

2.5.1.1.B. Laser Profilometer

It is more accurate compared to contact profilometer for surface texture measurements, due to higher resolution of laser beams.[205] However this method may lead to some artifact formations due to overshot production at sharp edges of groove floors.[205] Additionally wet surfaces may cause some precision impairments in measurements since the beam scatters in liquid.[209]

2.5.1.1.C. 3D Optical Profilometer (White Light Interferometer)

In 2005, 3D optical profilometer or white light interferometry is described as a non-destructive optical imaging method for measuring surface roughness and metrology of solid materials.[210,211] In this method, light reflects from the sample surface and does not penetrate due to the low wavelength of beams. These devices are meant to observe the 3-dimensional profile of a relatively wide area of a material. A white light illuminant is aimed towards beam splitter. Some beams are directed to the material whereas others are reflected off a reference mirror. The beams reflecting back from the material and mirror converge on the imaging detector located on the camera and form interference fringes if the beams reflecting back have almost same path lengths. (Figure 2.4.)[210]

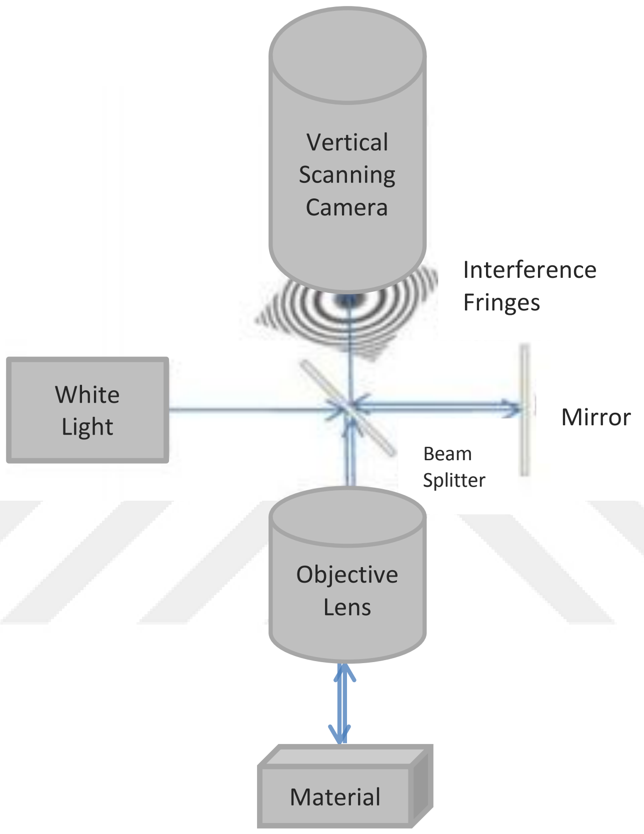

Figure 2.4. Diagram of white light interferometer

Topography images are taken during the vertical scanning interferometry mode.[209] The material gets lowered through a user-defined vertical range and variances in vertical level may be defined with 3 nanometer sensitivity.[210]

During measurements, the material should reflect the incoming light at least partially. Light absorbing surfaces could not transmit sufficient beam to camera to produce a contrast for accurate measurement. So samples having steep slopes usually do not reflect beams back in the direction of the camera lens and do not give correct measurements.[210]

2.5.1.1.D. Atomic Force Microscope

Atomic Force Microscope (AFM) is in the family of scanning probe microscopes.[209] The main purpose of AFM is to obtain topographic images in increased resolutions for various materials such as polymers, ceramics, metals, biomolecules and cells. It also produces 3D images of eroded teeth and corroded materials to measure surface roughness.[126,212] Various modes provide accurate inspection for surface topography, lateral surface composition and elasticity differences.

Highly sharpened stylus with radius of 4 to 60 nm is fixed onto a moveable cantilever which allows the scanning with nanometric high precision. The cantilever moves according to the surface topography. A diode laser beam is radiated from the source fixed behind the cantilever. Roughness becomes visible through the beams hitting the receiver as the stylus and cantilever move. Therefore a visual pattern of surface was constructed.[213]

The stylus works either in dynamic mode of which a pulsating stylus goes up and down, or in tapping mode of which stylus touches the surface. In non-dynamic mode, the tip goes in horizontal direction with permanent touch to surface. In non-contact mode, the stylus moves according to the intensity of van der Waals forces to measure the attraction between molecules.[126,209]

The resolution of images is higher compared to profilometer; yet scanned area is restricted only to 0.25 mm^2 and scanning duration is 60 minutes for this size.[209] The reason for that small area is because the scanning goes step by step. Surface roughness hence is depend on the scanned area and increases with broader scanning.[126]

Generally, it can measure the height differences on initial levels of material loss caused by erosion and abrasion.[209] If a profilometer and AFM was used together, investigation would be more reliable and precise.[126]

2.5.1.1.E. Confocal Laser Scanning Microscope

Confocal Laser Scanning Microscope (CLSM) is used to obtain images in increased resolution, three dimensional reconstructions and optical sections from samples. Major advantages of this method are the three dimensional inspections of eroded surfaces besides their increased resolution.[209] Advantages of CLSM may be counted as; sensitivity to obtain smaller roughness than contact profilometers, short process, simultaneous evaluation of topography and height profile, high-definition fully-focused images that can compete with scanning electron microscopes.[214] A limitation in the measurement of target area is the disadvantage on the other hand.[215]

CLSM workflow may be explained as follows: gas laser (e.g. Ar/Kr or He/Ar) light source is focused through the lens onto a small focal plane of an auto-fluorescent material or a material marked with fluorescent dyes. The laser may be emitted with specific wavelengths (488 nm generally). An integration of radiated fluorescent light and reflected laser light gathered from the enlightened area is collected by the objective lenses and a detector. The confocal property comes from same planes of the focus of illumination and the focal of detection. Sample topography informations may be gathered from different focal planes by elevation or decrease of the microscope stage. The computer creates three dimensional image of the surface from data collected as two dimensional images from consecutive focal areas.[209]

2.5.2. Surface Topography Assessment

Roughness is not an accurate representative for the actual topography of a material, since only certain parts are scanned with a profilometer rather than the entire surface.[216] Surface roughness results are often verified with scanning electron microscopy (SEM) images to specifically assess surface topography.[217,218]

SEM image is produced as a black-white image by selectively showering the material with electrons subsequently bouncing off the sample. In a vacuumed chamber, the source shoots electrons which are focused and navigated with electromagnets to scan the sample and produce a topographic image. The electrons are then detected with positively charged detectors that transform the acquired data into a black-white image. SEM allows three-dimensional evaluation of samples or wet cells and tissues through the use of variable pressure chambers. The vacuum prevents electrons from contacting with gas molecules and air particles that would hold them back from interacting with the specimen, resulting in bad quality image.[219,220]

Samples should be covered with a conductive coating to overcome the material overheating, which eventually improves image quality. A sputter coater is used to cover the material with a thin gold coating. A sputter coater utilizes argon ions to separate gold atoms from a gold plate and coat the surface to create a conductive gold layer.[220]

SEM imaging has provided more detailed results[216], because it provides a data collection about the texture in details with increased resolution and improves the quality of topography evaluation.[221,222] SEM images show the shape and contour changes that the surface profilometer may not show.[217]

Surface alterations following erosive attack may be qualitatively assessed using SEM imaging.[223,224] The severity of surface alteration may be graded on customized scales. [209]

2.5.3. Surface Microhardness Assessment

This determinant is calculated by estimating the opposition force of a material against various indenters creating unchangeable breakdown or perforation.[189]

Most ceramics possess higher hardness values in comparison with dental enamel and metallic alloys. It has been believed that hardness was associated with the antagonist wear severity; however, according to recent studies, the hardness of a restorative material alone is not a definitive indicator on abrasion of the antagonist structures.[225–227]

Heterogenic structure of dispersed crystals in a glassy matrix is associated with the defect mode when the indentations were done. Non-crystalline glass ceramics suffer indentation damage mainly through plastic deformation and following cracks of the weaker glass; while polycrystalline materials get damaged under indentation forces through the mechanism of dislocating the crystals in the matrix. Therefore the microhardness of polycrystalline materials is changed by the positioning of the indentation tip to the crystals.[227] Hardness difference between the glassy matrix and the crystals might be the reason for the inconsistent situation about wear and hardness.

Hardness does not define the intrinsic characteristics of all mass of the material; since it simply calculates the resistance to permanent deformation on the surface of a material by an indenter.[132,228]

As a result of environmental variabilities, characteristics of dental ceramics may be altered. Glass ceramics become harder when the value of the electrical zeta potential on the uppermost layer approaches 0, while they become softer when the positive surface charges on the surface are elevated. Moisty medium in the mouth imparts positive charges to the surface of glass ceramics, resulting in a loss of sodium ions to the interacting aqueous environment, thus decreasing surface hardness.[229] In support of these theories, relatively soft ceramics was shown to have a stronger abrasive effect on enamel than harder ceramics.[227]

2.5.3.1. Methods of Measuring Surface Microhardness

Micro-indentation methods and newly introduced nano-indentation methods are commonly used, especially for eroded surfaces. The main principle of micro- and nano-indentations can be explained as the certain load and dwell time of indentation with a diamond indenter having different geometries. Most commonly, 'Knoop' or 'Vickers' diamond tips are loaded on polished surfaces which are needed to observe indentations properly. The indentation of Knoop tip leaves a rhomboid mark and Vickers tip leaves a tetra-pyramidal mark. (Figure 2.5.)

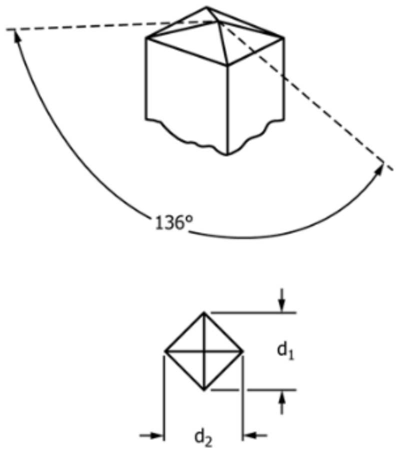

Figure 2.5. Shape and mark of Vickers indenter

The dimensions of d1 and d2 are measured via a light microscope, and 30-40 μm length is needed for accurate measurements. The Knoop or Vickers hardness numbers are calculated by a special formula.

Vickers hardness may be calculated and expressed either in units of GPa or as a dimensionless Vickers hardness number (VHN). The Vickers hardness number is calculated as follows: VHN=1.8544 x P/d2, where P is the force in kg.f (kilogram force) and d is the average length of the d1 and d2 in millimeters (mm).[230]

2.5.4. Fracture Toughness Assessment

This determinant is a feature interconnected with the stress intensity at a fracture tip on a surface and the length of the fracture, which changes according to the microstructure of material (e.g., crystal size, aspect ratio, and orientation; glass phase distribution; and porosity). Thus, it represents the counteraction of a material to quick fracture propagation under tensile stresses, such as occurs during the mastication.[231]

Fracture toughness is called the critical stress intensity factor. The stress intensity factor, which is referred as K and meaning how much stress concentrated at the tip of an existing flaw. K is a function of the generated stress, the geometry, and the length of the crack. As the stress is elevated, when K rises to a critical point (K_c), fracture propagates quickly and the material experiences catastrophic failure. During this process, different loading modes may be applied. Since brittle materials most often fail in mode I (opening mode), this is the most frequent mode for laboratory testing, so critical stress intensity factor in mode I is labeled as K_{Ic}. Therefore, K_{Ic}, the fracture toughness defines the amount of energy of which a material may absorb prior to catastrophic destruction occurred in the I failure mode.[232]

Fracture of a material is initiated when the applied load produces a stress at the tip of a flaw or crack equal to the internal strength of the vitreous matrix.[190] Since ceramic may fail without any visible plastic deformation, the importance of K_{Ic} in the ceramic wear process is important.[233] This type of wear process is initiated with formation and propagation of the crack subsequently and eventual catastrophic destruction of the material.[231] This behavior may be exacerbated with elevating strain rates under parafunctional forces and temperature changes, which are common in the mouth.[226] If the dental ceramic does not have enough toughness to resist fracture, brittle spalling may be formed. Brittle chipping occurred during the abrasion may be resulted in the re-sharpening of edges, thus wear risk is subsequently exacerbated. The sharp edges is not rounded rapidly due to their greater hardness.[189]

Because of the inherent difficulties in measuring the fracture toughness of dental ceramics, several efforts have been made to determine some standards for laboratory tests providing consistent and reproducible results.[232] These tests may be listed as follows: Indentation Fracture Toughness Test, Single Edge 'V' Notched Beam (SEVNB) Test, Single Edge Pre-Cracked Beam (SEPB) Test, Surface Crack in Flexure (SCF) 'Controlled Surface Flaw' Test, Chevron Notch Beam (CNB) Test.[232]

2.5.4.1. Indentation Fracture Toughness Test

The Vickers indentation fracture (VIF) test has a widespread use as an experimental method on estimating the fracture toughness of brittle ceramics since

1970s.[234] The concept of evaluating fractures produced by hardness indentations invited by Palmqvist[235] in the 1950s, however the concept was first introduced as a fracture toughness test by Evans and Charles[236] in the mid-1970s. the formula for the K_{Ic} value was proposed as: $K_{Ic}=0.0824 \times P/c^{3/2}$.[236]

Only little piece of sample is required and the measurements may be made rapidly with a quick preparation period with minimal cost. The VIF method is very advantageous in almost all respects, although it is admittedly a rather unconventional approach to the determination of fracture toughness.[234]

2.6. Optical Parameters of Esthetic Restorations

Successful esthetic dental restorations are determined by several critical factors. These factors may be listed as optical and mechanical properties. Material’s mechanical features may affect optical properties; and structural properties leading to the desired esthetics, color and translucency may also alter the mechanical properties like material strength, hardness and toughness. Therefore, the optical and mechanical properties must be considered together when selecting the ideal material for the patient's needs.

Mechanical and structural properties depend on the wear resistance, hardness, surface roughness and topography, strength, and toughness of the chosen material.[237] Inseparable from mechanical properties, optical properties have a critical impact on the success and esthetics of the esthetic restoration. Optical properties depend on the shade and translucency of the restoration, individual's shade perception, illuminant utilized on shade assessment, the surface and structural properties of both the tooth and the restorative materials chosen, and knowledge of some main principles of shade perception.

2.6.1. Color Determinant

2.6.1.1. Definition and Perception of Color

The phenomenon of color is the contact of light with a substance and the subjective experience of an observer.[238] Three factors may affect color perception: illuminant, spectral reflectivity of the substance and observer.[239]

Illuminant radiates light energy in different wavelengths in the visible spectrum. The influence on shade perception of an object is based on the content of different amounts of each visible wavelength radiated by illuminant.[239]

The spectral reflectance or transmittance defines the color of the substance. Curve of the spectral reflectance of the substance exhibit information graphically and shows a numerical quantification of the color. Different objects with different colors have different curves on the graph due to the distinct energy that is absorbed or reflected.[239]

Finally, the viewer's eye and brain referred as visual system influences the overall perception of color.[240] Normal human visible wavelength range of light is between 380–780 nm.[239]

2.6.1.2. Color Systems

When information about the shade of a restoration is exchanged between the dentist and dental technician, considerable controversy often arises. Therefore, several shade guides were created.[239]

In 1905, the Munsell Color Scale was an pioneer to classify shades to aid the dental communication.[241] In 1931, the Commission International de l'Eclairage (CIE), an organization concerned with color and appearance, published a scientific paper on the first standard for color matching and evaluation, describing an ideal illuminant, a standard observer, and outlining the process of visual system responding for particular shade.[242,243]

In 1976, CIE described new system called CIELab*.[244] Color differences between two objects were calculated using the ΔE_{ab} formula in the CIELab* system. Then in 1986, the HSB/HSV system was defined.[245] HSB stands for hue, saturation (chroma), lightness, while HSV stands for hue, saturation (chroma), value. The other systems for describing colors were CIELuv, XYZ, Lch, and RGB.[237] In 2004, the ΔE_{ab} formula calculating shade variations has been improved by the CIE and ΔE_{00} formula has been introduced.[246]

2.6.1.2.A. Munsell Color Scale

Color is defined in Munsell Color Scale by hue, value, chroma.[243]

Hue is an attribute which helps identify colors within different major color groups like red, blue, green. Value, an indicator of lightness, lies between absolute black and absolute white. Chroma is saturation level of a color; it defines the strength, intensity, vividness, or brightness of a color.[239]

The Munsell color scale may be represented as a sphere (Munsell's original concept) or as a cylinder.[247] (Figure 2.6.)

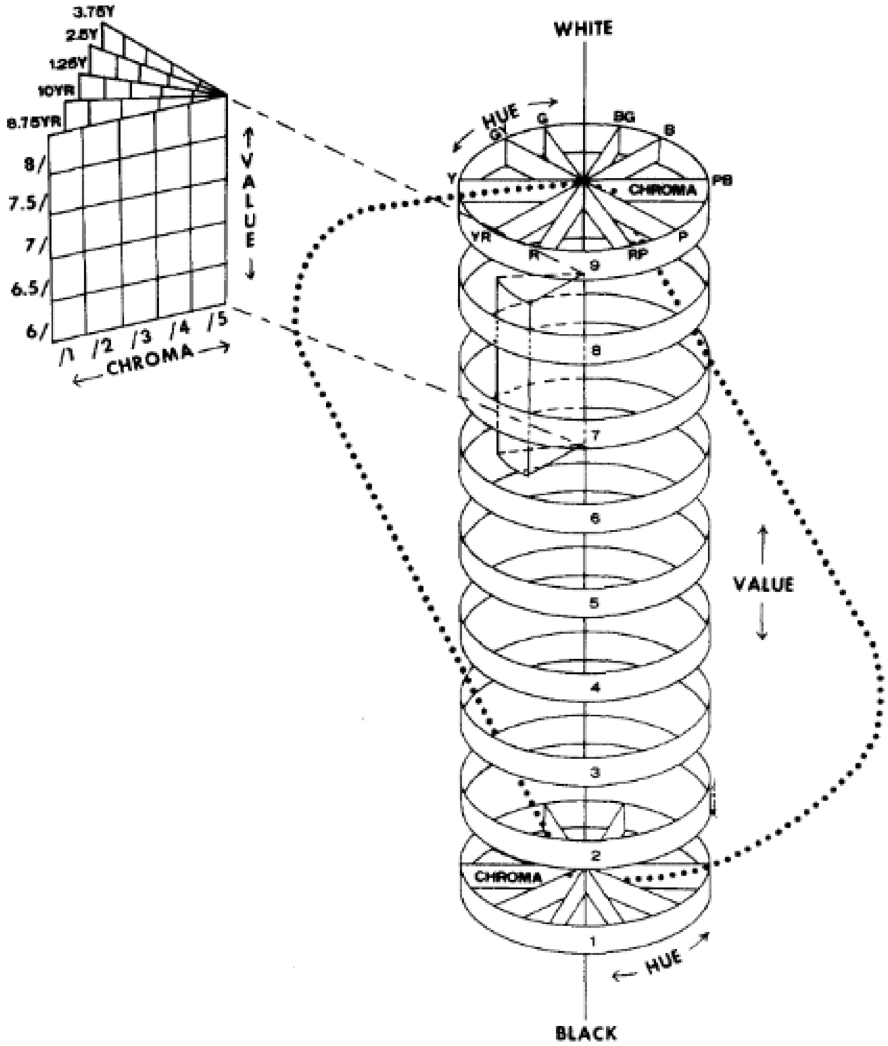

Figure 2.6. Cylindrical illustration of Munsell Color Scale[247]

Through the center of the cylinder runs a colorless and achromatic longitudinal axis, absolute white at the highest level, absolute black at the lowest level. Series of grays, passing through black to white in equal visual levels, attach those two ends. Ten shades (hues) are located around this skeleton in each step. Inside each hue, shades are organized according to the lightness/darkness (value - nine levels/wheels) and purity or strength (chroma). Lighter shades are at higher levels of the cylinder, darker shades are at lower levels. Shades are purest on the outer layer and become gradually grayer as they approach to the center. The intervals were organized as equal visual distances under a standard illuminant.[247]

- **Hue**

Hue is the property that distinguishes one color from others, e.g., red from yellow, green from blue, or violet etc.[248] Hues are designated by their initial letters in the Munsell system: R for red, YR for yellow-red, Y for yellow, etc.[247]

- **Value**

Value is the property that distinguishes a lighter color from a darker color. Value of zero means black, whereas Value of 10 refers to white. In the Munsell system, only nine (1-9) levels of value (gray) are used; while absolute white (10) and absolute black (0) do not count. Fractions may be used when finer scoring is necessary.[247,248]

Value differences may be more understandable when viewing a black and white television image. The real-life scene is full of colors, but only the lightness/darkness (value) of the color is transmitted; a blue, red, or yellow could all be transmitted as the same indistinctive gray when they have similar value. Shades with higher value would be transmitted as lighter grays and shades with lower value as darker grays, independent from hue or chroma.[247]

- **Chroma**

Chroma is the property that distinguishes a saturated shade from a weak and unsaturated shade.[248] Chroma defines the proportion of hue in a color.[247]

Chroma may be more understandable if the concept of painting a box is thought as painting one side as pure red. If some gray dye is added to the red dye before painting the second side, the red on the second side will be perceived as less pure red; thus chroma will be reduced. If some more gray dye is added before painting every other side, the color will progressively get closer to gray. Adding a gray always reduces the chroma, however theoretically has no effect on the hue. The change in value of the original color is associated with the value of the added gray. If a gray with a higher value than the original shade is used, the resulting shade will have the same hue, decreased chroma, and increased value. If a gray with the same value is added, only the chroma is affected and reduced.[247]

2.6.1.2.B. CIELab* Color System

This system was based on the theory of color perception, according to which the eye has three distinct color receptors (red, green and blue). Numerical expression of colors is possible with this system; additionally the calculation of clinically significant color difference between objects by a formula is also possible. The color of an object is described by three coordinates; L*, a* and b*. (Figure 2.7.)[237]

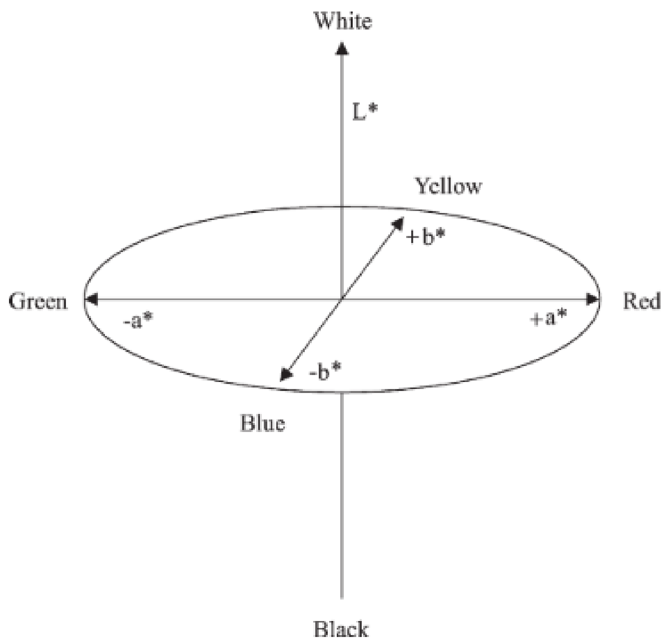

Figure 2.7. Color diagram according to CIELab* system

The L*, the lightness degree of the object, ranges from zero (perfect absorber black) to a hundred (perfect reflector white); the a* is the degree of redness ('+' a* values) or greenness ('-' a* values); and the b* is the degree of yellowness ('+' b* values) or blueness ('-' b* values).[237,239]

The a* and b* values become closer to 0 for neutral shades (white, gray, black) and become elevated in magnitude for more saturated or strong colors.[239]

$\Delta E_{ab} = [\ (L^*_1-L^*_2)^2 + (a^*_1-a^*_2)^2 + (b^*_1-b^*_2)^2\ ]^{1/2}$, is the formula for calculating color differences. This ΔE_{ab} value has become the cornerstone for color science, in industrial fields and dentistry.[237]

There are many researches on the clinical acceptability and perceptual thresholds of ΔE_{ab} for color changes.[116,249–252] O'Brien[116] has suggested the following ΔE_{ab} thresholds: if ΔE_{ab}=0, there are no color difference; if ΔE_{ab} is between 0.5 and 1, there is excellent color similarity; if ΔE_{ab} is between 1 and 2, the color similarity is good; if ΔE_{ab} is between 2 and 3.5, there is clinically perceptible yet acceptable color difference; and finally if ΔE_{ab} is higher than 3.5, the color difference is clinically unacceptable.

2.6.1.2.C. CIEDE2000 Color System

In 2004 the CIE has introduced a new and improved formula as ΔE_{00} instead of ΔE_{ab}[246], which is $\Delta E_{00} = \{\ [\Delta L' / (k_L \times S_L)]^2 + [\Delta C' / (k_C \times S_C)]^2 + [\Delta H' / (k_H \times S_H)]^2 + [R_t\ [[\Delta C' / (k_C \times S_C)] \times [\Delta H' / (k_H \times S_H)\ ]\ ]\ ]\ \}^{1/2}$. With this new formula, some new terms was introduced such as S_L, S_C, S_H, k_L, k_C and k_H. S_L, S_C, S_H are weighing functions, while k_L, k_C and k_H are parametric factors.[237,253] $\Delta L'$, $\Delta C'$ and $\Delta H'$ represents the difference of lightness, chroma and hue of original and reproduced images of an object, while R_t is the rotation function.[253] They allow the detection of variabilities in texture, background, separations, etc., for the lightness, chroma, and hue components. The purpose of introducing new terms and formulas was to enhance the relationship between visual and computed differences.[237]

Clinical acceptability and perceptibility thresholds for color change on ΔE_{00} were found 1.8 and 0.8, respectively.[254]

Even though the ΔE_{00} is considered to evaluate differences in distinct parameters such as lightness, chroma and hue; ΔE_{ab} and ΔE_{00} formulas are interchangeable with each other to evaluate the color differences.[255] Significant correlation was found between ΔE_{ab} and ΔE_{00} in spite of the involvement of weighting functions, and the use of ΔE_{00} was recommended.[256] When calculating a color difference, ΔE_{00} exhibits better consistency with human eye perceptibility acceptability thresholds.[252,257]

Despite the advantages of this improved formula, ΔE_{ab} is still more common in recent researches. This might be because of the complexity of ΔE_{00} formula and difficulties in making transformations of L*, a*, b* values to L′, a′, b′ via arithmetics.

Furthermore, the use of ΔE_{ab} provides great convenience in discussing the result s with previous researches done with ΔE_{ab}.[237] Therefore, the use of ΔE_{ab} is still very popular.

2.6.1.3. Main Definitions Related to Color and Appearance

The object's color with numerical data and outlook are not only relatable parameters in matching the shade. Geometric attributes and some optical phenomena are also relevant with this process. However, visual assessment of an object is still a gold standard along with color matching systems using color scales and systems.

Geometric attributes include scattering, translucency, transparency and opacity, while optical phenomena include opalescence, fluorescence, metamerism and gloss.[258]

2.6.1.3.A. Scattering

It is the process of redirecting light beams over a range of angles when the light passes through a granular, fibrous, or rough surface.[237]

2.6.1.3.B. Opalescence

This phenomenon is a process in which the object appears yellowish-red under the directly transmitted light, and appears blue under the condition that the directly transmitted light is scattered by the path. Therefore, two different colors are seen on the same material when viewed from different angles. The term opalescence is inspired by the appearance of the opal stone.[237]

2.6.1.3.C. Fluorescence

It is a phenomenon when a material absorbs light in the short wavelength range of 300-400 nm, in the ultraviolet spectrum or electromagnetic radiation, making it invisible to the naked human eye. Then, on the same material, the emission of light in longer wavelength happens as a visible bluish light.[237] If the absorbed light is in the UV spectrum, the only way for a human to see a visible light is to look at it with UV filters. When the source of the absorbed light is gone, the material stops radiating or emitting the visible light. This phenomenon is best explained by the fluorescent clothing worn by animators/showmen. These clothes start to glow when exposed to UV light. Therefore, absorbed invisible UV light with a short wavelength is converted into visible, bluish glowing light with a longer wavelength.

2.6.1.3.D. Metamerism

It is a phenomenon in which the colors of two objects of different spectral reflectance are the same under the illumination of one source. Under another light source with a different spectral composition, they may appear in different colors.[237]

2.6.1.3.E. Gloss

It is the attribute of the surface having a mirror-like reflection. Gloss is referred as shiny, glossy, or specular outlook.[237]

2.6.1.3.F. Opacity – Transparency - Translucency

Opacity is a feature of concealing what is behind. Transparency is a feature of an object in which an insignificant amount of transmitted light is scattered. A transparent object has no or minimal obscuring effect. Translucency is the feature of an object where the large amount of transmitted light is scattered.[237]

2.6.1.4. Color Measurement Methods

Generally, color in dentistry is evaluated by two methods, visual and instrumental.[259] Visual methods consist of shade guide systems, while instrumental methods are listed as RGB devices, colorimeters, spectrophotometers, and digital cameras.

2.6.1.4.A. Shade Guides

Tooth-colored shade guides are the most commonly used method of shade determination in dentistry.[197,259] However, it is also the most subjective method due to several factors related to the observer and the environment. The observer's age, experience, eye fatigue, eye health (e.g., color blindness), verbal utterances, ambient light intensity, and ambient light reflectance can be cited as examples of the subjectivity of this method.[70,239,260] However, in spite of those drawbacks, eye has great efficiency in detection of minor color variabilities between two materials.[261]

The most commonly used shade guides are the VITA Classical Shade Guide and VITA 3D Master Shade Guide System (VITA Zahnfabrik, Bad Säckingen, Germany). An addition to 3D Master Scale is VITA Bleached Guide which is primarily produced to monitor tooth whitening.[197] Recently, new types of shade guides have been produced, such as stump shade guides and gingival shade guides.

Especially stump shade guides have become very important, since the opacity or translucency of the restoration must be calculated for all ceramic restorations. Stump shades represent the shade of the abutment teeth, which has a major influence on the final esthetics of the restoration.

2.6.1.4.B. Spectrophotometers and Colorimeters

Spectrophotometers and colorimeters are utilized in industrial and searching fields to assess the color of broad variety of objects.[262]

- **Colorimeters**

They are usually set up for color measurement in XYZ or CIELab* systems. The instrument's color filter has the approximate spectrum of the standard observer's eye.[259,263] The colorimeter is relatively simpler and inexpensive compared to spectrophotometers.[237] These are produced to detect the shade of flat planes, so there might be accuracy problems in recording tooth color.[259] The filter wears out over time.[264]

- **Spectrophotometer**

It detects the quantity of visible energy radiated from the material, one wavelength at a time from the material’s entire visible spectrum. They measure and record emitted energy for value, chroma and hue.[265] However, they are expensive, complex and may be bulky to make measurements on patient.[266] They are able to convert data into various color systems.[237]

2.6.1.4.C. Digital Photography

Digital camera and photographs have taken place in shade taking due to disadvantages of spectrophotometers and colorimeters such as poor inter-device reliability and high-cost technology, that may not be affordable for a clinician.[237,267,268] However, digital cameras are among useful communication tools for a clinic and may be used for digital color detection, despite its variable subjectivity.[268] Those images may be simply stored and transferred to the dental technician, offering great quality of information related to different shades of tooth surface, form, and characteristics.[269]

Color matching skills of clinicians have been enhanced by this digital shade taking technique; but various determinants like exposure, white balance, film speed, aperture, light source, and resolution must be standardized.[270]

Various instruments are utilized with digital cameras to enhance the standardization of information and decreasing the degree of subjectivity related to color detection.[268] Cross-polarizing filters, gray cards, twin flashes are among these tools.

Cross-polarizing filters decrease light scatterings reflected from tooth surface, thus adjust the over-estimation of the prevalence of white opacities, when combined with twin-flashed photography. They also aid in detecting minor color differences on different tooth zones and distinguishing minor shade variabilities on shade guides accurately.[271] That filter such as the Polar Eyes Cross Polarization Filter (eLab, Emulation S.Hein, Breisgau, Germany) was found advantageous in displaying the internal color differences of natural teeth for shade analysis and remove diffuse light and unwanted reflections caused by the flash that can hide details and lead to problems in communication with a technician.[272] Thus, highest standard in shade taking and transferring this information to technician was found as cross-polarizing filters.[268]

Standardizing the white balance is also problematic. White balance removes unrealistic color sparkles from images.[273] The automatic balancing choice may be preferred for intra-oral images but should not be selected. Auto white balance incorrectly adds cyan shade to the scene to neutralize the increased percentage of redness of the soft tissues, whereas adding a blue shade to compensate for the yellowness of dental hard tissues.[268] An accurate white balance distinguishes healthy gingiva from inflamed gingiva. Correct color interpretation elicits tooth properties like translucency, caries, erosion, abrasion, and cervical dentin exposure.[273] A white balance reference card having defined color coordinates is advised to define the color accurately in tooth images on digital photography.[274,275]

2.6.2. Translucency Determinant

Translucency is a capacity of an object to transmit light.[276] It stands between pure opacity and transparency and an important determinant to choose correct restorative material.[277,278] Correct translucency determination of a restoration induces the desired shade and appearance, thus affects the harmony with surrounding structures.[279] Translucency of ceramics is associated with light reflection and absorption[237,276], crystal size[280], crystalline content[278], thickness[237,281], additives, density, porosity and sintering process.[282]

As an internal feature, translucency is classified as "absolute translucency" measuring the percentage of transmitted light, or "relative translucency" that expressed as variance in luminance and shade, when the object is evaluated on ideal black and white backgrounds.[283] Two indicators as translucency parameter (TP) and contrast ratio (CR) have been widely used for the relative translucency[284,285] that may be calculated by spectroradiometers and spectrophotometers.[277] These parameters are associated with the color of the white and black backgrounds.[2,3,286–288] Despite the recommendation of using backgrounds with ideal values, ideal white and black backgrounds are not commonly used because they are hard to find. The CIE color coordinates of ideal backgrounds were reported as CIE $L^* = 94.3$, $a^* = -0.4$, and $b^* = 1.4$ for the ideal white background, CIE $L^* = 0.2$, $a^* = 0.4$, and $b^* = -0.6$ for the ideal black background and CIE $L^* = 0.0$, $a^* = 0.0$, and $b^* = 0.0$ for a zero calibration box.[289,290] Generally use of CIE illuminant D65 was suggested as a reference illuminant.[290]

Recently, a declaration was made regarding the translucency parameter. When measurements are done on non-ideal backgrounds and when optical properties of the material are not similar throughout its thickness, translucency parameter should be named as 'relative translucency parameter' (RTP).

2.6.2.1. Translucency Parameter (TP)

The translucency parameter (TP) was first used on the assessment of translucency for maxillofacial elastomeric materials.[284] TP was defined as color difference for a material, at a particular thickness, on ideal black and white backings by CIELAB system.[277]

The CIE has recommended the utilization for TP.[246] However, the TP is still obtained with the CIELAB formula at the moment in the majority of translucency researches in dental literature.

TP is gathered by calculating the coordinate difference of a sample on two backgrounds; black (B) and white (W). TP formula according to CIELab is $[(LW^* - LB^*)^2 + (aW^* - aB^*)^2 + (bW^* - bB^*)^2]^{1/2}$, where subscript W refers to the color coordinates on an ideal white background and subscript B refers to those on an ideal black background.[284]

In addition, CIEDE2000 (1:1:1) color difference formula was also used to calculate the translucency parameter (TP_{00}) as following equation; $\{ [(L_B'-L_W') / (k_L \times S_L)]^2 + [(C_B'-C_W') / (k_C \times S_C)]^2 + [(H_B'-H_W') / (k_H \times S_H)]^2 + [R_t [[(C_B'-C_W') / (k_C \times S_C)] \times [(H_B'-H_W') / (k_H \times S_H)]]] \}^{1/2}$ where the subscripts "B" and "W" refer to lightness (L'), chroma (C') and hue (H') of the specimens on the black and the white backgrounds, respectively. R_T is the rotation function that means the relationship between chroma and hue differences in the blue region. Weighting functions, S_L, S_C, S_H set the total color difference for variation in the location of the color difference specimen over the B and W backgrounds in L', a', b' coordinates. The parametric factors, K_L, K_C, K_H, are correction terms for experimental conditions. In the present study, the parametric factors of the CIEDE2000 color difference formula were accepted as 1.[291]

When TP was calculated on a research; the illumination, the observer, the thickness of material and the color difference formula used for the calculations must also be presented.[292] The thickness of the translucent material is highly significant since it affects the perceived color coordinates on two backgrounds.[277] Similarly, spectral reflectance values of backgrounds, being ideal or non-ideal, also affect the calculated or observed color coordinates.[277,285]

2.6.2.2. Contrast Ratio (CR)

CR is defined as the ratio of spectral luminous reflectance (Y) of a sample on black (Yb) and white (Yw) backgrounds to give Yb/Yw.[285] 'Y' is described as the tristimulus value of transmittance by the CIE.[246] When Yb and Yw values are the same, the material completely masks the backgrounds and CR is 1, the highest possible measurement. When the material is completely transparent, the Yb and Yw are the values of the backgrounds, thus CR has the lower threshold which is the ratio of the Y of the black background to that of the white background.[277] Mean CR is calculated as the average CR values at each wavelength (10 nm intervals) in the range of 400 to 700 nm.[290]

The thickness of the transparent material and the reflectance values of the backings will significantly affect CR. Since Y is a function of the illuminant and the observer, each of these parameters must be defined clearly when using CR. Although CR is commonly associated with Y values, it is possible to calculate CR as a function of wavelength since the reflectance on each background may be defined as a function of wavelength.[277,285]

2.6.2.3. Translucency Thresholds

TP and CR values may be used interchangeably due to their high correlation.[293,294] ΔCR of 0.07 was observed as the perceivable limit, which could be transformed into ΔTP value of 2 by regression equations.[290]

Perceivable threshold for TP_{00} was found as 0.62 units; whereas acceptability threshold TP_{00} was observed as 2.62 units. Respective ΔTP CIELAB values are 1.33 for perception and 4.43 units for clinical acceptance.[291]

2.6.2.4. Factors Affecting Translucency Measurement

- Measuring instrument and method,
- Used formula as either TP or CR, or RTP,
- Sample thickness, particle contents, particle dispersion and intensity
- Color coordinates of backgrounds, being ideal or not,
- Illuminating conditions.[290]

3. MATERIALS AND METHODS

Experiments of the current research study have been performed in the hard tissue laboratory of Yeditepe University Faculty of Dentistry. SEM evaluations were completed in Biocidal, Research and Development Laboratory at Yeditepe University. 3D optical profilometer evaluation was performed at Yıldız Technical University Central Laboratory.

3.1. Power Analysis

Sample size was calculated using PASS 15 Power Analysis and Sample Size Software, 2017 (NCSS LLC, Kaysville, Utah, USA). Sample size of 18 is obtained for 6 subgroups whose means are to be compared.[295] The total sample of 108 subjects achieves 99% power to detect differences among the means versus the alternative of equal means using an F test with a 0.05 significance level.

3.2. Sample Preparations

Three esthetic CAD-CAM materials were selected as lithium disilicate glass ceramic (IPS e.max CAD, Ivoclar Vivadent, Schaan, Liechtenstein) (E) (Figure 3.1.); zirconia reinforced lithium silicate ceramic (Celtra Duo CAD, Dentsply Sirona, York, Pennsylvania) (C) (Figure 3.2.); monolithic zirconia (Ceramill Zolid HT+, Amann Girrbach AG, Koblach, Austria) (Z) (Figure 3.3.). Material contents and sample characteristics were shown at Table 3.1. and Table 3.2.

Figure 3.1. IPS e.max CAD C14 block, Ivoclar Vivadent, Schaan, Liechtenstein

Figure 3.2. Celtra Duo CAD C14 block, Dentsply Sirona, York, Pennsylvania

Figure 3.3. Ceramill Zolid HT+ 16 mm thick disc, Amann Girrbach AG, Koblach, Austria

Table 3.1. Material contents

Brand Name (Abbreviat.)	Lot Number	Material	Manufacturer	Composition (% weight)
IPS e.max CAD (E)	Y12494	Lithium Disilicate Glass Ceramic	Ivoclar Vivadent, Schaan, Liechtenstein	%57-80 SiO_2, %11-19 Li_2O, %0-13 K_2O, %0-11 P_2O_5, %0-8 ZrO_2, %0-8 ZnO, %0-5 MgO, %0-5 Al_2O_3, other oxides and ceramic pigments
Celtra Duo CAD (C)	16005083	Zirconia Reinforced Lithium Silicate Ceramic	Dentsply Sirona, York, Pennsylvania	%58 SiO_2, %18.5 Li_2O, %10 ZrO_2, %5 P_2O_5, %2 CeO_2, %1.9 Al_2O_3, %1 Tb_2O_3 and other oxides
Ceramill Zolid HT+ PS (Z)	2003000	%4 Yttria Stabilized Tetragonal Zirconia Polycrystalline Ceramic (4Y-TZP)	Amann Girrbach AG, Koblach, Austria	ZrO_2+HfO_2+Y_2O_3 ≥ %99.0 Y_2O_3: %6.7 to %7.2 HfO_2 ≤ %5 Al_2O_3 ≤ %0.5 Other oxides ≤ %1

Table 3.2. Characteristics of samples

<table>
<tr><th>Material</th><th>Translucency and Color</th><th>Form</th><th>Cutting Stage</th><th>Grinding and Polishing</th><th>Crystallization / Sinterization</th><th>Final Dimensions</th></tr>
<tr><td>IPS e.max CAD (E)</td><td rowspan="2">HT
A1</td><td rowspan="2">C14 Block
14 x 12
x 18 mm
dimensions</td><td rowspan="2">Cut at uncrystallized stage</td><td rowspan="3">600-800-1200-2500 Grit Silicon Carbide Papers and Optra Fine 3 Step Intraoral Polishing Kit</td><td rowspan="2">Crystallized after grinding</td><td rowspan="3">14 x 12
x 1.5 mm</td></tr>
<tr><td>Celtra Duo CAD (C)</td></tr>
<tr><td>Ceramill Zolid HT+ PS (Z)</td><td>HT
A1
(Pre-shaded)</td><td>Disc
at 16 mm thickness,
98 mm diameter</td><td>Cut at green stage</td><td>Sintered before grinding</td></tr>
</table>

3.2.1. Lithium Disilicate and Zirconia Reinforced Lithium Silicate Samples

E and C blocks were stabilized on a metal-acrylic holder piece (Figure 3.4. and Figure 3.5.) by using sticky wax (Polywax, Bilkimya, İzmir, Turkey) (Figure 3.6. and Figure 3.7.). Then, the piece was installed onto the sectioning saw (Isomet 1000, Buehler, Lake Bluff, Illinois) (Figure 3.8. and Figure 3.9.). Blocks were cut under the water cooling at standard speed of 275 rpm. Forty samples were sliced from each material into average thickness of 1.8 mm (± 0.2 mm) rectangular plates. After the cutting step has been completed, samples were ready to grinding and polishing step.

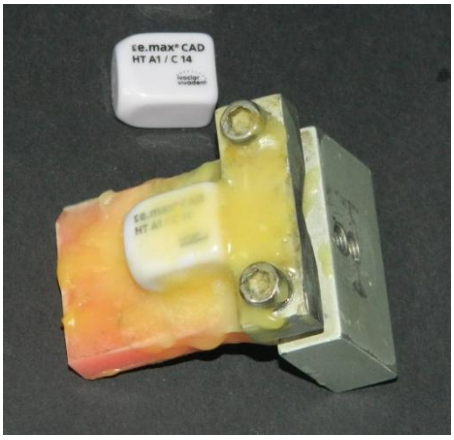

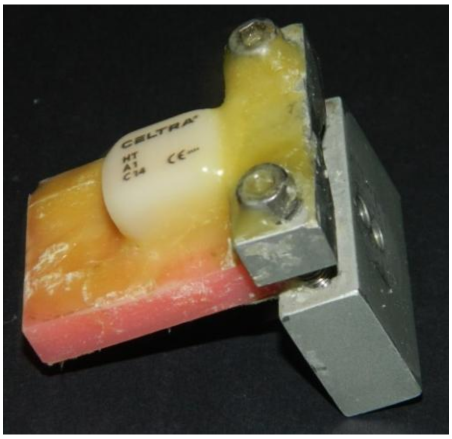

Figure 3.4. and Figure 3.5. E and C blocks stabilized onto metal-acrylic holder

Figure 3.6. and Figure 3.7. Polywax sticky wax, Bilkimya, İzmir, Turkey

Figure 3.8. Isomet 1000 sectioning saw, Buehler, Lake Bluff, Illinois

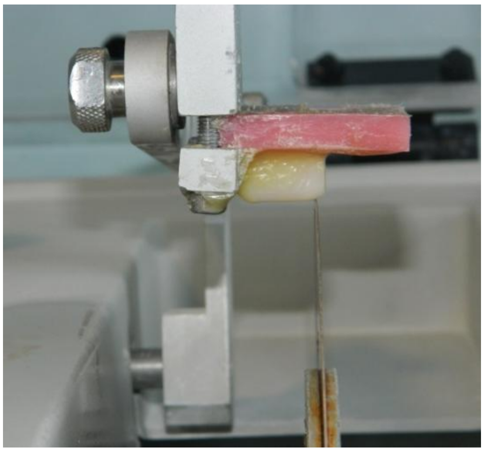

Figure 3.9. Block hold by metal-acrylic piece installed onto the sectioning saw

3.2.2. Monolithic Zirconia Samples

Z samples were designed onto solid disc by computer aided design (CAD) (Ceramill Mind 1.0 software, Amann Girrbach GmbH, Pforzheim, Germany) (Figure 3.10.) and forty samples dry milled from 16 mm thick disc by computer aided manufacturing (CAM) with 5 axis milling unit (Ceramill Motion 2; Amann Girrbach GmbH, Pforzheim, Germany) (Figure 3.11. and Figure 3.12.). Samples were designed %25 bigger than the desired final dimensions (Figure 3.13.).

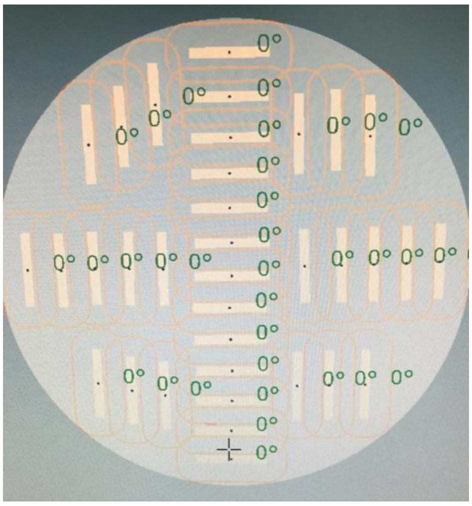

Figure 3.10. Samples designed onto disc by Ceramill Mind 1.0 software, Amann Girrbach GmbH, Pforzheim, Germany

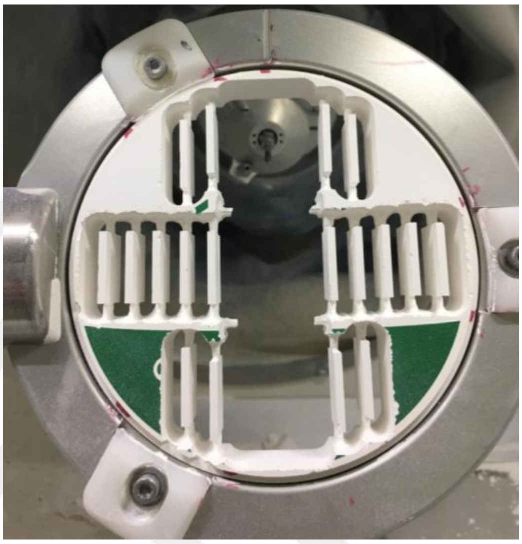

Figure 3.11. and Figure 3.12. Disc milled by Ceramill Motion 2,
Amann Girrbach GmbH, Pforzheim, Germany

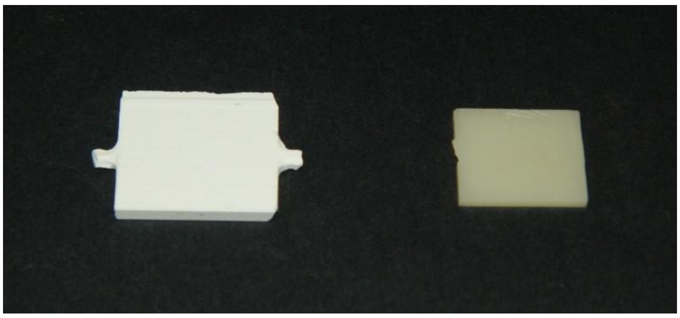

Figure 3.13. Z sample milled %25 bigger than desired dimensions

3.2.3. Sinterization of the Monolithic Zirconia Samples

After the dry milling step, samples were sintered at maximum 1450^{o}C according to the manufacturer’s instructions (HT Speed Sintering Furnace; MIHM-VOGT GmbH & Co., Stutensee, Germany) (Figure 3.14., Figure 3.15. and Figure 3.16.). Sintered samples were ready to grinding and polishing step.

Figure 3.14. and Figure 3.15. Before and after the sintering process

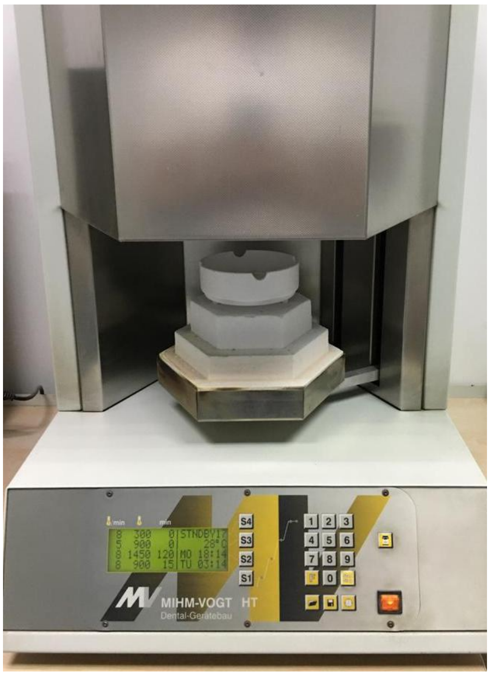

Figure 3.16. HT Speed Sintering Furnace, MIHM-VOGT GmbH & Co., Stutensee, Germany

3.2.4. Grinding Step

Sintered Z and uncrystallized E and C samples were polished under water-cooling on an automatic polishing machine at 600 rpm (Ecomet 250, Buehler, Lake Bluff, Illinois) (Figure 3.17.) with 600-800-1200-2500 grit silicon carbide papers (Waterproof Silicon Carbide Paper 188, English Abrasives & Chemicals Ltd., Stafford, UK; Buehler-Met II Silicon Carbide Grinding Paper, Buehler, Lake Bluff, Illinois) (Figure 3.18., Figure 3.19. and Figure 3.20.). Final thickness was measured with digital caliper (Digital ABS AOS Caliper, Mitutoyo Corp., Kanagawa, Japan) between polishing steps (Figure 3.21.). Material thickness was adjusted to 1.5 mm (± 0.2 mm) since complete crown was simulated. Similarly Arif et al.[296] studied the same thickness for complete crowns in a research.

Figure 3.17. Ecomet 250 automatic polishing machine, Buehler, Lake Bluff, Illinois

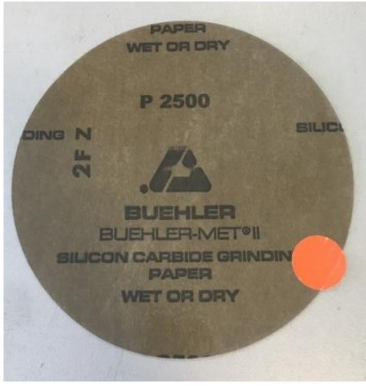

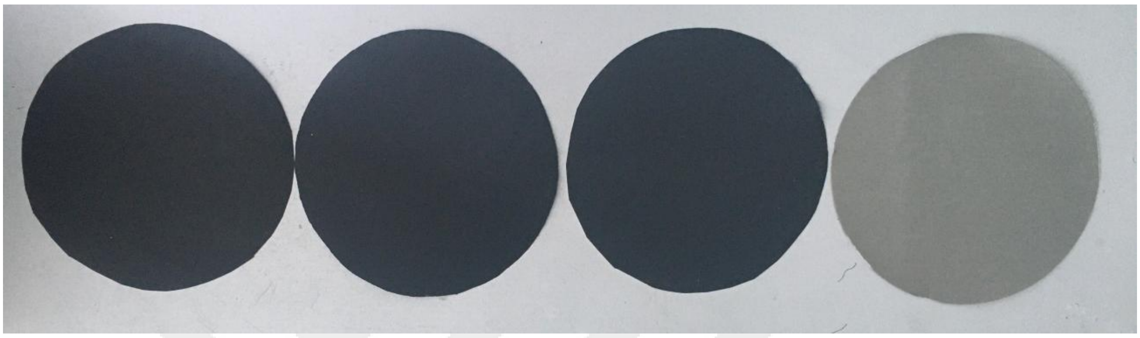

Figure 3.18., Figure 3.19. and Figure 3.20. 600- 800- 1200- 2500 grit silicon carbide papers (English Abrasives & Chemicals Ltd., Stafford, UK; Buehler, Lake Bluff, Illinois)

Figure 3.21. Digital caliper (Mitutoyo Corp., Kanagawa, Japan) measuring final thickness as 1.50 mm

3.2.5. Crystallization of the Lithium Disilicate and Zirconia Reinforced Lithium Silicate Samples

Polished E and C samples were crystallized by two furnaces (Programat P500, Ivoclar Vivadent, Schaan, Lichtenstein; Focus 2010 High Precision Dental Furnace, Shenpaz, Tel Aviv, Israel) according to manufacturer’s instructions. (Figure 3.22., Figure 3.23., Figure 3.24. and Figure 3.25.)

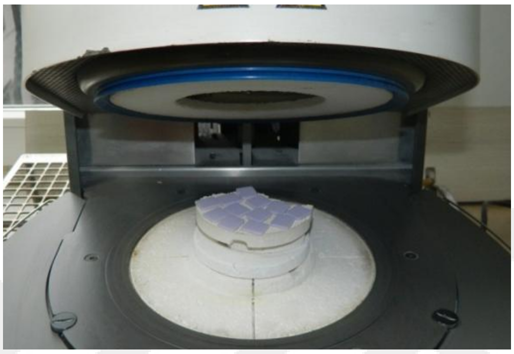

Figure 3.22. E samples before crystallization
with Programat P500, Ivoclar Vivadent, Schaan, Lichtenstein

Figure 3.23. E samples after crystallization with

Programat P500, Ivoclar Vivadent, Schaan, Lichtenstein

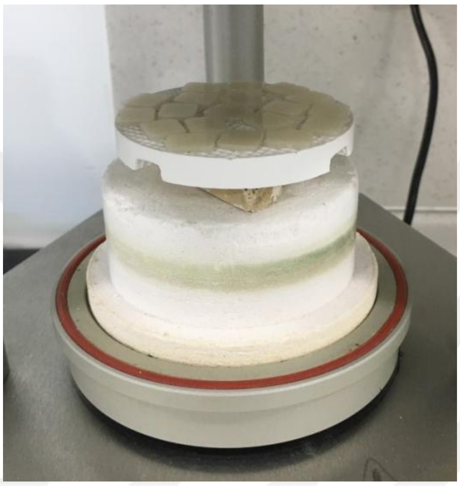

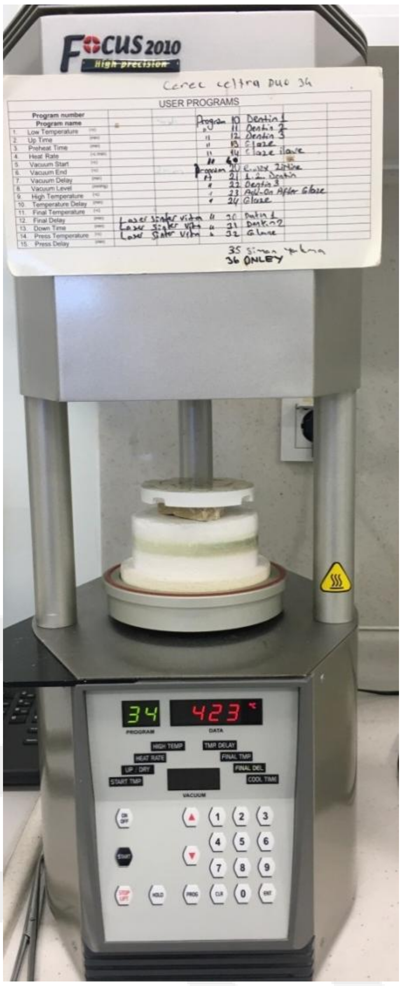

Figure 3.24. and Figure 3.25. C samples before and after crystallization with Focus 2010 Furnace, Shenpaz, Tel Aviv, Israel

3.2.6. Intra Oral Polishing Step and Cleaning of Samples

A marker was made with diamond round burr on the unpolished surface of all samples in order to determine which side has been the polished side of a sample. Then, unmarked side of all samples was polished with 3 step intraoral polishing kit (Optra Fine Intra Oral Polishing Kit, Ivoclar Vivadent, Schaan, Liechtenstein) (Table 3.3.).

Table 3.3. Optra Fine Intra Oral Polishing Kit

Step	Cooling	Lot Number	Speed and Application Time	Content
Finishing Step Light Blue Rubber Tip	Air & Water	ZL005B	Max 15.000 rpm for 30 seconds	Synthetic rubber, diamond granulate, titanium dioxide, stainless steel attachment
Polishing Step Dark Blue Rubber Tip				
High Polishing Step HP Polishing Paste Applied with Nylon Brush	Air		Max 10.000 rpm (5.000-7.000 rpm recommended speed) for 30 seconds	Paste: Diamond dust (2-4 µm), glycerine, sodium lauryl sulphate, propylene glycol Brush: Nylon fibers, stainless steel attachment

First step is finishing with light blue colored rubber tips, second step is polishing with dark blue colored rubber tips, and third step is high polishing with Optra Fine HP Polishing Paste and plastic brush (Figure 3.26.). First two steps were applied under water and air cooling with 15.000 rpm, third step was applied under just air cooling with 7.000 rpm contra-angled hand piece and micro motor (WD-79M, W&H, Salzburg, Austria; EA-51 LT, A-dec, Newberg, Oregon) (Figure 3.27.).

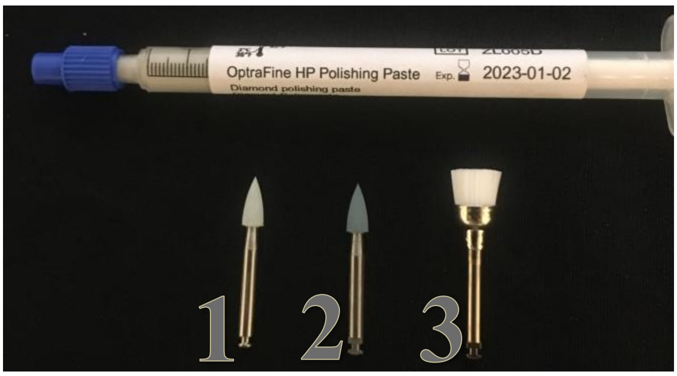

Figure 3.26. Optra Fine 3 step intra oral polishing kit, Ivoclar Vivadent, Schaan, Liechtenstein

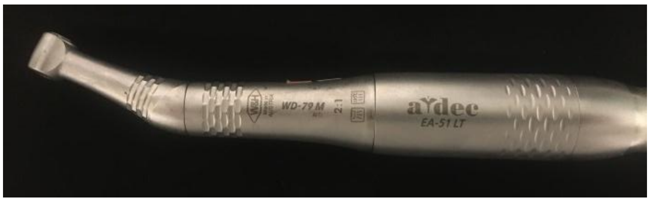

Figure 3.27. Contra-angled hand piece and micro motor (W&H, Salzburg, Austria; A-dec, Newberg, Oregon)

Each step was applied for 30 seconds, 15 seconds in one direction and 15 seconds in another direction - 90^{o} angle relative to the first direction - as manufacturer's instructions. Each sample was subjected to 90 seconds of total finishing and polishing time. Polishing was performed by same operator in order to obtain standardized polishing for all samples as much as possible.

All samples were cleaned ultrasonically (AS 8772 Ultrasonic Cleaner, General Home Orsay Ltd. Şti., İstanbul, Turkey) in distilled water for 20 minutes (Figure 3.28.) after all polishing procedures completed, distributed into subgroups and stored in clean distilled water at room temperature until all baseline measurements have been done.

Figure 3.28. Samples cleaned in distilled water for 20 minutes with ultrasonic cleaner (AS 8772 Ultrasonic Cleaner, General Home Orsay Ltd. Şti., İstanbul, Turkey)

3.2.7. Subgroup Formations

Forty samples of each material were divided into two subgroups as blumia nervosa group and control group. Total of 6 subgroups were obtained (n=18), two extra samples were assigned for SEM imaging and 3D optical profilometer evaluation. Six plastic boxes with color identified covers, each material type having different color, and stands made from plexi glass to hold samples upright have been prepared in order to store samples properly exposed to poured solutions (Figure 3.29., Figure 3.30. and Figure 3.31.). Plastic boxes and plexi glass stands were chosen as acid resistant.

Figure 3.29. Plastic box and upright standing samples via plexi glass holder

Figure 3.30 and Figure 3.31. Different color coded boxes

3.3. Solution Preparations

Two different solutions were prepared at Yeditepe University Faculty of Pharmacy as blumic (blumia nervosa solution) and control (artificial saliva solution) subgroups. Blumic subgroup was simulated under the conditions of 1.6 pH and 37°C. The control group which is control subgroup was simulated under the conditions of 7 pH and 37°C. Each solution's formula and pH has been demonstrated in Table 3.4. (Figure 3.32. and Figure 3.33.).

Table 3.4. Solution formulas and pH's table

Solution Name	pH	Temperature	Formula
Blumic Subgroup (Blumia Nervosa Solution)	1.6	37°C	0,5 g NaCl + 6 mol/L HCl + 99,5 mL distilled water[153]
Control Subgroup (Artificial Saliva Solution)	7		1,3 g NaCl + 0,03 g $MgCl_2.6H_2O$ + 0,08 g $CaCl_2.2H_2O$ + 0,3 g KCl + 0,9 g KOH + 472 µL H_3PO_4

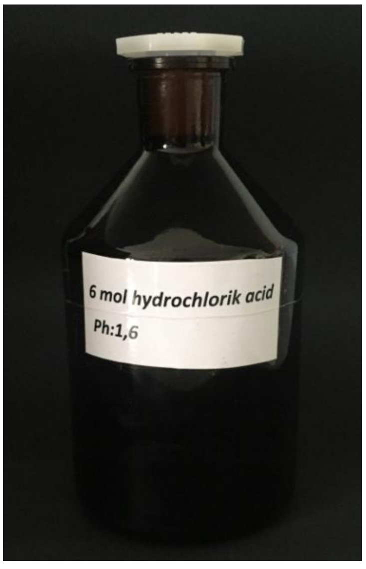

Figure 3.32. Blumia Nervosa Solution (Blumic Subgroup Solution)

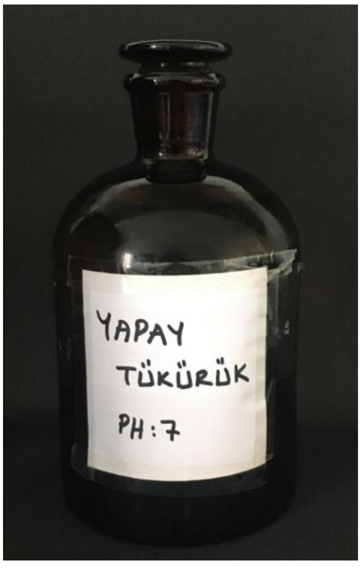

Figure 3.33. Artificial Saliva Solution (Control Subgroup Solution)

The pH’s of blumia nervosa solution and artificial saliva solutions were measured with digital pH meter (MP220 pH Meter, Mettler Toledo, Greifensee, Switzerland) (Figure 3.34.) and adjusted to 1.6 pH and 7 pH, respectively. Samples were aligned onto stands and then solutions were poured into the assigned box. The pH of every solution was checked every day along the immersion period and boxes were kept in incubator (Memmert BE 500 Incubator, Memmert GmbH + Co. KG, Schwabach, Germany) at 37^{o}C (Figure 3.35.). When the experiment time was completed, samples were taken out of solutions and rinsed under tap water for few seconds, placed onto tissues and wiped gently. Then, T1 measurements have been completed.

Figure 3.34. MP 220 Digital pH meter, Mettler Toledo, Greifensee, Switzerland

Figure 3.35. Samples stored in the incubator at 37ºC
(Memmert BE 500 Incubator, Memmert GmbH + Co. KG, Schwabach, Germany)

3.4. Measurements

Measurements were made at T0 and T1 times.

Baseline (T0) measurements were made before the samples were immersed in prepared solutions and demonstrated the initial optical and mechanical characteristics of samples. Color, translucency, surface roughness, surface microhardness, fracture toughness and surface topography were examined at T0 measurements.

T1 measurements were made after the time simulating five years of blumia nervosa exposure. In our study, average purging number in a day was selected as 8 times.[153] Effect of exposure period was revealed as 2 minutes conformed to the length of pH decline in saliva after an acid attack.[153,297] The exposure time to vomit for patients who have blumia nervosa for five years equals to 486.5 hours totally (approximately 20.2 days). The pH of the immersion solution was selected as 1.6 regarding that the physiologic pH of gastric juice after a complete meal is 1.6 pH.[165] Control groups were stored in artificial saliva until the experiment has been done. Changes in color, translucency, surface roughness, surface microhardness, fracture toughness and surface topography were examined at T1 measurements.

Summary of study design and measurement protocol is shown in Figure 3.36.

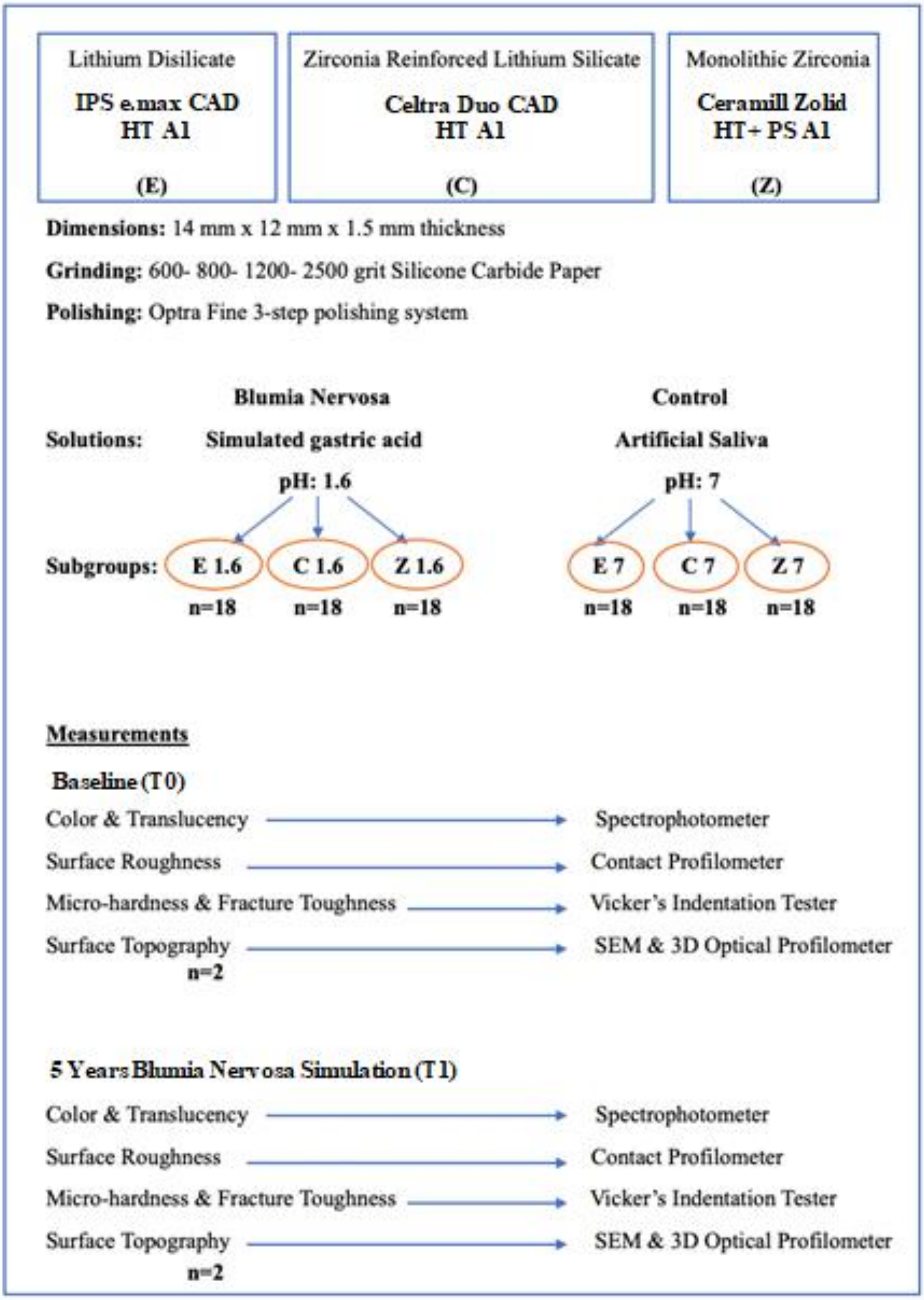

Figure 3.36. Summary of study design

3.4.1. Color Measurements

The color of the samples was analyzed before and after the solution exposure by using a spectrophotometer (CM-2600d, Konica Minolta, Tokyo, Japan) (Figure 3.37.) based on the CIELab system on a white background (L* 99.41, a* -0.09, b* -0.13) and measurement have been done on the center of polished surface of the sample (Figure 3.38.). Three measurements have been done on one sample and arithmetical mean was calculated by the software (Spectra Magic 3.1; Konica Minolta, Tokyo, Japan) (Figure 3.39.). Device has been calibrated before starting the measurement of each subgroup. ΔE, L*, a* and b* values were calculated. The color change (ΔE) between T0 and T1 was calculated by using the following equation:

$$\Delta E = [\ (\Delta L^*)^2 + (\Delta a^*)^2 + (\Delta b^*)^2\ ]^{1/2},$$

where L* is the lightness coefficient, ranging from black (=0) to white (=100), positive a* value indicates redness and negative a* value indicates greenness, and positive b* value indicates yellowness and negative b* value indicates blueness. In this study, ΔE higher than 3.5 was considered as clinically unacceptable.[116]

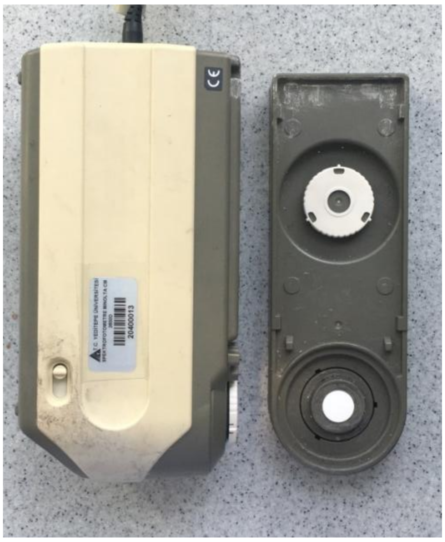

Figure 3.37. and Figure 3.38. Spectrophotometer (CM-2600d, Konica Minolta, Tokyo, Japan) and sample positioned on the center of white background

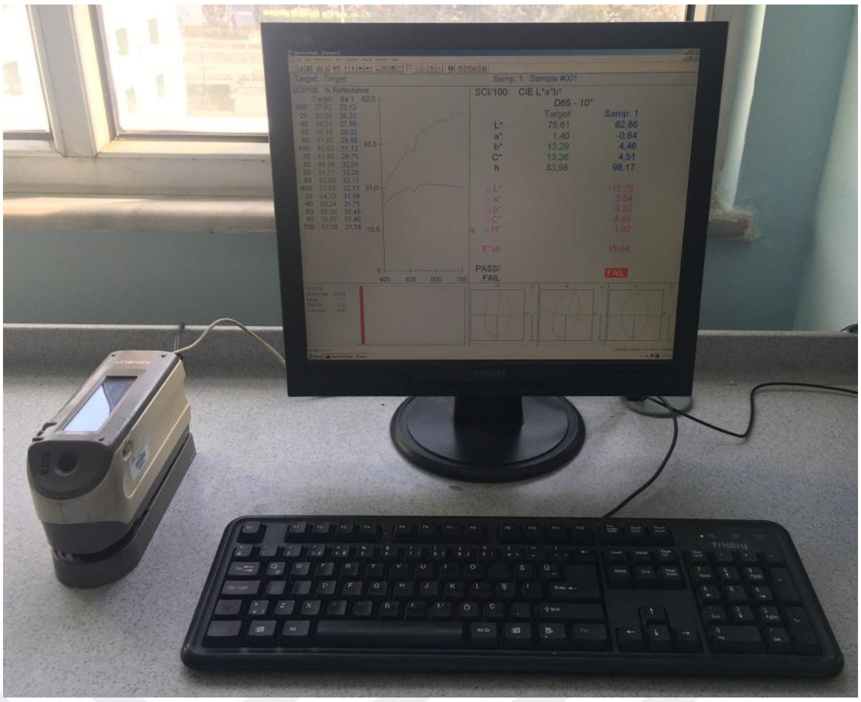

Figure 3.39. Spectrophotometer set up and
Spectra Magic 3.1 Software, Konica Minolta, Tokyo, Japan

3.4.2. Translucency Measurements

Sample translucency was determined with translucency parameter (TP). Same spectrophotometer (CM-2600d; Konica Minolta, Tokyo, Japan) was used for measurements. TP was determined by measuring the color difference of the sample over the white (L* 99.41, a* -0.09, b* -0.13) and black (L* 27.22, a* 0.01, b* 0.09) backgrounds (Figure 3.40. and Figure 3.41.) with the following formula[298]:

$$TP = [\ (L^*_W - L^*_B)^2 + (a^*_W - a^*_B)^2 + (b^*_W - b^*_B)^2\ ]^{1/2},$$

where subscript B refers to the color coordinates over the black background and subscript W refers to the color coordinates over the white background. If a material is totally opaque, the TP value is 0. While increased TP value means increased translucency of the material. Translucency difference in TP (ΔTP) value more than 2 was accepted visually perceptible in the study.[290] ΔTP was calculated as subtracting TP_{T0} from TP_{T1} ($\Delta TP = TP_{T1} - TP_{T0}$).

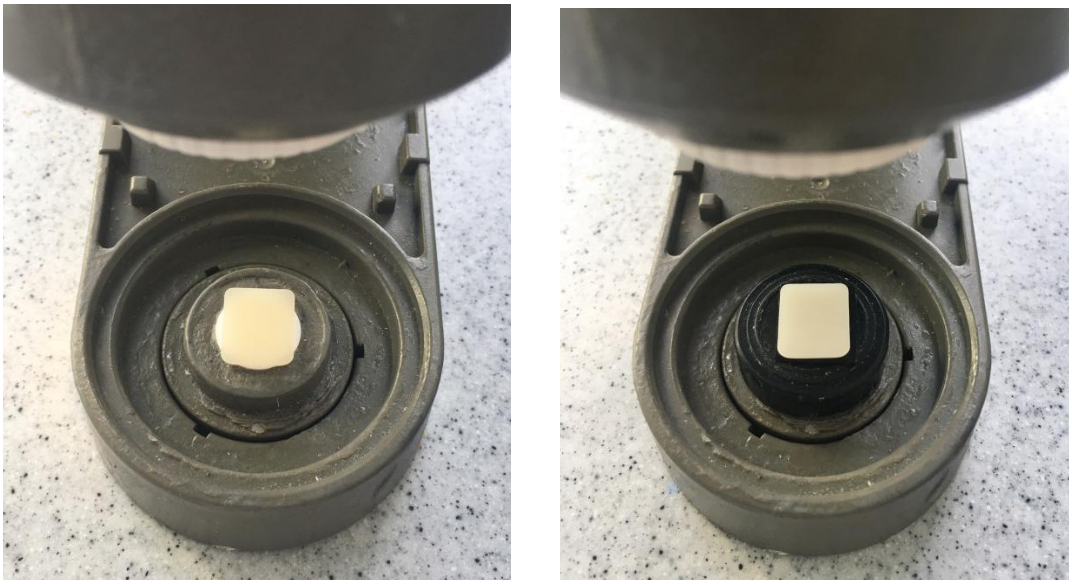

Figure 3.40. and Figure 3.41. Sample over white and black backgrounds

3.4.3. Surface Roughness Measurements

Surface roughness of the sample was assessed as Ra value (μm) by a contact profilometer (Perthometer M1, Mahr GmbH, Ingolstadt, Germany) (Figure 3.42.) set with 0.25 mm cutoff value, 0.5 mm/s stylus speed and 1.75 mm traversing length (Figure 3.43.). Three measurements on three different locations were made on the center of each sample to obtain the average surface roughness (Figure 3.44.). Calibration of the profilometer was performed using a standard reference specimen at the beginning of each subgroup's measurement. Mean of three R_a values of a sample was calculated. Ra values were recorded and compared between T0 and T1. Surface roughness difference (ΔRa) was calculated as subtracting Ra_{T0} from Ra_{T1} ($\Delta Ra = Ra_{T1} - Ra_{T0}$). Jones et al.[106] found that patients started to feel discomfort when the Ra value was higher than 0.5 μm. Bollen et al.[102] found that bacterial retention and biologic complications were appeared when the Ra value was higher than 0.2 μm. In the light of these informations, Ra higher than 0.2 μm was accepted as clinically unacceptable.

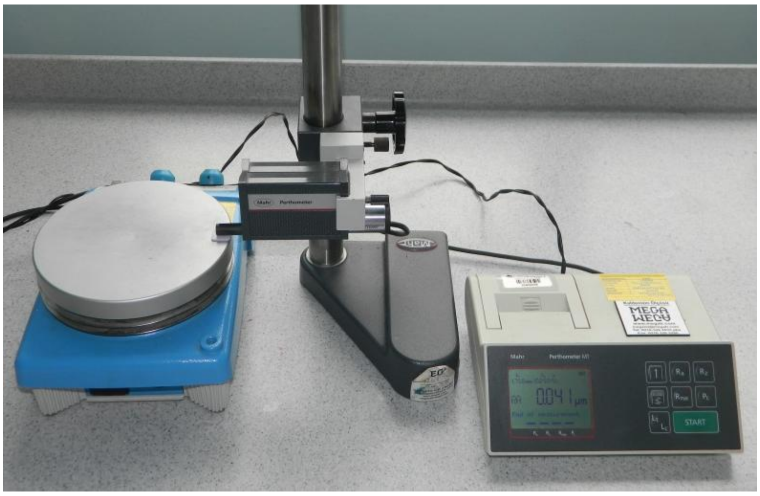

Figure 3.42. Contact profilometer (Perthometer M1, Mahr GmbH, Ingolstadt, Germany)

Figure 3.43. Settings of contact profilometer

Figure 3.44. Measuring the surface roughness on the center of a sample

3.4.4. Surface Microhardness Measurements

Surface microhardness was determined with a microhardness tester equipped with Vickers diamond indentation tip (Micromet 5114D, Buehler, Lake Bluff, Illinois) (Figure 3.45.) by the Vickers indentation technique under a load of 1 kg.f (9.8 N) for 15 second dwell time as indicated with ASTM C1327 Test Method for Vickers Indentation Hardness of Advanced Ceramics[230]. Five indentations were made on each sample at least 0.5 millimeters apart from each other using a Vickers diamond indenter to determine the mean microhardness value for each sample (Figure 3.46.). Dimensions of indentation marks were measured using the eyepiece of a microscope (Figure 3.47. and Figure 3.48.), and Vickers Hardness Number (VHN) values were calculated according to the following equation[230]:

$$VHN=1854.4 \times P / (d_1 x d_2),$$

where P is the load in g.f, while d_1 and d_2 are diameters of the mark of Vicker's indentation in micrometers (µm) (Figure 3.49.). Surface microhardness difference (ΔVHN) was calculated as subtracting VHN_{T0} from VHN_{T1} ($\Delta VHN = VHN_{T1} - VHN_{T0}$).

Figure 3.45. and Figure 3.46. Microhardness tester equipment (Micromet 5114D, Buehler, Lake Bluff, Illinois) and indentation made on the center of sample

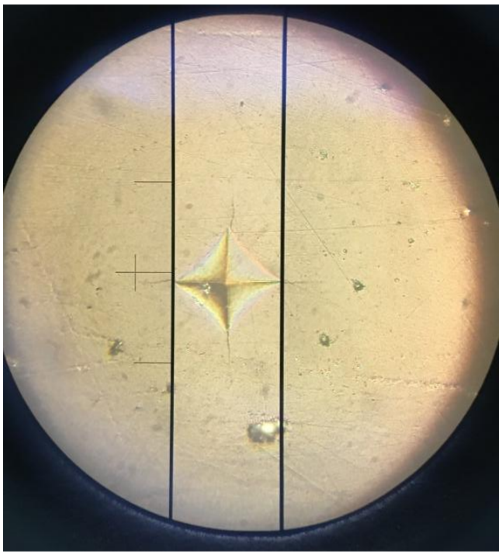

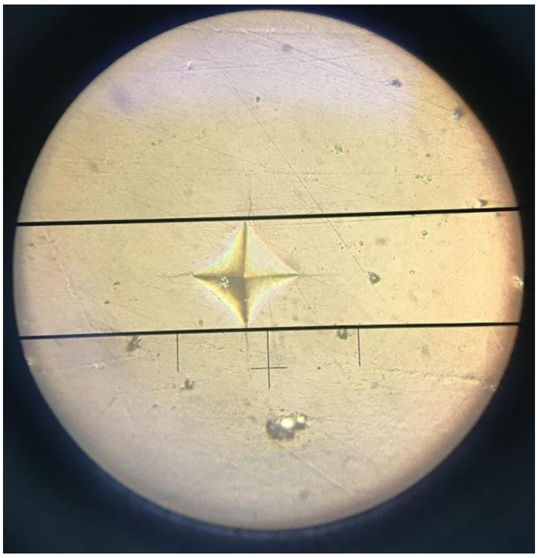

Figure 3.47. and Figure 3.48. Vickers indentation mark and border lines to measure d_1 and d_2 distance

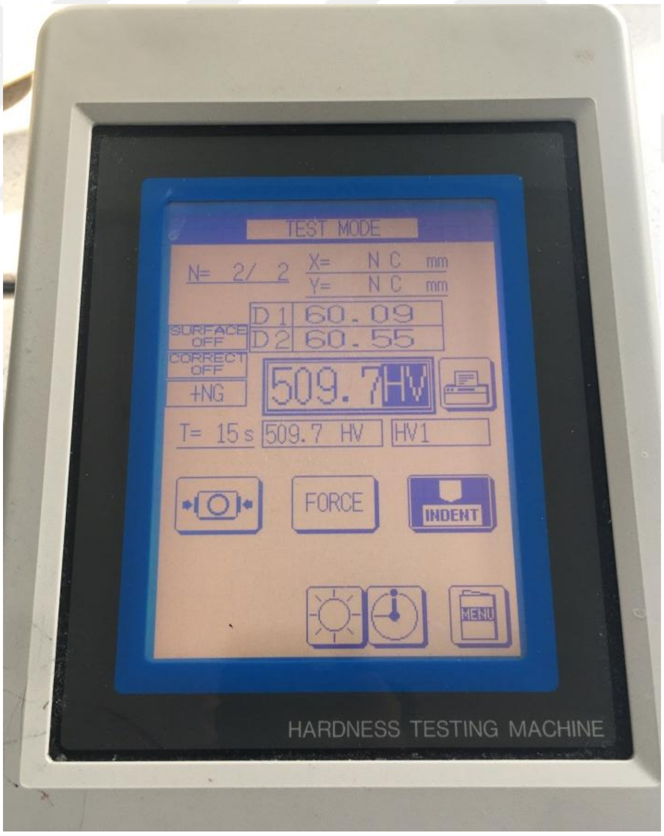

Figure 3.49. Screen showing the calculation of the Vickers Hardness Number (VHN)

3.4.5. Fracture Toughness Measurements

This measurement involves making a Vickers hardness indentation with sufficient load on the surface of a ceramic material in order to generate radial cracks arising from the indentation corners (Figure 3.50. and Figure 3.51.). On this study, in order to make comparison among different materials, indentation fracture toughness (K_{Ic}) was calculated according to the formula below[236];

$$K_{Ic} = (0.0824 \text{ x } P/c^{3/2})$$

where P is load in kg.f and c is the crack length in millimeters (mm). 1 kg.f load was applied for 15 seconds[232], then the cracks were observed and measured with microscope, mean values of five different indentation crack lengths were recorded. P and mean of five c values for one sample put into the formula and K_{Ic} value was obtained as MPa.m1/2. Fracture toughness difference (ΔK_{Ic}) was calculated as subtracting $K_{Ic\text{-}T0}$ from $K_{Ic\text{-}T1}$ ($\Delta K_{Ic} = K_{Ic\text{-}T1} - K_{Ic\text{-}T0}$).

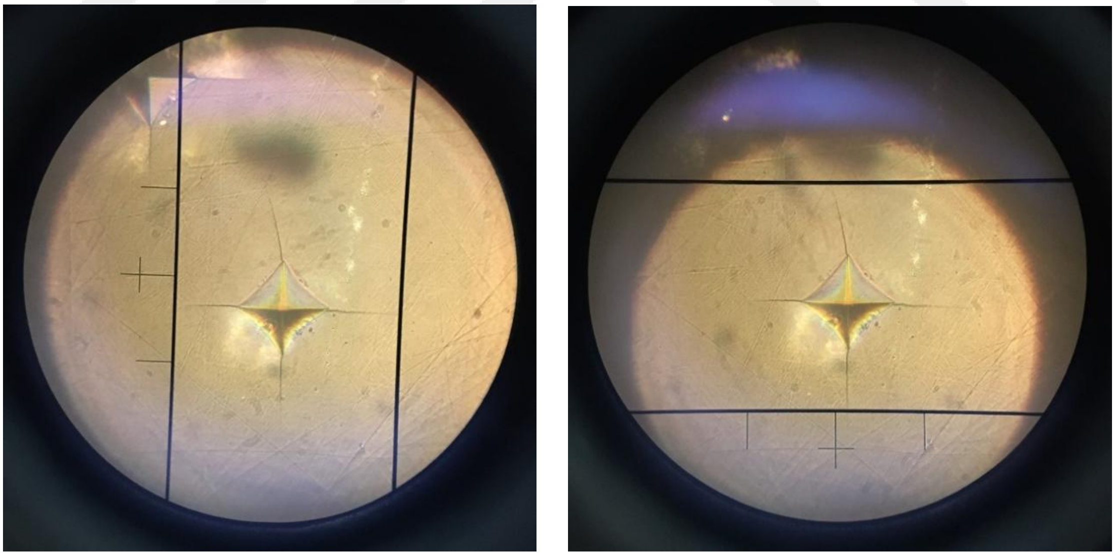

Figure 3.50. and Figure 3.51. Cracks formed on a sample by indentation

3.4.6. Surface Topography

Two extra samples from each group were prepared for surface morphology analysis, one for SEM imaging and one for 3D optical profilometer.

Samples were secured onto microscope slide with gold conducting tape and were gold-sputtered in a vacuum sputter coater (SCD 005 Sputter Coater, Bal-Tec, Balzers, Liechtenstein) (Figure 3.52.). Then, samples were examined by using scanning electron microscope (SEM) (EVO 40, Carl Zeiss Microscopy, Oberkochen, Germany) (Figure 3.53. and Figure 3.54.) at x1000, x5000 and x 10.000 magnification. Then, the images were compared with each other and qualitative evaluations of surface topography were made.

Figure 3.52. Vacuum sputter coater
(SCD 005 Sputter Coater, Bal-Tec, Balzers, Liechtenstein)

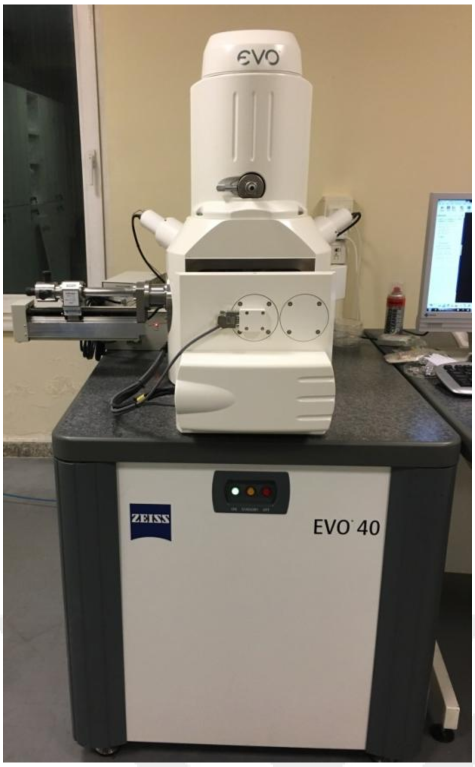

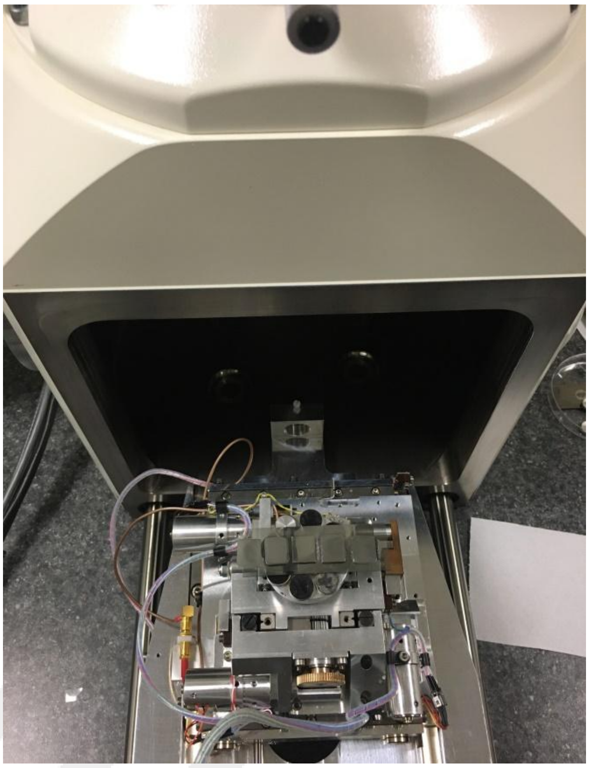

Figure 3.53. and Figure 3.54. Scanning electron microscope
(EVO 40, Carl Zeiss Microscopy, Oberkochen, Germany) and positioning of samples for examination

Besides these methods, surface topography and surface roughness was observed with 3D optical surface profilometer (Nanomap-500LS, AEP Technology, Santa Clara, California, USA) (Figure 3.55.) as two dimensional and three dimensional imaging under the white light interferometry and analysis was made by a software (Digital Surf version no 6.1.6001, TalyMap Platinum software, Leicester, England). Images were compared with each other for qualitative surface topography changes.

Figure 3.55. 3D Optical Profilometer
(Nanomap-500LS, AEP Technology, Santa Clara, California, USA)

3.5. Statistical Analysis

Data were analyzed with IBM SPSS Statistics 22 (IBM SPSS, Turkey). Normal distribution was evaluated with Kolmogorov-Smirnov and Shapiro-Wilks tests, and data were found normally distributed. Descriptive statistics of continuous data has shown as mean ± standard deviation, median, minimum and maximum. The effects of material and solution on surface roughness, surface microhardness, fracture toughness, color parameters (L*,a*, b*) and translucency parameter at T0 and T1 were evaluated with Repeated Measures Two-way ANOVA test. The differences between materials were evaluated with One-way ANOVA test. In differences found statistically significant, post hoc Tukey HSD test was used if the variances were homogenous and post hoc Tamhane's T2 test was used if the variances were not homogenous. T0-T1 differences were evaluated with Paired Samples t test. The effects of material and solution on the changes of surface roughness (ΔRa), surface microhardness (ΔVHN), fracture toughness (ΔK_{Ic}), color parameters (ΔE) and translucency parameter (ΔTP) were evaluated with Two-way ANOVA test. If $p<0.05$, the difference is statistically significant.

4. RESULTS

4.1. Mechanical Properties

Surface roughness, surface microhardness, fracture toughness and surface topography parameters were evaluated.

4.1.1. Surface Roughness

Average surface roughness (Ra) value was evaluated among three different CAD-CAM materials [IPS e.max CAD (E), Celtra Duo CAD (C) and Ceramill Zolid HT+ (Z)] on baseline (T_0) and after the immersions in two different solutions (T_1). Ra changes from T_0 to T_1 (ΔRa) were evaluated based on material and solution. Higher Ra value in ‘μm’ means that the material is rougher.

Descriptive statistics on surface roughness of six subgroups before and after the solution exposures were shown at Table 4.1.

Table 4.1. Descriptive statistics on surface roughness (μm) of six subgroups before and after the solution exposures

Surface Roughness (Ra)		n	x̄	SD	Min.	Max.	Median	Skewness	SE of Mean
T0 Ra	IPS e.max Blumic Subgroup	18	0,045	0,010	0,022	0,056	0,045	-0,989	0,002
	Celtra Duo Blumic Subgroup	18	0,030	0,006	0,022	0,040	0,0305	0,188	0,001
	Ceramill Zolid Blumic Subgroup	18	0,022	0,005	0,015	0,030	0,0215	0,188	0,001
	IPS e.max Control Subgroup	18	0,039	0,007	0,031	0,055	0,038	0,679	0,002
	Celtra Duo Control Subgroup	18	0,026	0,004	0,016	0,033	0,0265	-0,493	0,001
	Ceramill Zolid Control Subgroup	18	0,030	0,008	0,016	0,043	0,0315	-0,294	0,002
T1 Ra	IPS e.max Blumic Subgroup	18	0,049	0,010	0,032	0,067	0,0485	0,136	0,002
	Celtra Duo Blumic Subgroup	18	0,034	0,006	0,023	0,043	0,034	-0,224	0,001
	Ceramill Zolid Blumic Subgroup	18	0,025	0,007	0,016	0,038	0,024	0,376	0,002
	IPS e.max Control Subgroup	18	0,042	0,009	0,029	0,058	0,04	0,365	0,002
	Celtra Duo Control Subgroup	18	0,028	0,003	0,022	0,034	0,028	-0,126	0,001
	Ceramill Zolid Control Subgroup	18	0,030	0,006	0,020	0,040	0,0305	-0,049	0,001
ΔRa	IPS e.max Blumic Subgroup	18	0,004	0,005	-0,004	0,016	0,0035	0,573	0,001
	Celtra Duo Blumic Subgroup	18	0,004	0,003	0,000	0,011	0,004	0,303	0,001
	Ceramill Zolid Blumic Subgroup	18	0,004	0,003	-0,001	0,009	0,003	0,135	0,001
	IPS e.max Control Subgroup	18	0,002	0,003	-0,004	0,007	0,0015	-0,042	0,001
	Celtra Duo Control Subgroup	18	0,002	0,004	-0,005	0,006	0,004	-0,717	0,001
	Ceramill Zolid Control Subgroup	18	0,000	0,004	-0,006	0,005	0,0005	-0,177	0,001

4.1.1.1. Baseline (T_0) Surface Roughness (Ra) Evaluations among CAD-CAM Materials

Statistics for baseline (T_0) surface roughness (Ra) measurements were shown at Table 4.2.

Table 4.2. Baseline surface roughness (µm) evaluations among different materials and solutions.

Solution	Ra	IPS e.max CAD (E) x̄ ± SD	Celtra Duo CAD (C) x̄ ± SD	Ceramill Zolid HT+ (Z) x̄ ± SD	p
1.6 pH	**T_0**	0,045±0,01	0,030±0,006	0,022±0,005	0,000*
7 pH	**T_0**	0,039±0,007	0,026±0,004	0,030±0,008	0,000*

One-way ANOVA Test **p<0.05*

It was revealed that; the mean of baseline Ra values of three different materials assigned to blumic subgroups (1.6 pH) were found significantly different (p=0.000). The Ra values are ordered as; IPS e.max (0,045±0,01) > Celtra Duo (0,030±0,006) > Ceramill Zolid (0,022±0,005). Mean Ra of IPS e.max was found significantly higher than Celtra Duo and Ceramill Zolid (p=0.000, p=0.000 respectively); and mean Ra of Celtra Duo was found significantly higher than Ceramill Zolid (p=0.003) according to post-hoc Tukey Test.

The mean of baseline Ra values of three different materials assigned to control subgroups (7 pH) were found significantly different (p=0.000). The Ra values are ordered as; IPS e.max (0,039±0,007) > Ceramill Zolid (0,030±0,008) > Celtra Duo (0,026±0,004). Similarly, mean Ra of IPS e.max was found significantly higher than Celtra Duo and Ceramill Zolid (p=0.000, p=0.003 respectively). However, there is no statistically significant difference between the mean Ra values of Celtra Duo and Ceramill Zolid (p=0.140) according to post-hoc Tamhane's T2 Test.

4.1.1.2. Surface Roughness (Ra) Evaluations After Solution Exposures (T_1) Among CAD-CAM Materials

Statistics for T_1 surface roughness (Ra) measurements were shown at Table 4.3.

Table 4.3. Surface roughness (μm) evaluations among different materials and solutions at T_1.

Solution	Ra	IPS e.max CAD (E)	Celtra Duo CAD (C)	Ceramill Zolid HT+ (Z)	p
		$\bar{x} \pm SD$	$\bar{x} \pm SD$	$\bar{x} \pm SD$	
1.6 pH	**T_1**	0,049±0,01	0,034±0,006	0,025±0,007	0,000*
7 pH	**T_1**	0,042±0,009	0,028±0,003	0,030±0,006	0,000*

One-way ANOVA Test **p<0.05*

The mean Ra values of three different materials assigned to blumic subgroups (1.6 pH) at T_1 were found significantly different (p=0.000). The Ra values are ordered as; IPS e.max (0,049±0,01) > Celtra Duo (0,034±0,006) > Ceramill Zolid (0,025±0,007). Mean Ra of IPS e.max was found significantly higher than Celtra Duo and Ceramill Zolid (p=0.000, p=0.000 respectively) at T_1; and mean Ra of Celtra Duo was found significantly higher than Ceramill Zolid (p=0.003) at T_1 according to post-hoc Tukey Test.

The mean Ra values of three different materials assigned to control subgroups (7 pH) at T_1 were found significantly different (p=0.000). The Ra values are ordered as; IPS e.max (0,042±0,009) > Ceramill Zolid (0,030±0,006) > Celtra Duo (0,028±0,003). Similarly, mean Ra of IPS e.max was found significantly higher than Celtra Duo and Ceramill Zolid (p=0.000, p=0.001 respectively) at T_1. However, there is no statistically significant difference between the mean Ra values of Celtra Duo and Ceramill Zolid (p=0.587) at T_1 according to post-hoc Tamhane's T2 Test.

4.1.1.3. Surface Roughness (Ra) Evaluations of Each Subgroup Before and After the Solution Exposure (T_0-T_1)

All subgroups except control subgroup of Ceramill Zolid were found significantly affected by the respective solution exposures (Table 4.4.).

Table 4.4. Ra (µm) evaluations of six subgroups before and after (T_0-T_1) the solution exposure.

Solution	Ra	IPS e.max CAD (E)	Celtra Duo CAD (C)	Ceramill Zolid HT+ (Z)
		$\bar{x}$ ± SD	$\bar{x}$ ± SD	$\bar{x}$ ± SD
1.6 pH	**T_0**	0,045±0,01	0,030±0,006	0,022±0,005
	T_1	0,049±0,01	0,034±0,006	0,025±0,007
	p	0,007*	0,000*	0,000*
7 pH	**T_0**	0,039±0,007	0,026±0,004	0,030±0,008
	T_1	0,042±0,009	0,028±0,003	0,030±0,006
	p	0,012*	0,019*	1,000

Paired Samples t test **p<0.05*

The increases in mean surface roughness (Ra) values from T_0 to T_1 caused by blumic solution (1.6 pH) were statistically significant for IPS e.max, Celtra Duo and Ceramill Zolid (p=0.007, p=0.000, p=0.000 respectively). The increases in mean surface roughness (Ra) values from T_0 to T_1 on control solution (7 pH) were statistically significant for IPS e.max and Celtra Duo (p=0.012, p=0.019 respectively) samples; however control solution (7 pH) was not significantly affected the mean surface roughness (Ra) value between T_0 and T_1 on Ceramill Zolid samples (p=1.000).

4.1.1.4. Comparison of Surface Roughness Changes (ΔRa) on Different CAD-CAM Materials Exposed to Different Solutions

Surface roughness change (ΔRa) of a material is observed by two parameters; different solutions and different materials and the results are shown in Table 4.5.

Table 4.5. ΔRa (µm) Evaluation on Different Materials and Solutions

	ΔRa		
	1.6 pH	**7 pH**	
Material	**x̄ ± SD**	**x̄ ± SD**	**p**
IPS e.max (E)	0,0039±0,005	0,0022±0,003	0,255
Celtra Duo (C)	0,0042±0,003	0,0023±0,004	0,123
Ceramill Zolid (Z)	0,0037±0,003	0±0,004	0,004*
p	0,920	0,115	

Two-way ANOVA Test **p<0.05*

When the blumic solution's effect on surface roughness change (ΔRa) among three different materials were evaluated, no statistically significant differences were found (p=0.920). The effect of control solution on surface roughness change (ΔRa) among three different materials was not statistically significant either (p=0.115).

A comparison was made on the surface roughness change (ΔRa) of a material affected by two different solutions. The ΔRa values of IPS e.max and Celtra Duo blumic subgroups (0,0039±0,005; 0,0042±0,003 respectively) were found higher than control subgroups (0,0022±0,003; 0,0023±0,004 respectively). However, the ΔRa value differences between two solutions on these materials were not statistically significant (p=0.255, p=0.123 respectively). The ΔRa value of Ceramill Zolid samples exposed to blumic solution (0,0037±0,003) was higher than those exposed to control solution (0±0,004). The difference was statistically significant (p=0.004) (Figure 4.1.).

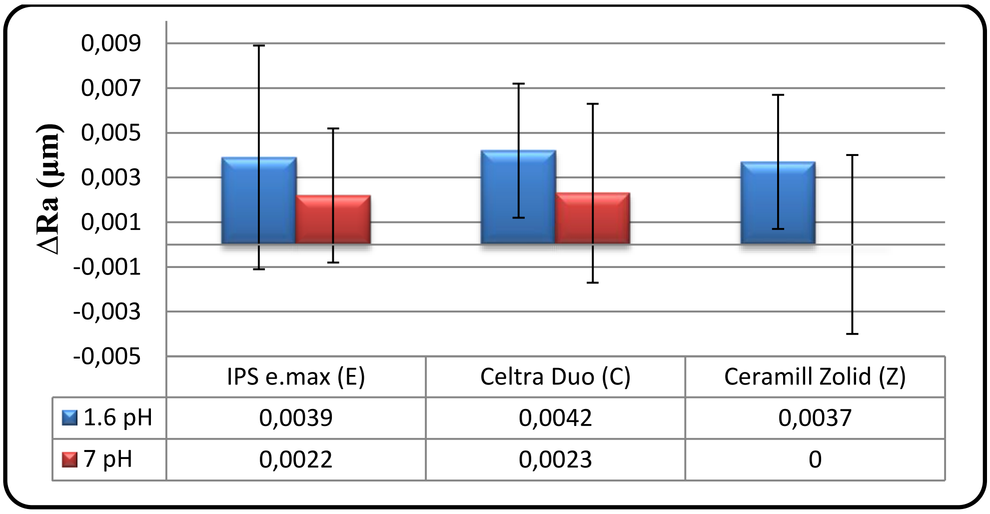

Figure 4.1. Surface roughness change evaluations on different materials and solutions

When the influences of material type, solution pH and their interactions on surface roughness change (ΔRa) were evaluated with the two-way analysis of variance, the results were found as seen on Table 4.6.

Table 4.6. Evaluation of the common effect of material and solution on ΔRa

ΔRa	**Type III Sum of Squares**	**df**	**Mean Square**	**F**	**p**
Material	0,00004	2	0,00002	1,416	0,247
Solution	0,00000	1	0,00000	10,488	0,002*
Material * Solution	0,00002	2	0,00001	0,69	0,504

Two-way ANOVA Test $^{*}p<0.05$

Material and material*solution interaction were not significantly affected the ΔRa ($F=1.416$, $p=0.247$; $F=0.69$, $p=0.504$). However, solution change was significantly affected ΔRa ($F=10.488$, $p=0.002$).

4.1.2. Surface Microhardness

Surface microhardness value (Vickers Hardness Number-VHN) was evaluated among three different CAD-CAM materials [IPS e.max CAD (E), Celtra Duo CAD (C) and Ceramill Zolid HT+ (Z)] on baseline (T_0) and after the immersion in two different solutions (T_1). VHN changes from T_0 to T_1 (ΔVHN) were evaluated based on material and solution. Higher VHN value means that the material is harder.

Descriptive statistics on surface microhardness of six subgroups before and after the solution exposures were shown at Table 4.7.

Table 4.7. Descriptive statistics on surface hardness (VHN) of six subgroups before and after the solution exposures

Surface Hardness (VHN)		n	x̄	SD	Min.	Max.	Median	Skewness	SE of Mean
T0 VHN	IPS e.max Blumic Subgroup	18	523,353	7,031	506,120	532,520	525,53	-1,022	1,657
	Celtra Duo Blumic Subgroup	18	580,460	7,772	570,700	597,840	578,08	0,956	1,832
	Ceramill Zolid Blumic Subgroup	18	1256,056	16,609	1219,600	1280,600	1256,8	-0,583	3,915
	IPS e.max Control Subgroup	18	525,740	6,972	514,540	538,700	524,04	0,139	1,643
	Celtra Duo Control Subgroup	18	574,781	4,838	562,780	585,840	574,44	-0,197	1,140
	Ceramill Zolid Control Subgroup	18	1253,367	11,425	1237,400	1276,200	1251,4	0,663	2,693
T1 VHN	IPS e.max Blumic Subgroup	18	541,607	7,858	520,400	557,400	542,68	-0,820	1,852
	Celtra Duo Blumic Subgroup	18	550,488	8,661	540,100	570,900	548,71	1,024	2,041
	Ceramill Zolid Blumic Subgroup	18	1260,789	15,750	1236,200	1287,000	1259,5	-0,012	3,712
	IPS e.max Control Subgroup	18	553,202	9,384	534,620	570,480	553,23	-0,086	2,212
	Celtra Duo Control Subgroup	18	560,280	4,394	551,620	567,680	560,36	0,060	1,036
	Ceramill Zolid Control Subgroup	18	1259,522	11,453	1234,600	1276,400	1261,4	-0,736	2,699
ΔVHN	IPS e.max Blumic Subgroup	18	18,253	3,979	13,620	26,740	16,98	0,961	0,938
	Celtra Duo Blumic Subgroup	18	-29,972	10,864	-49,180	-11,600	-29,57	-0,162	2,561
	Ceramill Zolid Blumic Subgroup	18	4,733	19,386	-20,200	29,800	15,4	-0,181	4,569
	IPS e.max Control Subgroup	18	27,462	7,141	15,600	39,740	27,47	0,032	1,683
	Celtra Duo Control Subgroup	18	-14,501	2,591	-18,760	-10,860	-14,2	-0,193	0,611
	Ceramill Zolid Control Subgroup	18	6,156	15,804	-22,000	29,000	10,8	-0,765	3,725

4.1.2.1. Baseline (T_0) Surface Microhardness (VHN) Evaluations Among CAD-CAM Materials

Statistics for baseline (T_0) surface microhardness measurements (VHN) were shown at Table 4.8.

Table 4.8. Baseline surface microhardness (VHN) evaluations among different materials and solutions.

Solution	VHN	IPS e.max CAD (E) $\bar{x} \pm SD$	Celtra Duo CAD (C) $\bar{x} \pm SD$	Ceramill Zolid HT+ (Z) $\bar{x} \pm SD$	p
1.6 pH	**T_0**	523,35±7,03	580,46±7,77	1256,06±16,61	0,000*
7 pH	**T_0**	525,74±6,97	574,78±4,84	1253,37±11,42	0,000*

One-way ANOVA Test **p<0.05*

The mean of baseline (T_0) VHN values of three different materials assigned to blumic subgroups (1.6 pH) were found significantly different (p=0.000). The mean VHN values are ordered as; Ceramill Zolid (1256,06±16,61) > Celtra Duo (580,46±7,77) > IPS e.max (523,35±7,03). Mean VHN value of Ceramill Zolid was found significantly higher than Celtra Duo and IPS e.max (p=0.000, p=0.000 respectively) at T_0; and mean VHN value of Celtra Duo was found significantly higher than IPS e.max (p=0.000) at T_0 according to post-hoc Tamhane's T2 Test.

The mean of baseline (T_0) VHN values of three different materials assigned to control subgroups (7 pH) were found significantly different (p=0.000). Similarly, the mean VHN values are ordered as; Ceramill Zolid (1253,37±11,42) > Celtra Duo (574,78±4,84) > IPS e.max (525,74±6,97). The mean VHN value of Ceramill Zolid was found significantly higher than Celtra Duo and IPS e.max (p=0.000, p=0.000 respectively) at T_0; and mean VHN value of Celtra Duo was found significantly higher than IPS e.max (p=0.000) at T_0 according to post-hoc Tamhane's T2 Test.

4.1.2.2. Surface Microhardness (VHN) Evaluations After Solution Exposures (T_1) Among CAD-CAM Materials

Statistics for T_1 surface microhardness measurements (VHN) were shown at Table 4.9.

Table 4.9. Surface microhardness (VHN) evaluations among different materials and solutions at T_1.

Solution	VHN	IPS e.max CAD (E) x̄ ± SD	Celtra Duo CAD (C) x̄ ± SD	Ceramill Zolid HT+ (Z) x̄ ± SD	p
1.6 pH	**T_1**	541,61±7,86	550,49±8,66	1260,79±15,75	0,000*
7 pH	**T_1**	553,2±9,38	560,28±4,39	1259,52±11,45	0,000*

One-way ANOVA Test **p<0.05*

The mean VHN values of three different materials assigned to blumic subgroups (1.6 pH) at T_1 were found significantly different (p=0.000). The VHN values are ordered as; Ceramill Zolid (1260,79±15,75) > Celtra Duo (550,49±8,66) > IPS e.max (541,61±7,86). Mean VHN value of Ceramill Zolid was found significantly higher than Celtra Duo and IPS e.max (p_1=0.000, p_2=0.000 respectively) at T_1; and mean VHN of Celtra Duo was found significantly higher than IPS e.max (p=0.008) at T_1 according to post-hoc Tamhane's T2 Test.

The mean VHN values of three different materials assigned to control subgroups (7 pH) at T_1 were found significantly different (p=0.000). The VHN values are ordered as; Ceramill Zolid (1259,52±11,45) > Celtra Duo (560,28±4,39) > IPS e.max (553,2±9,38). Similarly, mean VHN values of Ceramill Zolid was found significantly higher than Celtra Duo and IPS e.max (p_1=0.000, p_2=0.000 respectively) at T_1; and mean VHN of Celtra Duo was found significantly higher than IPS e.max (p=0.023) at T_1 according to post-hoc Tamhane's T2 Test.

4.1.2.3. Surface Microhardness (VHN) Evaluations of Each Subgroup Before and After the Solution Exposure (T_0-T_1)

All subgroups, except blumic subgroup and control subgroup of Ceramill Zolid, were found significantly affected by the respective solution exposures (Table 4.10.).

Table 4.10. VHN evaluations of six subgroups before and after (T_0-T_1) the solution exposure.

Solution	VHN	IPS e.max CAD (E) x̄ ± SD	Celtra Duo CAD (C) x̄ ± SD	Ceramill Zolid HT+ (Z) x̄ ± SD
1.6 pH	**T_0**	523,35±7,03	580,46±7,77	1256,06±16,61
	T_1	541,61±7,86	550,49±8,66	1260,79±15,75
	p	0,000*	0,000*	0,315
7 pH	**T_0**	525,74±6,97	574,78±4,84	1253,37±11,42
	T_1	553,2±9,38	560,28±4,39	1259,52±11,45
	p	0,000*	0,000*	0,117

Paired Samples t test   **p<0.05*

While the mean surface microhardness (VHN) value of blumic subgroup of IPS e.max was increasing significantly (p=0.000) from T_0 to T_1, the mean surface microhardness (VHN) value of blumic subgroup of Celtra Duo was significantly decreasing (p=0.000) from T_0 to T_1. However the increase of mean surface microhardness (VHN) value from T_0 to T_1 caused by blumic solution (1.6 pH) was not statistically significant for Ceramill Zolid samples (p=0.315). Similarly, the mean surface microhardness (VHN) value of control subgroup of IPS e.max was increasing significantly (p=0.000) from T_0 to T_1, the mean surface microhardness (VHN) value of control subgroup of Celtra Duo was significantly decreasing (p=0.000) from T_0 to T_1. The increase of mean surface microhardness (VHN) value from T_0 to T_1 caused by control solution (7 pH) was not statistically significant for Ceramill Zolid samples either (p=0.117).

4.1.2.4. Comparison of Surface Microhardness Changes (ΔVHN) on Different CAD-CAM Materials Exposed to Different Solutions

Surface microhardness change (ΔVHN) of a material is observed by two parameters; different solutions and different materials. The results are shown in Table 4.11. The absolute values of ΔVHN's were taken into consideration in order to see how great the change is, independent from whether it has a decrease or increase trend.

Table 4.11. ΔVHN Evaluation on Different Materials and Solutions

	ΔVHN		
	1.6 pH	**7 pH**	
Material	**$\bar{x}$ ± SD**	**$\bar{x}$ ± SD**	**p**
IPS e.max (E)	18,25±3,98	27,46±7,14	0,000*
Celtra Duo (C)	-29,97±10,86	-14,5±2,59	0,000*
Ceramill Zolid (Z)	4,73±19,39	6,16±15,8	0,811
p	0,000*	0,000*	

Two-way ANOVA Test **p<0.05*

When the effect of blumic solution (1.6 pH) on surface microhardness changes (ΔVHN) among different materials was evaluated, statistically significant differences were found (p=0.000). The absolute values of materials' ΔVHN were ordered as; Celtra Duo (29,97±10,86) > IPS e.max (18,25±3,98) > Ceramill Zolid (4,73±19,39). According to post-hoc Tamhane's T2 Test (Table 4.11.a.), surface microhardness change (ΔVHN) of Celtra Duo was significantly higher than IPS e.max and Ceramill Zolid (p=0.000, p=0.000 respectively) and Celtra Duo had a decrease tendency in VHN value. The surface microhardness change (ΔVHN) of IPS e.max was significantly higher than Ceramill Zolid (p=0.028). They both had increase tendencies in VHN values, but VHN increase of Ceramill Zolid was not significant (p=0.315) as aforementioned in Table 4.10.

Similarly, when the influence of control solution (7 pH) was evaluated on the surface hardness change (ΔVHN) of three different materials, statistically significant differences were found (p=0.000). The absolute values of materials' ΔVHN were ordered as; IPS e.max (27,46±7,14) > Celtra Duo (14,5±2,59) > Ceramill Zolid (6,16±15,8). According to post-hoc Tamhane's T2 Test (Table 4.11.b.), surface microhardness change (ΔVHN) of IPS e.max was significantly higher than Celtra Duo and Ceramill Zolid (p=0.000, p=0.000 respectively) and IPS e.max had an increase tendency in VHN value. The surface microhardness change (ΔVHN) of Celtra Duo was significantly higher than Ceramill Zolid (p=0.000). Celtra Duo had a decrease tendency in VHN value, while Ceramill Zolid had an increase tendency in VHN value yet this decrease was not significant (p=0.117) as aforementioned in Table 4.10.

Table 4.11.a. Multiple comparisons of blumic subgroups' surface hardness values

Solution	Δ VHN	Material 1	Material 2	Mean Difference (1-2)	SE	p	95% Confidence Interval	
							Lower Bound	Upper Bound
1.6 pH Blumic Solution		IPS e.max	Celtra Duo	48,22556*	2,727	0,000	41,167	55,285
			Ceramill Zolid	13,52000*	4,665	0,028	1,276	25,764
		Celtra Duo	IPS e.max	-48,22556*	2,727	0,000	-55,285	-41,167
			Ceramill Zolid	-34,70556*	5,238	0,000	-48,046	-21,366
		Ceramill Zolid	IPS e.max	-13,52000*	4,665	0,028	-25,764	-1,276
			Celtra Duo	34,70556*	5,238	0,000	21,366	48,046

Tamhane's T2 Test

Table 4.11.b. Multiple comparisons of control subgroups' surface hardness values

Solution	Δ VHN	Material 1	Material 2	Mean Difference (1-2)	SE	p	95% Confidence Interval	
							Lower Bound	Upper Bound
7 pH Control Solution		IPS e.max	Celtra Duo	41,96333*	1,791	0,000	37,327	46,600
			Ceramill Zolid	21,30667*	4,088	0,000	10,806	31,807
		Celtra Duo	IPS e.max	-41,96333*	1,791	0,000	-46,600	-37,327
			Ceramill Zolid	-20,65667*	3,775	0,000	-30,593	-10,720
		Ceramill Zolid	IPS e.max	-21,30667*	4,088	0,000	-31,807	-10,806
			Celtra Duo	20,65667*	3,775	0,000	10,720	30,593

Tamhane's T2 Test

A comparison was made on the surface microhardness change (ΔVHN) of a material affected by two different solutions. Surface hardness change (ΔVHN) of IPS e.max and Ceramill Zolid blumic subgroups was lower (18,25±3,98; 4,73±19,39 respectively) than IPS e.max and Ceramill Zolid control subgroups (27,46±7,14; 6,16±15,8). When the difference of IPS e.max was statistically significant in ΔVHN (p=0.000), the difference of Ceramill Zolid was not statistically significant in ΔVHN (p=0.811). Absolute value of surface hardness change (ΔVHN) of Celtra Duo blumic subgroup (29,97±10,86) was higher than the absolute ΔVHN value of Celtra Duo control subgroup (14,5±2,59). Blumic solution decreased Celtra Duo's VHN more than control solution and the difference was statistically significant (p=0.000) (Figure 4.2.)

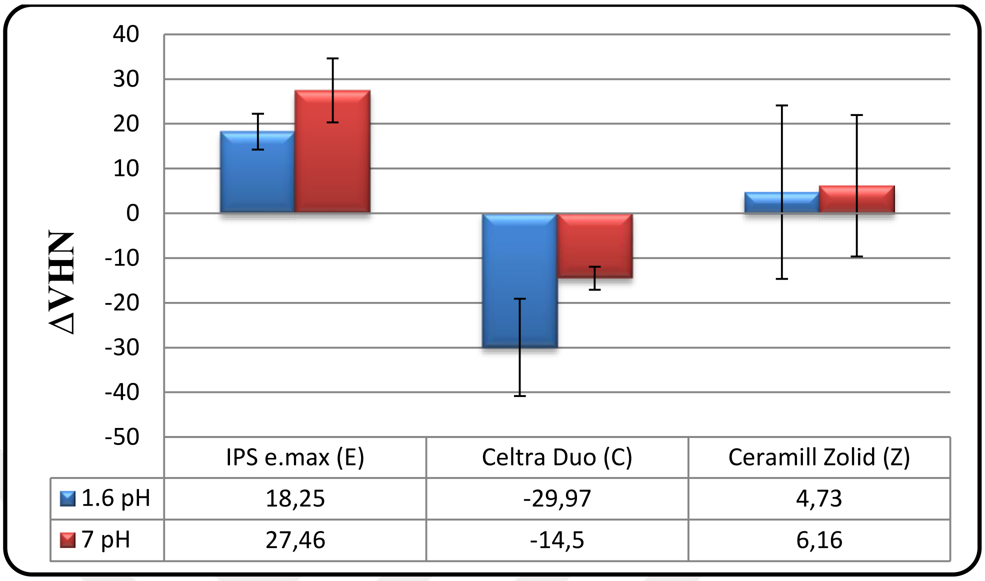

Figure 4.2. Surface microhardness change evaluations on different materials and solutions

When the influences of material types, solution pH and their interactions on surface microhardness change (ΔVHN) were evaluated with the two-way analysis of variance, the results were found as seen on Table 4.12.

Table 4.12. Evaluation of the common effect of material and solution on ΔVHN

ΔVHN	Type III Sum of Squares	df	Mean Square	F	p
Material	37235,72	2	18617,86	136,706	0,000*
Solution	2043,978	1	2043,978	15,008	0,000*
Material * Solution	891,657	2	445,828	3,274	0,042*

Two-way ANOVA Test **p<0.05*

It was shown that material change, solution change and material*solution interactions were significantly affected the ΔVHN (F:136.709, p:0.000; F:15.008, p:0.000; F:3.274, p:0.042 respectively). Material change has influenced ΔVHN more than solution change and material*solution interaction.

4.1.3. Fracture Toughness

Average fracture toughness (K_{Ic}) value was evaluated among three different CAD-CAM materials [IPS e.max CAD (E), Celtra Duo CAD (C) and Ceramill Zolid HT+ (Z)] on baseline (T_0) and after the immersions in two different solutions (T_1). K_{Ic} changes from T_0 to T_1 (ΔK_{Ic}) were evaluated based on material and solution. Higher K_{Ic} value in 'MPa.m$^{1/2}$' means that the material is tougher, thus the crack propagation was prevented more effectively.

Descriptive statistics on fracture toughness of six subgroups before and after the solution exposures were shown at Table 4.13.

Table 4.13. Descriptive statistics on fracture toughness (K_{Ic}) of six subgroups before and after the solution exposures

Fracture Toughness (K_{Ic})		**n**	**x̄**	**SD**	**Min.**	**Max.**	**Median**	**Skewness**	**SE of Mean**
T0 K_{Ic}	IPS e.max Blumic Subgroup	18	3,195	0,265	2,800	3,770	3,230	0,331	0,062
	Celtra Duo Blumic Subgroup	18	1,581	0,056	1,510	1,710	1,560	0,750	0,013
	Ceramill Zolid Blumic Subgroup	18	6,655	0,667	5,740	7,790	6,660	0,030	0,157
	IPS e.max Control Subgroup	18	2,818	0,209	2,490	3,290	2,810	0,889	0,049
	Celtra Duo Control Subgroup	18	1,554	0,062	1,450	1,680	1,555	0,298	0,015
	Ceramill Zolid Control Subgroup	18	6,269	0,583	5,500	7,300	6,075	0,710	0,138
T1 K_{Ic}	IPS e.max Blumic Subgroup	18	2,741	0,173	2,360	3,050	2,740	-0,231	0,041
	Celtra Duo Blumic Subgroup	18	1,844	0,135	1,610	2,100	1,855	0,051	0,032
	Ceramill Zolid Blumic Subgroup	18	5,847	0,669	4,740	7,030	5,750	0,245	0,158
	IPS e.max Control Subgroup	18	2,739	0,165	2,480	3,070	2,705	0,387	0,039
	Celtra Duo Control Subgroup	18	1,848	0,095	1,630	1,990	1,860	-0,643	0,022
	Ceramill Zolid Control Subgroup	18	6,181	0,575	5,390	7,180	6,100	0,300	0,136
Δ K_{Ic}	IPS e.max Blumic Subgroup	18	-0,454	0,207	-0,900	-0,200	-0,375	-1,009	0,049
	Celtra Duo Blumic Subgroup	18	0,263	0,130	0,070	0,530	0,200	0,285	0,031
	Ceramill Zolid Blumic Subgroup	18	-0,808	0,464	-1,620	-0,200	-0,705	-0,524	0,109
	IPS e.max Control Subgroup	18	-0,079	0,234	-0,600	0,200	-0,045	-0,770	0,055
	Celtra Duo Control Subgroup	18	0,294	0,086	0,080	0,440	0,305	-0,579	0,020
	Ceramill Zolid Control Subgroup	18	-0,088	0,307	-0,700	0,540	-0,075	-0,069	0,072

4.1.3.1. Baseline (T_0) Fracture Toughness (K_{Ic}) Evaluations among CAD-CAM Materials

Statistics for baseline (T_0) fracture toughness (K_{Ic}) measurements were shown at Table 4.14.

Table 4.14. Baseline fracture toughness ($MPa.m^{1/2}$) evaluations among different materials and solutions.

Solution	K_{Ic}	IPS e.max CAD (E)	Celtra Duo CAD (C)	Ceramill Zolid HT+ (Z)	p
		$\bar{x} \pm SD$	$\bar{x} \pm SD$	$\bar{x} \pm SD$	
1.6 pH	**T_0**	3,20±0,26	1,58±0,06	6,66±0,67	0,000*
7 pH	**T_0**	2,82±0,21	1,55±0,06	6,27±0,58	0,000*

One-way ANOVA Test **p<0.05*

The mean of baseline (T_0) K_{Ic} values of three different materials assigned to blumic subgroups (1.6 pH) were found significantly different (p=0.000). The K_{Ic} values are ordered as; Ceramill Zolid (6,66±0,67) > IPS e.max (3,20±0,26) > Celtra Duo (1,58±0,06). Mean K_{Ic} value of Ceramill Zolid was found significantly higher than IPS e.max and Celtra Duo (p=0.000, p=0.000 respectively) at T_0; and mean K_{Ic} value of IPS e.max was found significantly higher than Celtra Duo (p=0.000) at T_0 according to post-hoc Tamhane's T2 Test.

The mean of baseline (T_0) K_{Ic} values of three different materials assigned to control subgroups (7 pH) were found significantly different (p=0.000). Similarly, the K_{Ic} values are ordered as; Ceramill Zolid (6,27±0,58) > IPS e.max (2,82±0,21) > Celtra Duo (1,55±0,06). The mean K_{Ic} value of Ceramill Zolid was found significantly higher than IPS e.max and Celtra Duo (p=0.000, p=0.000 respectively) at T_0; and mean K_{Ic} value of IPS e.max was found significantly higher than Celtra Duo (p=0.000) at T_0 according to post-hoc Tamhane's T2 Test.

4.1.3.2. Fracture Toughness (K_{Ic}) Evaluations After Solution Exposures (T_1) Among CAD-CAM Materials

Statistics of T_1 fracture toughness measurements (K_{Ic}) were shown at Table 4.16.

Table 4.15. Fracture toughness (MPa.m$^{1/2}$) evaluations among different materials and solutions at T_1.

		IPS e.max CAD (E)	Celtra Duo CAD (C)	Ceramill Zolid HT+ (Z)	
Solution	K_{Ic}	**x̄ ± SD**	**x̄ ± SD**	**x̄ ± SD**	**p**
1.6 pH	T_1	2,74±0,17	1,84±0,13	5,85±0,67	0,000*
7 pH	T_1	2,74±0,17	1,85±0,09	6,18±0,58	0,000*

One-way ANOVA Test *$p<0.05$

The mean K_{Ic} values of three different materials assigned to blumic subgroups (1.6 pH) at T_1 were found significantly different (p=0.000). The K_{Ic} values are ordered as; Ceramill Zolid (5,85±0,67) > IPS e.max (2,74±0,17) > Celtra Duo (1,84±0,13). Mean K_{Ic} value of Ceramill Zolid was found significantly higher than IPS e.max and Celtra Duo (p=0.000, p=0.000 respectively) at T_1; and mean K_{Ic} value of IPS e.max was found significantly higher than Celtra Duo (p=0.000) at T_1 according to post-hoc Tamhane's T2 Test.

The mean K_{Ic} values three different materials assigned to control subgroups (7 pH) at T_1 were found significantly different (p=0.000). Similarly, the K_{Ic} values are ordered as; Ceramill Zolid (6,18±0,58) > IPS e.max (2,74±0,17) > Celtra Duo (1,85±0,09). The mean K_{Ic} value of Ceramill Zolid was found significantly higher than IPS e.max and Celtra Duo (p=0.000, p=0.000 respectively) at T_1; and mean K_{Ic} value of IPS e.max was found significantly higher than Celtra Duo (p=0.000) at T_1 according to post-hoc Tamhane's T2 Test.

4.1.3.3. Fracture Toughness (K_{Ic}) Evaluations of Each Subgroup Before and After the Solution Exposure (T_0-T_1)

All subgroups, except control subgroups of IPS e.max and Ceramill Zolid, were found significantly affected by the respective solution exposures as shown in Table 4.16.

Table 4.16. K_{Ic} ($MPa.m^{1/2}$) evaluations of six subgroups before and after (T_0-T_1) the solution exposure.

Solution	K_{Ic}	IPS e.max CAD (E)	Celtra Duo CAD (C)	Ceramill Zolid HT+ (Z)
		$\bar{x}$ ± SD	$\bar{x}$ ± SD	$\bar{x}$ ± SD
1.6 pH	**T0**	3,20±0,26	1,58±0,06	6,66±0,67
	T1	2,74±0,17	1,84±0,13	5,85±0,67
	p	0,000*	0,000*	0,000*
7 pH	**T0**	2,82±0,21	1,55±0,06	6,27±0,58
	T1	2,74±0,17	1,85±0,09	6,18±0,58
	p	0,170	0,000*	0,238

Paired Samples t test **p<0.05*

The mean fracture toughness (K_{Ic}) values of IPS e.max and Ceramill Zolid blumic subgroups were significantly decreased (p=0.000, p=0.000 respectively) from T_0 to T_1, while the mean fracture toughness (K_{Ic}) value of Celtra Duo blumic subgroup was significantly increased (p=0.000) from T_0 to T_1. The mean fracture toughness (K_{Ic}) values of IPS e.max and Ceramill Zolid control subgroups were decreasing from T_0 to T_1, however these decreases were not statistically significant (p=0.170, p=0.238 respectively). The mean fracture toughness (K_{Ic}) of Celtra Duo control subgroup was significantly increased (p=0.000) from T_0 to T_1.

4.1.3.4. Comparison of Fracture Toughness Changes (ΔK_{Ic}) on Different CAD-CAM Materials Exposed to Different Solutions

Fracture toughness change (ΔK_{Ic}) of a material is observed by two parameters; different solutions and different materials. The results are shown in Table 4.17. The absolute values of ΔK_{Ic} were taken into consideration in order to see how great the change is, independent from whether it has a decrease or increase tendency.

Table 4.17. ΔK_{Ic} ($MPa.m^{1/2}$) Evaluation on Different Materials and Solutions

	ΔK_{Ic}		
	1.6 pH	**7 pH**	
Material	**$\bar{x}$ ± SD**	**$\bar{x}$ ± SD**	**p**
IPS e.max (E)	-0,45±0,21	-0,08±0,23	0,000*
Celtra Duo (C)	0,26±0,13	0,29±0,09	0,405
Ceramill Zolid (Z)	-0,81±0,46	-0,09±0,31	0,000*
p	0,000*	0,000*	

Two-way ANOVA Test *$^*p<0.05$*

When the effect of blumic solution on fracture toughness change (ΔK_{Ic}) among three different materials were evaluated, statistically significant differences were found (p=0.000). The absolute ΔK_{Ic} values were ordered as; Ceramill Zolid (0,81±0,46) > IPS e.max (0,45±0,21) > Celtra Duo (0,26±0,13). According to post-hoc Tamhane's T2 Test (Table 4.17.a.), the absolute ΔK_{Ic} value of Ceramill Zolid was significantly higher than IPS e.max and Celtra Duo (p=0.021, p=0.000 respectively) and Ceramill Zolid had a decrease tendency in K_{Ic}. The absolute ΔK_{Ic} value of IPS e.max was significantly higher than Celtra Duo (p=0.000). While IPS e.max had a decrease tendency in K_{Ic}, Celtra Duo had an increase tendency.

When the influence of control solution was evaluated on the fracture toughness change (ΔK_{Ic}) among three different materials, statistically significant differences were found (p=0.000). The absolute ΔK_{Ic} values were ordered as; Celtra Duo (0,29±0,09) > Ceramill Zolid (0,09±0,31) > IPS e.max (0,08±0,23). According to post-hoc Tamhane's T2 Test (Table 4.17.b.), the absolute ΔK_{Ic} value of Celtra Duo was significantly higher than Ceramill Zolid and IPS e.max (p=0.000, p=0.000 respectively) and Celtra Duo had an increase tendency in K_{Ic}. There was no statistically significant difference between the fracture toughness changes (ΔK_{Ic}) of Ceramill Zolid and IPS e.max (p=0.999). They both had a decrease tendency in K_{Ic}, however these decreases were not statistically significant (p=0.170, p=0.238 respectively) as aforementioned in Table 4.17.

Table 4.17.a. Multiple comparisons of blumic subgroups' fracture toughness values

Solution	ΔK_{Ic}	Material 1	Material 2	Mean Difference (1-2)	SE	p	95% Confidence Interval Lower Bound	95% Confidence Interval Upper Bound
1.6 pH Blumic Solution		IPS e.max	Celtra Duo	-0,71722*	0,058	0,000	-0,864	-0,571
			Ceramill Zolid	0,35389*	0,120	0,021	0,046	0,662
		Celtra Duo	IPS e.max	0,71722*	0,058	0,000	0,571	0,864
			Ceramill Zolid	1,07111*	0,114	0,000	0,775	1,368
		Ceramill Zolid	IPS e.max	-0,35389*	0,120	0,021	-0,662	-0,046
			Celtra Duo	-1,07111*	0,114	0,000	-1,368	-0,775

Tamhane's T2 Test

Table 4.17.b. Multiple comparisons of control subgroups' fracture toughness values

Solution	ΔK_{Ic}	Material 1	Material 2	Mean Difference (1-2)	SE	p	95% Confidence Interval Lower Bound	95% Confidence Interval Upper Bound
7 pH Control Solution		IPS e.max	Celtra Duo	-0,37333*	0,059	0,000	-0,525	-0,221
			Ceramill Zolid	0,009	0,091	0,999	-0,220	0,239
		Celtra Duo	IPS e.max	0,37333*	0,059	0,000	0,221	0,525
			Ceramill Zolid	0,38278*	0,075	0,000	0,187	0,579
		Ceramill Zolid	IPS e.max	-0,009	0,091	0,999	-0,239	0,220
			Celtra Duo	-0,38278*	0,075	0,000	-0,579	-0,187

Tamhane's T2 Test

A comparison was made on the change of fracture toughness (ΔK_{Ic}) of a material affected by two different solutions. The absolute fracture toughness change (ΔK_{Ic}) values of IPS e.max and Ceramill Zolid blumic subgroups were higher (0,45±0,21; 0,81±0,46 respectively) than IPS e.max and Ceramill Zolid control subgroups (0,08±0,23; 0,09±0,31 respectively). These differences were statistically significant (p=0.000, p=0.000 respectively). The absolute fracture toughness change (ΔK_{Ic}) value of Celtra Duo control subgroup was slightly higher (0,29±0,09) than Celtra Duo blumic subgroup (0,26±0,13). The difference was not statistically significant (p=0.405) (Figure 4.3.).

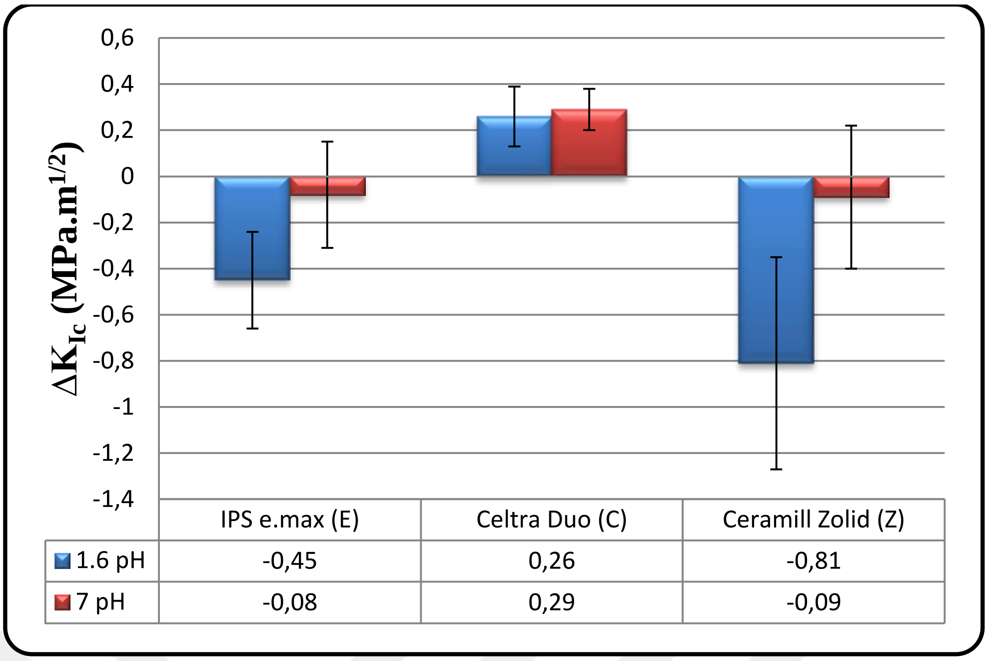

Figure 4.3. Fracture toughness change evaluations on different materials and solutions

When the influences of material change, solution pH and their interactions on fracture toughness change (ΔK_{Ic}) were evaluated with the two-way analysis of variance, the results were found as seen on Table 4.18.

Table 4.18. Evaluation of the common effect of material and solution on ΔK_{Ic}

ΔK_{Ic}	**Type III Sum of Squares**	**df**	**Mean Square**	**F**	**p**
Material	10,305	2	5,153	71,658	0,000*
Solution	3,801	1	3,801	52,855	0,000*
Material * Solution	2,132	2	1,066	14,826	0,000*

Two-way ANOVA Test *$p<0.05$

It was shown that material change, solution change and material*solution interactions were significantly affected the ΔK_{Ic} (F:71.658, p:0.000; F:52.855, p:0.000; F:14.826, p:0.000 respectively). When F values observed, statistics showed that material change has influenced ΔK_{Ic} more than solution change and material*solution interaction.

4.1.4. Surface Topography

3D optical profilometer and scanning electron microscope (SEM) images were compared subjectively.

4.1.4.1. 3D Optical Profilometer Evaluations

Before and after 3D optical profilometer images of six subgroups were shown at figures from Figure 4.4. to Figure 4.6.

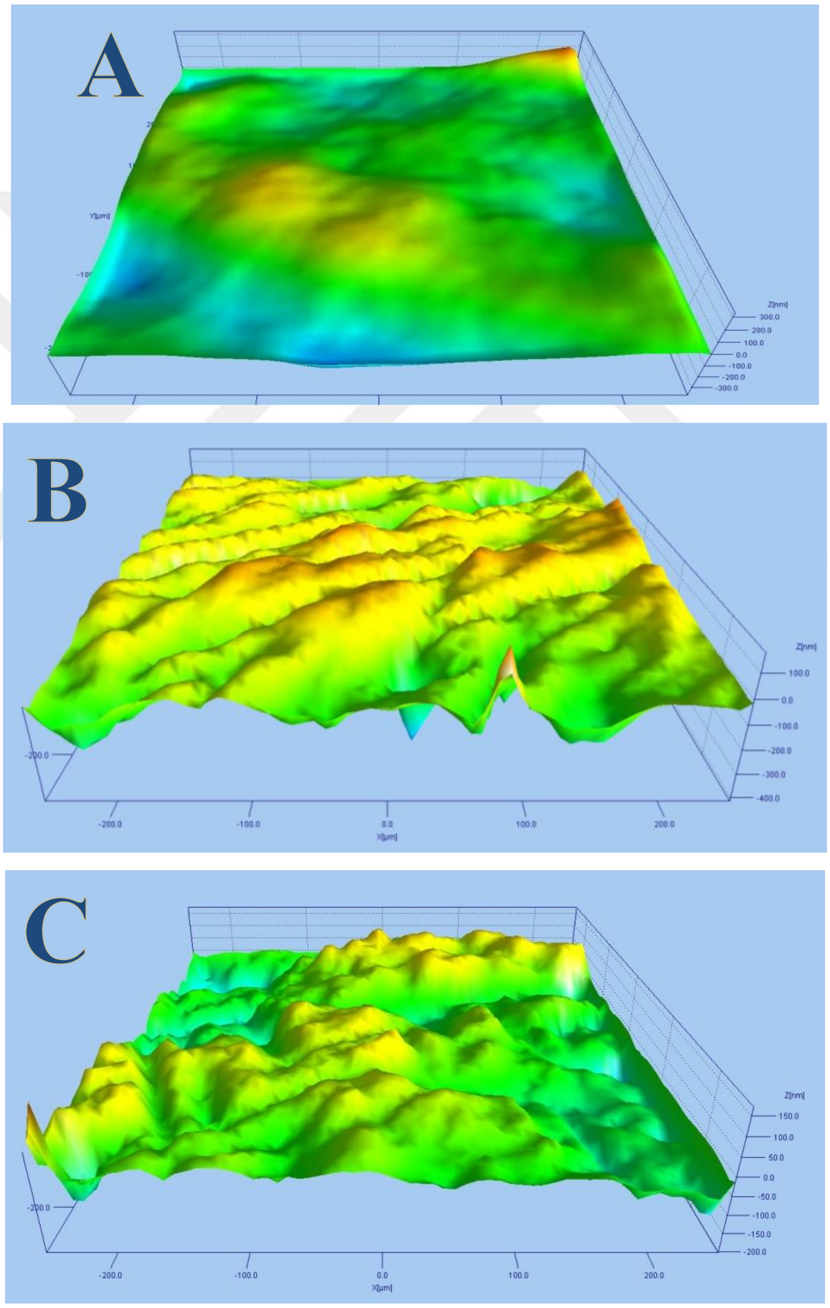

Figure 4.4. 3D topographic images of IPS e.max taken by 3D optical profilometer.
A, before solution exposure. B, after exposure of blumic solution. C, after exposure of control solution.

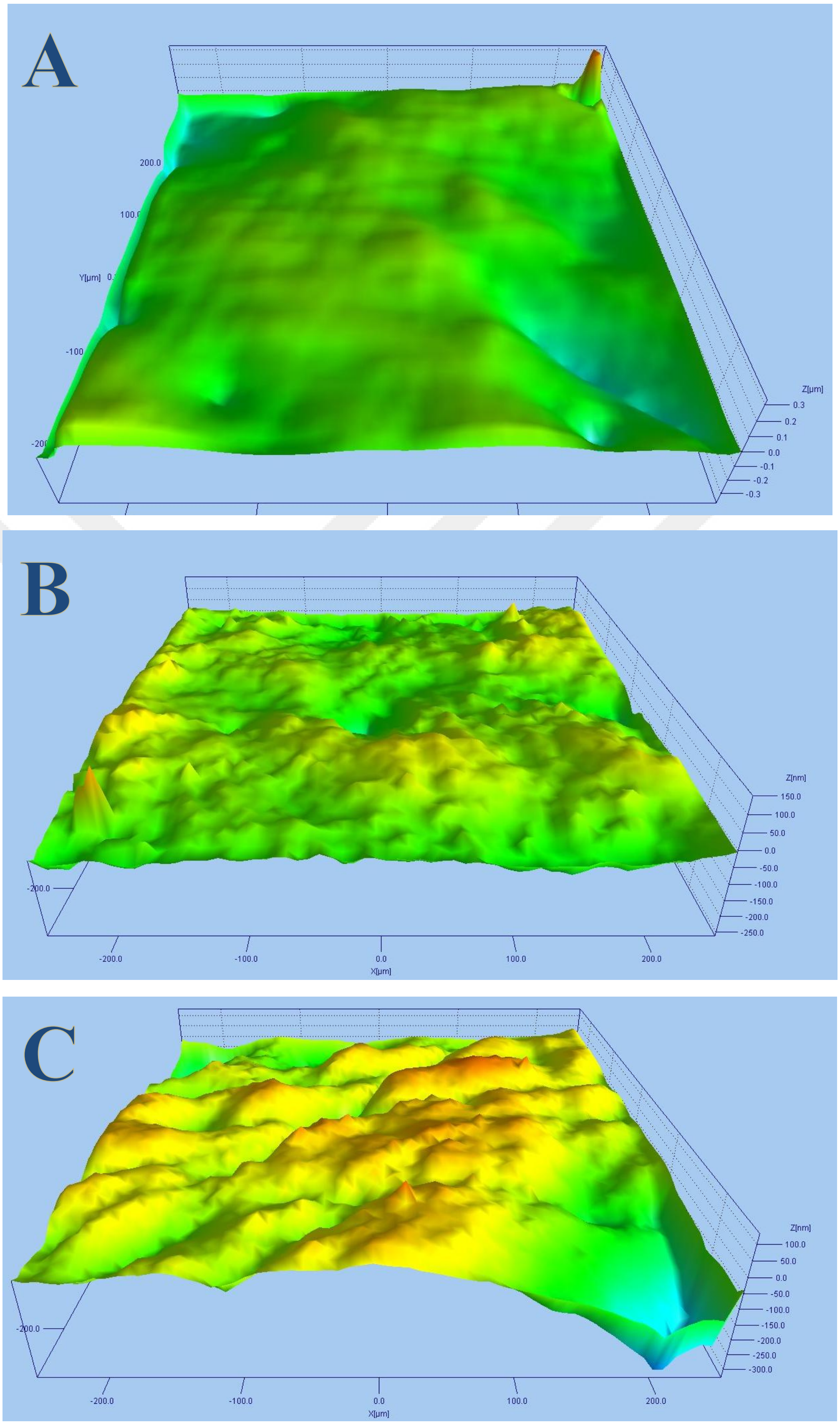

Figure 4.5. 3D topographic images of Celtra Duo taken by 3D optical profilometer.

A, before solution exposure. B, after exposure of blumic solution. C, after exposure of control solution.

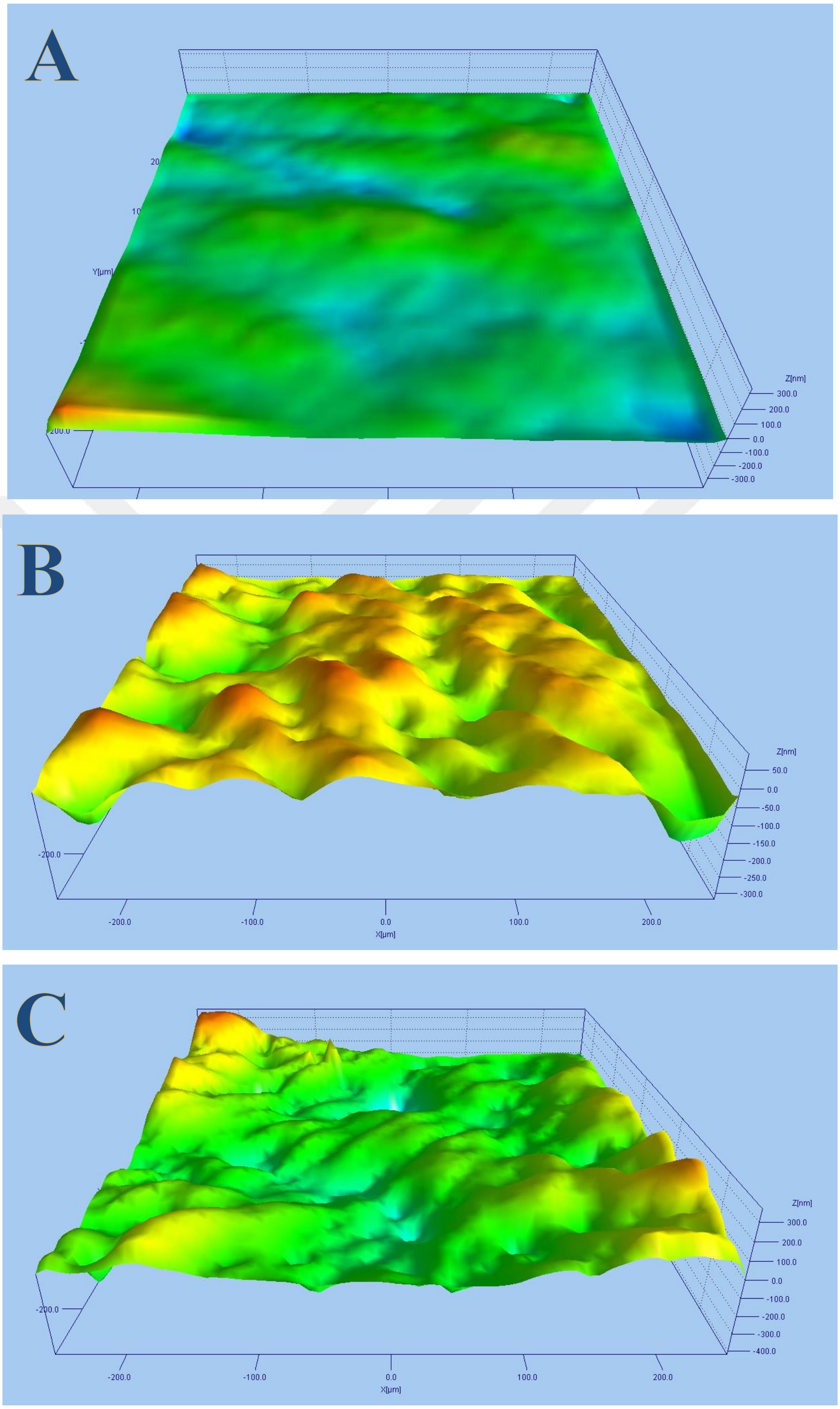

Figure 4.6. 3D topographic images of Ceramill Zolid taken by 3D optical profilometer.
A, before solution exposure. B, after exposure of blumic solution. C, after exposure of control solution.

4.1.4.2. Scanning Electron Microscope (SEM) Evaluations

Before and after SEM images of six subgroups were shown in figures from Figure 4.7. to Figure 4.9.

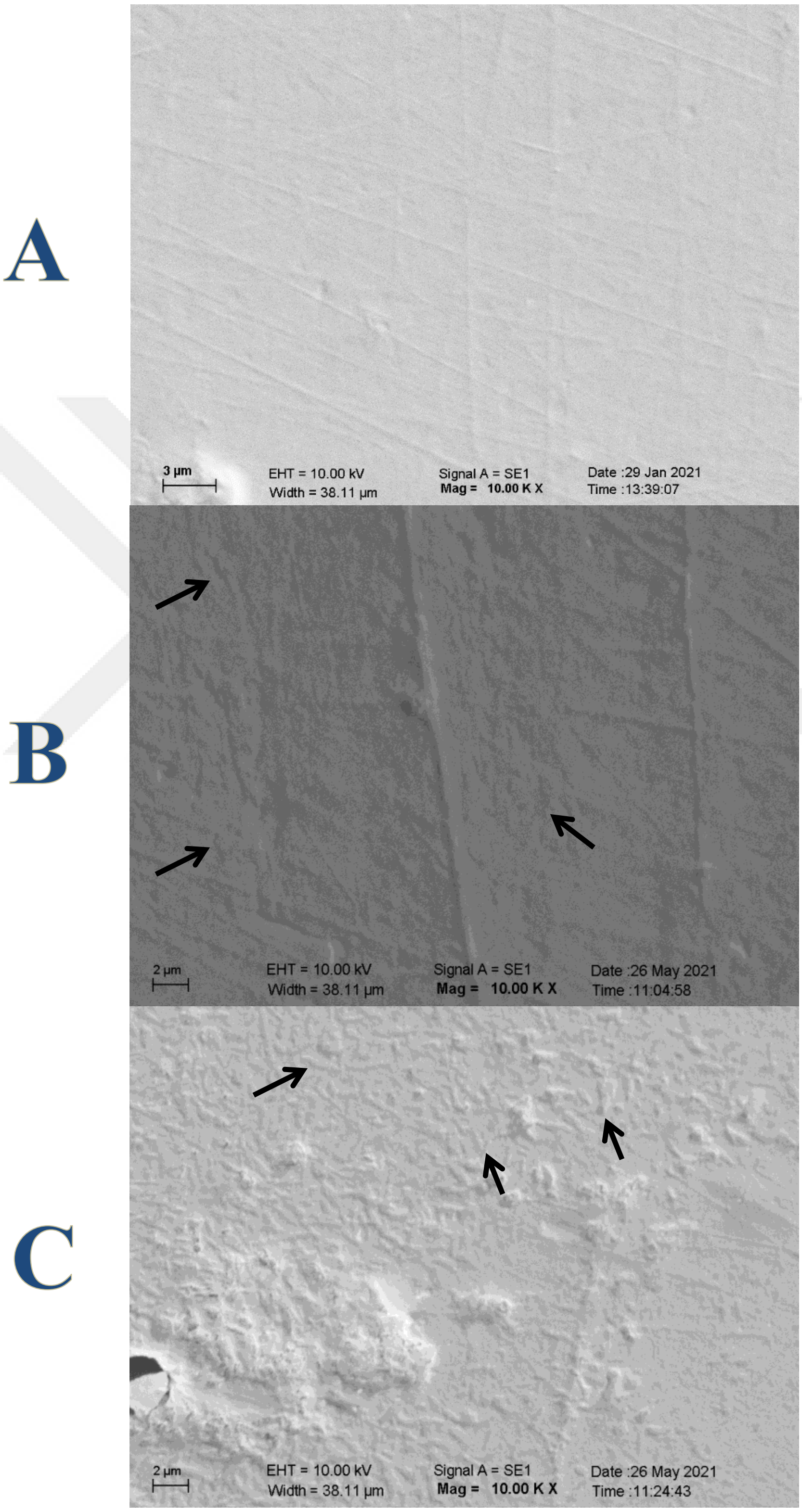

Figure 4.7. SEM images of IPS e.max with x10.000 original magnification.
A, before solution exposure. B, after blumic solution exposure. C, after control solution exposure.

A

B

C

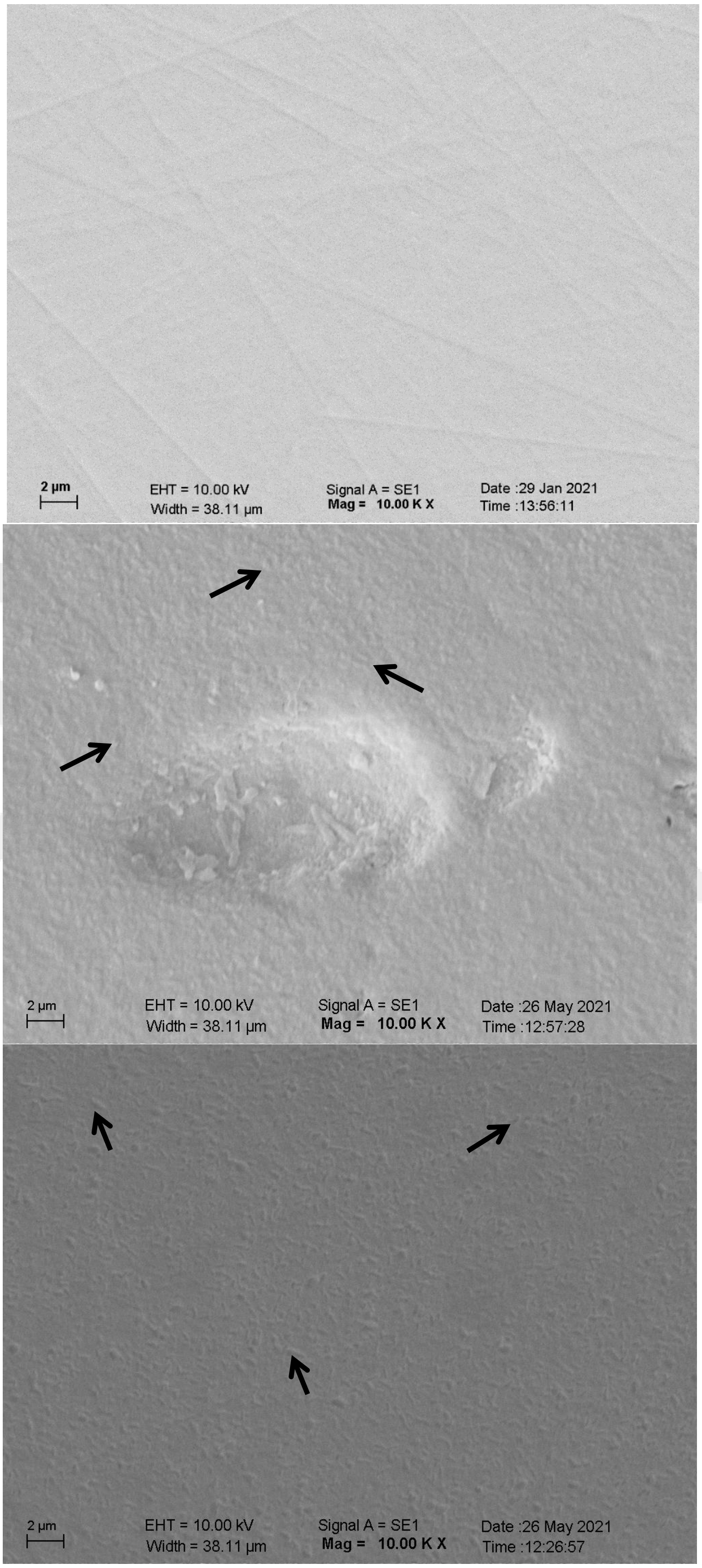

Figure 4.8. SEM images of Celtra Duo with x10.000 original magnification.
A, before solution exposure. B, after blumic solution exposure. C, after control solution exposure.

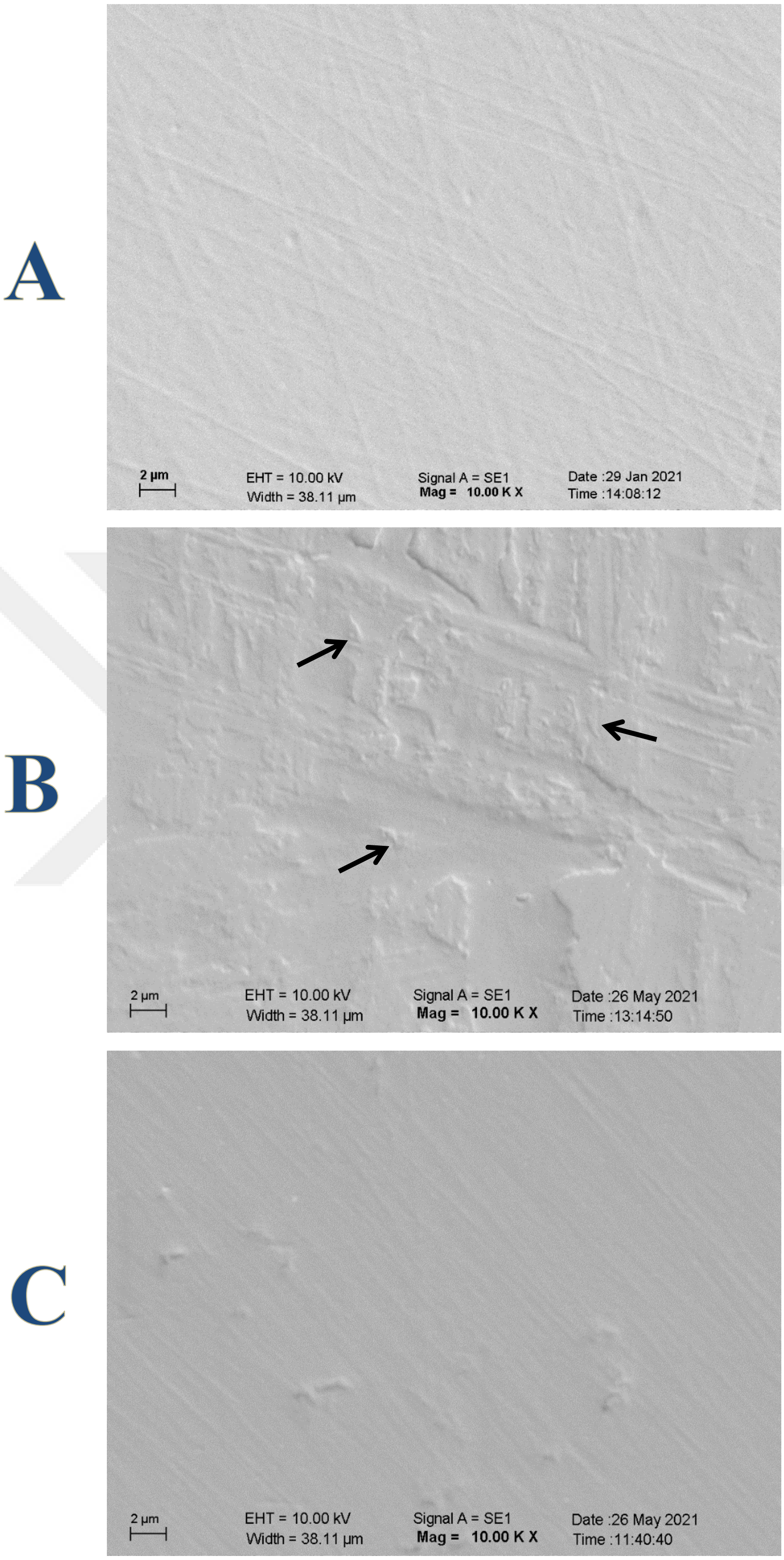

Figure 4.9. SEM images of Ceramill Zolid with x10.000 original magnification.

A, before solution exposure. B, after blumic solution exposure. C, after control solution exposure.

4.2. Optical Properties

Color and translucency parameters were evaluated.

4.2.1. Color

Color parameters (L*, a*, b*) were evaluated among three different CAD-CAM materials [IPS e.max CAD (E), Celtra Duo CAD (C) and Ceramill Zolid HT+ (Z)] on baseline (T_0) and after the immersions on two different solutions (T_1). The parameter of color change from T_0 to T_1 (ΔE) were evaluated based on material and solution. Higher ΔE value means that the material's color was changed more. Descriptive statistics on color parameters of six subgroups before and after the solution exposures were shown at Table 4.19.a., Table 4.19.b., Table 4.19.c. and Table 4.20.

Table 4.19.a. Descriptive statistics on color parameter (L*) of six subgroups before and after the solution exposures

L*		n	$\bar{x}$	SD	Min.	Max.	Median	Skewness	SE of Mean
T0	IPS e.max Blumic Subgroup	18	75,897	0,219	75,570	76,490	75,860	0,987	0,052
	Celtra Duo Blumic Subgroup	18	76,996	0,383	76,280	77,720	77,025	-0,148	0,090
	Ceramill Zolid Blumic Subgroup	18	77,666	0,442	76,800	78,280	77,700	-0,375	0,104
	IPS e.max Control Subgroup	18	75,594	0,225	75,290	76,240	75,545	1,415	0,053
	Celtra Duo Control Subgroup	18	77,726	0,508	76,600	78,360	77,865	-0,987	0,120
	Ceramill Zolid Control Subgroup	18	77,157	0,239	76,570	77,640	77,175	-0,394	0,056
T1	IPS e.max Blumic Subgroup	18	76,565	0,234	76,210	77,070	76,540	0,532	0,055
	Celtra Duo Blumic Subgroup	18	77,645	0,330	76,990	78,170	77,680	-0,444	0,078
	Ceramill Zolid Blumic Subgroup	18	78,877	0,271	78,440	79,330	78,900	0,008	0,064
	IPS e.max Control Subgroup	18	75,958	0,210	75,660	76,470	75,945	0,671	0,049
	Celtra Duo Control Subgroup	18	77,176	0,444	76,160	77,810	77,275	-1,276	0,105
	Ceramill Zolid Control Subgroup	18	77,419	0,136	77,250	77,720	77,340	0,741	0,032

Table 4.19.b. Descriptive statistics on color parameter (a*) of six subgroups before and after the solution exposures

a*		n	x̄	SD	Min.	Max.	Median	Skewness	SE of Mean
T0	IPS e.max Blumic Subgroup	18	1,403	0,043	1,340	1,490	1,4	0,418	0,010
	Celtra Duo Blumic Subgroup	18	1,221	0,053	1,090	1,290	1,23	-1,088	0,012
	Ceramill Zolid Blumic Subgroup	18	2,530	0,089	2,350	2,680	2,55	-0,405	0,021
	IPS e.max Control Subgroup	18	1,464	0,038	1,410	1,560	1,46	0,887	0,009
	Celtra Duo Control Subgroup	18	1,256	0,056	1,180	1,350	1,235	0,317	0,013
	Ceramill Zolid Control Subgroup	18	2,515	0,046	2,460	2,590	2,52	0,161	0,011
T1	IPS e.max Blumic Subgroup	18	1,166	0,036	1,090	1,240	1,17	-0,267	0,009
	Celtra Duo Blumic Subgroup	18	0,937	0,057	0,840	1,040	0,95	-0,177	0,013
	Ceramill Zolid Blumic Subgroup	18	2,038	0,114	1,720	2,170	2,075	-1,455	0,027
	IPS e.max Control Subgroup	18	1,297	0,039	1,240	1,360	1,305	-0,023	0,009
	Celtra Duo Control Subgroup	18	0,980	0,059	0,880	1,100	0,99	-0,077	0,014
	Ceramill Zolid Control Subgroup	18	2,453	0,049	2,370	2,510	2,47	-0,768	0,012

Table 4.19.c. Descriptive statistics on color parameter (b*) of six subgroups before and after the solution exposures

b*		n	x̄	SD	Min.	Max.	Median	Skewness	SE of Mean
T0	IPS e.max Blumic Subgroup	18	14,257	0,125	14,070	14,560	14,255	0,763	0,029
	Celtra Duo Blumic Subgroup	18	12,365	0,148	12,180	12,670	12,375	0,501	0,035
	Ceramill Zolid Blumic Subgroup	18	12,169	0,208	11,880	12,620	12,120	0,975	0,049
	IPS e.max Control Subgroup	18	14,291	0,125	14,090	14,590	14,275	0,586	0,030
	Celtra Duo Control Subgroup	18	12,447	0,189	12,090	12,750	12,485	-0,382	0,045
	Ceramill Zolid Control Subgroup	18	11,708	0,208	11,200	11,990	11,775	-0,925	0,049
T1	IPS e.max Blumic Subgroup	18	12,657	0,130	12,420	12,910	12,655	0,108	0,031
	Celtra Duo Blumic Subgroup	18	10,887	0,168	10,630	11,160	10,910	-0,007	0,040
	Ceramill Zolid Blumic Subgroup	18	10,148	0,217	9,880	10,730	10,070	1,279	0,051
	IPS e.max Control Subgroup	18	13,439	0,122	13,240	13,740	13,415	0,715	0,029
	Celtra Duo Control Subgroup	18	11,476	0,174	11,000	11,770	11,495	-0,850	0,041
	Ceramill Zolid Control Subgroup	18	10,819	0,258	10,410	11,480	10,905	0,575	0,061

Table 4.20. Descriptive statistics on color parameter (ΔE) of six subgroups before and after the solution exposures

ΔE	n	x̄	SD	Min.	Max.	Median	Skewness	SE of Mean
IPS e.max Blumic Subgroup	18	1,753	0,030	1,710	1,820	1,76	0,328	0,007
Celtra Duo Blumic Subgroup	18	1,647	0,032	1,600	1,710	1,64	0,689	0,008
Ceramill Zolid Blumic Subgroup	18	2,422	0,195	2,110	2,780	2,415	0,223	0,046
IPS e.max Control Subgroup	18	0,941	0,030	0,900	0,990	0,95	-0,061	0,007
Celtra Duo Control Subgroup	18	1,194	0,045	1,130	1,280	1,175	0,590	0,011
Ceramill Zolid Control Subgroup	18	0,970	0,087	0,800	1,070	0,995	-1,014	0,020

4.2.1.1. Baseline (T_0) Color Parameter (L*, a*, b*) Evaluations among CAD-CAM Materials

Statistics for baseline (T0) color parameter (L*, a*, b*) measurements were shown at Table 4.21., Table 4.22. and Table 4.23.

Table 4.21. Baseline L* parameter evaluations among different materials and solutions.

Solution	L*	IPS e.max CAD (E) x̄ ± SD	Celtra Duo CAD (C) x̄ ± SD	Ceramill Zolid HT+ (Z) x̄ ± SD	p
1.6 pH	**T_0**	75,9±0,22	77±0,38	77,67±0,44	0,000*
7 pH	**T_0**	75,59±0,23	77,73±0,51	77,16±0,24	0,000*

One-way ANOVA Test   **p<0.05*

The mean of baseline L* values of three different materials assigned to blumic subgroups (1.6 pH) were found significantly different (p=0.000). The L* values are ordered as; Ceramill Zolid (77,67±0,44) > Celtra Duo (77±0,38) > IPS e.max (75,9±0,22). Mean L* value of Ceramill Zolid was found significantly higher than IPS e.max and Celtra Duo (p=0.000, p=0.000 respectively) at T0; and mean L* value of Celtra Duo was found significantly higher than IPS e.max (p=0.000) at T0 according to post-hoc Tamhane's T2 Test.

The mean of baseline L* values of three different materials assigned to control subgroups (7 pH) were found significantly different (p=0.000). The L* values are ordered as; Celtra Duo (77,73±0,51) > Ceramill Zolid (77,16±0,24) > IPS e.max (75,59±0,23). The mean L* value of Celtra Duo was found significantly higher than Ceramill Zolid and IPS e.max (p=0.001, p=0.000 respectively) at T0; and mean L* value of Ceramill Zolid was found significantly higher than IPS e.max (p=0.000) at T0 according to post-hoc Tamhane's T2 Test.

Table 4.22. Baseline a* parameter evaluations among different materials and solutions.

		IPS e.max CAD (E)	**Celtra Duo CAD (C)**	**Ceramill Zolid HT+ (Z)**	
Solution	**a***	**$\bar{x}$ ± SD**	**$\bar{x}$ ± SD**	**$\bar{x}$ ± SD**	**p**
1.6 pH	**T_0**	1,40±0,04	1,22±0,05	2,53±0,09	0,000*
7 pH	**T_0**	1,46±0,04	1,26±0,06	2,52±0,05	0,000*

One-way ANOVA Test **p<0.05*

The mean of baseline a* values of three different materials assigned to blumic subgroups (1.6 pH) were found significantly different (p=0.000). The a* values are ordered as; Ceramill Zolid (2,53±0,09) > IPS e.max (1,40±0,04) > Celtra Duo (1,22±0,05). Mean a* value of Ceramill Zolid was found significantly higher than IPS e.max and Celtra Duo (p=0.000, p=0.000 respectively) at T0; and mean a* value of IPS e.max was found significantly higher than Celtra Duo (p=0.000) at T0 according to post-hoc Tamhane's T2 Test.

The mean of baseline a* values of three different materials assigned to control subgroups (7 pH) were found significantly different (p=0.000). The a* values are ordered as; Ceramill Zolid (2,52±0,05) > IPS e.max (1,46±0,04) > Celtra Duo (1,26±0,06). The mean a* value of Ceramill Zolid was found significantly higher than IPS e.max and Celtra Duo (p=0.000, p=0.000 respectively) at T0; and mean a* value of IPS e.max was found significantly higher than Celtra Duo (p=0.000) at T0 according to post-hoc Tukey Test.

Table 4.23. Baseline b* parameter evaluations among different materials and solutions.

		IPS e.max CAD (E)	Celtra Duo CAD (C)	Ceramill Zolid HT+ (Z)	
Solution	**b***	**$\bar{x} \pm SD$**	**$\bar{x} \pm SD$**	**$\bar{x} \pm SD$**	**p**
1.6 pH	**T_0**	14,26±0,13	12,37±0,15	12,17±0,21	0,000*
7 pH	**T_0**	14,29±0,13	12,45±0,19	11,71±0,21	0,000*

One-way ANOVA Test **p<0.05*

The mean of baseline b* values of three different materials assigned to blumic subgroups (1.6 pH) were found significantly different (p=0.000). The b* values are ordered as; IPS e.max (2,53±0,09) > Celtra Duo (1,40±0,04) > Ceramill Zolid (1,22±0,05). Mean b* value of IPS e.max was found significantly higher than Celtra Duo and Ceramill Zolid (p=0.000, p=0.000 respectively) at T0; and mean b* value of Celtra Duo was found significantly higher than Ceramill Zolid (p=0.002) at T0 according to post-hoc Tukey Test.

The mean of baseline b* values of three different materials assigned to control subgroups (7 pH) were found significantly different (p=0.000). The b* values are ordered as; IPS e.max (14,29±0,13) > Celtra Duo (12,45±0,19) > Ceramill Zolid (11,71±0,21). The mean b* value of IPS e.max was found significantly higher than Celtra Duo and Ceramill Zolid (p=0.000, p=0.000 respectively) at T0; and mean b* value of Celtra Duo was found significantly higher than Ceramill Zolid (p=0.000) at T0 according to post-hoc Tukey Test.

4.2.1.2. Evaluations of Color Parameters (L*, a*, b*) After Solution Exposures (T_1) Among CAD-CAM Materials

Statistics for T1 color parameters (L*, a*, b*) were shown at Table 4.23., Table 4.24. and Table 4.25.

Table 4.24. L* value evaluations among different materials and solutions at T_1.

Solution	L*	IPS e.max CAD (E)	Celtra Duo CAD (C)	Ceramill Zolid HT+ (Z)	p
		$\bar{x} \pm SD$	$\bar{x} \pm SD$	$\bar{x} \pm SD$	
1.6 pH	**T_1**	76,57±0,23	77,65±0,33	78,88±0,27	0,000*
7 pH	**T_1**	75,96±0,21	77,18±0,44	77,42±0,14	0,000*

One-way ANOVA Test **p<0.05*

The mean L* values of three different materials assigned to blumic subgroups (1.6 pH) at T1 were found significantly different (p=0.000). The L* values are ordered as; Ceramill Zolid (78,88±0,27) > Celtra Duo (77,65±0,33) > IPS e.max (76,57±0,23). Mean L* value of Ceramill Zolid was found significantly higher than Celtra Duo and IPS e.max (p=0.000, p=0.000 respectively) at T1; and mean L* value of Celtra Duo was found significantly higher than IPS e.max (p=0.000) at T1 according to post-hoc Tukey Test.

The mean L* values of three different materials assigned to control subgroups (7 pH) at T1 were found significantly different (p=0.000). Similarly, the L* values are ordered as; Ceramill Zolid (77,42±0,14) > Celtra Duo (77,18±0,44) > IPS e.max (75,96±0,21). The mean L* value of IPS e.max was found significantly lower than Celtra Duo and Ceramill Zolid (p=0.000, p=0.000 respectively) at T1; however there was no statistically significant difference between Celtra Duo and Ceramill Zolid (p=0.109) in terms of mean L* value at T1 according to post-hoc Tamhane's T2 Test.

Table 4.25. a* value evaluations among different materials and solutions at T_1.

Solution	a*	IPS e.max CAD (E) $\bar{x} \pm SD$	Celtra Duo CAD (C) $\bar{x} \pm SD$	Ceramill Zolid HT+ (Z) $\bar{x} \pm SD$	p
1.6 pH	**T_1**	1,17±0,04	0,94±0,06	2,04±0,11	0,000*
7 pH	**T_1**	1,30±0,04	0,98±0,06	2,45±0,05	0,000*

One-way ANOVA Test **p<0.05*

The mean a* values of three different materials assigned to blumic subgroups (1.6 pH) at T1 were found significantly different (p=0.000). The a* values are ordered as; Ceramill Zolid (2,04±0,11) > IPS e.max (1,17±0,04) > Celtra Duo (0,94±0,06). Mean a* value of Ceramill Zolid was found significantly higher than IPS e.max and Celtra Duo (p=0.000, p=0.000 respectively) at T1; and mean a* value of IPS e.max was found significantly higher than Celtra Duo (p=0.000) at T1 according to post-hoc Tamhane's T2 Test.

The mean a* values of three different materials assigned to control subgroups (7 pH) at T1 were found significantly different (p=0.000). Similarly, the a* values are ordered as; Ceramill Zolid (2,45±0,05) > IPS e.max (1,30±0,04) > Celtra Duo (0,98±0,06). The mean a* value of Ceramill Zolid was found significantly higher than IPS e.max and Celtra Duo (p=0.000, p=0.000 respectively) at T1; and mean a* value of IPS e.max was found significantly higher than Celtra Duo (p=0.000) at T1 according to post-hoc Tukey Test.

Table 4.26. b* value evaluations among different materials and solutions at T_1.

Solution	b*	IPS e.max CAD (E) $\bar{x} \pm SD$	Celtra Duo CAD (C) $\bar{x} \pm SD$	Ceramill Zolid HT+ (Z) $\bar{x} \pm SD$	p
1.6 pH	**T_1**	12,66±0,13	10,89±0,17	10,15±0,22	0,000*
7 pH	**T_1**	13,44±0,12	11,48±0,17	10,82±0,26	0,000*

One-way ANOVA Test **p<0.05*

The mean b* values of three different materials assigned to blumic subgroups (1.6 pH) at T1 were found significantly different (p=0.000). The b* values are ordered as; IPS e.max (12,66±0,13) > Celtra Duo (10,89±0,17) > Ceramill Zolid (10,15±0,22). Mean b* value of IPS e.max was found significantly higher than Celtra Duo and Ceramill Zolid (p=0.000, p=0.000 respectively) at T1; and mean b* value of Celtra Duo was found significantly higher than Ceramill Zolid (p=0.000) at T1 according to post-hoc Tukey Test.

The mean b* values of three different materials assigned to control subgroups (7 pH) at T1 were found significantly different (p=0.000). Similarly, the b* values are ordered as; IPS e.max (13,44±0,12) > Celtra Duo (11,48±0,17) > Ceramill Zolid (10,82±0,26). Similarly, the mean b* value of IPS e.max was found significantly higher than Celtra Duo and Ceramill Zolid (p=0.000, p=0.000 respectively) at T1; and mean b* value of Celtra Duo was found significantly higher than Ceramill Zolid (p=0.000) at T1 according to post-hoc Tamhane's T2 Test.

4.2.1.3. Evaluations of Color Parameters (L*, a*, b*) of Each Subgroup Before and After the Solution Exposure (T_0-T_1)

All six subgroups were found significantly affected by the respective solution exposures in terms of L*, a* and b* values, and detailed statistics were shown in Table 4.27., Table 4.28. and Table 4.29.

Table 4.27. L* value evaluations of six subgroups before and after (T_0-T_1) the solution exposure.

Solution	L*	IPS e.max CAD (E) $\bar{x} \pm SD$	Celtra Duo CAD (C) $\bar{x} \pm SD$	Ceramill Zolid HT+ (Z) $\bar{x} \pm SD$
1.6 pH	**T_0**	75,9±0,22	77±0,38	77,67±0,44
	T_1	76,57±0,23	77,65±0,33	78,88±0,27
	p	0,000*	0,000*	0,000*
7 pH	**T_0**	75,59±0,23	77,73±0,51	77,16±0,24
	T_1	75,96±0,21	77,18±0,44	77,42±0,14
	p	0,000*	0,000*	0,000*

Paired Samples t test *$p<0.05$*

With the exposure of blumic solution, the L* value of IPS e.max, Celtra Duo and Ceramill Zolid were significantly increased (p=0.000, p=0.000, p=0.000 respectively). When the L* values were compared before and after the exposure of control solution, L* values of IPS e.max and Ceramill Zolid were increased significantly (p=0.000, p=0.000 respectively), while L* value of Celtra Duo was significantly decreased (p. =0.000).

Table 4.28. a* value evaluations of six subgroups before and after (T_0-T_1) the solution exposure.

Solution	a*	IPS e.max CAD (E)	Celtra Duo CAD (C)	Ceramill Zolid HT+ (Z)
		x̄ ± SD	x̄ ± SD	x̄ ± SD
1.6 pH	**T_0**	1,40±0,04	1,22±0,05	2,53±0,09
	T_1	1,17±0,04	0,94±0,06	2,04±0,11
	p	0,000*	0,000*	0,000*
7 pH	**T_0**	1,46±0,04	1,26±0,06	2,52±0,05
	T_1	1,30±0,04	0,98±0,06	2,45±0,05
	p	0,000*	0,000*	0,000*

Paired Samples t test *$p<0.05$

With the exposure of blumic solution, the a* values of IPS e.max, Celtra Duo and Ceramill Zolid were significantly decreased (p=0.000, p=0.000, p=0.000 respectively). When the a* values were compared before and after the exposure of control solution, a* values of IPS e.max, Celtra Duo and Ceramill Zolid were also decreased significantly (p=0.000, p=0.000, p=0.000 respectively).

Table 4.29. b* value evaluations of six subgroups before and after (T_0-T_1) the solution exposure.

Solution	b*	IPS e.max CAD (E)	Celtra Duo CAD (C)	Ceramill Zolid HT+ (Z)
		x̄ ± SD	x̄ ± SD	x̄ ± SD
1.6 pH	**T_0**	14,26±0,13	12,37±0,15	12,17±0,21
	T_1	12,66±0,13	10,89±0,17	10,15±0,22
	p	0,000*	0,000*	0,000*
7 pH	**T_0**	14,29±0,13	12,45±0,19	11,71±0,21
	T_1	13,44±0,12	11,48±0,17	10,82±0,26
	p	0,000*	0,000*	0,000*

Paired Samples t test *$p<0.05$

With the exposure of blumic solution, the b* values of IPS e.max, Celtra Duo and Ceramill Zolid were significantly decreased (p=0.000, p=0.000, p=0.000 respectively). When the b* values were compared before and after the exposure of control solution, b* values of IPS e.max, Celtra Duo and Ceramill Zolid were also decreased significantly (p=0.000, p=0.000, p=0.000 respectively).

4.2.1.4. Comparison of Color Changes (ΔE) on Different CAD-CAM Materials Exposed to Different Solutions

Color change (ΔE) of a material was observed by two parameters; different solutions and different materials. The results are shown in Table 4.30.

Table 4.30. ΔE Evaluation on Different Materials and Solutions

	ΔE		
	1.6 pH	**7 pH**	
Material	**$\bar{x}$ ± SD**	**$\bar{x}$ ± SD**	**p**
IPS e.max (E)	1,75±0,03	0,94±0,03	0,000*
Celtra Duo (C)	1,65±0,03	1,19±0,05	0,000*
Ceramill Zolid (Z)	2,42±0,20	0,97±0,09	0,000*
p	0,000*	0,000*	

Two-way ANOVA Test **p<0.05*

When the effect of blumic solution (1.6 pH) on color change among different materials were evaluated, statistically significant differences were found (p=0.000). The color change (ΔE) values of materials were ordered as; Ceramill Zolid (2,42±0,20) > IPS e.max (1,75±0,03) > Celtra Duo (1,65±0,03). According to post-hoc Tamhane's T2 Test (Table 4.30.a.), the color change (ΔE) value of Ceramill Zolid was significantly higher than IPS e.max and Celtra Duo (p=0.000, p=0.000 respectively). The color change (ΔE) value of IPS e.max was significantly higher than Celtra Duo (p=0.000).

When the influence of control solution (7 pH) was evaluated on the color change (ΔE) of three different materials, statistically significant differences were found (p=0.000). The color change (ΔE) values were ordered as; Celtra Duo (1,19±0,05) > Ceramill Zolid (0,97±0,09) > IPS e.max (0,94±0,03). According to post-hoc Tamhane's T2 Test (Table 4.30.b.), color change (ΔE) value of Celtra Duo was significantly higher than Ceramill Zolid and IPS e.max (p=0.000, p=0.000 respectively). There were no statistically significant differences between the IPS e.max and Ceramill Zolid (p=0.462) in terms of color change (ΔE) values.

Table 4.30.a. Multiple comparisons of blumic subgroups' color change values

Solution	ΔE	Material 1	Material 2	Mean Difference (1-2)	SE	p	95% Confidence Interval Lower Bound	Upper Bound
1.6 pH Blumic Solution		IPS e.max	Celtra Duo	,10667*	0,010	0,000	0,081	0,133
			Ceramill Zolid	-,66889*	0,047	0,000	-0,792	-0,546
		Celtra Duo	IPS e.max	-,10667*	0,010	0,000	-0,133	-0,081
			Ceramill Zolid	-,77556*	0,047	0,000	-0,898	-0,653
		Ceramill Zolid	IPS e.max	,66889*	0,047	0,000	0,546	0,792
			Celtra Duo	,77556*	0,047	0,000	0,653	0,898

Tamhane's T2 Test *$p<0.05$

Table 4.30.b. Multiple comparisons of control subgroups' color change values

Solution	ΔE	Material 1	Material 2	Mean Difference (1-2)	SE	p	95% Confidence Interval Lower Bound	Upper Bound
7 pH Control Solution		IPS e.max	Celtra Duo	-,25333*	0,013	0,000	-0,286	-0,221
			Ceramill Zolid	-0,029	0,022	0,462	-0,085	0,027
		Celtra Duo	IPS e.max	,25333*	0,013	0,000	0,221	0,286
			Ceramill Zolid	,22389*	0,023	0,000	0,165	0,283
		Ceramill Zolid	IPS e.max	0,029	0,022	0,462	-0,027	0,085
			Celtra Duo	-,22389*	0,023	0,000	-0,283	-0,165

Tamhane's T2 Test *$p<0.05$

A comparison was made on the color change (ΔE) value of a material affected by two different solutions. ΔE values of IPS e.max, Celtra Duo and Ceramill Zolid blumic subgroups were higher (1,75±0,03; 1,65±0,03; 2,42±0,20 respectively) than IPS e.max, Celtra Duo and Ceramill Zolid control subgroups (0,94±0,03; 1,19±0,05; 0,97±0,09 respectively). These differences were statistically significant (p=0.000, p=0.000, p=0.000 respectively) (Figure 4.10.).

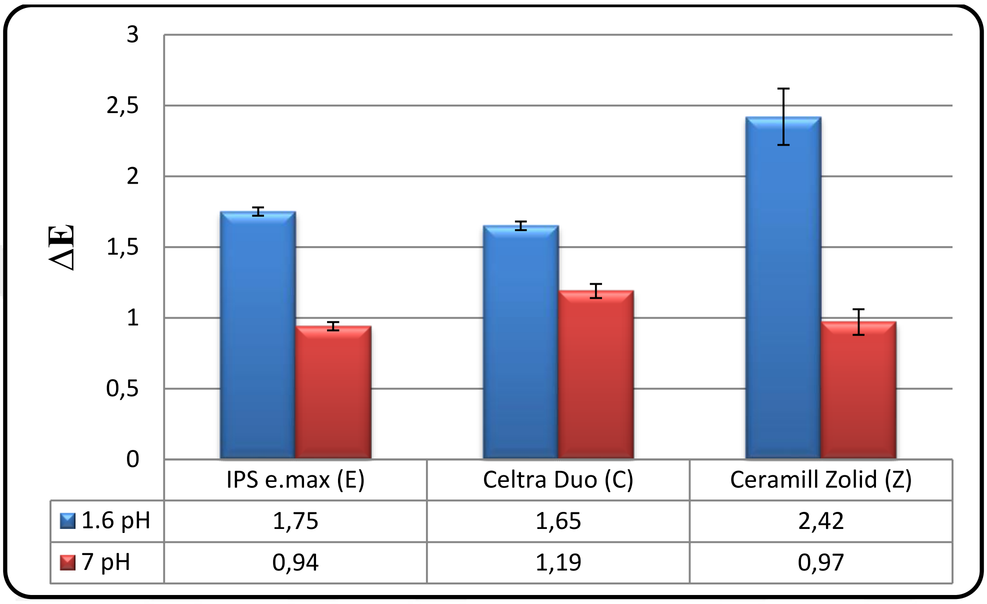

Figure 4.10. Color change evaluations on different materials and solutions

When the influences of material change, solution pH and their interaction on color change (ΔE) were evaluated with the two-way analysis of variance, the results were found as seen on Table 4.31.

Table 4.31. Evaluation of the common effect of material and solution on ΔE

	Type III Sum of Squares	**df**	**Mean Square**	**F**	**p**
Material	2,441	2	1,22	145,062	0,000*
Solution	22,159	1	22,159	2634,178	0,000*
Material * Solution	4,612	2	2,306	274,137	0,000*

Two-way ANOVA Test **p<0.05*

It was shown that material change, solution change and material*solution interactions were significantly affected the ΔE (F:145.062, p:0.000; F: 2634,178, p:0.000; F: 274,137, p:0.000 respectively). When F values observed, statistics showed that solution change has influenced ΔE more than material change and material*solution interactions.

4.2.2. Translucency Results

Translucency parameter (TP) was evaluated among three different CAD-CAM materials [IPS e.max CAD (E), Celtra Duo CAD (C) and Ceramill Zolid HT+ (Z)] on baseline (T_0) and after the immersions on two different solutions (T_1). The absolute values of the change of translucency parameter from T_0 to T_1 (ΔTP) were evaluated based on material and solution. Higher absolute ΔTP value means that the material's translucency changed more.

Descriptive statistics on translucency parameter of six subgroups before and after the solution exposures were shown at Table 4.32.

Table 4.32. Descriptive statistics on translucency parameter (TP) of six subgroups before and after the solution exposures

Translucency Parameter (TP)		n	x̄	SD	Min.	Max.	Median	Skewness	SE of Mean
T0 TP	IPS e.max Blumic Subgroup	18	16,80	0,20	16,42	17,14	16,775	0,15	0,05
	Celtra Duo Blumic Subgroup	18	17,50	0,23	17,18	17,90	17,460	0,31	0,05
	Ceramill Zolid Blumic Subgroup	18	8,81	0,25	8,37	9,15	8,870	-0,37	0,06
	IPS e.max Control Subgroup	18	16,53	0,21	16,23	16,91	16,515	0,46	0,05
	Celtra Duo Control Subgroup	18	17,33	0,21	17,02	17,72	17,290	0,36	0,05
	Ceramill Zolid Control Subgroup	18	8,13	0,21	7,76	8,62	8,125	0,67	0,05
T1 TP	IPS e.max Blumic Subgroup	18	15,75	0,16	15,37	15,97	15,775	-0,96	0,04
	Celtra Duo Blumic Subgroup	18	17,32	0,24	16,92	17,82	17,305	0,46	0,06
	Ceramill Zolid Blumic Subgroup	18	7,67	0,19	7,30	7,98	7,665	-0,17	0,05
	IPS e.max Control Subgroup	18	16,47	0,17	16,19	16,82	16,440	0,32	0,04
	Celtra Duo Control Subgroup	18	17,84	0,28	17,32	18,28	17,820	-0,32	0,07
	Ceramill Zolid Control Subgroup	18	7,66	0,26	7,26	8,26	7,680	0,83	0,06
ΔTP	IPS e.max Blumic Subgroup	18	-1,05	0,18	-1,35	-0,65	-1,06	0,54	0,04
	Celtra Duo Blumic Subgroup	18	-0,18	0,18	-0,68	0,03	-0,185	-1,23	0,04
	Ceramill Zolid Blumic Subgroup	18	-1,14	0,27	-1,58	-0,67	-1,195	0,29	0,06
	IPS e.max Control Subgroup	18	-0,05	0,19	-0,51	0,14	0,025	-1,46	0,05
	Celtra Duo Control Subgroup	18	0,51	0,30	0,10	1,12	0,395	0,76	0,07
	Ceramill Zolid Control Subgroup	18	-0,48	0,19	-0,79	-0,04	-0,49	0,54	0,04

4.2.2.1. Baseline (T_0) Evaluations of Translucency Parameter (TP) Among CAD-CAM Materials

Statistics for baseline (T0) translucency parameter (TP) measurements were shown at Table 4.33.

Table 4.33. Baseline TP parameter evaluations among different materials and solutions.

Solution	TP	IPS e.max CAD (E) $\bar{x}$ ± SD	Celtra Duo CAD (C) $\bar{x}$ ± SD	Ceramill Zolid HT+ (Z) $\bar{x}$ ± SD	p
1.6 pH	**T_0**	16,80±0,2	17,50±0,23	8,81±0,25	0,000*
7 pH	**T_0**	16,53±0,21	17,33±0,21	8,13±0,21	0,000*

One-way ANOVA Test *$p<0.05$

The mean baseline TP values of three different materials assigned to blumic subgroups (1.6 pH) were found significantly different (p=0.000). The TP values are ordered as; Celtra Duo (17,50±0,23) > IPS e.max (16,80±0,2) > Ceramill Zolid (8,81±0,25). Mean TP value of Celtra Duo was found significantly higher than IPS e.max and Ceramill Zolid (p=0.000, p=0.000 respectively) at T0; and mean TP value of IPS e.max was found significantly higher than Ceramill Zolid (p=0.000) at T0 according to post-hoc Tukey Test.

Similarly, the mean baseline TP values of three different materials assigned to control subgroups (7 pH) were found significantly different (p=0.000). The TP values are ordered as; Celtra Duo (17,33±0,21) > IPS e.max (16,53±0,21) > Ceramill Zolid (8,13±0,21). Mean TP value of Celtra Duo was found significantly higher than IPS e.max and Ceramill Zolid (p=0.000, p=0.000 respectively) at T0; and mean TP value of IPS e.max was found significantly higher than Ceramill Zolid (p=0.000) at T0 according to post-hoc Tukey Test.

4.2.2.2. Translucency Parameter (TP) Evaluations After Solution Exposures (T_1) Among CAD-CAM Materials

Statistics for T_1 translucency parameter (TP) measurements were shown at Table 4.34.

Table 4.34. Translucency parameter evaluations among different materials and solutions at T_1.

Solution	TP	IPS e.max CAD (E) $\bar{x} \pm SD$	Celtra Duo CAD (C) $\bar{x} \pm SD$	Ceramill Zolid HT+ (Z) $\bar{x} \pm SD$	p
1.6 pH	**T_1**	15,75±0,16	17,32±0,24	7,67±0,19	0,000*
7 pH	**T_1**	16,47±0,17	17,84±0,28	7,66±0,26	0,000*

One-way ANOVA Test **p<0.05*

The mean TP values of three different materials assigned to blumic subgroups (1.6 pH) at T1 were found significantly different (p=0.000). The TP values are ordered as; Celtra Duo (17,32±0,24) > IPS e.max (15,75±0,16) > Ceramill Zolid (7,67±0,19). Mean TP value of Celtra Duo was found significantly higher than IPS e.max and Ceramill Zolid (p=0.000, p=0.000 respectively) at T1; and mean TP value of IPS e.max was found significantly higher than Ceramill Zolid (p=0.000) at T1 according to post-hoc Tukey Test.

Similarly, the mean TP values of three different materials assigned to control subgroups (7 pH) at T1 were found significantly different (p=0.000). The TP values are ordered as; Celtra Duo (17,84±0,28) > IPS e.max (16,47±0,17) > Ceramill Zolid (7,66±0,26). Mean TP value of Celtra Duo was found significantly higher than IPS e.max and Ceramill Zolid (p=0.000, p=0.000 respectively) at T1; and mean TP value of IPS e.max was found significantly higher than Ceramill Zolid (p=0.000) at T1 according to post-hoc Tukey Test.

4.2.2.3. Translucency Parameter (TP) Evaluations of Each Subgroup Before and After the Solution Exposure (T_0-T_1)

All subgroups, except IPS e.max control subgroup, were found significantly affected by the respective solution exposures and statistical details were shown at Table 4.35.

Table 4.35. TP evaluations of six subgroups before and after (T_0-T_1) the solution exposure.

Solution	TP	IPS e.max CAD (E) x̄ ± SD	Celtra Duo CAD (C) x̄ ± SD	Ceramill Zolid HT+ (Z) x̄ ± SD
1.6 pH	**T_0**	16,80±0,2	17,50±0,23	8,81±0,25
	T_1	15,75±0,16	17,32±0,24	7,67±0,19
	p	0,000*	0,001*	0,000*
7 pH	**T_0**	16,53±0,21	17,33±0,21	8,13±0,21
	T_1	16,47±0,17	17,84±0,28	7,66±0,26
	p	0,254	0,000*	0,000*

Paired Samples t test *$p<0.05$*

The decreases in mean translucency parameter (TP) values from T0 to T1 were statistically significant for IPS e.max, Celtra Duo and Ceramill Zolid blumic subgroups (p=0.000, p=0.001, p=0.000 respectively). The changes in mean translucency parameter (TP) values from T0 to T1 were statistically significant for Celtra Duo and Ceramill Zolid control subgroups (p=0.000, p=0.000 respectively) materials. While TP of Celtra Duo control subgroup was increasing, TP of Ceramill Zolid control subgroup was decreasing. However there is no statistically significant difference in the decrease of mean translucency parameter (TP) value from t0 to t1 for IPS e.max control subgroup (p=0.254).

4.2.2.4. Comparison of Translucency Parameter Changes (ΔTP) on Different CAD-CAM Materials Exposed to Different Solutions

Translucency parameter change (ΔTP) of a material was observed by two parameters; different solutions and different materials. The results are shown in Table 4.36.

Table 4.36. ΔTP Evaluation on Different Materials and Solutions

	ΔTP		
	1.6 pH	**7 pH**	
Material	**x̄ ± SD**	**x̄ ± SD**	**p**
IPS e.max (E)	-1,05±0,18	-0,05±0,19	0,000*
Celtra Duo (C)	-0,18±0,18	0,51±0,30	0,000*
Ceramill Zolid (Z)	-1,14±0,27	-0,48±0,19	0,000*
p	0,000*	0,000*	

Two-way ANOVA Test **p<0.05*

When the effect of blumic solution on translucency parameter change (ΔTP) among different materials were evaluated, statistically significant differences were found (p=0.000). The absolute translucency parameter change (ΔTP) values of materials were ordered as; Ceramill Zolid (1,14±0,27) > IPS e.max (1,05±0,18) > Celtra Duo (0,18±0,18). According to post-hoc Tukey Test (Table 4.36.a.), the ΔTP of Celtra Duo was significantly lower than IPS e.max and Ceramill Zolid (p=0.000, p=0.000 respectively). There was no statistical difference in the ΔTP of IPS e.max and Ceramill Zolid (p=0.394). All of three material types had a decrease tendency in TP.

When the influence of control solution was evaluated on the translucency parameter change (ΔTP) of three different materials, statistically significant differences were found (p=0.000). The absolute values of translucency parameter change (ΔTP) were ordered as; Celtra Duo (0,51±0,30) > Ceramill Zolid (0,48±0,19) > IPS e.max (0,05±0,19). According to post-hoc Tamhane's T2 Test (Table 4.36.b.), ΔTP of Celtra Duo was significantly higher than Ceramill Zolid and IPS e.max (p=0.000, p=0.000 respectively), and the ΔTP of Ceramill Zolid was significantly higher than IPS e.max (p=0.000). While the TP of Celtra Duo was increased after the exposure to control solution, TP values of IPS e.max and Ceramill Zolid were decreased.

Table 4.36.a. Multiple comparisons of blumic subgroups' translucency change values

Solution	ΔTP	Material 1	Material 2	Mean Difference (1-2)	SE	p	95% Confidence Interval	
							Lower Bound	Upper Bound
1.6 pH Blumic Solution		IPS e.max	Celtra Duo	-,86556*	0,072	0,000	-1,039	-0,692
			Ceramill Zolid	0,094	0,072	0,394	-0,079	0,268
		Celtra Duo	IPS e.max	,86556*	0,072	0,000	0,692	1,039
			Ceramill Zolid	,96000*	0,072	0,000	0,787	1,134
		Ceramill Zolid	IPS e.max	-0,094	0,072	0,394	-0,268	0,079
			Celtra Duo	-,96000*	0,072	0,000	-1,134	-0,787

Tukey HSD Test **p<0.05*

Table 4.36.b. Multiple comparisons of control subgroups' translucency change values

Solution	ΔTP	Material 1	Material 2	Mean Difference (1-2)	SE	p	95% Confidence Interval	
							Lower Bound	Upper Bound
7 pH Control Solution		IPS e.max	Celtra Duo	-,56389*	0,077	0,000	-0,751	-0,377
			Ceramill Zolid	,42611*	0,077	0,000	0,239	0,613
		Celtra Duo	IPS e.max	,56389*	0,077	0,000	0,377	0,751
			Ceramill Zolid	,99000*	0,077	0,000	0,803	1,177
		Ceramill Zolid	IPS e.max	-,42611*	0,077	0,000	-0,613	-0,239
			Celtra Duo	-,99000*	0,077	0,000	-1,177	-0,803

Tamhane's T2 Test **p<0.05*

A comparison was made on the translucency parameter change (ΔTP) of a material affected by two different solutions. The absolute ΔTP values of IPS e.max and Ceramill Zolid blumic subgroups were higher (1,05±0,18; 1,14±0,27 respectively) than IPS e.max and Ceramill Zolid control subgroups (0,05±0,19; 0,48±0,19 respectively). The differences were statistically significant (p=0.000, p=0.000 respectively). The absolute ΔTP value of Celtra Duo blumic subgroup was lower (0,18±0,18) than Celtra Duo control subgroup (0,51±0,30). This difference was statistically significant (p=0.000). While the change of TP in Celtra Duo control subgroup had an increase tendency, the change of TP in Celtra Duo blumic subgroup had a decrease tendency (Figure 4.11.).

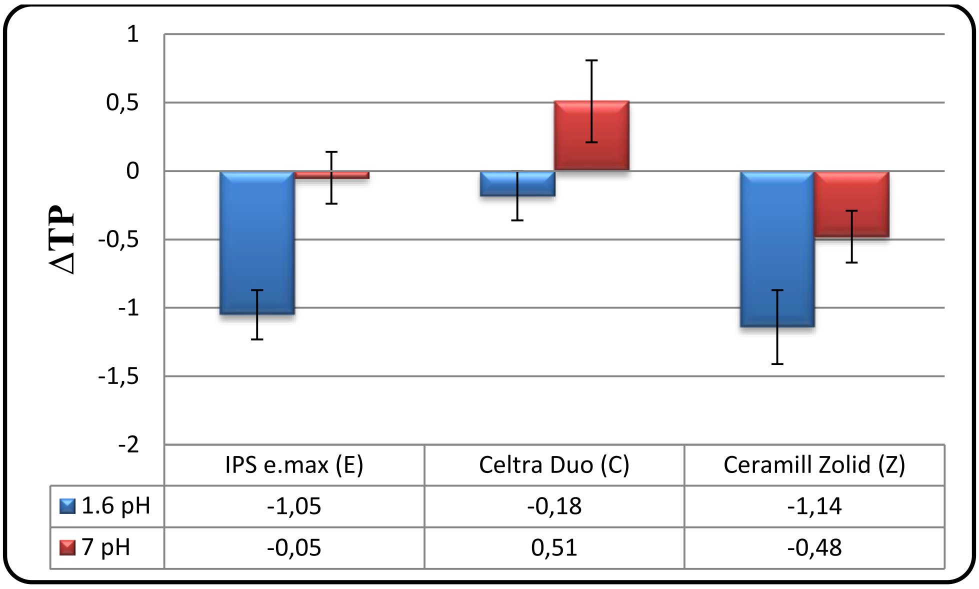

Figure 4.11. Translucency change evaluations on different materials and solutions

When the influences of material change, solution pH and their interactions on translucency parameter change (ΔTP) were evaluated with the two-way analysis of variance, the results were found as seen on Table 4.37.

Table 4.37. Evaluation of the common effect of material and solution on ΔTP

	Type III Sum of Squares	**df**	**Mean Square**	**F**	**p**
Material	18,350	2	9,175	182,805	0,000*
Solution	16,521	1	16,521	329,153	0,000*
Material * Solution	0,606	2	0,303	6,034	0,003*

Two-way ANOVA Test **p<0.05*

It was shown that material change, solution change and material*solution interactions were significantly affected the ΔTP (F:182.805, p:0.000; F: 329.153, p:0.000; F: 6.034, p:0.003 respectively). When F values observed, statistics showed that solution change has influenced ΔTP more than material change and material*solution interactions.

5. DISCUSSION

CAD-CAM systems have been introduced into our lives recently and enormous developments have been made in the field of different brands and different materials.[1] Many researches have been conducted on how CAD-CAM materials undergo changes under different clinical conditions.[7] Different intrinsic erosive conditions such as blumia nervosa may cause some changes on the mechanical and optical characteristics of CAD-CAM restorations.[7–9,16–20]

With the new diagnostic criteria about eating disorders[13], it was seen that blumia nervosa incidence has risen, since even symptoms with fewer frequencies have been counted as mild type of this disease. Thus, the investigations on this type of intrinsic conditions causing erosion and corrosion by gastric acid content on both teeth and dental restorations have gained attention.[7–9,16,299,300]

There is no clinical consensus in the literature for the most accurate method, pH and time of gastric acid exposition in regards to simulate the endogenous chemical clinical conditions. In the current in vitro study, blumia nervosa condition was simulated in vitro and compared with control conditions which were chosen as exposure to artificial saliva. Therefore, observing the different mechanical and optical parameters of three different CAD-CAM restorative materials was aimed under blumia and control conditions. According to the conducted literature review, same materials and same parameters were not evaluated under these experimental conditions in a study before.

While many studies[10,17,201,301–303] were conducted on extrinsic erosive conditions, some researchers have investigated the effects of mediums with different pH.[21,304] The carbonated drinks were significantly found less erosive on dental hard tissues compared to gastric juice.[166] This result was explained by the lower pH and higher acidity of gastric juice compared to the carbonated drinks. However, studies[7–9,16,299,300] investigating the effect of intrinsic corrosive conditions were less in number, having different designs with different conclusions. It was aimed to fill one of the possible gaps in the literature with the current study, therefore blumia nervosa patients' clinical situation was aimed to simulate firstly.

According to Schlueter et al.[153] blumic patients vomit 6-10 times a day regularly. In this current study, vomiting number in a day was selected as 8 times on average, consistent with that information. Effect of acidic vomit exposure on teeth was shown as 2 minutes conformed to the length of pH decline duration in saliva after an acid attack.[153,297] 5 years of exposure to blumia nervosa was calculated through the 2 minutes of contact happened for 8 times a day, therefore total immersion time was found as 486.5 hours which is approximately 20 days eventually. The pH of the immersion solution was selected as 1.6 regarding that the physiologic pH of gastric juice after a complete meal was found as 1.6.[165] Current immersion solution formula was adopted from Schlueter et al.'s research.[153] Mentioned researchers have added 'pepsin', which is a proteolytic enzyme degrading the organic matrix, into the blumia solution in order to see the effect on dentin organic matrix.[153] Pepsin was not expected to make any changes on dental ceramics, since there was no organic matrix in this study. So, pepsin was not added into the current study's solution.

Different immersion protocols based on immersion time, simulated period and solution pH were found in the literature.[16,18,305] Alnasser et al.[9] have used the HCl solution with 2 pH for 45 and 91 hours in order to simulate 6 months and 12 months of vomiting on blumia nervosa patients. Immersion time was calculated regarding the statement of Harryparsad et al.[16], who suggested that average daily exposure time of teeth to gastric acid in a patient with blumia nervosa is 15 minutes, because of the assumption that a blumic patient vomits three times a day which takes five minutes per vomit.[306] Backer et al.[300] have simulated a scenario of 2 and 8 years of vomiting with 6 and 24 hours of immersion in 1.2 pH solution. That blumic scenario was obtained from the study of Zaki et al.[18] who claimed that 6 hours immersion in 3.8 pH simulated gastric acid represents 2 years of vomiting on blumia nervosa.[166] Zaki et al.[18] studied 2 and 4 years of vomiting exposure as 6 and 12 hours of immersion periods. Cengiz et al.[19] have evaluated the effect of gastric juice with 1.14 pH with a design representing a gastroesophageal reflux disease (GERD) patient. However, the immersion time was only 24 hours. Immersion time was considered as a potential limitation by authors, while they claimed that their design was a worse-case scenario since the reflux attacks may occur several times a day. Sulaiman et al.[8] have used simulated gastric acid solution with 1.2 pH for 96 hours in 37^{o}C incubator in order to simulate over 10 years of clinical exposure according to Hunt et al.'s[305] method, which simulates 2-3 years in vivo conditions of endogenous dental erosion. Cruz et al.[7] have immersed materials into a solution prepared with HCl on 1.2 pH, and the immersion time was 18 hours and 25 minutes representing the average blumia patient who purges 3 times a day[7,306] for 2 years and estimated contact time was 30 seconds.[7,18]

These researchers have chosen different material types with different brands which may be listed as CAD-CAM glass matrix ceramics[7–9], polycrystalline ceramics such as monolithic zirconia[8,9] and resin matrix ceramics[7,9], CAD-CAM resin composites[300], conventional composites[18] and laboratory composites.[19] In current study, besides lithium disilicate and 4Y-TZP monolithic zirconia material, zirconia reinforced lithium silicate was preferred in fully crystallized state. Traini et al.[49] stated that zirconia reinforced lithium silicate materials exhibited more brittle characteristics in partially crystallized state. However, the manufacturer claimed that the material may be suitable in partially crystallized form.[307] They can be cemented when polished immediately after milling, thus creating a great advantage in chair-side work. Yet, the manufacturer also suggested that final crystallization may strengthen the materials optical and mechanical properties, despite not being obligatory.[307]

If the material allowed, glaze applications or polishing procedures were chosen in aforementioned studies as a surface treatment especially for glass ceramics and monolithic zirconia, or no surface treatment was applied after grinding the samples. For dental restorations, the main goal of surface treatments is always gathering the smoothest restoration surface in order to obtain long-term clinical success and durability for ceramic restorations.[117] Glazing was suggested as a way to provide highly desired smooth ceramic surface.[131] Despite decreasing the roughness of material and promoting surface smoothing, additional firings during glaze application might harmfully impact the material's fatigue strength, might cause defect formation on ceramic surfaces which leads to permanent corruption, and might delay the delivery of the restoration.[39,109] It was stated that if there are no esthetic obligations for glazing, polishing should be done especially on the occlusal surfaces of posterior restorations.[47] Glazing might be avoided because the resistance of the glaze is questionable when the restoration is in function.[123] Rapidly worn out glaze layer after functioning along a period or abraded via chair-side adaptation is a common issue especially for glazed monolithic zirconia.[127,137] Additionally, adequate bonding between glaze layer and Y-TZP ceramic could be hard to obtain.[133] After the glaze was disappeared, underlying unpolished rough zirconia could be exposed. If glaze application was requested to enhance final esthetic properties especially for monolithic zirconia, Amer et al.[127] and Zucuni et al.[109] suggested adequate polishing before glazing to generate smooth surface prior to glaze application for mechanic improvements and prevention of antagonist enamel abrasion. Thus, the restoration could be protected from further destructive effects caused by the chance of glaze layer loss in clinical use. The longevity of glaze could not be established well enough to sustain restoration smoothness under the functional forces, however polishing was found more durable and promising according to recent researches.[10,39,47,83,105,123,126,128–130] Therefore, polishing was chosen as the surface treatment in the current study. Besides, the materials' own characteristics against corrosive conditions could be observed instead of the characteristics of glaze layer.

Smooth and polished surfaces contribute to the higher esthetics of dental restorations by stabilizing color and translucency[138] and increasing luster[104]. The polished surfaces minimize bacterial adhesion[139] and improving biocompatibility[102] through increasing the adherence and reproduction of epithelial cells and fibroblasts of gingiva to the lithium disilicate glass ceramic besides diminishing the plaque retention.[47,140,141] Polished surfaces diminish the material exhaustion and risk of chipping or fracture[142], and enhance flexural strength[143] and fatigue behavior compared to glazing.[109] Furthermore, smooth surfaces experience lesser wear.[144,145] Consequently, they extend the lifetime of both the restoration and antagonist, because smooth surfaces lead to less antagonist wear as well.[144] Intraoral polishing aids in reducing the susceptibility to cross-contamination by removing requirements for recurring laboratory steps.[143]

Matzinger et al.[129], Vichi et al.[130], Amaya-Pajares et al.[126] and Zucuni et al.[109] recommended the use of polishing systems for lithium disilicate, zirconia reinforced lithium silicate and monolithic zirconia materials, including Optra Fine system. Several studies[123,129] suggested polishing systems with diamond polishing pastes to achieve optimal clinical performance and guaranteeing smooth surfaces, Ra being less than 0,2 µm.[102] High gloss polishing was found necessary due to significant reduction in surface roughness hereby with the decrease in fracture risk.[129] In the lights of these informations, polishing with three step Optra Fine polishing system was chosen as surface treatment and applied to all samples. Polishing time was chosen as 30 seconds per tip as recommended by manufacturer.

Contact profilometer was utilized in this study to mainly observe the surface roughness (Ra) due to its reliability in flat surfaces, availability and easy use. It has provided correct measurements on surface roughness of flat samples contained under corrosive environment.[205,206] The efficiency of surface roughness measurement methods depend on both sample and device. Device dependent factors may include stylus size, scanning speed, response frequency, sampling length or area. When the stylus size gets smaller, the original profile will be followed precisely even in very small defects. A device could not measure the defects smaller than its stylus tip. When the contact profilometer is compared with other methods, it was seen that atomic force microscope (AFM) presents greater details. AFM and 3D optical profilometer can show surface topography in three dimensional records.[126] Thus it might be offered to use AFM or 3D optical profilometer to contribute the information gathered by contact profilometer. Contact profilometer informations were supported by surface topography evaluations obtained by scanning electron microscope (SEM) images and 3D optical profilometer images in this study.

Average surface roughness value (Ra) is the mostly used parameter for two dimensional observations of surface roughness in dentistry.[126,128,147] However Ra value differs in different techniques and devices. So, studies that used the same profilometer type should be used to make comparisons. Furthermore, Al-Shammery et al.[202] suggested using other parameters such as Rz, Rq and Rmax together with Ra in order to distinguish peaks from valleys and correct profile shape. In the current study, in order to compare the results with other studies, only Ra value was measured.

When the surface roughness values of IPS e.max, Celtra Duo and Ceramill Zolid were observed under blumic and control conditions, it was shown that blumic solution significantly increased the surface roughness (Ra) of three different materials. However they were roughened similarly by blumic solution. It was seen that IPS e.max and Celtra Duo were roughened by the influence of control solution similar to the effect of blumic solution, but it could not affect the surface roughness and topography of Ceramill Zolid. These informations were supported with the SEM and 3D optical profilometer images between Figure 4.4. and Figure 4.9. In the evaluation of which material's roughness was affected more severely, not the Ra values but the ΔRa values should be taken into consideration carefully, since initial roughness values were different. ΔRa of Ceramill Zolid control subgroup was significantly lower than blumic subgroup. It might be explained by inertness of zirconia against neutral solutions, compared to low temperature degradation (LTD) causing blumic solution, while other subgroups roughened similarly as mentioned above. ΔRa values of other subgroups were not significantly different between blumic and control solutions.

Based on the suggestions of Esquivel-Upshaw et al.[21], it might be speculated that being in an aqueous environment affects the roughness of glassy matrix ceramics independent from pH. While comparing the corrosive effects of solutions with acidic, basic and neutral pH, Esquivel-Upshaw et al.[21] claimed that the common reaction occurred in acidic solution is the ion exchange between network modifiers in material and protons in solution. In basic solutions, hydroxyl ions in environment demolish the glass structure by breaking off the bonds of silicon-oxygen-silicon molecules, thus leading dissolution. Combination of these two reactions occurs in neutral solutions. Corrosion of glassy matrix ceramics is more complex than these reactions, because of both glassy and crystalline phase content. First, dissolution happens on the glassy matrix which leads to crystals to be exposed into environment.[21] The crystalline phase, such as lithium disilicate crystals and zirconia reinforced lithium silicate crystals, was dissolved in a slower rate than glass matrix. The coordination and bonding energy of the composing elements are stronger for the crystalline phase compared to glassy phase and this reduces the dissolution rate of the crystals.[299] As a proof of this information and consistent with the current study, IPS e.max and Celtra Duo exhibited rough surfaces after both HCl and saliva immersion.

In a research[8] evaluating the monolithic zirconia against erosive conditions, partially and fully stabilized monolithic zirconia samples were found to have bead-like structures of Al, Ca, K or Fe oxides on corroded surfaces observed in SEM images after the exposure of HCl solution, thus showing susceptibility to corrosion. After the EDX evaluation, some elements like yttria and hafnium were disappeared from the surface of zirconia, thus confirming the ion interaction between solution and material. The lesser yttria content was resulted in the more vulnerability to low temperature degradation (LTD) on zirconia. LTD leads to phase transformation from tetragonal to monoclinic, subsequent crystal size increase and then surface irregularities, similar to current study which can be observed on Figure 4.9.B. These surface irregularities lead to micro cracks and subsequent macro cracks.[64]

When the SEM images correlated with roughness results, blumic subgroups look smoother than control subgroups on IPS e.max and Celtra Duo. However their roughness values were not significantly different. This might be explained by different corrosion patterns against different pH's.[21] Additionally, long exposure time to acidic solution might lead not only glass matrix dissolution, but removal of crystals as well. Thus lithium disilicate particles could not be seen on IPS e.max blumic subgroup clearly, as crystals were less distinguishable in Celtra Duo blumic subgroup. Even small pores of removed crystals can be seen in Figure 4.4.B., 4.5.B., 4.7.B. and Figure 4.8.B. However on control subgroups, crystals were more visible. This might be due to glass matrix's total destruction caused by sequential basic reactions occurred in neutral solution.[21] Thus the crystals were intact due to mild environment and complete loss of glass matrix can be observed. In Figure 4.9.C., Ceramill Zolid control subgroup looks as smooth as baseline image Figure 4.9.A.

Zirconia reinforced lithium silicate has approximately 0.5 µm mean crystal size, whereas lithium disilicate glass ceramic has 1.5 µm mean crystal size.[307] These dimension differences, meaning smaller Celtra Duo crystals than IPS e.max crystals, might be observed by following the black arrows on Figure 4.7.C and Figure 4.8.C. In a research[130] comparing the Vita Suprinity and IPS e.max, Vita Suprinity exhibited higher polishability than IPS e.max CAD. This result is consistent with current study, since Vita Suprinity and Celtra Duo have similar molecular content; mainly consisting of SiO_2, Li_2O, ZrO_2.[129] They both are zirconia reinforced lithium silicate materials having homogenous glassy matrix containing crystalline component made of round and sub-micrometric elongated grains of lithium metasilicates. Lithium metasilicates were converted into lithium disilicates after crystallization process; additionally tetragonal zirconia fillers are added to increase strength values.[308] As claimed by aforementioned study, higher polishability of zirconia reinforced lithium silicate might be due to its finer microstructure compared to lithium disilicate and higher zirconium dioxide content of Vita Suprinity.[130] During polishing the zirconia reinforced lithium silicate crystal particles removed from the surface might be joining to polishing tip. These fine diamond particles may lead to the smoother and glossier surface topography.[130,309]

When the surface roughness values were evaluated in that study, it was shown that different materials may exhibit different polishabilities at baseline with same polishing protocol. Initial polishabilities of materials were as follows: IPS e.max had significantly lower polishability than Celtra Duo and Ceramill Zolid. Polishabilities of Celtra Duo and Ceramill Zolid were similar. As aforementioned above, this might be due to the material's internal characteristics such as different crystal forms, different particle sizes and dispersions, and different crystalline content. Also, it was speculated by Kou et al.[310] that zirconia particles might be the reason for superior polishability compared to Al_2O_3 containing materials. Additionally, lithium disilicate has higher crystalline phase content which might lead lower polishability.[130,308] On the contrary, Cruz et al.[7] found close baseline Sa roughness values between IPS e.max and Vita Suprinity (0.58 ±0.09 and 0.59 ±0.12 respectively) by 3D laser confocal microscope. This might be due to grinding only with abrasive papers instead of using polishing system. This study's roughness values could not be compared with the current study due to different device and different surface roughness parameter choices.

When the Ra values of each material were evaluated before and after the solution exposure in the current study, it was seen that none of them have exceeded the clinical success threshold. This threshold was determined as 0.2 µm.[102] When this limit was exceeded, bacterial retention began to progress and subsequent biological complications might be occurred. Despite different initial polishabilities, different baseline and final surface roughness values, each material exhibited values far below this threshold.

Confirming the surface roughness results of this study, Ban[64] stated that glass ceramics presented dissolution even in neutral solutions, their strength decreased after contact with a fluid, acid or water; and zirconia has high inertness and water resistance under neutral pH, while little susceptibility to dissolution under HCl acid contact. These results were found consistent with the current study.

Alnasser et al.[9] compared Ra values of lithium disilicate and monolithic zirconia after 45 and 91 hours of exposure to acidic solution with 2 pH by using 3D optical interferometer and no statistically significant changes were found. In current study, the immersion period in blumic solution was longer and solution pH was lower, so lithium disilicate and zirconia samples were thought to be affected by acid corrosion.

Cruz et al.[7] evaluated the effect of simulated gastric juice on surface roughness (Sa) of lithium disilicate glass ceramic and zirconia reinforced lithium silicate ceramic. They concluded that simulated gastric juice significantly decreased the roughness which was not found in our study. It is presumed by the authors that the superficial glassy matrix of IPS e.max CAD is removed initially, exposing the crystalline phase which begins to undergo acid attack and reducing the surface roughness. But they also found pores on both IPS e.max CAD and Vita Suprinity similar to this research's SEM images. Similar to Cruz et al.[7], Harryparsad et al.[16] claimed a hypothesis that longer periods of exposure would result in a smoother material compared with the baseline. On the contrary, Sulaiman et al.[8] represented longer period of exposure and immersed in acidic solutions for longer period compared to these two studies, and found significant increase in surface roughness consistent with current study. This controversy might be enlightened as follows; exposures lasting up to the 24 hours may decrease the roughness values, but more than 24 hours of exposures may lead to increase in roughness values.

So, the exposure time defined as ‘longer period’ by Cruz et al.[7] and Harryparsad et al.[16] was not really a longer period compared to Sulaiman et al.[8] and the current study.

Harryparsad et al.[16] suggested that IPS e.max would be the superior choice of material for patients with blumia and GERD. It is claimed by the current study that selected three materials may be the choice for blumic patients in terms of surface roughness parameter, because of the fact that Celtra Duo and Ceramill Zolid showed surface roughness changes similar to IPS e.max.

Surface microhardness is considered as an important mechanical property in the selection of appropriate restorative materials.[48] The surface microhardness of a material is a relative measurement of the resistance to permanent surface indentation or penetration.[311,312]

When the surface microhardness (VHN) changes were evaluated in the current study, it was found that Ceramill Zolid was affected neither by blumic solution nor by control solution. Slight increase in VHN was not statistically significant. It may be speculated by the authors that solution exposure did not cause any zirconia removal from the material surface but led some transformations between phases. Because of the fact that zirconia polycrystals were still intact on the surface, they resist against an incoming load and particles do not change their location.

It was showed that polycrystalline materials get damaged under indentation forces through the mechanism of dislocating the crystals in the matrix.[227] However, densely packaged zirconia polycrystals could not change their position because no gaps were formed by removal of zirconia crystals from surface. So, Ceramill Zolid samples were intact after both blumic and control solutions.

When the glassy matrix ceramics’ hardness change were considered, Alencar-Silva et al.[10] have found that after 5 years exposure of different extrinsic erosive and staining solutions, VHN of IPS e.max was significantly decreased ($p<0.05$). In the current study, consistent results were found for Celtra Duo. Hardness decrease of Celtra Duo in both blumic and control solutions was speculated by dissolution of silica glass matrix and leaching of alkaline ions from material as explained before. Heterogenic structure of dispersed crystals in a glassy matrix is associated with the defect mode when the indentations were done. The glass matrix part suffers indentation damage mainly through plastic deformation and following cracks of the weaker glass, while the remaining crystals are dislocated by indenter.[227] Thus it was thought by the authors that if indenter comes across to the glassy matrix part, VHN value would be lower due to deeper indentation as much as the dislocations of crystals allow; yet if the indenter comes across to the crystal, the VHN value would be higher due to crystals higher resistance compared to glass matrix. The hardness difference between the glassy matrix and the crystals might be the reason for the inconsistent situation about hardness.[227]

In the current study, VHN values of IPS e.max were increased significantly both after blumic and especially control solution exposure. The reason might be speculated as the higher chance for indenter to come across to the lithium disilicate particles which have greater dimensions than zirconia reinforced lithium silicate particles.[130] The ratio of lithium disilicate particles were higher in IPS e.max, while zirconia reinforced lithium silicate particles were lesser on Celtra Duo.[130,308] When the silica was dissolved by aqueous environment, larger gaps were formed in the microstructure of Celtra Duo, thus increasing the possibility of indenter to sink into these gaps and leading crystals to be dislocated more. However, minor gaps were formed on IPS e.max and hence higher possibility of indenter to come across onto the larger lithium disilicate crystals. These gap formations and gap dimensions between crystals may be clearly seen on SEM images of current study (Figure 4.7.C and Figure 4.8.C.). Still, there is a need to conduct more researches on this topic to enlighten the mechanism of hardness increase in IPS e.max and hardness decrease in Celtra Duo.

Surface microhardness increase on IPS e.max blumic subgroup was found significantly lower than IPS e.max control subgroup. The reason was thought as after acidic corrosion, some crystals were damaged on blumic subgroup, while control subgroup’s crystals were intact. Similarly, the crystals of Celtra Duo blumic subgroup were damaged or removed more than control subgroup. Therefore significantly higher hardness decrease occurred on Celtra Duo blumic subgroup compared to control subgroup. Since no significant changes in Ceramill Zolid samples’ hardness were found after each solution’s exposure, the hardness changes were not found significantly different as well. Blumic solution has affected Celtra Duo more than IPS e.max, while control solution has affected IPS e.max more than Celtra Duo.

Özdemir et al.[313] found that after hydrofluoric acid (HF) etching, the hardness of IPS e.max Press material was increased. They linked this finding with the information that the density of material might be increased. When the porosity was lowered and the density was elevated of the ceramic bulk, its hardness was increased.[314–317] This perspective might create another speculation on hardness increase of IPS e.max for the current findings, it might be due to density increase.

In the evaluation of which material's hardness was affected more severely, not only the VHN values but also the ΔVHN values should be taken into consideration carefully because initial hardness values could be very different. Even if the hardness of IPS e.max was increased and hardness of Celtra Duo was decreased, Celtra Duo was still harder than IPS e.max according to final hardness orders among blumic and control subgroups. Nevertheless, Ceramill Zolid was the hardest among three materials in every condition. T_0 and T_1 surface microhardness orders were as follows; Ceramill Zolid > Celtra Duo > IPS e.max after both blumic and control solution exposures.

When the surface microhardness differences between materials were evaluated in the current study, it was shown that different materials exhibited significantly different baseline and T_1 microhardness values. Monolithic zirconia had significantly highest VHN due to higher opposition resistance of zirconia polycrystals, while zirconia reinforced lithium silicate was significantly found harder than lithium silicate due to the zirconia content in Celtra Duo.[20] The baseline VHN values of IPS e.max and Celtra Duo polished HT samples were found as between the ranges of 506,120 to 538,700 and between the ranges of 562,780 to 597,840 respectively.

Materials' structure and surface treatment may change the surface microhardness. In the study of Alencar-Silva et al.[10], when the materials were grinded with abrasive papers as polishing procedure, the VHN values of HT IPS e.max samples were found 729,71±2,39. When the glaze was applied to same samples, the mean VHN value was found as 649,06±4,14. They have found that glazing significantly decreased the surface microhardness ($p<0.001$). The reason for finding higher VHN values compared to current study may be explained as the difference in hardness measuring method. In current study, indentation load was applied as 9,8 N and duration was 15 seconds as expressed in ASTM standards[230], however Alencar-Silva et al.[10] applied 2 N load for 15 seconds dwell time. Therefore VHN values were found higher.

In another study Lawson et al.[20] applied the same indentation protocol as ASTM declared onto the LT unpolished or unglazed IPS e.max (452,9±16,2), fired Celtra Duo (595,1±37,6) and un-fired Celtra Duo (463,5±26,6) samples. Unfired Celtra Duo and IPS e.max showed same VHN values, while Celtra Duo's surface microhardness significantly increased with firing process. VHN discrepancies with the current study might be explained by different surface treatment protocols and different crystal densities determining the translucency of samples. As a similarity with current study, fired Celtra Duo exhibited increased hardness compared to IPS e.max.

As seen in current research and other studies[7,10,20], IPS e.max, Celtra Duo and Ceramill Zolid materials have higher surface microhardness values than human enamel which has 347 VHN. Surface microhardness has been told to be the most important determinant on opposite enamel wear[318–321], however recent studies[225–227] showed that it is not the only determinant. But surface microhardness of CAD-CAM materials was found important in easy milling. If the hardness was lower, milling speed may be elevated due to less cutting force requirement.[20] Hardness is a special mechanical property that affects the clinical success of a material.[322] Materials with a lower surface hardness may deteriorate easily, and the deterioration of a surface causes fatigue to the material, which decreases its survival rate.[323]

Cruz et al.[7] found no statistically significant change after gastric juice exposure on any material; similar to that they could not find any significant roughness changes. It might be due to short immersion time compared to current study. VHN values were ordered as follows Vita Suprinity > IPS e.max CAD in both T_0 and T_1 periods similar to current results.

Pinto et al.[304] have compared the effect of mediums with different pH on Vickers hardness (GPa) and fracture toughness (K_{Ic}) of two porcelain types. Unlike the current study, the hardness values of materials were decreased as the pH increased. No statistically significant differences on fracture toughness were found between acidic, neutral and basic pH liquid medium. The fracture toughness results were not consistent with the current study either. These differences might be explained by different material selections.

The fracture toughness (K_{Ic}) value defines the critical stress intensity level at which catastrophic failure occurs due to a critical micro defect; so the lower the K_{Ic}, the lower the clinical reliability of the ceramic restoration.[43] Different test methods have been established to evaluate the fracture toughness values. In this study, the indentation technique was used, because it is a simple procedure and economical in terms of less preparation and used material. The greatest asset of the technique is the use of a small amount of specimen area.[43] The main limitation of the indentation based methods is that only a comparison between materials in the same study can be investigated. New ceramic material cannot be verified by indentation fracture toughness test. It has been reported that variations up to 48% from the true fracture toughness value occurred using the indentation fracture toughness test method.[322] However it was the most practical method that could be chosen for author's laboratory conditions and only meant to compare before and after results for different materials under identical conditions.

The fracture toughness is the material's resistance to crack propagation. The toughening mechanism of ceramics is mainly due to crack deflection, particle (fiber) bridging, stress dispersion in the crack tip.[317,324] For lithium disilicate glass ceramics, the toughening mechanism may be primarily attributed to crack deflection and particle bridging. Their fracture toughness depends on the size, aspect ratio, and orientation of the crystals.[52,324–327] Needle-shaped crystals of lithium disilicate material were homogeneously embedded in the glass matrix in an interlocking structure, and they play a major role in hindering crack propagation and elevating the flexural strength. In this microstructure, the growth of micro cracks can be avoided if they move vertically to needle crystals. If they move in parallel to needle crystals, crack propagation could not be stopped.[328] Apel et al.[329] showed that the crack propagation was an inter-granular process in lithium disilicate glass–ceramics because the crack propagated only through the residual glass matrix and not through the crystals. The high strength crystals of the interlocking microstructure are more resistant. Consequently, crack development takes place at the weaker interfaces between the crystals.[325,329–331] On the other hand, crack propagation limiting mechanism on zirconia material is known as transformation toughening.[24]

K_{Ic} values of IPS e.max and Ceramill Zolid samples were found significantly decreased by blumic solution. This might be explained by the resolution of lithium disilicate crystals deflecting crack in blumic solution besides glassy phase removal, thus prevention was weakened and toughness was decreased in IPS e.max blumic subgroup. The crystal orientations in microstructure and sparser distribution of lithium disilicate crystals after acid attacks may cause the inter-granular crack to propagate more easily through the residual glass matrix, causing a lower fracture toughness of the samples.[325,329,331] Similarly, increased LTD caused by the dissolved yttria in blumic corrosion conditions might be the reason of weakened crack propagation prevention, thus leading decreased fracture toughness in Ceramill Zolid blumic subgroup.

Consistent with current study, Turp et al.[332] evaluated three monolithic zirconia's fracture toughness after solution exposures with different pH's, and found that samples immersed into neutral solution had higher fracture toughness values compared to those immersed into acidic or alkali solutions. Monoclinic phase had become more prominent in acidic and alkaline solutions. Similarly, control solutions did not affect the fracture toughness properties of Ceramill Zolid significantly.

On the contrary, it was found that IPS e.max and Ceramill Zolid were not affected by control conditions with neutral pH. It might be speculated that control conditions did not cause lithium disilicate crystals to dissolve, only caused the loss of glassy matrix in IPS e.max, while it did not cause significant yttria loss and LTD, thus transformation toughening mechanism was intact in Ceramill Zolid. Exposition of an acidic environment influenced the fracture toughness of these two materials more than exposition of aqueous environment.

However in some dental ceramic materials, aqueous environment may lead to the prevention of crack propagation.[22,302] Fracture toughness of Celtra Duo was increased by two solutions and no significant changes in the increase of fracture toughness were observed between them (+0,26±0,13 and +0,29±0,09, p=0.405). So, both blumic solution and control solution were increased the toughness of Celtra Duo samples similarly. Even if the glass matrix was disappeared on Celtra Duo control subgroup, the zirconia reinforced lithium silicate crystals could be observed. Even though it looked like all crystals and glass matrix was dissolved in Celtra Duo blumic subgroup, fracture toughness was still increasing. It might be speculated that, intact zirconia particles may somehow prevent cracks to propagate more than initial situation, may be due to glassy matrix loss which normally leads a way for crack to propagate.[333] Prevention mechanisms as crack deflection, zone shielding, contact shielding, stress dispersion in the crack tip and particle bridging,[317,324,334] which were aiming different approaches to increase the energy required for crack propagation[326] might be included in Celtra Duo. This material was affected by being in an aqueous environment more than being in an acidic solution.

When the baseline and final fracture toughness of materials were compared, the order was Ceramill Zolid > IPS e.max > Celtra Duo. Although the fracture toughness of Celtra Duo was increased and the fracture toughness of IPS e.max was decreased, the order has not changed. That order was expected in terms of Ceramill Zolid, but Celtra Duo's lower toughness was not expected. The order may be based on the claim that the inter-granular crack may propagate more easily through the residual glass matrix.[333] The glass matrix ratio was higher for Celtra Duo than IPS e.max and crystal ratio preventing the crack was higher for IPS e.max at initial state.[130,308] Greater crystal sizes, orientation or bridging particles of IPS e.max might lead superior toughness than Celtra Duo having smaller crystal size.[130,333] Further investigations with different fracture toughness measuring methods may be needed to assess the initial values of these materials.

Fracture toughness of the dental enamel was reported as ranging between 0.7±0.2 MPa.m$^{1/2}$ and 1.77±0.2 MPa.m$^{1/2}$ [335]. Final K_{Ic} value order was as Ceramill Zolid (ranging between 4.74 MPa.m$^{1/2}$ and 7.18 MPa.m$^{1/2}$) > IPS e.max (ranging between 2.36 MPa.m$^{1/2}$ and 3.07 MPa.m$^{1/2}$) > Celtra Duo (ranging between 1.61 MPa.m$^{1/2}$ and 2.10 MPa.m$^{1/2}$). Regarding to that information, all three materials exhibited higher fracture toughness values than teeth after aqueous environment exposures. According to ISO 6872 standard, minimum fracture toughness should be 5 MPa.m$^{1/2}$ for a dental ceramic to be used in the fabrication of prostheses involving 4 or more units.[336] Although indentation fracture toughness was not the absolute method to determine materials exact fracture toughness, it gives an opinion about approximate values. So as a result of current study, only Ceramill Zolid seemed like an appropriate material to be used as 4 or more unit bridge restorations regarding to this standard.

While the CAD-CAM lithium disilicate ceramic was evaluated[337], fracture toughness values was reported ranging from 2.27±0.16 MPa.m$^{1/2}$ to 2.37±0.28 MPa.m$^{1/2}$, which are close to current study's IPS e.max values. Guazzato et al.[338] reported the fracture toughness of zirconia-based dental materials as ranging from 4.8±0.5 MPa.m$^{1/2}$ to 7.4±0.6 MPa.m$^{1/2}$. In another study[49] fully crystalized Vita Suprinity, which is zirconia reinforced lithium silicate same as Celtra Duo, presented values of fracture toughness as 4.7±0.8 MPa.m$^{1/2}$. They both are not consistent with the results of this study. Current results of fracture toughness values of monolithic zirconia was higher (ranging from 5.85±0.67 to 6.66±0.67 MPa.m$^{1/2}$) than values found by Zhang et al.[81] who compared two different zirconia materials (2.60±0.20 MPa.m$^{1/2}$ and 2.50±0.1 MPa.m$^{1/2}$). It might be due to different indentation forces. Even though same fracture toughness calculating method which was indentation fracture toughness method was used in both studies, they applied 10 kg indentation load for 10 seconds, while we applied 1 kg (9.8 N) indentation force for 15 seconds. 10 times more forces might be generated longer cracks in length, thus K_{Ic} value could be smaller. On the contrary, half of our indentation force was applied to leucite reinforced dental ceramic samples by Pinto et al.[304] Lower K_{Ic} values (ranging from 0.77±0.02 to 1.07±0.07 MPa.m$^{1/2}$) have been obtained when compared with this study's lithium disilicate and zirconia reinforced lithium silicate samples (ranging from 1.55±0,06 to 3.20±0,26 MPa.m$^{1/2}$). It might be due to material differences as leucite reinforced ceramic and feldspathic ceramic which are known to be weaker materials, despite lower indentation force applied. Load application between 1 kg.f and 2 kg.f was advised by Cesar et al.[232] on glassy matrix ceramics. Reason of 1 kg.f load application is based on Standard Test Method for Vicker's Indentation Hardness of Advanced Ceramics[230]. While measuring Vicker's hardness of IPS e.max and Celtra Duo, the indentation load was advised and applied as 1 kg.f equals to 9.8 N. K_{Ic} values was calculated according to crack length formed during this indentation for these two materials. In order to be able to compare the fracture toughness under same conditions, Ceramill Zolid samples were also evaluated under 1 kg.f indentation load for 15 seconds. Cracks were smaller compared to IPS e.max and Celtra Duo for Ceramill Zolid, so the K_{Ic} values were found higher. These fracture toughness values were not aimed to be used as absolute values for three material types, but meant to compare different materials under same conditions and observe the toughness change before and after the exposure to aqueous mediums with different pH.

When calculating the color difference, ΔE_{00} value exhibits better consistency with human eye perceptibility and acceptability thresholds.[252,257] Despite the superiority of this improved formula, the use of ΔE_{ab} value is still more common in recent researches. This might be because of the complexity of ΔE_{00} formula and difficulties in making transformations of L*, a*, b* values to L', a', b' via arithmetics. Furthermore, the use of ΔE_{ab} provides great convenience in discussing the results with previous researches done with ΔE_{ab}.[237] Therefore, the use of ΔE_{ab} is still very popular in the dental literature. In the current study, ΔE_{ab} was preferred due to these advantages.

When comparing the optical properties between blumic and control subgroups, it was seen in the current study that not only surface roughness but also the mechanisms leading surface ion exchange, loss or accumulation were found effective in the change of color and translucency.

The increase in surface roughness of ceramics has the potential to affect light reflection and color perception due to changes in surface topography.[339] Color change (ΔE) of blumic subgroups of all three materials was found significantly higher than control subgroups (Table 4.30.). Surface roughness values were higher in these blumic subgroups, when compared to control subgroups. Although these differences were not statistically significant, SEM images showed that the crystals were not resolved and removed from the surface in control groups. As shown in the Cruz et al.'s [7] and current study's SEM images, substance loss including crystals was more on blumic condition and pores were more obvious especially in glass based ceramics. This might lead to more color change in blumic subgroups of compared to control subgroups.

L*, a* and b* values were significantly affected by two solutions in every material, thus leading significant color changes. It might be concluded that being in an acidic environment might be more influential on color change, although aqueous environment also affected the color change.

In the blumic solution, color of Ceramill Zolid was changed significantly the most. This might be due to increased LTD and acid may altered the internal order and characteristics of zirconia crystals. In a low pH condition, dissolution of silica in the composition of glass ceramics occurs and results in the loss of alkaline ions.[201,301] Cruz et al.[7] found that color change of IPS e.max CAD and Vita Suprinity was found similar with each other. They found smaller ΔE_{ab} values for IPS e.max and Vita Suprinity (0.33 ±0.19 and 0.28 ±0.15 respectively) compared to current study conducted with IPS e.max and Celtra Duo (1.75±0.03 and 1.65±0.03 respectively). Although their solution was more acidic, ΔE_{ab} value differences might be due to different immersion times between Cruz et al.[7] and current study (as 18 hours 25 minutes and 20 days, respectively). Even though the color change values of IPS e.max and Celtra Duo were closer in the current study, Celtra Duo was significantly found more color resistant. This result may be attributed to the different crystal contents and configuration after acid attack.

These color changes in blumic subgroups were in the 'good color similarity' level for IPS e.max and Celtra Duo (ΔE_{ab} between 1 and 2), whereas color change of Ceramill Zolid was clinically perceptible (ΔE_{ab} between 2 and 3.5) according to O'Brien classification.[116] Ceramill Zolid was not suggested for anterior restorations by the authors under these circumstances.

However in the control conditions, Celtra Duo was significantly the mostly affected material, while Ceramill Zolid and IPS e.max were similarly affected less. Least affected surface was Ceramill Zolid, thus this result might be expected. Even if the roughness was increased in IPS e.max, intact lithium disilicate crystals might be reason of high color stability. Significant L* value decrease in Celtra Duo control subgroup was interesting and may be led to the greater color change. The L* coordinate corresponds to the value (lightness or darkness) of an object and is considered to be the most important aspect of color selection in dentistry.[339] Celtra Duo materials' lightness value was considered as diminished in saliva. Other subgroups' L* values were significantly elevated, while a* and b* values were significantly decreased by each solution. Consequently these differences led to lighter, less reddish and less yellowish samples in different color coordinates.[246,340]

Even though there were color differences under control solution exposure, these color changes was in ‘excellent color similarity’ level for IPS e.max and Ceramill Zolid (ΔE_{ab} between 0.5 and 1), and in ‘good color similarity’ level for Celtra Duo samples (ΔE_{ab} between 1 and 2) according to O’Brien classification.[116] It might be suggested that IPS e.max and Ceramill Zolid materials were more color stable and reliable to use at anterior region in healthy patients. However more researches are needed on Celtra Duo material.

Current study was the only research conducted about the color change of different materials exposed to blumic and control solutions for longer periods. Kulkarni et al.[339] compared different materials under blumic conditions for 108 minutes. Even under this short period of exposure, they found significant ΔE_{ab} differences between zirconia and IPS e.max materials ($p<0.05$).

Besides simulating the intrinsic erosive conditions, there are several studies[17,301,302] evaluating the effect of extrinsic erosive solutions on several materials. dos Santos et al.[301] have observed lithium disilicate ceramic (IPS e.max Press Impulse) after the glaze application in the way of color stability (ΔE_{ab}, L*) and translucency parameter and contrast ratio (TP, CR) change after exposure to orange juice, cola, coffee, red wine and artificial saliva. Control group was immersed in artificial saliva at 37^{o}C throughout the immersion period of experiment similar to current study. Close ΔE_{ab} value was found after artificial saliva immersion to the current study (approximate ΔE_{ab}=1.25 and 0.94±0.03, respectively). In consistency with current study, saliva exposition led to the lowest color change on IPS e.max. T1 L* and TP values were also closer to the current study’s results; approximate L* was 75 and TP was 17, while current study’s L* was 75.96±0.21 and TP 16.47±0.17. Significantly greater color change and lower L* values were observed after immersion in orange juice and cola, while only orange juice showed clinically unacceptable color change (ΔE_{ab}>3,5) according to ΔE_{ab} acceptance threshold of O’Brien.[116] Immersion in coffee resulted in greater opacity and lower translucency of the material in regard to the TP and CR.

When the translucency values were observed, Celtra Duo was significantly the most translucent and Ceramill Zolid was significantly the most opaque in both baseline and final with 1.5 mm thickness. Translucency values of all samples were significantly decreased after respective solution exposures, except the Celtra Duo control subgroup with significantly increased translucency, and IPS e.max control subgroup with no significant change. Different parameters including grain size, additive materials, and firing and sintering conditions can affect the translucency of zirconia and glass based ceramics.[341] The decrease of translucency was linked to the declined scattering in glazed specimens by Koçak et al.[287] Residual porosities at the grain boundaries, even at small sizes and quantities, have a detrimental effect on the translucency of zirconia by increasing the refractive index and light scattering.[77,342] Thus decreasing translucency may be explained by light scattering at the grain boundaries, pores, and secondary phases especially for zirconia samples after solution exposures.[215] It was found that IPS e.max and Ceramill Zolid were influenced significantly by the blumic solution compared to control solution, and control solution was found significantly more influential for Celtra Duo samples. Biggest change was found for Ceramill Zolid blumic subgroup consistent with those having the highest color change; and least TP change was found for IPS e.max control subgroup which was not considered as a significant clinical change. According to Culp et al.[343] and Ozturk et al.[344] lithium disilicate ceramic has excellent translucency because of a high content of lithium disilicate crystals. This advantage must be preserved on all materials for the longevity of the rehabilitation. It was seen that this advantage was still intact after the exposition of control solution on IPS e.max. However in acidic conditions, translucency of IPS e.max material was not stable, yet it was unrecognizable (ΔTP=1,05±0,18). Similarly after the exposition of blumic solution, translucencies of Celtra Duo and Ceramill Zolid were not stable and significantly decreased. However, the translucency changes (ΔTP) were both unrecognizable and in the clinical acceptability limits for Celtra Duo and Ceramill Zolid (0.18±0.18 and 1.14±0.27, respectively). Even if there were significant changes in translucency, they were not clinically recognizable due to ΔTP being less than 2 according to Lee et al.[290]

On the contrary to current study, Sulaiman et al.[8] compared the TP values of monolithic zirconia and IPS e.max CAD samples with 1.2 mm thickness after exposure to simulated gastric acid for 96 hours. They found minimal increase in the TP value of IPS e.max, which are most probably not detectable by the eye and therefore leading minimal threat to material’s esthetic appearance. Decrease of TP in the current study might be explained by different acid pH and exposure times or conditions leading different dissolutions in the crystals and material thickness differences. When the exposure time increases subsequently, increased translucency may be turned into increased opacity. There were no other studies in the literature to make further comparisons on IPS e.max or on any other materials.

After evaluating all these results, following inference was made; the strength of that study was seen as comparing blumic conditions with saliva control. Not only the influence of blumic solution, but the comparisons of blumic condition with the control condition could be done. Therefore, results could be interpreted via the differences between two conditions in accordance with clinical scenarios.

According to literature search based on this topic conducted on PubMed, there were no studies which had compared blumic conditions with control condition such as exposure to artificial saliva. Including a control solution and few control subgroups into the research has given the opportunity to see whether the changes in the different parameters of various materials were caused by acidic condition or the cause was just being in the aqueous environment. Further researches with this perspective may be done to compare the results with different materials and different surface treatments.

In the light of these informations unwanted changes in optical characteristics might have started with the surface roughening and particle loss or transformation. The authors and previous researches suggests that it might be appropriate to re-polish restorations periodically, thus roughness increase and crack propagations might be prevented bringing with higher color stability and more success over few years.[345]

Further researches are needed to see the effects of re-polishing of corroded materials and on microstructural level in order to comprehend internal changes for these materials according to authors. Even though this in-vitro research study could not demonstrated the exact clinical situation as a clinical research study, it has given important ideas about the behaviors of these three polished materials under blumic conditions compared to control condition selected as artificial saliva exposure.

Followings may be stated regarding the null hypothesis:

1) First null hypothesis as “there are no statistically significant changes in terms of mechanical (Ra, VHN, K_{Ic}) and optical (L*, a*, b*, TP) properties of different CAD-CAM materials after exposure to acidic blumia nervosa solution and artificial saliva solution” was partially rejected. There were significant differences after solution exposures in the properties of various selected materials. However, there were no

significant changes in surface roughness (Ra) of Ceramill Zolid control subgroup, surface microhardness (VHN) of both Ceramill Zolid blumic and control subgroups, fracture toughness (K_{Ic}) of IPS e.max and Ceramill Zolid control subgroups, and translucency (TP) of IPS e.max control subgroup.

2) Second null hypothesis as "solutions with different pH similarly affect the mechanical (ΔRa, ΔVHN, ΔK_{Ic}) and optical (ΔE_{ab}, ΔTP) properties' changes of a CAD-CAM material" was partially rejected. There were significant differences between the effects of solutions with different pH (blumic solution, 1.6 pH; and control solution, 7 pH) in terms of different parameters on various selected materials. However, there were no significant differences between the effects of two solutions in surface roughness changes (ΔRa) of IPS e.max and Celtra Duo materials, surface microhardness changes (ΔVHN) of Ceramill Zolid material, and fracture toughness changes (ΔK_{Ic}) of Celtra Duo material.

3) Third null hypothesis as "blumic solution affects the selected three CAD-CAM materials similarly on mechanical (ΔRa, ΔVHN, ΔK_{Ic}) and optical (ΔE_{ab}, ΔTP) properties' changes" was partially rejected. There were significant differences in terms of most parameters among three CAD-CAM materials exposed to blumic solution. However, there were no significant differences among three materials in surface roughness changes (ΔRa). Additionally, there were no significant differences between IPS e.max and Ceramill Zolid blumic subgroups in translucency parameter changes (ΔTP).

4) Fourth null hypothesis as "control solution affects the selected three CAD-CAM materials similarly on mechanical (ΔRa, ΔVHN, ΔK_{Ic}) and optical (ΔE_{ab}, ΔTP) properties' changes" was partially rejected. There were significant differences in terms of various parameters among three CAD-CAM materials exposed to control solution. However, there were no significant differences among three materials in surface roughness changes (ΔRa). Additionally, there were no significant differences between IPS e.max and Ceramill Zolid control subgroups in fracture toughness and color changes (ΔK_{Ic} and ΔE_{ab}, respectively).

6. CONCLUSIONS

The conclusions of the current study were as follows:

1) In terms of surface roughness, glassy matrix ceramics such as IPS e.max CAD and Celtra Duo CAD roughened not only by blumic mediums with acidic pH, but also by artificial saliva medium with neutral pH. These two materials were affected by being in an aqueous environment independent from different pH. In contrast to IPS e.max CAD and Celtra Duo CAD, Ceramill Zolid HT+ PS material was affected by acidic blumic medium rather than being only in an aqueous environment. It was found as the most inert material in terms of surface roughness change in the control conditions. After all, three selected materials exhibited Ra values lower than 0,2 µm in any condition, thus staying under the clinically unacceptable roughness threshold.

2) In terms of surface microhardness, IPS e.max CAD and Celtra Duo CAD were affected differently by two solution exposures, whereas Ceramill Zolid HT+ PS was not affected and remained very stable. The increase of surface microhardness was considered as a positive change. Being in an aqueous environment increased the surface microhardness value of IPS e.max CAD, when artificial saliva elevated surface microhardness more than blumic solution. Thus blumic solution having acidic pH had less contribution to material's resistance. Being in an aqueous environment decreased the surface microhardness value of Celtra Duo CAD. Blumic solution was affected the Celtra Duo CAD more negatively than artificial saliva.

3) Even though there was an increase in the surface microhardness of IPS e.max CAD and there was a decrease in the surface microhardness of Celtra Duo CAD after both solution exposures, final surface microhardness of Celtra Duo CAD was more superior to the IPS e.max CAD. Surface microhardness of Ceramill Zolid HT+ PS was the highest obviously in any time.

4) Fracture toughness values of IPS e.max CAD and Ceramill Zolid HT+ PS were decreased and cracks propagated further after blumic solution exposure. Stability of IPS e.max CAD and Ceramill Zolid HT+ PS was very high regarding to the fracture toughness under control conditions. Fracture toughness of Celtra Duo CAD was elevated after the exposure of two solutions.

5) Despite the increase in the fracture toughness values of Celtra Duo CAD in aqueous environments, fracture toughness of IPS e.max CAD was higher than Celtra

Duo CAD in any time. Ceramill Zolid HT+ PS was obviously the toughest among three selected materials after selected solutions' exposure.

6) Color of all samples was changed after immersion in different solutions. The color changes after the blumic solution exposures were higher than the control solution exposures among selected three materials.

7) Color change (ΔE_{ab}) order was as follows among blumic subgroups: Ceramill Zolid HT+ PS > IPS e.max CAD > Celtra Duo CAD (2,42±0,20; 1,75±0,03; 1,65±0,03, respectively). Ceramill Zolid HT+ PS had the highest color change and this level was clinically perceptible, yet in acceptable level (ΔE_{ab}<3.5). Least color changes were found in IPS e.max CAD and Ceramill Zolid HT+ PS exposed to control solution, and the changes were in the 'excellent color change' level ($0.5<\Delta E_{ab}<1$).

8) Acidic blumic solution affected the translucency parameters of IPS e.max CAD and Ceramill Zolid HT+ PS more than the control solution. On the contrary, Celtra Duo CAD was influenced by control solution more than blumic solution. Translucency changes (ΔTP) were under the clinically perceivable limit (ΔTP<2) for all materials and both solutions.

As a statement in accordance to these conclusions, inclusion of control solution and control subgroups instead of only comparing blumic subgroups is highly recommended to interpret differences between two conditions in accordance with clinical scenarios.

Following clinical recommendations may be made as a result of this study. In non-blumic patients, Ceramill Zolid HT+ PS was found as the most stable material choice, and then IPS e.max follows as the second stable material. Celtra Duo CAD needs further researches. In blumic patients, all materials' mechanical properties were found sufficient, but color stabilities of IPS e.max CAD and Celtra Duo CAD were superior to Ceramill Zolid HT+ PS. In blumic patients, high color change of polished Ceramill Zolid HT+ PS restricted its use at anterior region. After all, periodic re-polishing applications might be considered as a precaution against corrosive effects of aqueous environment. Materials' characteristics may be uncontrollably changed during a 5 year period depending on the severity, acidity and duration of blumia nervosa. So, periodic control sessions can be very important in blumic patients.

7. REFERENCES

1. Luthardt R, Sandkuhl O, Herold V, Walter M. Accuracy of mechanical digitizing with a CAD/CAM system for fixed restorations. *Int J Prosthodont*. 2001;14(2):146-151.
2. Subaşı MG, Alp G, Johnston WM, Yilmaz B. Effects of fabrication and shading technique on the color and translucency of new-generation translucent zirconia after coffee thermocycling. *J Prosthet Dent*. 2018;120(4):603-608.
3. Alp G, Subasi MG, Johnston WM, Yilmaz B. Effect of surface treatments and coffee thermocycling on the color and translucency of CAD-CAM monolithic glass-ceramic. *J Prosthet Dent*. 2018;120(2):263-268.
4. Yuan JCC, Barão VAR, Wee AG, Alfaro MF, Afshari FS, Sukotjo C. Effect of brushing and thermocycling on the shade and surface roughness of CAD-CAM ceramic restorations. *J Prosthet Dent*. 2018;119(6):1000-1006.
5. Schwindling FS, Rues S, Schmitter M. Fracture resistance of glazed, full-contour ZLS incisor crowns. *J Prosthodont Res*. 2017;61(3):344-349.
6. Kim SH, Choi YS, Kang KH, Att W. Effects of thermal and mechanical cycling on the mechanical strength and surface properties of dental CAD-CAM restorative materials. *J Prosthet Dent*. 2021.
7. Cruz MEM, Simões R, Martins SB, Trindade FZ, Dovigo LN, Fonseca RG. Influence of simulated gastric juice on surface characteristics of CAD-CAM monolithic materials. *J Prosthet Dent*. 2020;123(3):483-490.
8. Sulaiman TA, Abdulmajeed AA, Shahramian K, et al. Impact of gastric acidic challenge on surface topography and optical properties of monolithic zirconia. *Dent Mater*. 2015;31(12):1445-1452.
9. Alnasser M, Finkelman M, Papathanasiou A, Suzuki M, Ghaffari R, Ali A. Effect of acidic pH on surface roughness of esthetic dental materials. *J Prosthet Dent*. 2019;122(6):567.e1-567.e8.
10. Alencar-Silva FJ, Barreto JO, Negreiros WA, Silva PGB, Pinto-Fiamengui LMS, Regis RR. Effect of beverage solutions and toothbrushing on the surface roughness, microhardness, and color stainability of a vitreous CAD-CAM lithium disilicate ceramic. *J Prosthet Dent*. 2019;121(4):711.e1-711.e6.
11. Habsha E. The etiology and pathogenesis of tooth wear: Part I. *Oral Health*. 1999;10:83-92.

12. Castillo M, Weiselberg E. Bulimia Nervosa/Purging Disorder. *Curr Probl Pediatr Adolesc Health Care*. 2017;47(4):85-94.
13. American Psychiatric Association. *DSM-V. Diagnostic and Statistical Manual of Mental Disorders*. 5th edition. Washington, DC: APA Press; 2013.
14. Lo Russo L, Campisi G, Di Fede O, Di Libeto C, Panzarella V, Lo Muzio L. Oral manifestations of eating disorders: a critical review. *Oral Dis*. 2018;14(6):479-484.
15. Saksena R, Bartlett DW, Smith BG. The role of saliva in regurgitation erosion. *Eur J Prosthodont Restor Dent*. 1999;7(4):121-124.
16. Harryparsad A, Dullabh H, Sykes L, Herbst D. The effects of hydrochloric acid on all-ceramic restorative materials: an in-vitro study. *J South African Dent Assoc*. 2014;69(3):106-111.
17. Wan Bakar WZ, McIntyre J. Susceptibility of selected tooth-coloured dental materials to damage by common erosive acids. *Aust Dent J*. 2008;53(3):226-234.
18. Zaki DYI, Hamzawy EMA, El Halim SA, Amer MA. Effect of simulated gastric juice on surface characteristics of direct esthetic restorations. *Aust J Basic Appl Sci*. 2012;6(3):686-694.
19. Cengiz S, Sarac S, Özcan M. Effects of simulated gastric juice on color stability, surface roughness and microhardness of laboratory-processed composites. *Dent Mater J*. 2014;33(3):343-348.
20. Lawson NC, Bansal R, Burgess JO. Wear, strength, modulus and hardness of CAD/CAM restorative materials. *Dent Mater*. 2016;32(11):e275-e283.
21. Esquivel-Upshaw JF, Dieng FY, Clark AE, Neal D, Anusavice KJ. Surface degradation of dental ceramics as a function of environmental pH. *J Dent Res*. 2013;92(5):467-471.
22. Anusavice KJ. Degradability of dental ceramics. *Adv Dent Res*. 1992;6(1962):82-89.
23. Ornstein R, Rosen D, Mammel K, et al. Distribution of eating disorders in children and adolescents using the proposed DSM-5 criteria for feeding and eating disorders. *J Adolenscent Heal*. 2013;53(2):303-305.
24. Zarone F, Russo S, Sorrentino R. From porcelain-fused-to-metal to zirconia: Clinical and experimental considerations. *Dent Mater*. 2011;27:83-96.

25. Bajraktarova-Valjakova E, Korunoska-Stevkovska V, Kapusevska B, Gigovski N, Bajraktarova-Misevska C, Grozdanov A. Contemporary Dental Ceramic Materials, A Review: Chemical Composition, Physical and Mechanical Properties, Indications for Use. *Open Access Maced J Med Sci*. 2018;6(9):1742-1755.
26. Babu PJ, Alla RK, Alluri VR, Datla SR, Konakanchi A. Dental Ceramics : Part I – An Overview of Composition, Structure and Properties. *Am J Mater Eng Technol*. 2015;3(1):13-18.
27. Ho GW, Matinlinna JP. Insights on Ceramics as Dental Materials. Part I: Ceramic Material Types in Dentistry. *Silicon*. 2011;3:109-115.
28. Alla RK. *Dental Materials Selection*. New Delhi: Jaypee Brothers Medical Publishers; 2013.
29. İşisağ Ö, Şahin O, Köroğlu A. Dişhekimliğinde Tam Seramik Sistemler. *Uluslararası Dişhekimliği Bilim Derg*. 2016;1:19-25.
30. Denry I, Holloway J. Ceramics for dental applications: A Review. *Materials (Basel)*. 2010;3:351-368.
31. Yoshinari M, Dérand T. Fracture strength of all-ceramic crowns. *Int J Prosthodont*. 1994;7(4):329-338.
32. Denry I. How and when does fabrication damage adversely affect the clinical performance of ceramic restorations? *Dent Mater*. 2013;29(1):85-96.
33. Zhang R, Sailer I, Lawn B. Fatigue of Dental Ceramics. *J Dent*. 2013;41(12):1135-1147.
34. Zhang Y, Lawn B, Rekow E, Thompson V. Effect of sandblasting on the long-term performance of dental ceramics. *J Biomed Mater Res Part B Appl Biomater*. 2004;71(2):381-386.
35. Zortuk M, Bolpaca P, Kilic K, Ozdemir E, Aguloglu S. Effects of fingure pressure applied by dentists during cementation of all-ceramic crowns. *Eur J Dent*. 2010;4(4):383-388.
36. Rochette A. A ceramic restoration bonded by etched enamel and resin for fractured incisors. *J Prosthet Dent*. 1975;33(3):287-293.
37. Santos Jr. G, Santos M, Rizkalla A. Adhesive Cementation of etchable ceramic esthetic restorations. *J Can Dent Assoc (Tor)*. 2009;75(5):379-384.
38. Helvey G. Classification of Dental Ceramics. *Insid Dent*. 2013;(April):62-76.

39. Kelly J, Benetti P. Ceramic materials in dentistry: Historical evolution and current practice. *Aust Dent J*. 2011;56(1 Supplement):84-96.

40. Datla SR, Alla RK, Alluri VR, P JB, Konakanchi A. Dental Ceramics: Part II – Recent Advances in Dental Ceramics. *Am J Mater Eng Technol*. 2015;3(2):19-26.

41. Gracis S, Thompson VP, Ferencz JL, Silva NRFA, Bonfante EA. A New Classification System for All-Ceramic and Ceramic-like Restorative Materials. *Int J Prosthodont*. 2015;28(3):227-235.

42. Bajraktarova-Valjakova E, Grozdanov A, Guguvcevski L, et al. Acid Etching as Surface Treatment Method for Luting of Glass-Ceramic Restorations, Part 1: Acids, Application Protocol and Etching Effectiveness. *Open Access Maced J Med Sci*. 2018;6(3):568-573.

43. Yilmaz H, Aydin C, Gul BE. Flexural strength and fracture toughness of dental core ceramics. *J Prosthet Dent*. 2007;98:120-128.

44. Fradeani M, Redemagni M. An 11-year clinical evaluation of leucite-reinforced glass-ceramic crowns: a retrospective study. *Quintessence Int (Berl)*. 2002;33(7):503-510.

45. Layton DM, Clarke M. A systematic review and meta-analysis of the survival of non-feldspathic porcelain veneers over 5 and 10 years. *Int J Prosthodont*. 2013;26(2):111-124.

46. Zarone F, Ferrari M, Mangano FG, Leone R, Sorrentino R. “Digitally Oriented Materials”: Focus on Lithium Disilicate Ceramics. *Int J Dent*. 2016;2016:9840594.

47. Zarone F, Di Mauro MI, Ausiello P, Ruggiero G, Sorrentino R. Current status on lithium disilicate and zirconia: A narrative review. *BMC Oral Health*. 2019;19:134-147.

48. Elsaka SE, Elnaghy AM. Mechanical properties of zirconia reinforced lithium silicate glass-ceramic. *Dent Mater*. 2016;32(7):908-914.

49. Traini T, Sinjari B, Pascetta R, et al. The zirconia-reinforced lithium silicate ceramic: lights and shadows of a new material. *Dent Mater J*. 2016;35(5):748-755.

50. D’Arcangelo C, Vanini L, Rondoni G, De Angelis F. Wear properties of dental ceramics and porcelains compared with human enamel. *J Prosthet Dent*. 2016;115:350-355.

51. Zarone F, Ruggiero G, Leone R, Breschi L, Leuci S, Sorrentino R. Zirconia-Reinforced Lithium Silicate (ZLS) mechanical and biological properties: a literature review. *J Dent*. 2021:103661.
52. Guazzato M, Albakry M, Ringer S, Swain M. Strength, fracture toughness and microstructure of a selection of all-ceramic materials. Part II. Zirconia-based dental ceramics. *Dent Mater*. 2004;20:449-456.
53. Gorman C, Horgan K, Dollard R, Stanton K. Effects of repeated processing on the strength and microstructure of a heat-pressed dental ceramic. *J Prosthet Dent*. 2014;112:1370-1376.
54. Coldea A, Swain M, Thiel N. In-vitro strength degradation of dental ceramics and novel PICN material by sharp indentation. *J Mech Behav Biomed Mater*. 2013;26:34-42.
55. Garrido M, Giráldez I, Ceballos L, Rodríguez J. On the possibility of estimating the fracture toughness of enamel. *Dent Mater*. 2014;30:1224-1233.
56. Leung BTW, Tsoi JKH, Matinlinna JP, Pow EHN. Comparison of mechanical properties of three machinable ceramics with an experimental fluorophlogopite glass ceramic. *J Prosthet Dent*. 2015;114(3):440-446.
57. Li RWK, Chow TW, Matinlinna JP. Ceramic dental biomaterials and CAD/CAM technology: State of the art. *J Prosthodont Res*. 2014;58(4):208-216.
58. Borges GA, Sophr AM, de Goes MF, Sobrinho LC, Chan DCN. Effect of etching and airborne particle abrasion on the microstructure of different dental ceramics. *J Prosthet Dent*. 2003;89(5):479-488.
59. Kern M, Wegner SM. Bonding to zirconia ceramic: adhesion methods and their durability. *Dent Mater*. 1998;14(1):64-71.
60. Scherrer S, Quinn G, Quinn J. Fractographic failure analysis of a Procera AllCeram crown using stereo and scanning electron microscopy. *Dent Mater*. 2008;24:1107-1113.
61. Piconi C, Maccauro G. Zirconia as a ceramic biomaterial. *Biomaterials*. 1999;20:1-25.
62. Helmer J, Driskell T. Use of Ceramics as Surgical Implants. In: *Research on Bioceramics.* South Carolina (USA): Clemson University; 1969.
63. Christel P, Meunier A, Dorlot JM, et al. Biomechanical Compatibility and Design of Ceramic Implants for Orthopedic Surgery. *Ann N Y Acad Sci*. 1988;523:234-256.

64. Ban S. Chemical durability of high translucent dental zirconia. *Dent Mater J*. 2020;39(1):12-23.
65. Dion I, Bordenave L, Levebre F. Physico-chemistry and cytotoxicity of ceramics. *J Mater Sci Mater Med*. 1994;5:18-24.
66. Denry I, Kelly R. State of the art of zirconia for dental applications. *Dent Mater*. 2008;24:299-307.
67. Scarano A, Piattelli M, Caputi S, Favero G, Piattelli A. Bacterial adhesion on commercially pure titanium and zirconium oxide disks: an in vivo human study. *J Periodontol*. 2004;75:292-296.
68. Chevalier J, Gremillard L, Virkar A, Clarke D. The tetragonal-monoclinic transformation in zirconia: Lessons learned and future trends. *J Am Ceram Soc*. 2009;92:1901-1920.
69. Della Bona A, Kelly J. The clinical success of all-ceramic restorations. *J Am Dent Assoc*. 2008;139 Supple:8S-13S.
70. Ariel J, Raigrodski A, Hillstead M, Meng G, Chung K. Survival and complications of zirconia-based fixed dental prostheses: A systematic review. *J Prosthet Dent*. 2012;107:170-177.
71. Hisbergues M, Vendeville S, Vendeville P. Zirconia: established facts and perspectives for a biomaterial in dental implantology. *J Biomed Mater Res Part B Appl Biomater*. 2009;88:519-529.
72. Zhang Y, Lawn BR. Novel Zirconia Materials in Dentistry. *J Dent Res*. 2018;97(2):140-147.
73. Luthardt R, Sandkuhl O, Reitz B. Zirconia-TZP and alumina- advanced technologies for the manufacturing of single crowns. *Eur J Prosthodont Restor Dent*. 1999;7(4):113-119.
74. Winchester L. Bond strengths of five different ceramic brackets: an in vitro study. *Eur J Orthod*. 1991;13(4):293-305.
75. Meyenberg K, Lüthy H, Schärer P. Zirconia posts: a new all-ceramic concept for nonvital abutment teeth. *J Esthet Dent*. 1995;7(2):73-80.
76. Stawarczyk B, Keul C, Figge D, Edelhoff D, Lümkemann N. Three generations of zirconia: From veneered to monolithic. Part I. *Quintessence Int (Berl)*. 2017;48(5):369-380.
77. Zhang Y. Making yttria-stabilized tetragonal zirconia translucent. *Dent Mater*. 2014;30(10):1195-1203.

78. Zhang F, Reveron H, Spies B, Van Meerbeek B, Chevalier J. Trade-off between fracture resistance and translucency of zirconia and lithium-disilicate glass ceramics for monolithic restorations. *Acta Biomater*. 2019;91:24-34.
79. Lughi V, Sergo V. Low temperature degradation-aging-of zirconia: A critical review of the relevant aspects in dentistry. *Dent Mater*. 2010;26(8):807-820.
80. Stawarczyk B, Keul C, Fgge D, Edelhof D, Lümkemann N. Three generations of zirconia: From veneered to monolithic. Part II. *Quintessence Int (Berl)*. 2017;48(6):441-450.
81. Zhang F, Van Meerbeek B, Vleugels J. Importance of tetragonal phase in high-translucent partially stabilized zirconia for dental restorations. *Dent Mater*. 2020;36(4):491-500.
82. Baldissara P, Wandscher F, Estivalete M, Parisi C, Ciocca L. Translucency of IPS e.max and cubic zirconia monolithic crowns. *J Prosthet Dent*. 2018;120(2):269-275.
83. Zucuni CP, Pereira GKR, Valandro LF. Grinding, polishing and glazing of the occlusal surface do not affect the load-bearing capacity under fatigue and survival rates of bonded monolithic fully-stabilized zirconia simplified restorations. *J Mech Behav Biomed Mater*. 2020;103:103528.
84. Hannink R, Kelly P, Muddle B. Transformation toughening in zirconia-containing ceramics. *J Am Ceram Soc*. 2000;83:461-487.
85. Pereira GKR, Guilardi LF, Dapieve KS, Kleverlaan CJ, Rippe MP, Valandro LF. Mechanical reliability, fatigue strength and survival analysis of new polycrystalline translucent zirconia ceramics for monolithic restorations. *J Mech Behav Biomed Mater*. 2018;85(May):57-65.
86. Sulaiman TA, Abdulmajeed AA, Shahramian K, Lassila L. Effect of different treatments on the flexural strength of fully versus partially stabilized monolithic zirconia. *J Prosthet Dent*. 2017;118(2):216-220.
87. Raigrodski A. Contemporary materials and technologies for all-ceramic fixed partial dentures: a review of the literature. *J Prosthet Dent*. 2004;92:557-562.
88. Dirxen C, Blunck U, Preissner S. Clinical performance of a new biomimetic double network material. *open Dent J*. 2013;6(7):118-122.
89. He L, Swain M. A novel polymer infiltrated ceramic dental material. *Dent Mater*. 2011;27(6):527-534.

90. Coldea A, Swain M, Thiel N. Mechanical properties of polymer-infiltrated-ceramic-network materials. *Dent Mater*. 2013;29(4):419-426.
91. Mörmann W, Stawarczyk B, Ender A, Sener B, Attin T, Mehl A. Wear characteristics of current aesthetic dental restorative CAD/CAM materials: Two-body wear, gloss retention, roughness and Martens hardness. *J Mech Behav Biomed Mater*. 2013;20(4):113-125.
92. Lauvahutanon S, Takahashi H, Shiozawa M, et al. Mechanical properties of composite resin blocks for CAD/CAM. *Dent Mater J*. 2014;33(5):705-710.
93. Miyazaki T, Nakamura T, Matsumura H, Ban S, Kobayashi T. Current status of zirconia restoration. *J Prosthodont Res*. 2013;57:236-261.
94. Mörmann W, Brandestini M. Cerec-System: computerized inlays, onlays and shell veneers. *Zahnarztl Mitt*. 1987;77:2400-2405.
95. Andersson M, Oden A. A new all-ceramic crown. A dense-sintered, high-purity alumina coping with porcelain. *Acta Odontol Scand*. 1993;51:59-64.
96. Raigrodski A. Clinical and laboratory considerations for the use of CAD⁄CAM Y-TZP-based restorations. *Pract Proced Esthet Dent PPED*. 2003;15:469-476.
97. Duret F, Preston J. CAD/CAM imaging in dentistry. *Curr Opin Dent*. 1991;1(2):150-154.
98. Miyazaki T, Hotta Y, Kunii J, Kuriyama S, Tamaki Y. A review of dental CAD/CAM: Current status and future perspectives from 20 years of experience. *Dent Mater J*. 2009;28(1):44-56.
99. Hickel R, Manart J. Longevity of restorations in posterior teeth and reasons for failure. *J Adhes Dent*. 2001;3:45-64.
100. Al-Wahadni A, Martin DM. Glazing and Finishing Dental Porcelain: A Literature Review. *J Can Dent Assoc*. 1998;64(8):580-583.
101. Quirynen M, Bollen C. The influence of surface roughness and surface-free energy on supra- and subgingival plaque formation in man. A review of the literature. *J Clin Periodontol*. 1995;22:1-14.
102. Bollen CML, Papaioanno W, Van Eldere J, Schepers E, Quirynen M, Van Steenberghe D. The influence of abutment surface roughness on plaque accumulation and peri-implant mucositis. *Clin Oral Implants Res*. 1996;7(3):201-211.

103. Obregon A, Goodkind R, Schwabacher W. Effects of opaque and porcelain surface texture on the color of ceramometal restorations. *J Prosthet Dent*. 1981;46:330-340.

104. Lawson N, Burgess J. Gloss and stain resistance of ceramic-polymer CAD/CAM restorative blocks. *J Esthet Restor Dent*. 2016;28(Supplementary 1):S40-45.

105. Mohammadibassir M, Rezvani MB, Golzari H, Moravej Salehi E, Fahimi MA, Kharazi Fard MJ. Effect of Two Polishing Systems on Surface Roughness, Topography, and Flexural Strength of a Monolithic Lithium Disilicate Ceramic. *J Prosthodont*. 2019;28(1):e172-e180.

106. Jones CS, Billington RW, Pearson GJ. The in vivo perception of roughness of restorations. *Br Dent J*. 2004;196(1):42-45.

107. Kurt M, Bankoğlu Güngör M, Karakoca Nemli S, Turhan Bal B. Effects of glazing methods on the optical and surface properties of silicate ceramics. *J Prosthet Dent*. 2020;64(2):202-209.

108. Haralur SB. Evaluation of efficiency of manual polishing over autoglazed and overglazed porcelain and its effect on plaque accumulation. *J Adv Prosthodont*. 2012;4(4):179-186.

109. Zucuni CP, Guilardi LFF, Rippe MPP, Pereira GKR, Valandro LFF. Fatigue strength of yttria-stabilized zirconia polycrystals: Effects of grinding, polishing, glazing, and heat treatment. *J Mech Behav Biomed Mater*. 2017;75(May):512-520.

110. Griggs J, Thompson J, Anusavice K. Effects of flaw size and auto-glaze treatment on porcelain strength. *J Dent Res*. 1996;75(6):1414-1417.

111. Sgura R, Reis MC, Hernandes AC, de Abreu Fantini MC, Andreeta Marcelllo Rubens Barsi, Medeiros IS. Surface treatment of dental porcelain: CO2 laser as an alternative to oven glaze. *Lasers Med Sci*. 2015;30(2):661-667.

112. Ahmad R, Wu BM, Morgano SM. Polishing Mechanism and Its Effect on the Mechanical Properties of Ceramic Restorations - A Review of the Literature. *Ann Dent Univ Malaya*. 2001;8:57-61.

113. Jefferies SR. Abrasive Finishing and Polishing in Restorative Dentistry: A State of the Art Review. *Dent Clin North Am*. 2007;51(2):379-397.

114. No Jones C, Billington R, Peason G. Interoperator variability during polishing. *Quintessence Int (Berl)*. 2006;37(3):183-190.

115. Karagöz Motro PF. Tam Seramik Materyallerinde Glaze ve Cila İşlemlerinin Yüzey Pürüzlülüğü ve Renk Stabilitesi Üzerine Etkilerinin İncelenmesi. 2011.
116. O'Brien W. *Dental Materials and Their Selection*. 4th Edition. Hanover Park, IL: Quintessence Publishing Co; 2008.
117. Fasbinder D. Clinical performance of chairside CAD/CAM restorations. *J Am Dent Assoc*. 2006;137:22-31.
118. Albakrya M, Guazzatoa M, Swain M. Effect of sandblasting, grinding, polishing and glazing on the flexural strength of two pressable all-ceramic dental materials. *J Dent*. 2004;32:91-99.
119. Fasbinder DJ, Neiva GF. Surface Evaluation of Polishing Techniques for New Resilient CAD/CAM Restorative Materials. *J Esthet Restor Dent*. 2016;28(1):56-66.
120. Song X, Ren H, Yin L. Machinability of lithium disilicate glass ceramic in in vitro dental diamond bur adjusting process. *J Mech Behav Biomed Mater*. 2016;53:78-92.
121. Corazza P, de Castro H, Feitosa S, Kimpara E, Della Bona A. Influence of CAD-CAM diamond bur deterioration on surface roughness and maximum failure load of Y-TZP-based restorations. *Am J Dent*. 2015;28(2):95-99.
122. Silva T, Salvia A, Carvalho R, Pagani C, Rocha D, Silva E. Polishing for glass ceramics: Which protocol ? *J Prosthodont Res*. 2014;58(3):160-170.
123. Steiner R, Beier US, Heiss-Kisielewsky I, Engelmeier R, Dumfahrt H, Dhima M. Adjusting dental ceramics: An in vitro evaluation of the ability of various ceramic polishing kits to mimic glazed dental ceramic surface. *J Prosthet Dent*. 2015;113(6):616-622.
124. Sulik W, Plekavich E. Surface finishing of dental porcelain. *J Prosthet Dent*. 1981;46:217-221.
125. Klausner L, Cartwright C, Charbeneau G. Polished versus autoglazed porcelain surfaces. *J Prosthet Dent*. 1982;47:157-162.
126. Amaya-Pajares SP, Ritter A V., Vera Resendiz C, Henson BR, Culp L, Donovan TE. Effect of Finishing and Polishing on the Surface Roughness of Four Ceramic Materials after Occlusal Adjustment. *J Esthet Restor Dent*. 2016;28(6):382-396.
127. Amer R, Kürklü D, Kateeb E, Seghi R. Three-body wear potential of dental yttrium-satbilized zirconia ceramic after grinding, polishing, and glazing treatments. *J Prosthet Dent*. 2014;112(5):1151-1155.

128. Gönüldaş F, Öztürk C, Atalay P, Öztaş D. Influence of different surface finishing techniques on machinable feldspathic and leucite-reinforced ceramics. *Dent Mater J*. 2019;38(2):317-322.

129. Matzinger M, Hahnel S, Preis V, Rosentritt M. Polishing effects and wear performance of chairside CAD/CAM materials. *Clin Oral Investig*. 2019;23(2):725-737.

130. Vichi A, Fabian Fonzar R, Goracci C, Carrabba M, Ferrari M. Effect of finishing and polishing on roughness and gloss of lithium disilicate and lithium silicate zirconia reinforced glass ceramic for CAD/CAM systems. *Oper Dent*. 2018;43(1):90-100.

131. Aravind P, Razak P, Francis P, Issac JK, Shanoj R, Sasikumar T. Comparative evaluation of the efficiency of four ceramic finishing systems. *J Int Oral Heal*. 2013;5:59-64.

132. Anusavice KJ, Phillips RW. *Phillip's Science of Dental Materials*. 11th edition. St. Louis: Elsevier; 2003.

133. Denry I, Kelly JR. Emerging ceramic-based materials for dentistry. *J Dent Res*. 2014;93(12):1235-1242.

134. Borba M, de Araújo MD, de Lima E, et al. Flexural strength and failure modes of layered ceramic structures. *Dent Mater*. 2011;27(12):1259-1266.

135. Wuttiphan S, Lawn B. Crack suppression in strongly bonded homogeneous/ heterogeneous laminates: a study on glass/glass-ceramic bilayers. *J Am Ceram Soc*. 1996;70(3):634-640.

136. Pozzobon JL, Pereira GKR, Wandscher VF, Dorneles LS, Valandro LF. Mechanical behavior of yttria-stabilized tetragonal zirconia polycristalline ceramic after different zirconia surface treatments. *Mater Sci Eng C*. 2017;77:828-835.

137. Janyavula S, Lawson N, Cakir D, Beck P, Ramp LC, Burgess JO. The wear of polished and glazed zirconia against enamel. *J Prosthet Dent*. 2013;109:22-29.

138. Awad D, Stawarczyk B, Liebermann A, Ilie N. Translucency of esthetic dental restorative CAD/CAM materials and composite resins with respect to thickness and surface roughness. *J Prosthet Dent*. 2015;113(6):534-540.

139. Bollen C, Lambrechts P, M. Q. Comparison of surface roughness of oral hard materials to the threshold surface roughness for bacterial plaque retention: a review of the literature. *Dent Mater*. 1997;13(4):258-269.

140. Tetè S, Zizzari V, Borelli B, et al. Proliferation and adhesion capability of human gingival fibroblasts onto zirconia, lithium disilicate and feldspathic veneering ceramic in vitro. *Dent Mater J*. 2014;33(1):7-15.
141. Forster A, Ungvári K, Györgyey Á, Kukovecz Á, Turzó K, Nagy K. Human epithelial tissue culture study on restorative materials. *J Dent*. 2014;42(1):7-14.
142. Anusavice K, Kakar K, Ferree N. Which mechanical and physical testing methods are relevant for predicting the clinical performance of ceramic-based dental prostheses? *Clin Oral Implants Res*. 2007;18:218-231.
143. de Jager N, Feilzer A, Davidson C. The influence of surface roughness on porcelain strength. *Dent Mater*. 2000;16:381-388.
144. Preis V, Behr M, Handel G, Schneider-Feyrer S, Hahnel S, Rosentritt M. Wear performance of dental ceramics after grinding and polishing treatments. *J Mech Behav Biomed Mater*. 2012;10:13-22.
145. Heintze S, Cavalleri A, Forjanic M, Zellweger G, Rousson V. Wear of ceramic and antagonist–a systematic evaluation of influencing factors in vitro. *Dent Mater*. 2008;24:433-449.
146. Karan S, Toroglu M. Porcelain refinishing with two different polishing systems after orthodontic debonding. *Angle Orthod*. 2008;78:947-953.
147. Sarikaya I, Guler AU. Effects of different polishing techniques on the surface roughness of dental porcelains. *J Appl Oral Sci*. 2010;18:10-16.
148. Pindborg J. *Pathology of Dental Hard Tissues.* Copenhagen: Munksgaard; 1970.
149. Asher C, Read M. Early enamel erosion in children associated with the excessive consumption of citric acid. *Br Dent J*. 1987;162(10):384-387.
150. Jones R, Cleaton-Jones P. Depth and area of dental erosions and dental caries in bulimic women. *J Dent Res*. 1989;68(8):1275-1278.
151. Schroeder P, Filler S, Ramirez B, Lazarchik D, Vaezi M, Richter J. Dental erosion and acid reflux disease. *Ann Intern Med*. 1995;122(11):809-815.
152. Barron R, Carmichael R, Marcon M, Sandor G. Dental Erosion in Gastroesophageal Reflux Disease. *J Can Dent Assoc*. 2003;69(2):84-89.
153. Schlueter N, Ganss C, Hardt M, Schegietz D, Klimek J. Effect of pepsin on erosive tissue loss and the efficacy of fluoridation measures in dentine in vitro. *Acta Odontol Scand*. 2007;65(5):298-305.
154. Amaechi B, Higham S, Edgar W. Use of transverse microradiography to quantify mineral loss by erosion in bovine enamel. *Caries Res*. 1998;32:351-356.

155. Attin T, Koidl U, Buchalla W, Schaller H, Kielbassa A, Hellwig E. Correlation of microhardness and wear in differently eroded bovine dental enamel. *Arch Oral Biol*. 1997;42:243-250.

156. Hara A, Lussi A, Zero D. Biological factors. In: Lussi A, ed. *Dental Erosion-from Diagnosis to Therapy*. Basel: Karger; 2006:88-99.

157. Butler W, Ritchie H. The nature and functional significance of dentin extracellular matrix proteins. *Int J Dev Biol*. 1995;39:169-179.

158. Breschi L, Gobbi P, Mazzotti G, Falconi M, Ellis T, Stangel I. High resolution SEM evaluation of dentin etched with maleic and citric acid. *Dent Mater*. 2002;18:26-35.

159. Ganss C, Klimek J, Starck C. Quantitative analysis of the impact of the organic matrix on the fluoride effect on erosion progression in human dentine using longitudinal microradiography. *Arch Oral Biol*. 2004;49:931-935.

160. Vanuspong W, Eisenburger M, Addy M. Cervical tooth wear and sensitivity: erosion, softening and rehardening of dentine; effects of pH, time and ultrasonication. *J Clin Periodontol*. 2002;29:351-357.

161. Pace F, Pallotta S, Tonini M, Vakil N, Bianchi Porro G. Systematic review: gastro-esophageal reflux disease and dental lesions. *Aliment Pharmacol Ther*. 2008;27:1179-1186.

162. Lazarchik D, Filler S. Dental erosion: predominant oral lesion in gastroesophageal reflux disease. *Am J Gastroenterol*. 2000;95(Supplementary 8):S33-38.

163. Bartlett D, Smith B. Clinical investigations of gastro-esophageal reflux: Part 1. *Dent Updat*. 1996;23(5):205-208.

164. Ibbetson R, Eder A. Tooth surface loss: editors' introduction. *Br Dent J*. 1999;186(2):60-66.

165. Newton JL, James OFW, Williams G V., Allen A. The diurnal profile of gastric pepsin activity is reduced with Helicobacter pylori infection. *Dig Dis Sci*. 2004;49(7-8):1103-1108.

166. Bartlett DW, Coward PY. Comparison of the erosive potential of gastric juice and a carbonated drink in vitro. *J Oral Rehabil*. 2001;28(11):1045-1047.

167. Tonami K, Ericson D. Protein profile of pepsin-digested carious and sound human dentine. *Acta Odontol Scand*. 2005;63:17-20.

168. Kleter G, Damen J, Buijs M, ten Cate J. The Maillard reaction in demineralized dentin in vitro. *Eur J Oral Sci*. 1997;105:278-284.
169. Russell G. Bulimia nervosa: an ominous variant of anorexia nervosa. *Psychol Med*. 1979;9(3):429-448.
170. Russell GFM. Thoughts on the 25th anniversary of bulimia nervosa. *Eur Eat Disord Rev*. 2004;12(3):139-152.
171. Kruger D. Bulimia nervosa: easy to hide but essential to recognize. *J Am Acad Physician Assist*. 2008;21(1):48-52.
172. American Psychiatric Association. *DSM-III. Diagnostic and Statistical Manual of Mental Disorders.* 3rd edition. Washington, DC: APA Press; 1980.
173. American Psychiatric Association. *DSM-III-R. Diagnostic and Statistical Manual of Mental Disorders.* 3rd edition. Washington, DC: APA Press; 1987.
174. Palmer R. Bulimia nervosa: 25 years on. *Br J Psychiatry*. 2004;185(6):447-448.
175. American Psychiatric Association. *DSM-IV. Diagnostic and Statistical Manual of Mental Disorders.* 4th edition. Washington, DC: APA Press; 1994.
176. MacDonald D, McFarlane T, Olmsted M. "Diagnostic shift" from eating disorder not otherwise specified to bulimia nervosa using the DSM-5 criteria: a clinical comparison with DSM-IV bulimia. *Eat Behav*. 2014;15(1):60-62.
177. Call C, Walsh T, Attia E. From DSM-IV to DSM-V: changes to eating disorder diagnoses. *Curr Opin Psychiatry*. 2013;26(6):532-536.
178. Grilo C, Ivezaj V, White M. Evaluation of the DSM-V severity indicator for bulimia nervosa. *Behav Res Ther*. 2015;67:41-44.
179. Campbell K, Peebles R. Eating disorders in children and adolescents: state of the art review. *Pediatrics*. 2014;134(3):582-592.
180. Smink F, van Hoeken D, Hoek H. Epidemiology of eating disorders: incidence, prevalence and mortality rates. *Curr Psychiatry Rep*. 2012;14(4):406-414.
181. Bulik C. Exploring the gene-environment nexus in eating disorders. *J Psychiatry Neurosci*. 2005;30(5):335-339.
182. Keski-Rahkonen A, Mustelin L. Epidemiology of eating disorders in Europe. *Curr Opin Psychiatry*. 2016;29(6):340-345.
183. Utzinger LM, Haukebo JE, Simonich H, et al. A latent profile analysis of childhood trauma in women with bulimia nervosa: Associations with borderline personality disorder psychopathology. *Int J Eat Disord*. 2016;49(7):689-694.

184. Golden N, Katzman D, Kreipe R, et al. Society for Adolescent Medicine. Eating disorders in adolescents: position paper of the Society for Adolescent Medicine. *J Adolesc Heal*. 2003;33:496-503.

185. Sangvai D. Eating disorders in the primary care setting. *Prim Care*. 2016;43(2):301-312.

186. Ganss C, Klimek J, K. G. Dental erosion in children and adolescents – a cross-sectional and longitudinal investigation using study models. *Community Dent Oral Epidemiol*. 2001;29(4):264-271.

187. Eccles J, Jenkins W. Dental erosion and diet. *J Dent*. 1974;2(4):153-159.

188. Milleding P, Haraldsson C, Karlsson S. Ion leaching from dental ceramics during static in vitro corrosion testing. *J Biomed Mater Res*. 2002;61:541-550.

189. Oh W, Delong R, Anusavice KJ. Factors affecting enamel and ceramic wear: A literature review. *J Prosthet Dent*. 2002;87:451-459.

190. Southan D, Jorgensen K. The endurance limit of dental porcelain. *Aust Dent J*. 1974;19:7-11.

191. Newton R. The durability of glass—a review. *Glas Technol*. 1985;26:21-38.

192. Ernsberger F. The role of molecular water in the diffusive transport of protons in glasses. *Phys Chem Glas*. 1980;21:146-149.

193. Anusavice K, Zhang N. Chemical durability of Dicor and lithia-based glass ceramics. *Dent Mater*. 1997;13:13-19.

194. Milleding P, Wennerberg A, Alaeddin S, Karlsson S, E S. Surface corrosion of dental ceramics in vitro. *Biomaterials*. 1999;20:733-746.

195. Wunderlich R, Yaman P. In vitro effect of topical fluoride on dental porcelain. *J Prosthet Dent*. 1986;55:385-388.

196. Sulikowski Y. Surface Texture: A systematic approach for accurate and effective communication. *Quintessence Dent Technol*. 2003;26:10-20.

197. Bhat V, Krishna Prasad D, Sood S, Bhat A. Role of colors in prosthodontics: Application of color science in restorative dentistry. *Indian J Dent Res*. 2011;22(6):804-809.

198. Park J, Park S, Lee K, Yun K, Lim H. Antagonist wear of three CAD/CAM anatomic zirconia ceramics. *J Prosthet Dent*. 2014;111:20-29.

199. Flury S, Peutzfeldt A, Lussi A. Influence of surface roughness on mechanical properties of two computer-aided design/computer-aided manufacturing (CAD/CAM) ceramic materials. *Oper Dent*. 2012;37:617-624.

200. Field J, Waterhouse P, German M. Quantifying and qualifying surface changes on dental hard tissues in vitro. *J Dent*. 2010;38:182-190.
201. Ccahuana VZS, Özcan M, Mesquita AMM, Nishioka RS, Kimpara ET, Bottino MA. Surface degradation of glass ceramics after exposure to acidulated phosphate fluoride. *J Appl Oral Sci*. 2010;18(2):155-165.
202. Al-Shammery H, Bubb N, Youngson C, Fasbinder D, Wood D. The use of confocal microscopy to assess surface roughness of two milled CAD-CAM ceramics following two polishing techniques. *Dent Mater*. 2007;23:736-741.
203. Flury S, Lussi A, Zimmerli B. Performance of different polishing techniques for direct CAD/CAM ceramic restorations. *Oper Dent*. 2010;35:470-481.
204. Heurich E, Beyer M, Jandt KD, et al. Quantification of dental erosion-a comparison of stylus profilometry and confocal laser scanning microscopy (CLSM). *Dent Mater*. 2010;26(4):326-336.
205. Whitehead S, Shearer A, Watts D, Wilson N. Comparison of two stylus methods for measuring surface texture. *Dent Mater*. 1999;15:79-86.
206. Paepegaey AM, Barker ML, Bartlett DW, et al. Measuring enamel erosion: a comparative study of contact profilometry, non-contact profilometry and confocal laser scanning microscopy. *Dent Mater*. 2013;29:1265-1272.
207. Al-Hiyasat A, Saunders W, Sharkey S, Smith G, Gilmour W. Investigation of human enamel wear against four dental ceramics and gold. *J Dent*. 1998;26:487-495.
208. Fuzzi M, Zaccheroni Z, Vallania G. Scanning electron microscopy and profilometer evaluation of glazed and polished dental porcelain. *Int J Prosthodont*. 1996;9:452-458.
209. Attin T, Wegehaupt FJ. Methods for assessment of dental erosion. *Erosive Tooth Wear From Diagnosis to Ther*. 2012;25:123-142.
210. Larimer C, Suter J, Bonheyo G, Addleman R. In situ non-destructive measurement of biofilm thickness and topology in an interferometric optical microscope. *J Biophotonics*. 2016;9:656-666.
211. Holme B, Hove L, Tveit A. Using white light interferometry to measure etching of dental enamel. *Measurement*. 2005;38:137-147.
212. Poggio C, Lombardini M, Vigorelli P, Colombo M, Chiesa M. The role of different toothpastes on preventing dentin erosion: an SEM and AFM study®. *Scanning*. 2014;36(3):301-310.

213. Barbour M, Rees J. The laboratory assessment of enamel erosion: a review. *J Dent*. 2004;32:591-602.
214. Uhlmann E, Oberschmidt D, Kunath-Fandrei G, eds. 3D-analysis of microstructures with confocal laser scanning microscopy. In: *ASPE Winter Topical Meeting on Machines and Processes for Micro-Scale and Meso-Scale Fabrication, Metrology and Assembly*. Gainesville; 2003.
215. Zhang F, Inokoshi M, Batuk M, et al. Strength, toughness and aging stability of highly-translucent Y-TZP ceramics for dental restorations. *Dent Mater*. 2016;32(12):e327-e337.
216. Oliveira-Junior O, Buso L, Fujiy F, et al. Influence of polishing procedures on the surface roughness of dental ceramics made by different techniques. *Gen Dent*. 2013;61(1):e4-e8.
217. Fuzzi M, Zaccheroni Z, Vallania G. Scanning electron microscopy and profilometer evaluation of glazed and polished dental porcelain. *Int J Periodontics Restorative Dent*. 1996;9:452-458.
218. Milleding P, Karlsson S, Nyborg L. On the surface elemental composition of non-corroded and corroded dental ceramic materials in vitro. *J Mater Sci Mater Med*. 2003;14:457-466.
219. Talbot M, White R. Cell surface and cell outline imaging in plant tissues using the backscattered electron detector in a variable pressure scanning electron microscope. *Plant Methods*. 2013;9(1):40.
220. Nguyen J, Harbison A. Scanning Electron Microscopy Sample Preparation and Imaging. *Methods Mol Biol*. 2017;1606:71-84.
221. No Valian A, Moravej-Salehi E. Surface treatment of feldspathic porcelain: scanning electron microscopy analysis. *J Adv Prosthodont*. 2014;6:387-394.
222. Moravej-Salehi E, Moravej-Salehi E, Valian A. Surface topography and bond strengths of feldspathic porcelain prepared using various sandblasting pressures. *J Investig Clin Dent*. 2016;7:347-354.
223. Magalhaes A, Romanelli A, Rios D, et al. Effect of a single application of TiF4 and NaF varnishes and solutions combined with Nd:YAG laser irradiation on enamel erosion in vitro. *Photobiomodulation, Photomed Laser Surg*. 2011;29:537-544.
224. Torres C, Chinelatti M, Gomes-Silva J, et al. Surface and subsurface erosion of primary enamel by acid beverages over time. *Braz Dent J*. 2010;21:337-345.

225. Dahl B, Oilo G. In vivo wear ranking of some restorative materials. *Quintessence Int (Berl)*. 1994;25:561-565.
226. Callister Jr. W. *Materials Science and Engineering: An Introduction.* 4th edition. New York: John Wiley & Sons; 1997.
227. Seghi R, Rosenstiel S, Bauer P. Abrasion of human enamel by different dental ceramics in vitro. *J Dent Res*. 1991;70:221-225.
228. Lawn B. A model for the wear of brittle solids under fixed abrasive conditions. *Wear*. 1975;33:269-272.
229. Westwood A, Latanision R. Environment sensitive machining behavior of nonmetals. Technical report. *Res Inst Adv Stud Martin Marietta Corp Balt*. 1970;10:70-100.
230. *ASTM Standard C1327. Standard Test Method for Vickers Indentation Hardness of Advanced Ceramics*. West Conshohocken, PA; 2015.
231. Mecholsky J. Fracture mechanics principles. *Dent Mater*. 1995;11:111-112.
232. Cesar PF, Della Bona A, Scherrer SS, et al. ADM guidance—Ceramics: Fracture toughness testing and method selection. *Dent Mater*. 2017;33(6):575-584.
233. Powers J, Allen L, Craig R. Two-body abrasion of commercial and experimental restorative and coating resins and an amalgam. *J Am Dent Assoc*. 1974;89:1119-1122.
234. Quinn GD, Bradt RC. On the vickers indentation fracture toughness Test. *J Am Ceram Soc*. 2007;90(3):673-680.
235. Palmqvist S. Method att Bestamma Segheten hos Spread Material, Sarskilt Hardmetaller. *Jernkortorets Ann*. 1957;141:300-307.
236. Evans A, Charles E. Fracture Toughness Determination by Indentation. *J Am Ceram Soc*. 1976;59:371-372.
237. Vichi A, Louca C, Corciolani G, Ferrari M. Color related to ceramic and zirconia restorations : A review. *Dent Mater*. 2011;27:97-108.
238. Bridgeman I. The nature of light and its interaction with matter. In: McDonald R, ed. *Colour Physics for Industry*. Huddersfield: H. Charlesworth & Co Ltd; 1987:1-34.
239. Joiner A. Tooth colour: A review of the literature. *J Dent*. 2004;32(SUPPL.):3-12.
240. Hill A. How we see colour. In: McDonald R, ed. *Colour Physics for Industry*. Huddersfield: H. Charlesworth & Co Ltd; 1987:211-281.

241. Clark E. Tooth color selection. *J Am Dent Assoc*. 1933;20:1065-1073.
242. Commission Internationale de l'Eclairage. *Standard Colorimetric Observer X2 (Lambda), Y2 (Lambda), Z2 (Lambda).* Vienna, Austria: Bureau Central de la CIE; 1931.
243. McLaren K. Colour space, colour scales and colour difference. In: McDonald R, ed. *Colour Physics for Industry*. Huddersfield: H. Charlesworth & Co Ltd; 1987:97-115.
244. Commission Internationale de l'Eclairage. *Light as a True Visual Quantity: Principles of Measurement*. Vienna, Austria: Bureau Central de la CIE; 1978.
245. Commission Internationale de l'Eclairage. *Colorimetry-Technical Report.* Vienna, Austria: Bureau Central de la CIE; 1986.
246. Commission Internationale de l'Eclairage. *Colorimetry—Technical Report.* Vienna, Austria: Bureau Central de la CIE; 2004.
247. Sproull RC. Color matching in dentistry. Part I. The three-dimensional nature of color. *J Prosthet Dent*. 1973;29(4):416-424.
248. Munsell AH. *A Color Notation*. 11th edition. Baltimore: Munsell Color Company, Inc.; 1961.
249. Kuehni R, Marcus R. An experiment in visual scaling of small colour differences. *Color Res Appl*. 1979;4:83-91.
250. Da Silva J, Park S, Weber H, Ishikawa-Nagai S. Clinical performance of a newly developed spectrophotometric system on tooth color reproduction. *J Prosthet Dent*. 2008;99:361-368.
251. Alghazali N, Burnside G, Moallem M, Smith P, Preston A, Jarad F. Assessment of perceptibility and acceptability of color difference of denture teeth. *J Dent*. 2012;40(Supplement 1):e10-e17.
252. Ghinea R, Pérez MM, Herrera LJ, Rivas MJ, Yebra A, Paravina RD. Color difference thresholds in dental ceramics. *J Dent*. 2010;38 S:e57-e64.
253. Johnson GM, Fairchild MD. A Top Down Description of S-CIELAB and CIEDE2000. *Color Res Appl*. 2003;28(6):425-435.
254. Paravina RD, Ghinea R, Herrera LJ, et al. Color difference thresholds in dentistry. *J Esthet Restor Dent*. 2015;27(S1):S1-S9.
255. Lee Y. Comparison of CIELAB DeltaE(*) and CIEDE2000 color-differences after polymerization and thermocycling of resin composites. *Dent Mater*. 2005;21:678-682.

256. Pérez Mdel M, Saleh A, Yebra A, Pulgar R. Study of the variation between CIELAB delta E* and CIEDE2000 color-differences of resin composites. *Dent Mater J*. 2007;26:21-28.
257. Wee A, Lindsey D, Shroyer K, Johnston W. Use of a porcelain color discrimination test to evaluate color difference formulas. *J Prosthet Dent*. 2007;98:101-109.
258. Hunter R. *The Measurement of Appearance.* 2nd ed. New York: John Wiley and Sons, Inc.; 1987.
259. Van der Burgt T, Ten Bosch J, Borsboom P, Kortsmit W. A comparison of new and conventional methods for quantification of tooth color. *J Prosthet Dent*. 1990;63:155-162.
260. Watts A, Addy M. Tooth discolouration and staining: a review of the literature. *Br Dent J*. 2001;190:309-316.
261. Paul S, Peter A, Pietroban N, Hammerle C. Visual and spectrophotometric shade analysis of human teeth. *J Dent Res*. 2002;81:578-582.
262. Patterson D. Instruments for the measurement of the colour of transparent and opaque objects. In: McDonald R, ed. *Colour Physics for Industry.* Huddersfield: H. Charlesworth & Co Ltd; 1987:35-62.
263. Tung F, Goldstein G, Jang S, Hittelman E. The repeatability of an intraoral dental colorimeter. *J Prosthet Dent*. 2002;88:585-590.
264. Douglas R. Precision of in vivo colorimetric assessments of teeth. *J Prosthet Dent*. 1997;77:464-470.
265. Paul S, Peter A, Pietrobon N, Hammerle C. Visual and spectrophotometric shade analysis of human teeth. *J Dent Res*. 2002;81:578-592.
266. Chu S, Devigus A. Fundamentals of Colors. In: *Fundamentals of Colors.* Chicago: Quintessence Publishing; 2004:23.
267. Sarafianou A, Kamposiora P, Papavasiliou G, Goula H. Matching repeatability and interdevice agreement of 2 intraoral spectrophotometers. *J Prosthet Dent*. 2012;107:178-185.
268. Sampaio CS, Atria PJ, Hirata R, Jorquera G. Variability of color matching with different digital photography techniques and a gray reference card. *J Prosthet Dent*. 2019;121(2):333-339.
269. Schropp L. Shade matching assisted by digital photography and computer software. *J Prosthodont*. 2009;18:235-241.

270. Sajjadi S, Khosravanifard B, F M, Rakhshan V, Esmaeilpour M. Effects of three types of digital camera sensors on dental specialists' perception of smile esthetics: a preliminary double-blind clinical trial. *J Prosthodont*. 2016;25:675-681.
271. Gurrea J, Gurrea M, Bruguera A, et al. Evaluation of dental shade guide variability using cross-polarized photography. *Int J Periodontics Restorative Dent*. 2016;36:76-81.
272. Bazos P, Magne P. Bio-emulation: biomimetically emulating nature utilizing a histoanatomic approach: visual synthesis. *Int J Esthet Dent*. 2014;9:330-352.
273. Casaglia A, De Dominicis P, Arcuri L, Gargari M, Ottria L. Dental photography today. Part 1: Basic concepts. *Oral Implantol*. 2016;8:122-129.
274. Hein S, Zangl M. The use of a standardized gray reference card in dental photography to correct the effects of five commonly used diffusers on the color of 40 extracted human teeth. *Int J Esthet Dent*. 2016;11:246-259.
275. Fondriest J. Shade matching in restorative dentistry; The science and strategies. *Int J Periodontics Restorative Dent*. 2003;23:467-479.
276. Brodbelt R, O'Brien W, Fan P, Frazer-Dib J, Yu R. Translucency of human dental enamel. *J Dent Res*. 1981;60:1749-1753.
277. Johnston WM. Review of translucency determinations and applications to dental materials. *J Esthet Restor Dent*. 2014;26(4):217-223.
278. Kelly J, Nishimura I, Campbell S. Ceramics in dentistry: historical roots and current perspectives. *J Prosthet Dent*. 1996;75:18-32.
279. Lee Y. Translucency of human teeth and dental restorative materials and its clinical relevance. *J Biomed Opt*. 2015;20:045002.
280. Li J, Watanabe R. Phase transformation in Y2O3-partially-stabilized ZrO2 polycrystals of various grain sizes during low-temperature aging in water. *J Am Ceram Soc*. 1998;81:2687-2691.
281. Heffernan MJ, Aquilino SA, Diaz-Arnold AM, Haselton DR, Stanford CM, Vargas MA. Relative translucency of six all-ceramic systems. Part I: Core materials. *J Prosthet Dent*. 2002;88(1):4-9.
282. Kim M, Ahn J, Kim J, Kim H, Kim W. Effects of the sintering conditions of dental zirconia ceramics on the grain size and translucency. *J Adv Prosthodont*. 2013;5:161-166.

283. Spink L, Rungruanganut P, Megremis S, Kelly J. Comparison of an absolute and surrogate measure of relative translucency in dental ceramics. *Dent Mater*. 2013;29:702-707.

284. Johnston W, Ma T, Kienle B. Translucency parameter of colorants for maxillofacial prostheses. *Int J Prosthodont*. 1995;8:79-86.

285. Miyagawa Y, Powers J, O'Brien W. Optical properties of direct restorative materials. *J Dent Res*. 1981;60:890-894.

286. Alp G, Johnston WM, Yilmaz B. Optical properties and surface roughness of prepolymerized polymethyl methacrylate denture base materials. *J Prosthet Dent*. 2019;121(2):347-352.

287. Koçak EF, Uçar Y, Kurtoğlu C, Johnston WM. Color and translucency of zirconia infrastructures and porcelain-layered systems. *J Prosthet Dent*. 2019;121(3):510-516.

288. Manziuc MM, Gasparik C, Burde A V., Colosi HA, Negucioiu M, Dudea D. Effect of glazing on translucency, color, and surface roughness of monolithic zirconia materials. *J Esthet Restor Dent*. 2019;31(5):478-485.

289. Lee Y, Lu H, Powers J. Optical properties of four esthetic restorative materials after accelerated aging. *Am J Dent*. 2006;19:155-158.

290. Lee YK. Criteria for clinical translucency evaluation of direct esthetic restorative materials. *Restor Dent Endod*. 2016;41(3):159.

291. Salas M, Lucena C, Herrera LJ, Yebra A, Della Bona A, Pérez MM. Translucency thresholds for dental materials. *Dent Mater*. 2018;34(8):1168-1174.

292. Mikhail S, Schricker S, Azer S, Brantley W, Johnston W. Optical characteristics of contemporary dental composite resin materials. *J Dent*. 2013;41:771-778.

293. Yu B, Lee Y. Translucency of varied brand and shade of resin composites. *Am J Dent*. 2008;21:229-232.

294. Yu B, Ahn J, Lee Y. Measurement of translucency of tooth enamel and dentin. *Acta Odontol Scand*. 2009;67:57-64.

295. Palla ES, Kontonasaki E, Kantiranis N, et al. Color stability of lithium disilicate ceramics after aging and immersion in common beverages. *J Prosthet Dent*. 2018;119(4):632-642.

296. Arif R, Yilmaz B, Johnston WM. In vitro color stainability and relative translucency of CAD-CAM restorative materials used for laminate veneers and complete crowns. *J Prosthet Dent*. 2019;122(2):160-166.

297. Meurman J, Rytömaa I, Kari K, Laakso T, Murtomaa H. Salivary pH and Glucose after Consuming Various Beverages, Including Sugar-Contining Drinks. *Caries Res*. 1987;21:353-359.
298. Johnston W, Ma T, Kienle B. Translucency parameter of colorants for maxillofacial prostheses. *Int J Prosthodont*. 1995;8(1):79-86.
299. Swain M V. Impact of oral fluids on dental ceramics: What is the clinical relevance? *Dent Mater*. 2014;30(1):33-42.
300. Backer AD, Münchow EA, Eckert GJ, Hara AT, Platt JA, Bottino MC. Effects of Simulated Gastric Juice on CAD/CAM Resin Composites—Morphological and Mechanical Evaluations. *J Prosthodont*. 2017;26(5):424-431.
301. dos Santos DM, da Silva EVF, Watanabe D, Bitencourt SB, Guiotti AM, Goiato MC. Effect of different acidic solutions on the optical behavior of lithium disilicate ceramics. *J Prosthet Dent*. 2017;118(3):430-436.
302. Kukiattrakoon B, Hengtrakool C, Kedjarune-Leggat U. Chemical durability and microhardness of dental ceramics immersed in acidic agents. *Acta Odontol Scand*. 2010;68(1):1-10.
303. Catelan A, Briso ALF, Sundfeld RH, Goiato MC, Dos Santos PH. Color stability of sealed composite resin restorative materials after ultraviolet artificial aging and immersion in staining solutions. *J Prosthet Dent*. 2011;105(4):236-241.
304. Pinto MM, Cesar PF, Rosa V, Yoshimura HN. Influence of pH on slow crack growth of dental porcelains. *Dent Mater*. 2008;24(6):814-823.
305. Hunt D, McIntyre J. The development of an in vitro model of dental erosion. *J Dent Res*. 1992;71:985.
306. Hetherington MM, Altemus M, Nelson ML, Bernat AS, Gold PW. Eating behavior in bulimia nervosa: Multiple meal analyses. *Am J Clin Nutr*. 1994;60(6):864-873.
307. Dentsply Sirona. Celtra Duo® Technical Product Information. 2017. https://www.dentsplysirona.com/content/dam/dentsply/pim/manufacturer/Prosthetics/Fixed/High_strength_glass_ceramic/Celtra_Duo/Celtra Duo brochure_EN.pdf.
308. Goharian P, Nemati A, Shabanian M, Afshar A. Properties, crystallization mechanism and microstructure of lithium disilicate glass-ceramic. *J Non Cryst Solids*. 2010;356(4-5):208-214.

309. Al-Wahadni AM, Martin DM. An in vitro investigation into the wear effects of glazed, unglazed and refinished dental porcelain on an opposing material. *J Oral Rehabil*. 1999;26(6):538-546.
310. Kou W, Molin M, Sjögren G. Surface roughness of five different dental ceramic core materials after grinding and polishing. *J Oral Rehabil*. 2006;33(2):117-124.
311. Lauvahutanon S, Takahashi H, Shiozawa M, et al. Mechanical properties of composite resin blocks for CAD/CAM. *Dent Mater J*. 2014;33:705-710.
312. Mandikos M, McGivney G, Davis E, Bush P, Carter J. A comparison of the wear resistance and hardness of indirect composite resins. *J Prosthet Dent*. 2001;85:386-395.
313. Özdemir H, Özdoğan A. The effect of heat treatments applied to superstructure porcelain on the mechanical properties and microstructure of lithium disilicate glass ceramics. *Dent Mater J*. 2018;37(1):24-32.
314. Yang Y, Wang Y, Tian W, et al. Reinforcing and toughening alumina/titania ceramic composites with nano-dopants from nanostructured composite powders. *Mater Sci Eng A*. 2009;508:161-166.
315. Chavan NM, Ramakrishna M, Phani PS, Rao DS, Sundararajan G. The influence of process parameters and heat treatment on the properties of cold sprayed silver coating. *Surf Coatings Technol*. 2011;205:4798-4807.
316. Zhong H, Wang L, Fan Y, et al. Mechanical properties and bioactivity of β-Ca2SiO4 ceramics synthesized by spark plasma sintering. *Ceram Int*. 2011;37:2459-2465.
317. Tang X, Nakamura T, Usami H, Wakabayashi K, Yatani H. Effects of multiple firings on the mechanical properties and microstructure of veneering ceramics for zirconia frameworks. *J Dent*. 2012;40(5):372-380.
318. Hudson J, Goldstein G, Georgescu M. Enamel wear caused by three different restorative materials. *J Prosthet Dent*. 1995;74:647-654.
319. Jagger D, Harrison A. An in vitro investigation into the wear effects of selected restorative materials on dentine. *J Oral Rehabil*. 1995;22:349-354.
320. Olivera A, Marques M. Esthetic restorative materials and opposing enamel wear. *Oper Dent*. 2008;33:332-337.
321. Gore G, Gates J. Effect of hardness on three very different forms of wear. *Wear*. 1997;203:544-563.

322. Fischer H, Marx R. Fracture toughness of dental ceramics: comparison of bending and indentation method. *Dent Mater*. 2002;18:12-19.
323. Rawls K. Mechanical properties of dental materials. In: Anusavice K, ed. *Phillips' Science of Dental Materials*. 11th edition. St. Louis: W.B. Saunders; 2003:69-143.
324. Yoshimura H, Gonzaga C, Cesar P, Miranda JW. Relationship between elastic and mechanical properties of dental ceramics and their index of brittleness. *Ceram Int*. 2012;38:4715-4722.
325. Albakry M, Guazzato M, Swain MV. Fracture toughness and hardness evaluation of three pressable all-ceramic dental materials. *J Dent*. 2003;31:181-188.
326. Albakry M, Guazzato M, Swain M. Influence of hot pressing on the microstructure and fracture toughness of two pressable dental glass-ceramics. *J Biomed Mater Res Part B Appl Biomater*. 2004;71:99-107.
327. Pollington S, van Noort R. Manufacture, characterisation and properties of novel fluorcanasite glass–ceramics. *J Dent*. 2012;40:1006-1017.
328. Goharian P, Nemati A, Shabanian M, Afshar A. Properties, crystallization mechanism and microstructure of lithium disilicate glass-ceramic. *J Non Cryst Solids*. 2010;356(4-5):208-214.
329. Apel E, Deubener J, Bernard A, et al. Phenomena and mechanisms of crack propagation in glass–ceramics. *J Mech Behav Biomed Mater*. 2008;1(313-325).
330. Kang SH, Chang J, Son HH. Flexural strength and microstructure of two lithium disilicate glass ceramics for CAD/CAM restoration in the dental clinic. *Restor Dent Endod*. 2013;38:134-140.
331. Yuan K, Wang F, Gao J, et al. Effect of sintering time on the microstructure, flexural strength and translucency of lithium disilicate glass–ceramics. *J Non Cryst Solids*. 2013;362:7-13.
332. Turp V, Tuncelli B, Sen D, Goller G. Evaluation of hardness and fracture toughness, coupled with microstructuralanalysis of zirconia ceramics stored in environments with differen pH values. *Dent Mater J*. 2012;31(6):891-902.
333. Tang X, Tang C, Su H, Luo H, Nakamura T, Yatani H. The effects of repeated heat-pressing on the mechanical properties and microstructure of IPS e.max press. *J Mech Behav Biomed Mater*. 2014;40:390-396.

334. Swain M. Toughening mechanisms for ceramics. In: Salama K, Ravi-Chandar K, Taplin DMR, Rama Rao P, eds. *Proceedings of the 7th International Conference On Fracture (ICF7)*. Pergamon; 1989:3739-3786.
335. Garrido M, Giráldez I, Ceballos L, Rodríguez J. On the possibility of estimating the fracture toughness of enamel. *Dent Mater*. 2014;30:1224-1233.
336. ISO 13356:2015. Implants for surgery — Ceramic materials based on yttria-stabilized tetragonal zirconia (Y-TZP). 2015.
337. Coldea A, Swain M, Thiel N. In-vitro strength degradation of dental ceramics and novel PICN material by sharp indentation. *J Mech Behav Biomed Mater*. 2013;26:34-42.
338. Guazzato M, Albakry M, Ringer S, Swain M. Strength, fracture toughness and microstructure of a selection of all-ceramic materials. Part II. Zirconia-based dental ceramics. *Dent Mater*. 2004;20:449-456.
339. Kulkarni A, Rothrock J, Thompson J. Impact of Gastric Acid Induced Surface Changes on Mechanical Behavior and Optical Characteristics of Dental Ceramics. *J Prosthodont*. 2020;29(3):207-218.
340. Nogueira A, Della Bona A. The effect of a coupling medium on color and translucency of CAD-CAM ceramics. *J Dent*. 2013;41:e18-23.
341. Maerten A, Zaslansky P, Mochales C, et al. Characterizing the transformation near indents and cracks in clinically used dental yttria- stabilized zirconium oxide constructs. *Dent Mater*. 2013;29:241-251.
342. Zhang F, Vanmeensel K, Batuk M, et al. Highly-translucent, strong and aging-resistant 3Y-TZP ceramics for dental restoration by grain boundary segregation. *Acta Biomater*. 2015;16:215-222.
343. Culp L, McLaren E. Lithium disilicate: the restorative material of multiple options. *Compend Contin Educ Dent*. 2010;31(716-720, 722,724-5).
344. Ozturk O, Uludag B, Usumez A, Sahin V, G. C. The effect of ceramic thickness and number of firings on the color of two all-ceramic systems. *J Prosthet Dent*. 2008;100:99-106.
345. Kursoglu P, Karagoz Motro PF, Kazazoglu E. Correlation of surface texture with the stainability of ceramics. *J Prosthet Dent*. 2014;112(2):306-313.